Bioremediation of uranium from acidic and alkaline solutions using genetically engineered *Deinococcus radiodurans*.

By

Sayali Kulkarni

LIFE 01201204001

Bhabha Atomic Research Centre, Mumbai

A thesis submitted to the
Board of Studies in Life Sciences

In partial fulfilment of requirements
for the Degree of
DOCTOR OF PHILOSOPHY
of
HOMI BHABHA NATIONAL INSTITUTE

June, 2016

STATEMENT BY AUTHOR

This dissertation has been submitted in partial fulfilment of requirements for an advanced degree at Homi Bhabha National Institute (HBNI) and is deposited in the library to be made available to borrowers under rules of the HBNI.

Brief quotations from this dissertation are allowable without special permission, provided that accurate acknowledgement of source is made. Requests for permission for extended quotation from or reproduction of this manuscript in whole or in part may be granted by the Competent Authority of HBNI when in his or her judgment the proposed use of the material is in the interests of scholarship. In all other instances, however, permission must be obtained from the author.

Sayali Kulkarni

DECLARATION

I, hereby declare that the investigation presented in the thesis has been carried out by me. The work is original and has not been submitted earlier as a whole or in part for a degree at this or any other Institution / University.

Sayali Kulkarni

List of Publications arising from the thesis

Journal:

1. Sayali Kulkarni, Anand Ballal and Shree Kumar Apte* (2013) Bioprecipitation of uranium from alkaline waste solutions using recombinant *Deinococcus radiodurans*, **J**. **Hazard**. **Mater**. 262: 853-861.

2. **Sayali Kulkarni**, Chitra Seetharam Misra, Alka Gupta, Anand Ballal and Shree Kumar Apte* Interaction of uranium with bacterial cell surface: Implications from phosphatase mediated uranium precipitation- (**Appl. Env. Microbiol.** doi:10.1128/AEM.00728-16).

Conferences:

1. Kulkarni S, Misra C, Ballal A, Gupta A, Apte S.K. (2014) Studies on phosphatase mediated bioprecipitation in recombinant *E. coli* / *D. radiodurans* using electron microscopy; International Conference on Electron Microscopy and XXXV Annual Meeting of Electron Microscopy Society of India (EMSI-2014); Page 205 (P-IC318); University of Delhi, Delhi, India.

2. **Kulkarni S**, Misra C, Gupta A, Ballal A, Apte S.K. (2015) Effect of pH /uranyl species on localization of uranyl phosphate precipitate in recombinant *D. radiodurans* expressing PhoN/PhoK; DAE-BRNS Life Science Symposium, 2015, page- 142 (P-50), Mumbai, India.

3. Ballal A, **Kulkarni S**, Misra C, Gupta A, Apte S. K. (2015) Transmission electron microscopy to visualize the localization of uranyl phosphate precipitate in *E. coli*; Conference on Electron Microscopy and XXXVI Annual Meeting of Electron Microscopy Society of India (EMSI-2015); Page 301; CIDCO convention centre, Vashi, Navi Mumbai.

Sayali Kulkarni

Dedicated to my Parents……

Acknowledgements

Pursuing PhD is not only an academic challenge; but much more non-scientific exercise too in every aspect. The going has been rough at times and fortunately I have been blessed to have the most wonderful people around me during those strenuous times. They have made this journey facile with words of encouragement and support all the time. I would like to acknowledge people from whom I received enormous help, and moral support to achieve this.

I would like to express my sincere gratitude first to my guide, Dr. Shree Kumar Apte for guiding my work in spite of a very busy schedule and for improving my scientific writing skills. This thesis would not have come up to into good shape without his critical evaluation and useful suggestions. There is a lot I have learnt that will stand me in good stead throughout my life.

I thank my co-guide, Dr. Anand Ballal, for supporting me throughout my work and teaching me basic skills of molecular biology. His guidance helped me in proper data interpretation, presentation and writing scientific articles. I thank my doctoral committee chairperson Dr. J. S Melo and Dr. Celin Acharya, member, for their encouragement, valuable suggestions and critical inputs that helped in elevating the standard of this work. I was fortunate to be able to discuss my work without any inhibitions with Dr. Celin Acharya on account of her friendly and cordial demeanour. Her patience and support helped me overcome my crisis situations and finish this thesis. I am indebted to Dr. Hema Rajaram, Dean, Life Sciences to whom I went very often for all Ph.D related paperwork as well as for personal advices. Her help and constant support helped me today to reach this moment.

I sincerely thank to Dr. S. Chattopadhyay for his generous attitude and support throughout the tenure of this work and for his words that boosted my moral.

I thank my wonderful colleagues Dr. Chitra Seetharam who not only supported me for PhD/academic work but also on personal front. I am thankful to Dr. Shyam Sunder and former colleague Saraswathi Perumal- they have been a family for me and one could not wish for more helpful colleagues (rather friends) than them.

Some people are invaluable in terms of support and help. I would not have seen this day of finishing my thesis without their support. They were able to a spread smile on my face during crisis situation. Our scientific as well as non-scientific discussions over lunch sessions are the best part of every day in BARC. I wish to thank my friends Akhilesh, Arvind, Nilesh, Dr. Prashant Raghvan, Papiya Dey and Ashwini for being with me all the time. My friends Pallavi Gaikwad and Ganesh Nikalje need a special mention for their invaluable help whenever asked for.

I wish to thank my lab-mates Mrs. Pallavi Chandwadkar and Mr. Pawan Nimje for all their help and moral support all the time and for all the fun we had in past few years. Thanks to techno-

savvy Divya for keeping the mood in the lab young and vibrant. I always enjoyed a talk with her and latest updates about electronic world.

I thank my colleagues, Dr. Alka Gupta, Namrata Jadhav for electron microscopic studies, Dr. Salil Verma, Mr. Deepak Tyagi for help in XRD analysis of samples and interpretation of results, Dr. Chitra R and Dr. Rajul Chaudhary for an un-complainingly processing my samples for XRD analysis and giving valuable scientific inputs.

This would never have happened without enormous support from my parents and husband. But I will surely fall short of words when it comes to thanking my parents. I therefore, dedicate this thesis to my parents.

Finally I am also thankful to Department of Atomic Energy and Bhabha Atomic Research Centre for providing funds and all the necessary aid to carry out this work. To all those, whom I have inadvertently left out but have contributed to my work, thank you very much.

ABBREVIATIONS

Ap	Ampicillin
APS	Ammonium per sulphate
ATP	Adenosine triphosphate
AU	Arbitrary unit
β-GP	Glycerol-2-phosphate
bp	Base pairs
Cm	Chloramphenicol
Cb	Carbenicillin
CBB	Coomassie Brilliant Blue
Cs	Caesium
D/W	Distilled water
EDTA	Ethylene diamine tetra acetic acid
GC	Geochemical condition
h	hour/s
IPTG	Isopropyl-β-D-thiogalactopyranoside
Kan	Kanamycin
kb	kilo bases
kDa	kilo Dalton
LB	Luria-Bertani
MG	Methyl Green
MOPS	3-(N-mopholino) propane sulfonic acid
mM	millimolar
mg	milligrams
ml	millilitre
min	minutes
Ni^{+2}-NTA	Ni^{2+} -nitrilotriacetic acid
NBT-BCIP	Nitro Blue Tetrazolium / 5'Bromo 4' Chloro 3-Indolyl Phosphate
NEB	New England biolabs
ng	nanogram

nm	nanometer
nmoles	nanomoles
OD	Optical Density
ORF	Open Reading Frame
PAGE	Polyacrylamide gel electrophoresis
PCR	Polymerase Chain Reaction
pmoles	picomoles
PDP	Phenolphthalein Di-Phosphate
P_i	Inorganic phosphate
p-NP	para-Nitro Phenol
p-NPP	para-Nitro Phenyl Phosphate
RT	Room temperature
SDS	Sodium dodecyl sulphate
SEM	Scanning Electron Microscopy
S-layer	Surface layer
TBE	Tris-Borate EDTA buffer
TEM	Transmission Electron Microscopy
TEMED	N,N,N`,N`-Tetramethylenediamine
TGY	Tryptone, Glucose, Yeast Extract
Tris	Tris (hydroxymethyl)-aminomethane
U	Uranium
UV	Ultra violet
µg	microgram
µl	microlitre
µM	micromloar
XRD	X-ray diffraction

Contents

Synopsis		v
List of figures		xix
List of tables		xxii

Chapter 1. Introduction

1.1	Sources of Uranium in the environment	2
1.2.	Environmental impact of uranium	4
1.3	Uranium- Chemistry and speciation	6
1.4	Microbial bioremediation of heavy metals and uranium	8
1.4.1	Biosorption	10
1.4.2	Bioaccumulation	12
1.4.3	Bioreduction	12
1.4.4	Biomineralization	15
1.5	Phosphatase mediated bioprecipitation of heavy metals- A preferred approach for bioremediation	17
1.6	Bacterial phosphatases	18
1.6.1	Acid phosphatases	20
1.6.2	Alkaline phosphatases	21
1.7	Phosphatase mediated bioremediation of uranium to date	23
1.8	*Deinococcus radiodurans* - A promising candidate for uranium bioremediation	25
1.9	This study	27

Chapter 2. Materials and Methods

2.1	Bacterial strains, growth media and culture conditions	31
2.2	Histochemical screening of recombinant bacterial strains expressing PhoN/PhoK	32
2.3	Recombinant DNA techniques	33
2.3.1	Isolation of plasmid DNA	33
2.3.2	Restriction endonuclease digestion and electrophoresis of DNA	34
2.3.3	Amplification of DNA by Polymerase Chain Reaction	34
2.3.4	Ligation and transformation	36
2.4	Extraction, estimation and electrophoresis of cellular proteins	36
2.5	Determination of phosphatase activity	38
2.5.1	*In vitro* acid/alkaline phosphatase activity by zymogram analysis	38

2.5.2	*In vivo* cell-based acid phosphatase activity	39
2.6	Western Blotting and immunodetection of PhoK protein	40
2.7	Determination of surface charge of cells	40
2.8	Uranium precipitation/biosorption assays	40
2.9	Radiation response studies	42
2.10	Uranium sensitivity studies	43
2.11	X-ray diffraction analysis	44
2.12	Fluorimetric analysis	44
2.13	Transmission Electron Microscopy	45
2.14	Lyophilisation	45
2.15	Immobilization of cells/proteins	46
2.15.1	Immobilization of *Deino-PhoK*/*Deino-PhoN*K cells in calcium alginate	46
2.15.2	Immobilization of *Deino-PhoK* cells in polyacrylamide gel and uranium precipitation in flow through system	46
2.15.3	Immobilization of PhoK on Ni^{+2}-NTA matrix	47
2.15.4	Uranium precipitation using immobilized PhoK	48
2.16	PhoK inactivation assays	49

Chapter 3. Construction of recombinant *D. radiodurans* strains expressing acid/alkaline phosphatases for bioprecipitation of U

3.1	Cloning of phoK in *E. coli -D. radiodurans* plasmid shuttle vector pRAD1	52
3.2	Transformation of plasmid pK1 into *D. radiodurans*	57
3.3	Expression and activity of PhoK in recombinant strains	59
3.3.1	*In vivo* cell associated phosphatase activity	59
3.3.2	*In vitro* PhoK activity by zymogram analysis	61
3.4	Optimization of PhoK expression	62
3.5	Radiation response of *Deino-PhoK*	65
3.5.1	Effect of gamma radiation on survival of *Deino-PhoK*	66
3.5.2	Effect on cell associated PhoK activity under radiation stress	66
3.6	Uranium precipitation studies using *Deino-PhoK* cells	68
3.6.1	Optimization of uranium precipitation conditions	68
3.6.2	Kinetics of uranium precipitation by *Deino-PhoK* cells	69
3.6.3	Uranium precipitation at different concentrations of β-GP	71
3.6.4	Comparison of U precipitation by *Deino-PhoK* and *Deino-PhoN* strains	72

3.6.5	Uranium precipitation by *Deino-PhoK* at different input U concentrations	73
3.6.6	Uranium precipitation by *Deino-PhoK* cells post irradiation	75
3.7	Construction of recombinant *Deinococcus* strain co-expressing both acid (PhoN) and alkaline phosphatase (PhoK)	78
3.8	Phosphatase expression, cell associated enzyme activity and in-gel zymogram assays of *Deino-PhoNK* strain	80
3.9	Evaluation of U precipitation by *Deino-PhoNK* strain	83
3.10	Discussion	84

Chapter 4. Characterization and localization of uranyl phosphate, precipitated by recombinant strains

4.1	Characterization of uranium, precipitated by *Deino-PhoK* cells	91
4.1.1	Identification of chemical nature of precipitate by XRD analysis	91
4.1.2	Fluorimetric analysis of uranyl phosphate precipitate	91
4.2	Electron microscopic visualization and localization studies of U precipitation	94
4.2.1	Location of uranyl phosphate precipitate in *Deino-PhoK* cells under GC2	94
4.2.2	Location of uranyl phosphate precipitate in *Deino-PhoN* cells under GC1	96
4.2.3	Localisation of uranyl phosphate precipitate on reversing the precipitation conditions for *Deinococcus* expressing PhoN/PhoK.	100
4.3	Confirmation of the uranyl phosphate precipitated under GC1 or GC2 by XRD analysis	104
4.4	Uranyl phosphate localisation studies in E. coli expressing PhoN/PhoK	106
4.5	Uranyl phosphate localisation in *Deino-PhoNK*	108
4.6	Demonstration of differential biosorption of uranium under GC1 and GC2	110
4.7	U sensitivity towards *D. radiodurans* and *E. coli*	112
4.8	Discussion	116

Chapter 5. Uranium precipitation by lyophilized or immobilized recombinant strains

5.1	Lyophilisation of *Deino-phoK* cells	124
5.1.1	Effect of lyophilization on survival of the recombinant *Deino-PhoK* cells	124
5.1.2	Alkaline phosphatase activity of lyophilized cells	125
5.1.3	Uranium precipitation ability of lyophilized *Deino-PhoK* cells.	126
5.2	Lyophilisation of *Deino-PhoK* cells	127
5.2.1	Phosphatase activity of lyophilized *Deino-PhoNK* cells	127
5.2.2	Uranium precipitation ability of lyophilized *Deino-PhoNK* cells	128

5.3	Immobilization of *Deino-PhoK*/*Deino-PhoNK* cells and evaluation of their uranium precipitation ability	129
5.3.1	U precipitation using immobilized *Deino-PhoK* cells in batch process	130
5.3.2	U precipitation by calcium alginate immobilized *Deino-PhoNK* cells in batch process	135
5.3.3	U bioprecipitation by calcium alginate immobilized *Deino-PhoK* cells in a	136
5.4	Use of immobilised PhoK protein in column-based U bioprecipitation	139
5.4.1	Immobilisation of PhoK and its activity	140
5.4.2	Uranium precipitation by immobilised PhoK in batch process	142
5.4.3	Uranium precipitation by immobilised PhoK in continuous flow through process	143
5.5	Discussion	147
Chapter 6. Summary and Conclusions		151
References		157
Publications from this work		172

Homi Bhabha National Institute

Ph. D. PROGRAMME

1. Name of the Student:	Sayali Kulkarni
2. Name of the Constituent Institution:	Bhabha Atomic Research Centre
3. Enrolment No.:	LIFE01201204001
4. Title of the Thesis:	Bioremediation of uranium from acidic and alkaline solutions using genetically engineered *Deinococcus radiodurans*
5. Board of Studies:	Life Sciences

Synopsis

Heavy metal pollution is a major environmental problem today. Most of the heavy metal ions are toxic to living organisms. The non-degradable nature of these heavy metals makes it more difficult to remove them, leading to their accumulation in the environment (1). Waste from the nuclear industry predominantly consists of radioactive or non-radioactive heavy metals like U, Cs, Sr, Pu, Am, Ni, Cd, Zn. Co, Pb etc, which are difficult to remove (2-3). Among these, uranium (U) is most commonly found radioactive component of the nuclear waste. Large amount of U-containing acid/alkaline radioactive waste is generated from activities such as U mining and extraction, fuel fabrication, reactor operation, spent fuel reprocessing and its disposal. Elsewhere in USA and the erstwhile USSR, groundwater has been contaminated in some places with radioactivity and heavy metals released from corrosion of nuclear stockpiles (2). Hence, it is of particular importance to efficiently remove U from such waste solutions.

Strategies for remediation of metal and radionuclide contaminated soils or groundwater include physical, chemical (abiotic) and biotic methods. Physico-chemical processes such as excavation, ion-exchange, oxidation and reduction, filtration, reverse

osmosis, chemical precipitation, conditioning and disposal are the widely practiced remediation techniques (4). High reagent requirements and unpredictable metal ion removal are some of the disadvantages associated with such techniques. Further, strong reagents like alkali solutions, acids are used for desorption, resulting in toxic sludge and secondary environmental pollution (5). Bioremediation involves minimizing the mobility of contaminants by transferring them to a stable, non-labile phase using biological entities or microbe mediated processes. For large areas of contaminated soil and aquifer sediments, application of biological methods is appealing since it is much less disruptive to the ecosystem and hydrology, reduces the risk of worker's exposure during remediation and is typically less expensive than conventional technologies (5-6). However, scope of this thesis is limited to U bioremediation from aqueous effluent waste.

Among the biological mechanisms involved in metal remediation, enzymatic bioprecipitation of heavy metals as metal phosphates is particularly attractive and is considered a promising approach for bioremediation of U (4). A major attraction of this method is treatment of waste even at very low concentrations of metal, which are not amenable to physico-chemical methods. Bioprecipitation of metals as phosphates is mediated by phosphatases which cleave a phospho-monoester substrate to release the phosphate moiety, which in turn precipitates heavy metals such as U, Cd, Ni, Am, Pu etc from solutions (7-8). Successful bioprecipitation of U and other heavy metals (e.g. cadmium) from acidic wastes using bacterial acid phosphatases has been demonstrated (7, 9-10). Genetic engineering has also been successful in endowing microbes, which occur and grow in waste, with ability to remediate metals and in enhancing their bioremediation potential. For example, *E. coli* has been genetically manipulated for such purpose and offers the advantage of convenient expression of foreign proteins (11-13), but is highly radiosensitive.

Radioactive waste sites pose a unique problem since their remediation requires a radio-resistant system which must not only remove metals but also endure such environment. Radiation resistant bacteria which can remediate these metals are better choices to address radioactive wastes (14-15). The bacterium *Deinococcus radiodurans*, known to survive extreme ionizing radiation stress has been a candidate of choice for studies on bioremediation in high radiation environments. *D. radiodurans* can tolerate very high doses of ionizing radiation and exhibits remarkable resistance to DNA damage caused by ionizing radiation, desiccation and other stresses (16-17). The organism has been engineered earlier for degradation of toluene, and detoxification of Hg and Cr in radioactive environment (1, 18). It has also been successfully manipulated to express acid phosphatase (PhoN) from other bacteria to precipitate U from aqueous waste solution. Such recombinant *D. radiodurans* cells exhibited metal precipitation even after being subjected to 6 kGy dose of gamma radiation, while *E. coli* cells carrying the same construct failed to do so (19-21).

Although, U bioprecipitation from acidic to neutral conditions has received considerable attention, bioprecipitation of U from alkaline waste has been relatively less explored so far. Precipitation of U(VI) as uranyl phosphate from alkaline solution is rather difficult on account of extremely high solubility of uranyl carbonate complexes at basic pH. Precipitation is feasible only at log (PO_4^{3-}/CO_3^{2-}) values of > -3 (22). While it is chemically difficult to achieve such a favorable (PO_4^{3-}/CO_3^{2-}) ratio, an active enzymatic process can generate localized high concentration of inorganic phosphate for such precipitation. Recently, our laboratory identified a novel alkaline phosphatase enzyme, PhoK, having very high specific activity from a *Sphingomonas* sp. strain BSAR-1 (23-24). This *Sphingomonas* strain could precipitate U, albeit with a low efficiency, under alkaline conditions indicating that the required (PO_4^{3-}/CO_3^{2-}) ratio for U precipitation could be attained by this enzyme. Bioprecipitation efficiency of PhoK could be enhanced several fold by cloning and

overexpressing the *Sphingomonas phoK* gene in *E. coli* (23). However, utility of these strains remained limited to non-radioactive waste. The present study was undertaken with an aim to construct a single recombinant bacterial strain capable of bioprecipitation of U from alkaline or acidic-neutral conditions in high radiation environment.

Chapter 1. General Introduction:

This chapter provides a brief overview of the problem of heavy metal pollution, in particular U contamination. The development of U attenuation processes is dependent on the chemical behavior of U in aqueous systems (25). Determination of the active species of U in aqueous systems under various environmental conditions is of primary importance for the understanding of U transport mechanism from the waste towards water bodies. U and its decay products are hazardous because of their radio-toxicity as well as chemical toxicity. Hence various attributes of U such as, its sources, mining, chemistry and speciation, toxicity and environmental impact are discussed in detail. The chapter also describes microbial remediation of U, including various mechanisms of biosorption, bioaccumulation, bioreduction and biomineralization. Phosphatase mediated bioprecipitation of heavy metals, especially U, and how this is a preferred strategy over others is highlighted. The chapter discusses bacterial phosphatases, their role in microbial metabolism and their use as tool for bioremediation and briefly reviews bacterial acid and alkaline phosphatases. An account of recent studies on use of native or engineered bacteria for bioremediation of U is provided. The radio-resistant *D. radiodurans* is highly suited for remediation of radioactive waste solutions and has been used for bioremediation of metals likely to be present in such waste solutions. The chapter summarizes the available information on bioremediation using *D. radiodurans*. It discusses possibilities of engineering *D. radiodurans* for bioprecipitation of alkaline waste solutions, and how co-expression of acid and alkaline phosphatases can enable

use of single microbe under both acidic-neutral and alkaline conditions. The chapter ends by delineating the specific objectives of this study which are as follow.

1. Cloning of *phoK* gene from *Sphingomonas* into *E. coli-D. radiodurans* shuttle vector and to ascertain its expression in *E. coli* and *D. radiodurans.*
2. Optimization of PhoK expression, activity and U precipitation by recombinant strain under ambient and high radiation environment.
3. Identification and localization of uranyl phosphate, precipitated by the recombinant strain
4. Lyophilization of *D. radiodurans* cells expressing PhoK to preserve their U precipitation ability and to extend shelf life.
5. Comparison of U precipitation in a batch versus continuous-flow process.
6. Construction of recombinant *D. radiodurans* co-expressing both acid and alkaline phosphatase and evaluating its U precipitation ability.

Chapter 2. Materials & Methods:

This chapter provides details of methodologies used in various experiments. Different bacterial strains used for the cloning and protein purification studies like *E. coli* JM109, *E. coli* (DE3), PhoK overexpressing *E. coli* (DE3), wild type as well as recombinant *D. radiodurans* strains generated in this study, are enlisted. Nutrient media used were LB for *E. coli* and TGY for *D. radiodurans* supplemented with appropriate antibiotics. The optimized growth conditions and methods used for growth in terms of increase in turbidity (Absorbance at 600 nm) or by scoring colony forming units are specified. Standard protocols for plasmid isolation, restriction digestion, ligation, transformation, sequencing etc. used in all the cloning work are described in this chapter. A binary shuttle vector for *E. coli* and *D. radiodurans,* pRAD1, was used for cloning. The deinococcal P_{groESL} promoter was employed for expression of genes in *D. radiodurans*. Expression of proteins was assessed using (a)

electrophoresis, (b) Western blotting followed by immunodetection, (c) zymogram analysis, and (d) phosphatase activity assays using substrates like para-nitrophenyl phosphate (*p*-NPP) or β-glycerophosphate (β-GP). The chapter provides details of U precipitation assays performed, along with appropriate controls. U precipitation assays were carried out under two different geochemical conditions, in ambient environment or after exposure to gamma radiation. U was estimated spectrophotometrically using the Arsenazo III reagent. Protocols used for characterization of precipitated U, like XRD and spectrofluorimetry analysis are described. Transmission electron microscopy was used as the main tool for visualization of precipitate and its pH based localization studies. Protocols for U toxicity studies with recombinant strains are included. Details of lyophilization of cells have been specified. Methods for immobilization of cells in calcium alginate matrix, and for immobilization of PhoK on Ni-NTA matrix are mentioned in detail. Protocols for batch and column based precipitation studies are also discussed.

Chapter 3. Construction of recombinant *D. radiodurans* strains expressing acid/alkaline phosphatases for bioprecipitation of U

This chapter describes the construction of recombinant *D. radiodurans* strains expressing PhoK alone or co-expressing PhoK and PhoN enzymes together and U precipitation abilities of these strains at different pH conditions. For heterologous expression of *phoK* gene, which encodes a novel alkaline phosphatase PhoK, the gene was cloned in *D. radiodurans*/*E. coli* shuttle plasmid vector pRAD1 downstream of a strong deinococcal promoter P_{groESL}. The recombinant plasmid construct, pK1, was transformed into *E. coli* (*E. coli-PhoK*) as well as *D. radiodurans* (*Deino-PhoK*). The recombinant strain *Deino-PhoK* exhibited remarkably high alkaline phosphatase activity as evidenced by cell based enzyme activity assays and also by *in gel* zymographic analysis. When assayed using whole cells, exponential phase *Deino-PhoK* cells showed 4-5 fold higher PhoK activity than *E. coli-PhoK*

and over 75-fold higher phosphatase activity than *Deino-PhoN* (*Deinococcus* expressing a non specific acid phosphatase, PhoN) cells, constructed earlier.

Deino-PhoK cells were assessed for their U precipitation ability, using either *p*-NPP or β-glycerophosphate (β-GP) as substrates. The cells showed very high phosphatase activity (~15000 units) as well as a very rapid U removal ability compared to those reported in earlier studies (19). Initial precipitation kinetics revealed a more rapid precipitation of U with *p*-NPP than with β-GP. However, notwithstanding these initial differences, both the substrates resulted in more than 90% U precipitation of initial input U at the end of 2 h. At higher concentrations of input U (1-10 mM), more than 80% U was precipitated within 2 h. The important factors for microbial bioremediation process are the time required for maximal metal removal, the range of working concentration and the minimum amount of biomass required. The *Deino-PhoK* strain excelled in all these attributes and at a relatively low cell density (OD_{600nm}~1), these cells could efficiently bioprecipitate over 90% of input U within 2 h. The maximal U loading capacity of *Deino-PhoK* cells was found to be 10.7 g U/ g dry weight of cells (at input U concentration of 10 mM), which to our knowledge, is the highest reported so far. The expression of PhoK did not compromise the inherent radioresistance or the bioprecipitation ability of the recombinant *Deino-PhoK* strain. Both, *Deino-pRAD1* and *Deino-PhoK* strains showed D_{10} values of around 15.6 kGy, indicating that introduction of *phoK* gene did not affect the inherent radioresistance of *D. radiodurans.*

To facilitate U bioprecipitation from both acidic and alkaline waste using a single microbe, a recombinant *Deinococcus* strain co-expressing both *phoN* and *phoK* genes was constructed. For this, *phoK* gene was cloned in previously constructed plasmid pPN1 which carries the *Salmonella typhimurium phoN* gene cloned in pRAD1 vector (19). The new plasmid, pK2, thus generated, harbored both the *phoN* and *phoK* genes, which were each expressed independently from a strong deinococcal promoter, P_{groESL}. The plasmid pK2 was

transformed into *D. radiodurans* R1 to obtain the strain *Deino-PhoNK*. Whole cell phosphatase activity, Western blotting based immunodetection and zymogram analyses confirmed that both PhoN and PhoK phosphatases were actively expressed in the recombinant strain and were fully active at their appropriate pH optima. U precipitation ability of *Deino-PhoNK* cells was evaluated at acidic and alkaline pH separately. The precipitation kinetics shown by *Deino-PhoNK* strain under alkaline conditions (> 85% U precipitation within 3 h) was very similar to that shown by the stationary phase *Deino-PhoK* strain. Rate of U precipitation at 1 mM metal concentration by the *Deino-PhoNK* strain under acidic conditions (>80-85% precipitation within 6 h), was comparable to that shown by the *Deino-PhoN* strain under similar conditions. Under alkaline conditions, at same input U concentration (i.e. 1 mM), *Deino-PhoNK* cells achieved 1.07 g loading of U/g of dry weight of cells whereas *Deino-PhoK* cells were loaded with 1.08 g of U/dry weight of cells at 1 mM U. Under acidic conditions *Deino-PhoNK* strain showed loading of 0.34 g U/g of dry weight of cells which was comparable to *Deino-PhoN* cells that showed ~ 0.35 g U/g dry weight of cells.

Chapter 4. Characterization and localization of uranyl phosphate, precipitated by recombinant strains.

This chapter describes physicochemical characterization of uranyl phosphate (UP) precipitated by recombinant strains, localization of the precipitated U using transmission electron microscopy (TEM) and effect of pH on localization of UP precipitate. In all previous studies, PhoN based U precipitation using uranyl nitrate at pH 6.8 resulted invariably in cell-associated U precipitates (20-21). In contrast, cell harbouring PhoK, tested with uranyl carbonate at pH 9, showed extracellular precipitation of U. The respective uranyl salts for U bioprecipitation studies were used to keep U soluble under the pH conditions optimal for the respective phosphatase activities. This chapter describes experiments which tested both the

enzymes, with different uranyl salts under both pH conditions, to determine whether U speciation has an influence on precipitation process. The assay conditions were described as geochemical condition 1 (GC1) and geochemical condition 2 (GC2). GC1 is a carbonate deficient condition at pH 6.8, while GC2 is a carbonate abundant condition at pH 9.0.

Deino-PhoK cells, under GC2, precipitated uranyl phosphate extracellularly as observed by transmission electron microscopy (TEM). X-ray diffraction (XRD) and fluorescence analysis identified the precipitated uranyl phosphate species as uranyl hydrogen phosphate hydrate, $H_2(UO_2)_2(PO_4)_2.8H_2O$ also known as chernikovite (meta-autunite). However, the same *Deino-PhoK* cells, when incubated with U under GC1, clearly showed a cell associated precipitate like the similarly treated *Deino-PhoN* cells. Interestingly, *Deino-PhoN* cells incubated with U under GC2 exhibited extracellular precipitation. Identical results were observed with recombinant *E. coli* strains, individually expressing PhoN/PhoK phosphatases. XRD analysis of uranyl phosphate, precipitated under both geochemical conditions, confirmed that the precipitated uranyl phosphate species remained the same i.e. chernikovite, irrespective of pH or phosphatase enzyme used. TEM analysis revealed that the cell-bound or extracellular location of the precipitate was determined not by the location of the corresponding enzyme (PhoN-periplasmic or PhoK-extracellular) or the uranyl salt used, but by the uranyl species prevalent under particular GC. Thus UP precipitate was cell surface associated under GC1 and extracellular under GC2. It was also demonstrated that U is adsorbed on to cell surface more under GC1 than under GC2. U adsorption was found to be 8.5% under GC1 and only about 2.2% under GC2. Differential adsorption of uranyl ions to cell surface also resulted in differential U toxicity to cells under the two GCs employed. Only 10 % growth was obtained at 1.5 mM input U concentration under GC1, and at 25 mM under GC2. Thus, U was far less inhibitory under GC2.

In terms of bioremediation, enzyme-based bioprecipitation was found to circumvent U toxicity to cells, by preventing entry and intracellular accumulation of U. Under both GC1 and GC2, the phosphatase expressing cells could survive at inhibitory concentration of U (2 mM for GC1, 30 mM for GC2), while phosphatse negative cells did not show any growth after exposure to these U concentrations. Thus, the issue of metal sensitivity can be avoided by PhoN/PhoK mediated U bioprecipitation.

Chapter 5. Uranium precipitation by lyophilized or immobilized recombinant *Deinococcus* strains

Lyophilization of *Deino-PhoK* or *Deino-PhoNK* cells was carried out to convert the biomass into a dry powdered form. Lyophilized recombinant cells fully retained phosphatase activity as well as U precipitation ability at ambient temperature for >1 year for both the recombinant strains (*Deino-PhoK* and *Deino-PhoNK*) during storage. This facilitated easy recovery of precipitated metal with the biomass. Most importantly, lyophilization significantly extended the shelf life of the product in terms of metal precipitation for prolonged period which increased the ease of handling, storage, transport and application.

Under GC1, the cell bound precipitate makes cells heavy causing them to settle down, thus facilitating easy recovery of the precipitated U without centrifugation. However, the uranyl phosphate, precipitated under GC2 by PhoK expressing cells remained extracellular and required centrifugation for complete recovery. In order to achieve easier separation of uranyl phosphate precipitate from the bulk volume, bioprecipitation was attempted with *Deino-PhoK* and *Deino-PhoNK* cells immobilized in calcium alginate beads. These beads could remove ~ 90% U from 1 mM solution within 2 h. On exposure to UV, these beads showed bright green colored fluorescence, while the supernatant of incubation medium did not, indicating that the precipitate was entirely entrapped into beads. The beads settled down to the floor of the flask quickly and could be easily harvested to facilitate separation and

recovery of the bioprecipitated U. The beads precipitated ~ 0.5 g of U /g of dry weight of biomass at 1 mM input U concentration under GC2.

A column based approach for U bioprecipitation provides the advantage of a continuous flow system for removal and recovery of U. For this purpose, the His-tagged PhoK was immobilized onto the Ni-NTA (Ni^{+2}-nitrilotriacetic acid) affinity matrix and tested in batch process or in column studies. The immobilized PhoK was able to precipitate more than 90% U from 1mM uranyl carbonate within 3 h in batch process, thus showing impressive loading capacities. Ni-NTA bound PhoK showed 30 µg of U/µg of PhoK protein in the first round and 21 µg of U/µg of PhoK in the second round. In column studies, 220 µg U/ µg of PhoK was precipitated in the first round while 175 µg was precipitated in second round, which is approximately 8 fold higher per µg of PhoK than in the batch process. The precipitated U could be eluted out in 0.2 M carbonate – bicarbonate buffer with 80 % efficiency. However, in the third round negligible U was precipitated (8-9% only) possibly due to loss of activity of purified PhoK. Prolonged incubation of PhoK at room temperature in presence of U inhibited the activity of purified PhoK. When kept at room temperature for 24 h, activity of purified PhoK was reduced to 33±5%, while incubation in the presence of 1 mM U under GC2 reduced the activity of purified PhoK to 40-45%. These results suggest that though Ni-NTA based U precipitation exhibited impressive loading capacities, whole cells are superior in terms of actual application for effluent waste treatment, since purified enzyme is prone to inactivation at room temperature as well as to poisoning of activity by U.

Whole cells of *Deino-PhoK* were immobilized and tested for their U precipitation (input concentration 1 mM) in batch and column processes under GC2. Although, U loading was higher in column process (0.85 g U/g of dry biomass) as compared to batch process (0.5 g U/ g of dry biomass), the time required to achieve this loading was rather long. In flow-through process, 0.85 g U loading was achieved over 8 days of continuous flow of U

solution, while in batch process, 0.5 g U loading could be achieved within 4 h. Also, the potential of flow-through system appeared to be seriously limited due to clogging of the column by the precipitate formed. Thus the use of immobilized whole cells in batch process appears to be more appropriate for actual bioremediation of waste solutions and additionally, batch operation provides better control over the system processes, which is a priority while handling radioactive waste.

Chapter 6. Summary and Conclusions.

The salient findings of this study are summarized in the last chapter. The radioresistant bacterium *D. radiodurans* (*Deino-PhoK*) overexpressed an alkaline phosphatase PhoK, exhibited many fold higher phosphatase activity and precipitated U efficiently over wide range of metal concentration under ambient conditions even after exposure to high radiation environment. At low uranyl concentrations (1 mM), the strain precipitated >90% of U within 2 h efficiently. Maximal U loading capacity of around 10.7 g U/g of dry weight of cells was achieved at 10 mM U concentration under alkaline conditions. To enable use of single bacterium over a wide pH range, the *Deino-PhoNK* was constructed which could precipitate U as efficiently under both acidic and alkaline conditions, as the individual *Deino-PhoN* and *Deino-PhoK* strains.

TEM analysis revealed that the cell-bound or extracellular location of the uranyl phosphate precipitate was determined not by the nature of uranyl salt or enzyme or localization of the corresponding enzyme but by the uranyl species prevalent under particular geochemical condition (GC). The precipitate was cell surface associated under GC1, wherein U dissociates to form positively charged uranyl-hydroxide ions. In contrast, under GC2 U is precipitated extracellularly, when the negatively charged uranyl carbonate complexes predominate. Also, uranyl-hydroxide ions were adsorbed strongly on to the negatively charged bacterial cell surface resulting in cell-bound precipitation. In comparison, Uranyl

carbonate complexes were adsorbed poorly probably due to electroststatic repulsion by cell surface leading to extracellular precipitation. The higher toxicity of U under GC1 than in GC2 can, thus, also be attributed to the preferential adsorption of U under GC1 to cell surfaces.

Lyophilization provided a good value addition to phosphatase mediated bioremediation by increasing the shelf life of recombinants and making their handling and storage easier, while preserving their U precipitation capability. Immobilization of *Deino-PhoK* or *Deino-PhoNK* into calcium alginate beads facilitated the separation of extracellular precipitate entrapping the precipitate inside beads. Immobilization of PhoK on Ni-NTA matrix yielded impressively high loading capacities of U in a column based flow through system. But direct contact with U inhibited the enzyme activity *in vitro*, suggesting superiority of cell-based system over purified enzyme. In cell based immobilization studies, batch process was found to be more appropriate for application, over continuous flow-through column process.

References

1. Brim H, McFarlan SC, Fredrickson JK, Minton KW, Zhai M, et al. 2000. *Nature Biotechnology* 18: 85-90
2. Raj K, Prasad KK, Bansal NK. 2006. *Nuclear Engineering and Design* 236: 914-30
3. IAEA. 2002. *Management of low and intermediate level radioactive wastes with regard to their chemical toxicity. Rep. ISSN 1011–4289*, international atomic energy agency Austria
4. Newsome L, Morris K, Lloyd JR. 2014. *Chemical Geology* 363: 164-84
5. Malik A. 2004. *Environment International* 30: 261-78
6. M.F.AbdEl-Sabour. 2007. *Electronic journal of environmental, agriculture and food chemistry* 6 2009-13
7. Macaskie LE, Bonthrone KM, Yong P, Goddard DT. 2000. *Microbiology* 146: 1855-67
8. Macaskie LE, Jeong BC, Tolley MR. 1994. *FEMS Microbiology Reviews* 14: 351-67
9. Macaskie L, Jeong B, Tolley M. 1994. *FEMS Microbiology Reviews* 14: 351-68
10. Macaskie LE, Dean ACR. 1984. *Microbiology* 130: 53-62
11. Deng X, Yi X, Liu G. 2007. *Journal of hazardous materials* 139: 340-4
12. Yuan C, Lu X, Qin J, Rosen BP, Le XC. 2008. *Environmental Science & Technology* 42: 3201-6
13. Seetharam C, Soundarajan S, Udas AC, Rao AS, Apte SK. 2009. *Process Biochemistry* 44: 246-50
14. Daly MJ. 2000. *Current Opinion in Biotechnology* 11: 280-5
15. Prakash D, Gabani P, Chandel AK, Ronen Z, Singh OV. 2013. *Microbial Biotechnology* 6: 349-60
16. Battista JR. 1997. *Annu Rev Microbiol* 51: 203-24

17. Venkateswaran A, McFarlan SC, Ghosal D, Minton KW, Vasilenko A, et al. 2000. *Appl Environ Microbiol* 66: 2620-6
18. Lange CC, Wackett LP, Minton KW, Daly MJ. 1998. *Nature Biotechnology* 16: 929-33
19. Appukuttan D, Rao AS, Apte SK. 2006. *Applied and Environmental Microbiology* 72: 7873-8
20. Appukuttan D, Seetharam C, Padma N, Rao AS, Apte SK. 2011. *Journal of Biotechnology* 154: 285-90
21. Misra CS, Appukuttan D, Kantamreddi VSS, Rao AS, Apte SK. 2012. *Bioengineered Bugs* 3: 44-8
22. Zheng Z, Wan J, Song X, Tokunaga TK. 2006. *Colloids and Surfaces A: Physicochemical and Engineering Aspects* 274: 48-55
23. Nilgiriwala KS, Alahari A, Rao AS, Apte SK. 2008. *Applied and Environmental Microbiology* 74: 5516-23
24. Nilgiriwala KS, Bihani SC, Das A, Prashar V, Kumar M, et al. 2009. *Acta Crystallographica Section F: Structural Biology and Crystallization Communications* 65: 917-9
25. Markich SJ. 2002. *The Scientific World Journal* 2: 707-29

Signature of Student: Date:

S. No.	Name	Designation	Signature	Date
1.	Dr. J. S. Melo	Chairman		
2.	Dr. S. K. Apte	Guide / convener		
3.	Dr. Anand Ballal	co-guide/member		
4.	Dr. Celin Acharya	Member		

List of Figures

Chapter 1. Introduction

1.1 Distribution of aqueous U(VI) species as a function of pH as predicted by modelling program MINQEL 8

1.2 Different mechanisms of bacterial interactions with metals 10

1.3 TEM of typical tetrad of *Deinococcus radiodurans* 26

Chapter 3. Construction of recombinant *D. radiodurans* strains expressing acid/alkaline phosphatases for bioprecipitation of U

3.1 Schematic maps of plasmids (A) pRAD1 and pPN1, and (B) pEK2 52

3.2 Schematic representation of construction of pK1 plasmid 54

3.3 Histochemical screening of *E. coli* transformants on PDP-MG plate 54

3.4 Restriction digestion of plasmid pK1 isolated from *E. coli-PhoK* 55

3.5 Alignment of sequence of P_{groESL} + *phoK* from the database with the actual sequence obtained from *E. coli-PhoK* transformant 56

3.6 Screening of *Deinococcus* transformed with pK1 on histochemical plate 57

3.7 Qualitative affirmation of extracellular secretion of PhoK in recombinant *Deinococcus* strains 58

3.8 Colony PCR of recombinant *Deinococcus* transformants 59

3.9 Comparison of cell associated PhoK activity using *p*-NPP as substrate 60

3.10 Zymographic analysis and Western blotting of PhoK 62

3.11 Phosphatase activity as a function of growth in *E. coli-PhoK* 63

3.12 Phosphatase activity as a function of growth in *Deino-PhoK* 64

3.13 Zymogram analysis as a function of growth 65

3.14 Radioresistance of *Deino-PhoK* strain 66

3.15 Effect on cell associated PhoK activity after radiation stress 67

3.16 Uranl ion spectra in the presence or absence of MOPS 69

3.17 Kinetics of U precipitation by *Deino-PhoK* cells with two different substrates 71

3.18 U precipitation by *Deino-PhoK* cells at different input concentrations of substrate (β-GP) 72

3.19 Comparison of uranium bioprecipitation by *Deino-PhoK* and *Deino-PhoN* strains 73

3.20 U precipitation by *Deino-PhoK* cells at different input U concentrations 74

3.21 Post irradiation uranium precipitation ability of *Deino-PhoK* cells 76

3.22 Construction of plasmid pK2 79

3.23 Screening of *Deinococcus* carrying pK2 on histochemical plates 80
3.24 Zymogram analysis of protein extracts (20 µg) of recombinant *Deinococc*us strains 82
3.25 Western blotting and immune-detection with PhoK antiserum 82
3.26 Evaluation of U precipitation by *Deino-PhoNK* cells. 84

Chapter 4. Characterization and localization of uranyl phosphate, precipitated by recombinant strains

4.1 Scanning electron micrograph of *Deino-PhoN* or *Deino-pRAD1* cells after U precipitation 89
4.2 Identity of the precipitated uranium by *Deino-PhoK* cells 92
4.3 Qualitative affirmation of fluorescent property of uranyl phosphate 93
4.4 Fluorimetric analysis of bioprecipitation by *Deino-PhoK* cells 94
4.5 Localization of precipitate in *Deino-PhoK* cells after U precipitation under GC1 96
4.6 Localization of precipitate in *Deino-PhoN* cells after U precipitation under GC1 97
4.7 U precipitation by recombinant *Deinococcus* cells under GC1 (A) or GC2 (B) 101
4.8 Localization of U precipitate in recombinant *D. radiodurans* cells on reversing the U precipitation conditions 102
4.9 XRD analyses of uranyl phosphate after precipitation under GC1 or GC2 105
4.10 Fluorescence of uranyl phosphate precipitate under GC1 or GC2 105
4.11 Determination of uranyl phosphate precipitate localization in *E. coli* cells 106
4.12 Localization of U precipitate in recombinant *E. coli* cells after U precipitation 107
4.13 Localization of U precipitate *Deino-NK* cells after U precipitation under GC1 or GC2 109
4.14 Biosorption of U by *D. radiodurans* and *E. coli* 111
4.15 Uranium sensitivity of *D. radiodurans* and *E. coli* under GC1 or GC2 113
4.16 Uranium sensitivity of *D. radiodurans* and *E. coli* 114
4.17 Effect of U toxicity in *Deino-PhoNK* cells under precipitating conditions 115

Chapter 5. Uranium precipitation by lyophilized or immobilized recombinant strains

5.1 U precipitation by lyophilized *Deino-PhoK* cells 127
5.2 U Precipitation by lyophilized *Deino-PhoNK* cells under GC1 or GC2 129
5.3 U precipitation by immobilized *Deino-PhoK* cells 132
5.4 Qualitative affirmation of uranyl phosphate in beads 133
5.5 Spectrofluorimetric analysis of bioprecipitation by recombinant cells immobilized 134

in beads
5.6 U precipitation by immobilized *Deino-PhoNK* cells under GC2 136
5.7 Standardization of procedure for column studies 137
5.8 U precipitation by immobilised *Deino-PhoK* cells in column 138
5.9 Uranium precipitation by immobilized *Deino-PhoK* cells in continuous flow through system 139
5.10 Binding of PhoK on Ni^{+2}-NTA matrix 140
5.11 Zymogram analysis of immobilized PhoK 141
5.12 U bioprecipitation using PhoK immobilized on Ni^{+2}-NTA in batch process 143
5.13 U bioprecipitation using PhoK immobilized on Ni^{+2}-NTA in a column 145
5.14 Effect of U on PhoK activity 147

List of Tables

Chapter 2. Materials & Methods

2.1 Bacterial strains used in this study 32

2.2 Plasmids used in this study 34

2.3 Primers used in this study 35

2.4 Composition of polyacrylamide gels 37

2.5 Composition of reagents used for protein electrophoresis 38

Chapter 3. Construction of recombinant *D. radiodurans* strains expressing acid/alkaline phosphatases for bioprecipitation of uranium

3.1 Cell associated phosphatase activity of different recombinant strains 60

3.2 Activity of cells in terms of phosphate hydrolysis from substrate 61

3.3 U removal in biotic and abiotic controls 70

3.4 Effect of radiation and heavy metals on U precipitation ability of *Deino-PhoK* 77

3.5 Phosphatase activity of recombinant *Deinococcus* strains in terms of hydrolysis of β-GP 81

3.6 Comparison of uranium precipitation ability of various bacterial strains 86

Chapter 4. Characterization and localization of uranyl phosphate, precipitated by recombinant strains

4.1 U speciation in GC1 or GC2 as predicted by MINTEQ modelling 99

4.2 Cell associated activity (%) of PhoN/PhoK in *Deinococcus* 103

Chapter 5. Uranium precipitation by lyophilized or immobilized recombinant strains

5.1 Viability of lyophilized *Deino-PhoK* cells 125

5.2 Alkaline phosphatase activity of lyophilized *Deino-PhoK* cells 126

5.3 PhoN/PhoK activity of lyophilized *Deino-PhoNK* cells 128

5.4 *p*-NPP activity of *Deino-PhoK* cells after immobilization into beads 131

5.5 U removal (%) in control Ca-alginate beads under GC1 135

5.6 Activity of PhoK immobilized on Ni^{+2}-NTA matrix 141

5.7 Comparison of U precipitation in batch verses column process using immobilized PhoK protein 144

5.8 Activity of PhoK when stored at room temperate and at 4°C 146

Chapter 1

Introduction

Life on planet Earth is habitable due to its ambience and natural resources. We depend on these resources for food, energy, clean water etc., which not only make life possible but also drive the economy. Industrialisation and economic growth, though hallmark of civilization, have also created new problems of waste management. Effluents coming from many industries such as corrosion of water pipes, photography, electrolysis, mining, energy and fuel production, pesticide, iron and steel, fertilizer, leather, aerospace and nuclear industry installations etc. are the main sources that generate waste containing heavy metals [1]. Heavy metal pollution is one of the major environmental problems today. Most of heavy metal ions are toxic to living organisms. The non-degradable nature of these heavy metals makes them more difficult to remove, making them persist in the environment [2]. The removal and recovery of heavy metals from effluent streams is essential for the protection of the environment and human health. In recent years, nuclear energy is becoming an important part of worldwide energy production programs, due to its better sustainability [3]. This has increased the demand and search for newer sources of uranium which is the main fuel for nuclear reactors. Waste from the nuclear industry predominantly consists of radioactive or non-radioactive heavy metals like U, Cs, Sr, Pu, Am, Ni, Cd, Zn. Co, Pb etc. most of which are difficult to remove [4-5]. Among these, uranium (U) is the most commonly radioactive component present in nuclear waste.

1.1 Sources of Uranium in the environment

Uranium is a metal of high density (18.9 g/cm^3) with atomic number 92. The earth's crust contains an average of about 3 ppm (3 g/t) U, and seawater harbours approximately 3 ppb (3 mg/t) U. Naturally occurring U has three isotopes, all of which are radioactive: U-238, U-235, and U-234 [6]. An ore grade of 1% U_3O_8 is equivalent to 0.848% U, and 1 million lbs U_3O_8 are equivalent to 385 metric tonnes of U (http://www.wise-uranium.org/rup.html). The major demand for U is by commercial power generating facilities for use in fuel rods. U

supply is broadly classified into two categories-primary and secondary. Primary supply includes all newly mined and processed U [7]. Secondary supply includes high enriched U (HEU), natural and low enriched U (LEU), reprocessed uranium (Rep U) and depleted U (tails).

The U content of the ore is often low between only 0.1% and 0.2%. Therefore, large amounts of ore have to be mined to obtain U. The preliminary step in U processing comprises of conventional mining followed by acid/alkaline leaching [8]. Leaching is the process of dissolution of U containing minerals from the ore. A leaching liquid is pumped through drill-holes into underground U deposits, and the U bearing liquid is pumped out from below [6, 9]. The selection of leaching procedure for dissolving uranium minerals is dependent partly on the physical characteristics of the ore such as: type of mineralization, nature of other constituent minerals present etc. [10-12]. The risk of leaching liquid excursions beyond the U deposit and subsequent contamination of ground water is one of the major disadvantages of *in situ* leaching methods, which generate large quantities of dilute acidic or alkaline waste. After completion of the *in situ* leaching, the waste sludge must be dumped in a final deposit and the ore zone aquifer must be restored to pre-leaching conditions. While closing down a U mill, large amounts of radioactively contaminated scrap is produced, which has to be disposed in a safe manner [11].

Nuclear power is mainly produced in reactors fuelled with enriched uranium. In the enrichment process, for each kilogram of enriched uranium produced, an average of 8 kg of depleted uranium (range 5 to 10 kg) is also produced [7, 13]. Consequently, more than three quarters of the total uranium devoted to fuelling reactors is in the form of depleted U (or tails), and the accumulated stockpiles of tails represent a significant quantity of U. Whether the depleted U stockpiles represent a valuable energy source or a waste to be disposed of has been debated for three decades [7]. Uranium mill tailings are waste by-product of U mining

and milling. They are normally dumped as sludge in special ponds or piles, where they are abandoned [6]. Due to technical limitations, all of the U present in the ore can't be extracted. Therefore, the sludge also contains 5% to 10% of the U initially present in the ore. In addition, the sludge contains heavy metals and other contaminants such as arsenic, as well as chemical reagents used during the milling process. Radionuclides contained in U tailings emit 20 to 100 times as much gamma radiation as natural background levels on deposit surfaces. Gamma radiation levels decrease rapidly with distance from the pile [14].

India has consciously developed the three stage nuclear program to explore the possibility of tapping nuclear energy for the purpose of power generation. It has been targeted with the objectives of using two naturally occurring elements Uranium and Thorium having good potential to be utilized as fuel in Nuclear Power Reactors. Indian U ore deposits are of low grade and medium tonnage. The first U processing plant was commissioned in 1967 at Jaduguda by UCIL (Uranium Corporation of India limited). UCIL at present produces U through two process plants treating low grade U. The first one treats ore obtained from the East Singhbhum belt of India, is based on acid leaching process whereas the other plant, located in Tumallapalle, Andhra Pradesh, is based on the alkaline leaching process [12]. In both U ore processing operations, acid/alkaline waste is generated which needs to be disposed safely. Hence simultaneous research activities aimed at development of environment friendly technologies for waste treatment are very desirable.

1.2 Environmental impact of Uranium

The development of uranium attenuation processes is strongly dependent on the chemical behaviour of U in aqueous systems. Particularly, the determination of the reactive species of U in aqueous systems under various environmental conditions is of primary importance for the understanding of U removal from the waste. U and its decay products are hazardous because of their chemical toxicity as well [15-16]. Although ubiquitous in the

environment, U has no known metabolic function in animals and is currently regarded as non-essential [17]. Following ingestion, uranium rapidly appears in the bloodstream where it is associated primarily with the red cells; non- diffusible uranyl–albumin complex is formed in equilibrium with a diffusible ionic uranyl hydrogen carbonate complex in the plasma. Because of their high affinity for phosphate, carboxyl and hydroxyl groups, uranyl compounds readily combine with proteins and nucleotides to form stable complexes [17-18]. Clearance of U from the bloodstream is also rapid, and the U subsequently accumulates predominantly in the kidneys and the skeleton, whereas little is found in the liver [19]. The skeleton is the major site of U accumulation; the uranyl ion replaces calcium in the hydroxyapatite complex of bone crystals. It is reported that the long-term ingestion of U by humans may produce interference with kidney function at the elevated levels of U. The maximum permissible concentration of U metal in the kidney is 3 mg/kg of kidney (http://www.gulflink.osd.mil/du/index.html). Soluble U, which is absorbed in the blood, is eliminated rapidly through the kidney in urine. About 67% is excreted within the first day without being deposited in any organ. Approximately 11% is initially deposited in the kidney and excreted with a 15-day half-life. Most of the remaining 22% is deposited mainly in the bone and in other organs and tissues. The observed effects may represent a manifestation of sub-clinical toxicity, which will not necessarily lead to kidney failure or overt illness. It may however, be the first step in a series of progressive or irreversible renal injury resulting from the chronic intake of elevated levels of uranium over time [20-21].

The potential toxicity of U towards the microbial communities is poorly understood. Studies published till now have considered only few of the bacterial species such as *Thermoterrabacterium ferrireducens*, *Pseudomonas aeruginosa*, *Clostridium* sp. ATCC 53464 that can tolerate higher concentrations of U(VI) [22]. Although many studies have signified the uranium-bacterial interactions for U transport and its fate, the exact mechanism

of U toxicity in bacteria is yet to be elucidated. Recent studies have suggested that UO_2^{2+} is potential inhibitor of flavoproteins [23-24]. Therefore, knowledge of the distribution of U among its various physicochemical forms (i.e., speciation) is paramount to understanding the interaction of U with the cells and its biological effects.

1.3 Uranium –chemistry and speciation

Uranium occurs naturally in the +2, +3, +4, +5 and +6 valence states, but it is most commonly found in the hexavalent form. Tetravalent uranium U(IV) which is often present as uraninite mineral, U_3O_8, is reasonably stable but has very poor solubility. Hexavalent uranium U(VI) is commonly associated with oxygen as the uranyl ion; UO_2^{2+} is most reactive and soluble species [22]. The uranyl ion is linear $[O=U=O]^{2+}$ with strong covalent bonds between oxygen and U atoms which remain intact during the complexation reactions. The mobility of U in environment is mainly controlled by pH, oxidation-reduction reactions and complexation. U has strong tendency to form complexes with organic or inorganic ligands [25-26]. The uranyl ion is a hard acid and preferentially reacts with hard anions, particularly oxygen-containing ligands, and strongly hydrolyzes water [27].

$$x\,UO_2^{2+} + y\,H_2O \rightarrow (UO_2)_x(OH)_y^{2x-y} + y\,H^+ \qquad (1.1)$$

The aqueous chemistry of U(VI) is complex due to coordination and hydrolytic reactions. In aquatic systems, U occurs in a variety of physicochemical forms, including the free metal ion (U^{4+} or UO_2^{2+}) and complexes with inorganic ligands (e.g., uranyl carbonate or uranyl phosphate) [28]. U is present as U(VI) in oxic waters (pH 5 to 9). The free uranyl ion (UO_2^{2+}) is calculated to be the predominant species at pH $\leq$ 5, but starts to become insignificant as pH increases. The formation of UO_2OH^+ is of secondary importance to UO_2^{2+} at pH $\leq$ 5. The primary hydrolyzed species of UO_2^{2+} at typical groundwater concentrations and circumneutral pH are UO_2OH^+, $(UO_2)_2(OH)_2^{2+}$, $(UO_2)_3(OH)_5^+$, $UO_2(OH)_2^0$ and $UO_2(OH)_3^-$.

An increase in pH of the solution favours the formation of positively charged uranyl-hydroxide, $(UO_2)^3(OH)^{5+}$ or $(UO_2)^4(OH)^{7+}$complexes that are transformed to negatively charged ones at higher pH. Uranyl ion preferentially forms complexes with functional groups such as carboxylates, carbonyls, alcohols, and ammonia [27]. Complexes with multidentate ligands, such as CO_3^{2-}, tend to have greater stability than those with monodentate ligands. Uranyl carbonates are highly soluble and play a dominant role in the migration of U in neutral or alkaline groundwater [29]. In strongly alkaline conditions, negatively charged carbonato-uranyl complexes like $[UO_2(CO_3)_2]^{-2}$ and $UO_2(CO_3)_3]^{-4}$ are predominant [30-31]. Carbonate strongly binds to U. It occupies two coordinate positions in the major species $[UO_2(CO_3)_2]^{-2}$ and $[UO_2(CO_3)_3]^{-4}$ forming a highly stable four member ring with UO_2^{2+} and displaces other ligands, including hydroxyls at pH > 7 [32] (Fig. 1.1). These uranyl carbonate complexes are highly stable affecting the speciation of U(VI) and also prevent adsorption to some mineral surfaces. Carbonate exerts a strong influence on U(VI) speciation at circumneutral pH but plays as such less significant role in the speciation of U at lower pH because carbonate is primarily protonated below pH 6.

Phosphate in natural systems can control the mobility of U(VI) in groundwater and soils. Uranyl phosphates are widely distributed in nature with over 70 minerals identified with U:P stoichiometric ratios of 1:1 (autunite and meta-autunite groups), 3:2 (phosphuranylite group), and 1:2 (walpurgite group) [29, 33-34]. Some earlier studies showed that UO_2^{2+} or UO_2OH^+ are major bioavailable forms of U(VI). Uranyl complexes with carbonates or phosphates reduce the bioavailability of U by reducing activity of UO_2^{2+}. Such studies have potentially important implications for the protection of aquatic ecosystem and in developing bioremediation strategies.

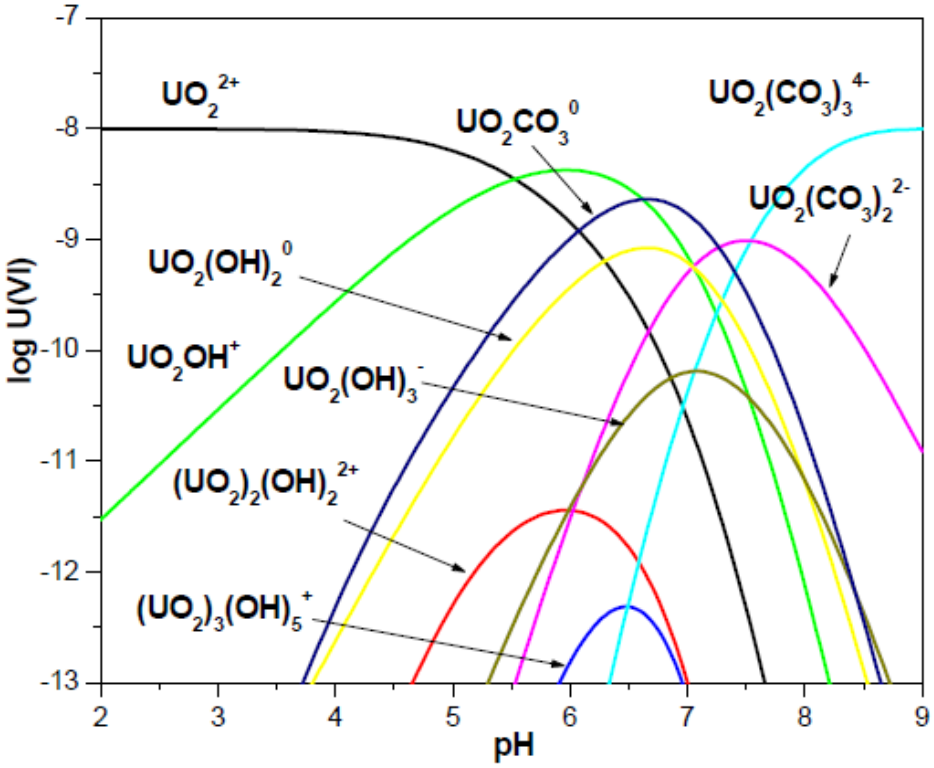

Fig. 1.1 Distribution of aqueous U(VI) [10^{-8} M]species as a function of pH as predicted by modelling program MINQEL (Source – Melanie J Beazley, 2009).

1.4 Microbial bioremediation of heavy metals and uranium

Metals constitute about 75% of the known elements; they are ubiquitous in the biosphere, and vital to our industry, infrastructure and daily life. The essential metals like Na, K, Mg, Ca, V, Mn, Fe, Co, Ni, Cu, Zn, Mo, etc. with known biological functions are required for enzyme catalysis, nutrient transport, protein structure, control of osmotic pressure [35]. Many heavy metals are required as micronutrients and act as cofactors in enzymatic processes and in metabolic pathways. However, when they are present in high concentration, they exert toxic effects in biological systems. Other metals, e.g. Cs, Al, Cd, Hg, Pb, etc. have no known essential metabolic functions but can all be accumulated [36]. Human activities associated with industrial-scale production of electrical components, fabrics, fertilizers, inks and dyes, mining, paints, paper, pesticides, pharmaceuticals, plastics etc. contribute to the degradation of surface-subsurface sediments and water quality. More than 1 million metric

tons of metal waste per year is predicted to be produced every year [37]. Lead (Pb), cadmium (Cd), and zinc (Zn) represent a subset of the most frequently reported metal contaminants in sediments and groundwater [37], thirteen trace metals and metalloids (Ag, As, Be, Cd, Cr, Cu, Hg, Ni, Pb, Sb, Se, Tl, Zn) are considered as priority pollutants [36].

Strategies for the remediation of metal and radionuclide contaminated soils or groundwater include physical, chemical (i.e., abiotic) and biologically mediated methods. Remediation techniques such as ion-exchange, chelation, oxidation and reduction, reverse osmosis, chemical precipitation, conditioning and disposal are practised as physico-chemical processes [38]. High reagent requirement, unpredictable metal ion removal are some disadvantages associated with such techniques. Further, many of the reagents used for desorption, are themselves pollutant which result in generation toxic sludge and secondary environmental pollution. Bioremediation involves minimizing the mobility of contaminants by transferring them to stable, non-labile phases using biological entities or microbe mediated processes. It uses microorganisms to reduce, eliminate, contain, or transform contaminants present in soils, sediments, water, and air [35].

Heavy metals need to be converted to less toxic form to remove them effectively. For a large area of contaminated soil and aquifer sediments, application of biological methods is appealing since it is much less disruptive to the ecosystem and hydrology, reduces the risk of worker's exposure during remediation and is typically less expensive than conventional technologies [38-39]. Microorganisms have evolved various measures to respond to heavy-metal stress (Fig. 1.2) via processes such as bioaccumulation [23, 40-41], biosorption to cell walls [42-45] and entrapment in extracellular capsules, precipitation [36, 46-47], complexation and bioreduction [48-51]. Microbes have proven capability to take up heavy metals from aqueous solutions, with varied range of metal concentrations in the effluent.

These factors have promoted extensive research on different bioremediation methods. However the focus of this study is limited to bioremediation of U using microbes.

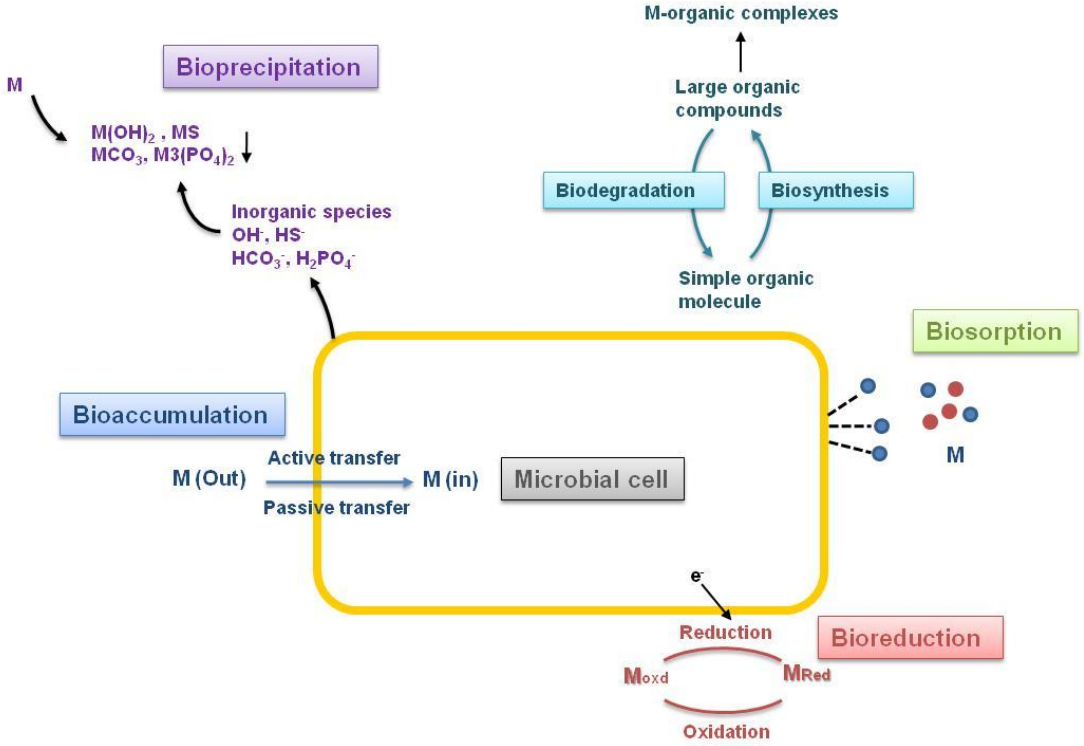

Fig. 1.2 Different mechanisms of bacterial interactions with metals (Source- Remaoudaki et al, 2007 [51]).

1.4.1 Biosorption

Biosorption is the metabolism independent, passive sorption of metal to the surface of living or dead biomass. It is a rapid phenomenon of metal sequestration which utilizes various natural materials of biological origin, including bacteria, fungi, yeast, algae, etc [1, 40]. When bacterial cell surface is in direct contact with the environment, the charged groups within the surface layers are able to interact with ions or charged molecules present in the external milieu. In both Gram-positive and Gram-negative bacteria cell envelopes possess an electronegative charge, which can attract metal cation to the cell surface [52-53]. Ligands in the cell wall such as carboxyl, amine, hydroxyl, phosphate and sulfhydryl groups bind metals through chemical sorption. Ability of microbial biomaterials to bind and concentrate heavy

metals from even the most dilute aqueous solutions, offers a technically feasible and economically attractive alternative [54]. Therefore, biosorption is perhaps best suited for treating effluents with low to medium metal concentrations because binding to cell wall is faster than uptake into the cell. Also cell bound metals can be eluted in appropriate solvents from a cell surface to regenerate the biosorbent. Dead biomass is often a better biosorbent as the effects of metal toxicity are not important. Microbial U biosorption in bacteria ranges from 45 to 615 mg g^{-1} cell dry weight [27, 40]. Low cost, high efficiency, minimization of chemical sludge, no additional nutrient requirement and regeneration of biosorbent are some advantages of biosorption. Use of algal biomass as biosorbent is emerging as an attractive method over use of other microbial cells. Algae have low nutrient requirements, being autotrophic they produce a large biomass, and unlike bacteria and fungi, they generally do not produce toxic substances [55]. Recently algae-silica preparation called Alga-SORB have been used as potential biosorbent for removal of Cu, As etc [56].

Although high biosorptive potential for several types of biomass have been reported, their strength in actual field application remains to be tested [38]. Despite the good potential for U removal, biosorption is unlikely to be useful in the context of U bioremediation. Problems associated with biosorption are that desorption from cell surfaces can be as rapid as sorption, and other cations compete for binding sites. Cell surfaces can also quickly become saturated, preventing further biosorption [40]. The potential for biological process improvement (e g. through genetic engineering of cells) is limited because cells are not metabolizing and it is a passive process and there is no potential for biologically altering the valency of metal state like in bioreduction [55]. Hence challenges for an adequate long-term solution for *in situ* bioremediation using alternative mechanisms still need to be explored.

1.4.2 Bioaccumulation

Bioaccumulation is defined as the uptake of toxicant by living cells and its transport into the cell [23, 38]. It is a growth and metabolism dependent process mediated by only living biomass. With certain metals, adventitious uptake may occur because the transported metals are similar to essential elements needed for cell functioning and are actively taken up into the cell [40]. Sometimes metals are sequestered intracellularly due to binding with specific components like metallothioneins or metal binding peptides [57]. The reactivity of cytosolic polyphosphates has been shown to facilitate intracellular sequestration of Cd, Cu, Hg, Pb, U, and Zn in naturally occurring archaeal and bacterial strains as well as genetically engineered bacterial strains [58-61]. Electron microscopy analyses of cells exposed to these elements demonstrated intracellular localization with phosphate-rich granules, suggesting that contaminant sequestration may be achieved by polyphosphates and may protect sensitive cytosolic molecules from oxidative damage. In addition to polyphosphate chelation of metals, an engineered *Pseudomonas aeruginosa* strain overexpressing the *ppk* gene (encoding polyphoaphate kinase) was shown to enhance intracellular polyphosphate concentrations when compared to the wild type strain [60] with enhanced the accumulation of U inside cells. Thus, polyphosphate metabolism that promotes intracellular sequestration of metals and radionuclides represents a good remediation approach [62]. However, bioaccumulation is prone to severe chemical toxicity for cellular activities. Also as metal gets accumulated within cell against a concentration gradient, higher amount of metal can't be removed from solutions.

1.4.3 Bioreduction

Bacteria can also immobilise certain heavy metals through their capacity to reduce elements to a lower redox state, a process called bioreduction. Reduction of an element from a higher to a lower oxidation state or to an elemental form affects its solubility, resulting in

precipitation, hence the process is also called as reductive biomineralization [38, 50]. In the absence of oxygen, bacteria are able to use different electron acceptors to gain energy for metabolism. Sulphate reducing bacteria (SRB) are anaerobic heterotrophs utilizing a range of organic substrates and SO^{2-} as a terminal electron acceptor. The sulphide produced from sulphate reduction in turn plays a major role in precipitating metals like Cu, Hg, Cd, As etc. as metal sulphides. Some metal sulphides like Co, Zn, Ni, Fe require more alkaline environment to ensure complete precipitation [63]. Metals or metalloids that form insoluble precipitates when reduced include Se(0), Cr(III), Tc(IV) and U(IV). A wide range of Archaea and bacteria are able to conserve energy though the reduction of Fe(III) (ferric iron) to Fe(II) (ferrous iron). Many of these organisms are also able to grow through the reduction of Mn(VI) to Mn(II) [41, 50].

Genes encoded by mercury resistance operon is a well-studied metal resistance system. Mercuric ion, Hg^{2+}, can be enzymatically reduced to metallic mercury by bacteria and fungi, which serves as a resistance and detoxification mechanism as Hg^0 is volatile [36, 41, 50]. Hg(II) is transported into the cell via the MerT transporter protein, and detoxified by reduction to relatively nontoxic volatile elemental mercury by an intracellular mercuric reductase (MerA). Some bacteria can use selenate (SeO_4^{-2}) as a terminal electron acceptor in dissimilatory reduction and incorporate Se into organic components, e.g. selenoproteins SeO_4^{-2} and selenite (SeO_3^{-2}) can be reduced to Se^0 [36]. Enzymatic reduction of plutonium, Pu(IV) to the more soluble Pu(III) under anaerobic conditions was demonstrated for *Geobacter metallireducens* GS-15 *and Shewanella oneidensis* MR-1 [64]. Tellurium (Te) may also be transformed by reduction and methylation. Reduction of tellurite (TeO_3^{-2}) to Te^0 by *Deinococcus radiodurans* has been reported recently [65].

Sulphur and sulphate reducing bacteria are particularly important in reductive precipitation of U(VI), Cr(VI), Tc(VII) and Pd(II) [36, 50, 66]. Anaerobically, hexavalent

U(VI) can be reduced to tetravalent U(IV) by a number of bacteria using either H_2 or one of a variety of organic electron donors [36]. Uranium bioreduction was first observed in the 1960s. However it only received attention after the work of Lovley *et al.* in the late 1980s [67]. The enzymatic reduction of soluble U(VI) to insoluble U(IV), as uraninite (UO_2(s)), under anaerobic conditions, is one of the most studied biological process of uranium immobilization [32]. *Desulfovibrio vulgaris* remains the only organism in which the enzyme system responsible for U(VI) reduction has been characterised in detail. Purified tetrahaem cytochrome C_3 was shown to function as a U(VI) reductase in vitro, in combination with hydrogenase, its physiological electron donor [68]. The most radiation resistant organism, *D. radiodurans* also has shown the potential to reduce U(VI) to U(IV) under anaerobic conditions [69].

Most research in the past decade has focused on understanding the bioreduction of U(VI) and on characterizing the stability of the reduced mineral product, with the overall objective of developing an *in situ* bioremediation approach [70]. Uranium bioreduction has been demonstrated in field experiments (*in situ*) in the USA [71-72]. Two types of environment have been targeted, (1) subsurface sediments at the US DOE Field Research Centre (FRC) in Oak Ridge, Tennessee (http://www.esd.ornl.gov/nabirfrc) (2) investigations on removal of uranium from contaminated groundwater at a 'Uranium Mill Tailings Remedial Action' or 'UMTRA' site in Rifle, Colorado. The approach adopted was in *situ* stimulation of dissimilatory metal-reducing bacteria, through the injection of the electron donor acetate into the subsurface [73-74].

Maintaining low U(VI) concentrations in groundwater over long periods of time may require a repeated supply of electron donor. Numerous factors determine whether bioreduction will be successful or not, from the presence of a suitable electron donor, to competition from other processes such as nitrate and sulphate reduction. Environmental

conditions also control the composition of the microbial community and population dynamics. The long-term stability of the mineral phases formed is crucial to the success of bioreduction; the more insoluble a mineral is, the less likely it will be remobilised. Uraninite is rapidly oxidized to the more mobile and reactive uranyl ion in oxic conditions. It is also chemically oxidised by Mn oxides, ferrihydrite, and under nitrate reducing conditions by nitrite or reactive Fe(III) oxy-hydroxides [70]. Also, it is important to avoid clogging of the injection well and aquifer through biomass growth or excess mineral precipitation. Therefore, in spite of being mostly studied mechanism in U bioremediation, some issues still need to be addressed to make it successful at field levels.

1.4.4 Biomineralization

The non-reductive biomineralization of metals is the formation of metal precipitates due to interaction with ligands such as carbonates, phosphates, hydroxides etc. generated by microbes. Microbes release metal complexing agents or certain metabolites in localised conditions near cell surface, which then precipitate metals externally as phosphates, hydroxides, carbonates etc. The nature of the resultant precipitate may depend on the nature of the cell surface, the cellular microenvironment, and the presence of reactive anions [75]. Precipitation, nucleation and deposition of crystalline material on or within cell walls are influenced by factors such as pH and cell wall composition. Most biominerals are calcium carbonates, silicates, iron oxides or sulphides. Biomineralization is itself an important interdisciplinary research area, and one that overlaps closely with geomicrobiology [36].

Among carbonates, mostly mineralised species are Ca and Mg carbonates. Carbonate precipitates are found in association with bacterial biofilms. Certain green, brown and red algae deposit calcium carbonate as cell-surface structures, while some protozoa (Foraminifera) use it for shells [76]. The range of composition and crystallization of carbonate precipitates produced by microbial communities is influenced by environmental

conditions and community species composition. Microbially produced extracellular polymeric substances provide a template for carbonate nucleation. Insoluble carbonates are formed as the result of organic and inorganic acid formation due to microbial metabolic activity. Bacteria can precipitate and deposit Fe(III) oxides and hydroxides (e.g. FeOOH, Fe_3O_4) around their cells by enzymatic, e.g. *Gallionella* sp., and non-enzymatic processes, e.g. *Leptothrix* sp [36].

Bioprecipitation by both sulphides and phosphates has been investigated because of the low solubility of many of their metal complexes. Release of phosphate via the hydrolysis of an organic phosphate has been shown to be an effective method for precipitation of metals, as insoluble metal phosphates [47, 77]. Phosphatase mediated precipitation of metals have been studied for metals like Cd, Cu, Pb, U, Am, Pu and Zn [46-47, 77]. In addition, metal precipitation by secreted phosphate generated from polyphosphate hydrolysis has been suggested as a mechanism to remove metals and actinides from aqueous waste streams. *Acinetobacter johnsonii* was effective in removing lanthanum from solution [78-79]. In the context of bioremediation, precipitation of metal species by reduction is generally limited to anaerobic processes and is ineffective against single-oxidation-state metals. Precipitation by other means has the advantage of producing chemically stable forms of metal, and its use is not limited to reducible metals. The importance of biomineralization in the sequestration of inorganic pollutants is obvious, especially at field sites where the metabolic activity of microorganisms can be artificially stimulated for bioremediation purposes. A group of studies have shown that the secretion of phosphate groups due to phosphatase activity can induce a significant immobilization of uranium in the form of autunite at acidic and alkaline pH [32, 80-81]. Thus the non-reductive biomineralization of U(VI) provides a promising new approach for *in situ* uranium bioremediation [32].

1.5 Phosphatase mediated bioprecipitation of heavy metals - A preferred approach for bioremediation

Phosphatases are enzymes that cleave the phosphate group from phosphoric acid monoesters into a phosphate ion and an alcohol. The action is opposite to that of phosphorylases and kinases, which attach phosphate group to their substrates by using energy molecules like ATP. Enzymatic bioprecipitation of metals is the process in which intrinsically produced phosphatases (by microbes) hydrolyse organic phosphate substrates and release inorganic phosphate which then interacts with metal in the solution to precipitate it as metal phosphate. According to metal chemistry, the concentration of residual free metal at equilibrium is governed by solubility product of metal complexes, that varies from 10^{-30} to 10^{-20}. Most of the metal can be removed from solution if provided with excess of ligand through chemical precipitation. Advantage of enzyme based bioprecipitation is generation of metal desolubilizing ligands on a continuous basis with the deposition of metal-ligand complexes on the external surface of the cell [46, 82]. This is much more advantageous than direct addition of ligand to the solution as in the previous case, metal precipitation will occur only when metal-ligand solubility product exceeds in the micro-environment near cells. The ligand is locally produced in high concentration, in juxtaposition to cellular components making judicious use of ligand in precipitating metal. Also, for very dilute metal solutions large quantities of ligands are required, generating secondary pollution due to excessive ligand addition [32, 80].

Early work of phosphatase mediated biomineralization of metals and radionuclides focused on the acid phosphatase activity of *Serratia* sp. NCIMB 40259 (formerly *Citrobacter* species) by Macaskie et al [46-47, 77]. Bioprecipitation is an aerobic process, which is neither limited by the finite sorption capacities nor by intracellular metal toxicity due to accumulation of metal inside cells. Also as metal is deposited in an altered chemical state,

they are less sensitive to spontaneous desorption. U(VI) forms highly insoluble phosphate minerals with a 1:1 stoichiometry at a wide range of pH [83]. These minerals comprise of the members of autunite/meta-autunite group, including calcium autunite [$Ca(UO_2)_2(PO_4)_2$], chernikovite [$H_2(UO_2)_2(PO_4)_2$], sale´eite [$Mg(UO_2)_2(PO_4)_2$], and ankoleite [$K_2(UO_2)_2(PO_4)_2$], and remain stable for long periods of time, suggesting that uranyl phosphates may provide a long-term sink for uranium in contaminated environments [70]. In bioprecipitation, high loading capacities can be obtained, e.g. *Citrobacter* sp. has shown a U loading of 9 g/g bacterial dry biomass in continuous flow through process [47]. Moreover, generation of inorganic phosphate for bioprecipitation is a single enzyme mediated process and therefore, is more amenable to genetic manipulation [77]. Finally, organophosphates commonly found in soils, such as phytate, which is ubiquitous plant waste or TBP which is another waste product generated during U processing, may provide substrate for phosphate to immobilize uranium via U–P bioprecipitation [84-85]. Hence enzymatic bioprecipitation of metal is more promising approach over other aspects of bioremediation.

1.6 Bacterial phosphatases

Inorganic and organic phosphates which comprise of orthophosphates, pyrophosphates, nucleotides, sugar phosphates etc. are essential for living organisms. Phosphatases are ubiquitous among prokaryotes and eukaryotes that catalyse the dephosphorylation of various substrates by hydrolysis of phosphoester or phosphoanhydride bonds [86-87]. Phosphatases play a crucial role in supporting microbial nutrition by releasing assimilable phosphate from organic source. Phosphatases are either secreted outside the plasma membrane, where they are released in a soluble form or retained as membrane-bound proteins. These secreted phosphatases are believed to function essentially in scavenging organic phosphoester (such as nucleotides, sugar phosphates and phytic acid) that can't cross the cytoplasmic membrane. Thus inorganic phosphate (P_i) and organic by-products are

released, that can be transported across the membrane, providing the cell with essential nutrients. Some secreted phosphatases have evolved specialized functions relevant to microbial virulence [88-89], whilst other phosphatases are found in the cytosolic compartment where they may be involved in dephosphorylating reactions occurring in signal transduction as well as in several metabolic pathways [90]. In general phosphatases hydrolyze phosphate monoesters as shown in the scheme below [91].

Traditionally, phosphatases are broadly categorised as acid and alkaline phosphatases based on the optimum pH required for their activity. Classification was initially based on the functional and biophysical properties of the phosphatases. With the advent of molecular sequence data, attempts to group phosphatases into molecular families on the basis of amino acid sequence similarity were carried out. The structural criterion has led to the definition of various molecular families of phosphatases for which signature sequence motifs have been defined [91-92]. Current knowledge on bacterial phosphatases is, however, far from complete. Most of the available information is derived from studies performed in the enterobacteriacea family [93] and information on phosphatases of other bacterial species is limited. The study of microbial phosphatases, therefore, remains an active investigational field, with relevance to various aspects of microbial physiology and biotechnology. The interest in bacterial phosphatases is, however, not only related to their multiple roles in the biology of the prokaryotic cell or to their involvement in microbial pathogenecity, but also to the possibility of exploiting these enzymes as investigative tools in regulation of gene expression and for bioremediation in environmental microbiology [77, 94].

1.6.1 Acid phosphatases

Bacterial non-specific acid phosphatases (NSAPs) (EC 3.1.1.2) are enzymes that function as soluble periplasmic proteins or retained as membrane bound proteins [87]. NSAPs are found to be widely distributed among many Gram positive or Gram negative bacterial species. They exhibit optimal catalytic activity at acidic to neutral pH values [91]. NSAPs have been classified into three distinct molecular families (Class A, B and C) based on amino acid sequence relatedness. Class A NSAPs are secreted monomeric to oligomeric proteins containing a polypeptide component of approximately 25-27 kDa [91, 95]. This class of enzymes has been isolated from *Zymomonas mobilis* (PhoC-Zm) [96], *Salmonella typhimurium* (PhoN) [97], *Morganella morganii* (PhoC) [98] and other bacteria. The *Zymomonas mobilis* PhoC-Zm enzyme represents the major P_i- irrepressible acid phosphatse and was the first Class A enzyme to be sequenced [96]. Class B NSAPs are secreted as homotetrameric metallo-proteins containing a 25-30 kDa polypeptide component [91, 99] that are completely unrelated to class A enzymes at the sequence level. The *Salmonella enterica* AphA-Se enzyme was the first class B NSAP purified and characterized in detail [99-100]. Class C NSAPs are secreted as bacterial lipoproteins that contain a polypeptide component with a molecular mass of approximately 30 kDa and share conserved sequence motifs [91]. At the sequence level Class C appear to be related, although distantly, to Class B NSAPs and also a few plant acid phosphophydrolases. This represents the first example of family bacterial NSAPs that has a relatively close eukaryotic counterpart. The first identified Class C enzyme was OlpA enzyme of *Chryseobacterium meningosepticum* [101]. Du Plessis *et al* reported characterization of another class C NSAP, from *Staphylococcus aureus* strain [86]. All the three classes contain conserved signature sequence motifs. There is also a completely new class of acid phosphatases termed as purple acid phosphatases (PAPs) that comprise a family of binuclear metal containing hydrolases, which have been isolated from

plants, mammals and fungi mostly. Enzymes isolated from mammalian source have shown to have a role in iron transport. In bacteria, PAPs may be restricted to a small number of organisms and help in aiding virulence. In *M. tuberculosis*, PAP may assist the pathogen's survival by reducing the respiratory burst of its host and/or removing potentially lethal free radicals, as purple acid phosphatase can remove reactive oxygen species in a Fenton like reaction [102].

1.6.2 Alkaline Phosphatases

Alkaline phosphatase (AP) (EC.3.1.3.1), a hydrolase enzyme functioning at alkaline pH and is ubiquitously distributed and highly conserved in bacteria, archaea, yeast, plants and mammalian cells [103]. The active AP hydrolyzes phosphates from many types of molecules like nucleotides, proteins, alkaloids, phosphate esters and anhydrides of phosphoric acid. APs play an indispensable role in phosphate metabolism, signal transduction, virulence and production of AP is regulated by the phosphoester compounds available in the environment [103]. Divalent metal ions are required for the activity of APs while chelators such as EDTA inhibit their activity. With few exceptions, APs are homodimeric enzymes and each catalytic site contains three metal ions, i.e., two Zn and one Mg, necessary for enzymatic activity [104].

While the main features of the catalytic mechanism are conserved comparing mammalian and bacterial APs, mammalian APs have higher specific activity and K_m values. They have a more alkaline pH optimum; display lower heat stability; are membrane-bound and are inhibited by L-amino acids and peptides through an uncompetitive mechanism. Studies on bacterial alkaline phosphatases are less focused even though several APs have been investigated from microorganisms [103]. Alkaline phosphatase of *Escherichia coli* is the most studied prokaryotic AP [105-106]. Bradshaw *et al*. determined the complete amino acid sequence of alkaline phosphatase monomer of *E. coli* [107]. Biosynthesis, structure and

catalytic properties of *E. coli* alkaline phosphatase have been extensively studied [108]. Alkaline phosphatases having high thermo-stability were described from different strains of bacteria such as, *Thermus thermophilus* [109], *Thermus caldophilus* [110], *Bacillus stearothermophilus* [111], *Bacillus licheniformis* [112] etc. Recently a novel alkaline phosphatase, PhoK, from *Sphingomonas* sp. has been characterized from our laboratory and its x-ray crystallographic structure was elucidated [113-115]. The specific activity of PhoK is significantly higher as compared to other bacterial APs, and requires Ca^{+2} and Zn^{+2} for its activity, whereas Mg^{+2} has no effect on its activity unlike *E. coli* AP [115]**.**

The expression of AP in bacteria is regulated in complex ways. Characterization of Pho regulon, especially the discovery of promoter was a major breakthrough [105]. Most APs are induced by P_i limitation and their kinetics of de-repression is well studied in various organisms. In *E. coli* around 90 proteins are synthesized at an increased rate during P_i starvation and synthesis of proteins under normal condition is regulated by phoB-phoR operon [108, 116]. In *Bacillus*, the two component signal transduction system involves PhoP and PhoR for regulation of gene expression in response to phosphate starvation [117]. AP is reported to be induced by starvation of pyrimidines or guanine in presence of excess phosphate. Hence, AP is induced not only by lowering of the internal orthophosphate pool, but also due to changes in the levels of nucleotide pool in the cell [118]. APs are part of a super-family which include nucleotide phosphodiesterases (NPP), co-factor independent phosphoglycerate mutases (iPGM), phosphonate monoester hydrolases (PMH) and aryl sulfatases (AS). All these are metalloenzymes, but the number and nature of metal ions required is widely different within the AP super-family [115].

Alkaline phosphatases are critical in cellular signalling and there is fine tuning of AP levels in cells for signal transduction cascade to function efficiently. APs appear to be very promising for future technologies in molecular biology. Due to its catalytic ability with

various chromogenic substrates, APs form key components of molecular techniques. The applications of APs in diverse areas such as molecular biology, immunology, diagnostics and dairy technology have been well documented [103].

1.7 Phosphatase mediated bioremediation of uranium to date

One of the best documented examples using phosphatase mediated bioprecipitation is that of *Citrobacter* strain (renamed as *Serratia* sp. NCIMB 40259) isolated from polluted soil and was shown to precipitate heavy metals like Cd, U, Pu, Am etc as cell bound metal phosphates [46-47, 77, 82, 119]. When supplied with glycerol-2-phosphate, the cellular phosphatse activity cleaved the organic phosphate to release inorganic phosphate, which precipitated U(VI) as uranyl hydrogen phosphate minerals. The efficiency of metal removal depends on P_i liberation and the solubility product of metal phosphate. Additionally, biofilms of *Serratia* sp. NCIMB 40259 that promoted the precipitation of $H_2(UO_2)_2(PO_4)_2$ (chernikovite) further removed 85% and 97% of co-occurring ^{60}Co and ^{137}Cs, respectively, via substitution of H^+ within chernikovite [120]. The *Citrobacter* acid phosphatase was subsequently characterized and was found to have a significant homology with the PhoN of *Salmonella*. The recombinant *E. coli* expressing multiple copies of PhoN from *Salmonella* sp. was reported to precipitate heavy metals more efficiently than wild type *Citrobacter* [94]. The phosphatase enzyme remained functional in resting cells, facilitating the use of pre-grown cells. Recently, PhoN from *Salmonella typhimurium* was cloned and overexpressed in *E. coli* and *D. radiodurans* in our laboratory and these engineered strains were used for the removal of cadmium and uranium from acidic-neutral solutions [121-123]. Naturally occurring bacterial strains like *Arthrobacter*, *Bacillus*, and *Rahnella* showing intrinsic phosphatase activity were isolated from metal contaminated soils of Oak Ridge Field Research Centre (ORFRC) site and were found to precipitate ~ 200 µM U from synthetic groundwater [124]. Thomas and Macaskie showed that by employing a phosphatase-

mediated bioprecipitation approach using *Pseudomonas*, two types of wastes i.e. TBP-containing and heavy metal-containing, can be simultaneously targeted [40, 85]. Another approach is to stimulate phosphatase activity of native microorganisms in subsurface area by injecting glycerol phosphate as the sole carbon and phosphorous source and to precipitate uranium at acidic pH (5.5) [70]. These studies demonstrated the potential for *in situ* bioremediation of uranyl phosphate as a result of microbial phosphatase activity through the introduction of an organophosphate source [125]. The stability of metal phosphates over a broad pH range provides an ideal insoluble phase for long term contaminant sequestration within the subsurface environment. Another two-stage system utilized *P. aeruginosa*, chosen for its metal tolerance and ability to accumulate large amounts of polyphosphates. Metal binding occurred after the degradation of the polyphosphate and concomitant release of phosphate from the cells [60]. Recently two bacterial strains, *Bacillus sphaericus* JG-7B and *Sphingomonas* sp. S15-S1 both recovered from extreme environments, were reported to bioprecipitate U at from pH 2-4.5 in the absence of externally supplied organophosphate substrate due to their intrinsic phosphatase activity [126]. Although, U bioprecipitation from acidic to neutral conditions has received considerable attention, bioprecipitation of U from alkaline waste remains relatively unexplored so far. Precipitation of U(VI) as uranyl phosphate from alkaline solution is rather difficult on account of extremely high solubility of uranyl carbonate complexes at basic pH. Precipitation is feasible only at log (PO_4^{-3}/CO_3^{-2}) values of > -3 [127]. While it is chemically difficult to achieve a favourable (PO_4^{-3}/CO_3^{-2}) ratio, an active enzymatic process can generate a high localized concentration of inorganic phosphate for precipitation. Recently, our laboratory identified a novel alkaline phosphatase enzyme, PhoK, having very high specific activity from a *Sphingomonas* sp. [35-37]. This *Sphingomonas* strain could precipitate uranium, albeit with a low efficiency, under alkaline conditions indicating that the required (PO_4^{-3}/CO_3^{-2}) ratio for U precipitation could be

achieved by this enzyme. In view of these earlier reports, more detailed studies on bioprecipitation from acidic-neutral or alkaline conditions were targeted in this study.

1.8 *Deinococcus radiodurans*- A promising candidate for uranium bioremediation from high radiation environment

Microbial genes can be efficiently expressed into suitable hosts and these genetically engineered microbes can be employed for bioremediation of heavy metals. Numerous organisms have the ability to degrade, detoxify, transform or immobilise pollutants, metals as described in previous sections. However, radiosensitivity of microbes e.g. *Citrobacter*, *E. coli*, *Pseudomonas*, *Sphingomonas* often limits their bioremediation capabilities in radioactive waste. Radiation resistant bacteria which can remediate these metals are better choices to address these wastes [128-129]. Bacteria belonging to the family *Deinococcaceae* have become more popular for the use in bioremediation due to their high level of tolerance to ionizing radiation, ultraviolet radiation, oxidising agents, desiccations, mutagenic agents etc. [130-131]. Both *Deinococcus* and *Thermus* genera belong to one phylum containing the unusual amino acid ornithine, that forms the cross bridging component of peptidoglycan layer which is the signature of these genera. Out of 47 species of *Deinococcus* genus, *D. radiodurans* R1 (American type culture collection 13939) and SARK (ATCC 35073) are the best studied (https://en.wikipedia.org/wiki/Deinococcus). The bacterium *D. radiodurans* is an ancient Gram positive, aerobic, vegetative, non-pathogenic organism which was identified in 1956 as a contaminant of heavily irradiated food [131]. *D. radiodurans* tends to grow as tetrads in culture and occasionally as dyads (Fig 1.3).

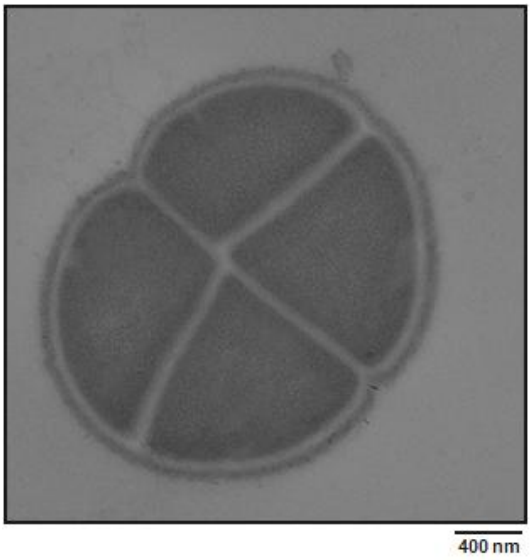

Fig. 1.3. TEM of typical tetrad of *Deinococcus radiodurans*. (Source - This study).

It has been reported to survive up to 1.5 MRad of ionizing radiation and up to 100 double strand breaks without mutagenesis [130]. For comparison, radiation tolerance of this organism is about 3000 times more than that tolerated by human cells [132]. It stains Gram positive but has complicated layered wall typical of Gram negative character, the inner membrane, the unusual thick peptidoglycan layer, an outer membrane and a surface layers (S-layer) of protein consisting of hexagonally symmetric units [133-134].

The tolerance of *D. radiodurans* to so many stresses has been attributed to phenomenal efficiency of DNA repair, chromosomal alignment, morphology facilitating torroid genome structure and high concentration of Mn^{+2} complexes which protect proteins during oxidative stress [131]. Combining the high radiation resistance with its non-pathogenic, non-sporulating phenotype, *D. radiodurans* has been positioned as safe candidate for development of microbiological treatment of waste. The whole genome sequence of this organism made it more feasible for genetic manipulations [135]. Strategies involving both chromosomal integration as well as vector based expression of foreign genes in trans have proved effective in this organism [136].

Bioremediation using *D. radiodurans* began in 1997, with the demonstration of its ability to grow in the presence of ionizing radiation at 60 Gy/h comparable to most DOE radioactive waste sites [137]. Genes coding for toluene deoxygenase from *Pseudomonas putida* were functionally expressed in *D. radiodurans* to produce recombinant strain which could oxidise toluene, chlorobenzene, indole etc. *Deinococcus*, engineered to degrade toluene, was also able to facilitate Cr (VI) reduction under radioactive conditions [138]. *D. radiodurans* was also engineered with mercury detoxifying genes (mer operon from *E. coli*) and these recombinant strains were shown to reduce highly toxic mercury ion Hg(II) to less toxic elemental Hg(0) [2]. Under anaerobic conditions, *D. radiodurans* reduced Fe(III)-nitrilotriacetic acid, coupled to oxidation of lactate to CO_2 and acetate. It also reduced U(VI) and Cr(VI) in presence of AQDS (anthraquinone,2-6-disulphonate) [69]. Recently *D. radiodurans* was also shown to degrade DBP (Di-*n*- butyl phalate) and could survive in activated sludge waste for 7 days [139]. Di-n-butyl phthalate (DBP) is a group of phthalate esters (PAEs) that are widely used in cosmetics, perfumes, and plasticizers and have been classified as endocrine disruptor by most countries. In another study from our laboratory, *phoN* gene encoding a NSAP was cloned in *D. radiodurans* under strong deinococcal promoter, P_{groESL}. Nearly, 90% of 1 mM U could be precipitated from acidic-neutral solutions in 6 h by recombinant strain (*Deino-PhoN*). Further *Deino-PhoN* could bring about metal precipitation even after 6 kGy gamma radiation, while corresponding *E. coli* failed to do so [121]. In batch process, *Deino-PhoN* cells could precipitate uranium from a concentration range of (0.5-20 mM) resulting in maximum loading of 5.7 g U/g dry weight of cells at 20 mM input concentration in 17 days [122].

1.9 This Study

As mentioned earlier, U bioremediation from acidic to neutral conditions has received considerable attention, but bioremediation of U from alkaline waste remains

relatively unexplored so far. To perform bioremediation of U(VI) in alkaline solutions, studies were initiated in our research group. A *Sphingomonas* strain producing novel and highly active alkaline phosphatase, PhoK, was isolated in our laboratory. The corresponding gene was cloned and over expressed in *E. coli* [113]. But bioremediation of nuclear waste using recombinant *E. coli* or naturally occurring bacteria limits their usage for radioactive waste, due to their radiosensitivity. Earlier studies have shown the potential of *D. radiodurans* in bioremediation studies (section 1.8 above). In view of this, *D. radiodurans* appears to be promising candidate for further exploration of bioremediation of alkaline waste. Studies in this thesis are focused on cloning of the *phoK* gene in *D. radiodurans* and examining the bioremediation abilities of the recombinant strains. It would be extremely beneficial if both alkaline and acidic waste, containing U could be bioremediated by single microbe. This study therefore proposes engineering of bacterium that can perform bioprecipitation from both alkaline and acidic waste by pyramiding PhoN (acid phosphatase as well as PhoK (alkaline phosphatse) in single microbe. Further, in terms of biotechnological applications, stabilisation of biomass by lyophilization, immobilisation is also attempted. The specific objectives of this study are:

1. Cloning of *phoK* gene from *Sphingomonas* into *E. coli-D. radiodurans* shuttle vector and to ascertain its expression in *E. coli* and *D. radiodurans.*
2. Optimization of PhoK expression, activity and uranium precipitation by recombinant strain under ambient and high radiation environment.
3. Lyophilization of *D. radiodurans* cells expressing PhoK to preserve their uranium precipitation ability and to extend shelf life.
4. Comparison of uranium precipitation in a batch versus continuous-flow process.
5. Construction of recombinant *D. radiodurans* co-expressing both acid and alkaline phosphatase and evaluating its U precipitation ability.

The work carried out is described in following chapters.

Chapter 2. Materials and methods

It outlines the bacterial strains and culture media used, different experimental conditions, protocols used for cloning, biochemical assays, U precipitation, characterization of precipitate, lyophilisation, immobilization of cells etc.

Chapter 3. Construction of recombinant *D. radiodurans* strains – Expressing Acid/alkaline phosphatase and evaluation of U precipitation.

This chapter describes construction of recombinant *D. radiodurans* strains expressing alkaline phosphatase, or co-expressing both acid and alkaline phosphatse with evaluation of their U precipitation ability.

Chapter 4. Localization and characterization of uranyl phosphate precipitated by recombinant strains.

This chapter describes characterization of precipitated U by using different techniques, precipitate localization studies and factors governing the location of precipitate.

Chapter 5. Uranium precipitation by lyophilized or immobilized recombinant *Deinococcus* strains.

This chapter describes use of *Deinococcus* strains in terms of application. For this, lyophilisation and immobilisation was carried out and U precipitation was evaluated in batch/column processes using these cells.

Chapter 6- Summary and Conclusions.

This chapter summarizes all the major findings of the study.

Chapter 2

Materials and Methods

This chapter describes in detail the materials used in various experiments and details of the methods used to address the specific objectives of the current study. Growth media and culture conditions for various organisms including screening of recombinant organisms; the recombinant DNA techniques involved in gene cloning; extraction, electrophoretic resolution and immune-detection of proteins; *in vitro* and *in vivo* phosphatase activity measurements, protocols used for U precipitation studies and for characterization of precipitated U by X-ray diffraction and electron microscopy are detailed in this chapter. Protocols used for lyophilization and immobilisation of cells and PhoK enzyme and their use for U precipitation are also presented.

2.1 Bacterial strains, growth media and culture conditions.

E. coli cells were grown aerobically in Luria–Bertani (LB) growth medium (1% Bacto-Tryptone, 0.5% NaCl, and 0.5% yeast extract, pH 7.2) at 37°C under agitation (150 rpm) unless otherwise specified. *D. radiodurans* strain R1 was routinely grown aerobically in TGY (1% Bacto-Tryptone, 0.1% glucose, and 0.5% yeast extract, pH 7) liquid medium at 32°C under agitation (150 rpm).

Bacterial growth was assessed by measuring turbidity (OD_{600nm}) of liquid cultures or by determining colony forming units (CFUs) on appropriate agar plates (1.5% Bacto Agar). The antibiotic concentration used for selection of *E. coli* transformants was 100 µg/ml of Carbenicillin for recombinants carrying pRAD1 [140] based constructs, or 50 µg/ml of Kanamycin and 33 µg/ml of Chloramphenicol for pET29b based constructs. For *D. radiodurans*, growth medium was supplemented with 3 µg/ml chloramphenicol for pRAD1 based constructs. The different bacterial strains used in this study are described in Table 2.1

Table 2.1. Bacterial strains used in this study

Strain	Characteristics	Source/Reference
E. coli JM109	F' *traD36 proA$^+$B$^+$ lacI^q Δ(lacZ)M15/ Δ(lac-proAB) mcrB$^+$ glnV44 e14$^-$ gyrA96 recA1 relA1 endA1 thi hsdR17($r_k^-m_k^+$)*	Lab collection
E. coli DH5α	F' *recA41 endA1 gyrA96 thi-1 hsdr17*(r^{K-} m^{K+}) *supE44 relAλ lacU169*	Lab collection
E. coli BL21 (DE3) pLysS	(F' *ompT gal dcm lon hsdSB(rB- mB-) λ(DE3) pLysS(cmR)*	Lab collection
EK2	*E. coli* DH5α containing a 3-kb PstI-BglII fragment from BSAR-1 in PstI/BamHI sites of the pBluescriptII SK(-) vector	[113]
EK4	*E. coli* (BL21)(DE3) containing complete *phoK* gene in pET29b vector	[113]
E. coli-PhoN	*E. coli* DH5α containing plasmid pPN1 (*phoN* ORF, gene bank accession no X59036, in plasmid pRAD1 under P_{groESL} promoter)	[121]
E. coli-PhoK	*E. coli* DH5α containing plasmid construct pK1 (*phoK* ORF, gene bank accession no EF143994, in plasmid pRAD1 under P_{groESL} promoter)	This study
E. coli-pRAD1	*E. coli* DH5α containing shuttle vector plasmid pRAD1	This study
D. radiodurans R1	Wild-type strain	Lab collection
Deino-PhoN	*D. radiodurans* R1 containing plasmid construct pPN1	[121]
Deino-pRAD1	*Deinococcus radiodurans* R1 containing empty shuttle vector plasmid pRAD1	This Study
Deino-PhoK	*Deinococcus radiodurans* R1 containing plasmid construct pK1	This study
Deino-PhoNK	*Deinococcus radiodurans* R1 containing plasmid construct pK2	This study

2.2 Histochemical screening of recombinant bacterial strains expressing PhoN/PhoK.

Histochemical screening was used for detection of phosphatase activity of PhoN/PhoK expressing clones. Screening of *E. coli* clones was carried out by growing cells

on LB plates containing phenolphthalein diphosphate (PDP) at 1 mg/ml and methyl green (MG) at 50 µg/ml [141]. For screening of *D. radiodurans* strains, the MG concentration was reduced to 5 µg /ml, as higher concentration of MG was found to be toxic. Recombinant cells, which display cell based phosphatase activity displayed dark green coloured colonies on PDP-MG plates. Phosphoric acid released from PDP due to action of phosphatases causes local acidification of medium leading to pH indicator dye, MG stain turning dark green. Precipitation of the dark green MG on phosphatase producing colonies forms the basis for screening of phosphatase positive strains.

For qualitative determination of extracellular release of PhoN/PhoK enzyme, 10 µl supernatant medium of overnight grown cultures of either *D. radiodurans* or *E. coli* clones was spotted on appropriated nutrient media supplemented with PDP-MG (1 mg/ml) or *para*-nitrophenol phosphate (*p*-NPP) in 1.5% agar plate.

2.3 Recombinant DNA techniques

2.3.1 Isolation of plasmid DNA.

Plasmid DNA was isolated from *E. coli* cells by alkaline lysis method using the High Pure Plasmid Isolation Kit, from Roche Diagnostics, Germany, as per the manufacturer's protocol. For plasmid isolation from *Deinococcus*, the above mentioned kit was used with certain modifications. Overnight grown culture (10 ml) of *Deinococcus* was centrifuged, washed twice in chilled ethanol, followed by two washes in Tris-EDTA (TE) buffer (10 mM Tris and 1 mM EDTA, pH 8) and finally re-suspended in suspension buffer provided in the kit. To this lysozyme was added to a final concentration of 2 mg/ml and cell suspension was incubated at 37°C for 1 h. Subsequently, Proteinase K was added to a final concentration of 4 mg/ml and the mixture incubated for 10-15 min at 70°C. The rest of the procedure was followed as per the manufacturer's protocol. Various plasmids used in the study are listed in Table 2.2.

Table 2.2. Plasmids used in this study.

Sl. no.	Plasmid	Description of construct	Source/Reference
1.	pRAD1	*E. coli-D. radiodurans* shuttle vector, Ap^r, Cm^r, (6.28 kb)	[140]
2.	pEK2	pBluescriptII SK(+) vector containing a 3-kb PstI-BglII fragment from BSAR-1 in PstI/BamHI sites.	[113]
3.	pPN1	pRAD1 containing *S. typhi phoN* gene with deinococcal *groESL* promoter (7.35 kb)	[121]
4.	pK1	pRAD1 containing phoK ORF with deinococcal *groESL* promoter (8.21 kb)	This study
5.	pK2	pPN1 containing phoK ORF with deinococcal *groESL* promoter in Xho/BglII restriction sites 9.38 kb	This study

2.3.2 Restriction endonuclease digestion and electrophoresis of DNA

Restriction endonuclease digestion of DNA was carried out according to the manufacturer's protocol (New England Biolabs, UK). The digested DNA (with appropriate amount of 6X loading dye: 30% glycerol, 6 mM EDTA, 0.01% bromophenol blue, 0.01% xylene cyanol) was resolved on 1% agarose gel containing 0.5 µg/ml ethidium bromide prepared in 0.5 X TBE (4.45 mM Tris, 4.45 mM boric acid, 0.1 mM EDTA, pH 8.3) buffer. Electrophoresis was carried out at 8V/cm and DNA fragments were visualized using UV transilluminator at λ= 380 nm. The 1 kb and 100 bp DNA ladder from New England Biolabs, UK were used as markers to calculate the molecular size of the various DNA fragments. The desired DNA fragments were eluted from the gel using QIAquick Gel extraction kit (QIAGEN, Germany) when required.

2.3.3 Amplification of DNA by Polymerase Chain Reaction

Primers used in this study are listed in Table 2.2**.** All primers used or cloning and DNA sequencing were obtained from Pramukh Health Care Pvt. Ltd, India.

Table 2.3. Primers used in this study

Primer	Sequence
P5	5'GGAGCGGATAACAATTTCACACA-3'
P6	5'AACGCGGCTGCAAGAATGGTA-3'
F_{ow}	5'CCAGTTATTGGCGATGATGCC-3'
R_{ow}	5'GGAGCCTGATCCAGGAAGCG-3'
DAG-f	5'GCCTCTAGACATGTTCAG-3' (XbaI)
Gro-r	5-GTTTCAGCATCTAGAGTCCTCCTG-3' (Xba I)
FDNE	5'GGAATTCCATATGTTGAAACACGTCGCCGCTGCC-3' (NdeI)
RDBE	5'CGCGGATCCTTACTGCCCGGCGCAGCTGTCGTCCCTTG-3'(Bam HI)

*The underlined sequence in the primer corresponds to the restriction site indicated in the parenthesis.

PCR amplification was generally carried out using 20 pmoles of each primer, 200 µM dNTPs, 1.5 U Taq DNA polymerase in 1X Taq buffer (Bangalore Genei Ltd., India). For PCR of longer DNA fragments from deinococcal chromosome, the GC Rich PCR amplification kit from Roche Diagnostics, Germany was used. The template for PCR was either recombinant plasmid (10-20 ηg) or a colony (in case of colony PCR). In case of *D. radiodurans*, colony PCR was carried out by making a suspension of cells taken from the colony in 10 µl distilled water which was placed in a boiling water bath for 20 min. Five µl of this suspension was directly used as template in PCR reactions. A typical PCR cycle involved quick denaturation at 94°C for 3 min followed by 30-32 amplifications cycles. Each amplification cycle comprised of three steps, denaturation at 94°C for 1 min followed by annealing at 50-65°C for 1-2 min (depending on T_m of primers used) and extension at 72°C for varying time depending on the length of fragment to be amplified (approximately 1 min extension was used for amplifying 1 kb DNA fragment). The PCR products were purified by PCR purification kit supplied by Roche Diagnostics, Germany when required.

DNA sequencing of cloned *phoK* gene was done commercially (Bangalore Genei Pvt. Ltd). Computational analysis of DNA sequences were performed using internet based programs. Similarity searches were carried out using the BLAST algorithms available at http://www.ncbi.nlm.nih.gov/BLAST/. Multiple sequence alignment comparison was performed using ClustalW (http://www.ebi.ac.uk/clutsalw/).

2.3.4 Ligation and transformation

Ligation of DNA insert to the vector was typically carried out in 3:1 to 5:1 molar ratio. The Rapid Ligation Kit from Roche Diagnostics, Germany was used for DNA ligation. About 2.5 Units of T4 DNA ligase was added to a 20 µl reaction containing the T4 ligase buffer, vector, insert and DNA dilution buffer according to the manufacturer's protocol (Roche Diagnostics, Germany). The ligated DNA (50–100 ng) was used to transform competent *E. coli* cells prepared using $CaCl_2$ protocol and transformation of such cells was carried out as described earlier [142]. *Deinococcus* transformations were carried out as described earlier [143] with some modifications. Briefly, exponentially grown cells were chilled on ice for 10 min and subjected to centrifugation. They were re-suspended in 3 ml TGY with 30 mM $CaCl_2$. To 100 µl cell suspension aliquot, 1 µg plasmid DNA was added and kept on ice for 45 min. Cells were then incubated at 32°C for 45 min. About 900 µl TGY was added to the cells and incubated at 32°C under agitation (180 rpm) overnight. The following day, the cells (100µl) were plated on TGY agar medium containing 3 µg/ml chloramphenicol. The transformants growing on the antibiotic supplemented plates were then screened for phosphatase activity on histochemical plates as described in section 2.2.

2.4 Extraction, estimation and electrophoresis of cellular proteins

Cultures of *E. coli* or *D. radiodurans* were harvested by centrifugation, washed in distilled water twice and re-suspended in chilled distilled water. The concentrated cell suspensions were then sonicated (Branson Sonicator, Germany) with total pulse time of 2 min

(1 sec ON and 1 sec OFF). The cell-free extracts containing total cellular proteins were obtained by centrifugation at 13,000 rpm for 30 min at 4°C. Protein concentrations in the cell free lysate was estimated by using SIGMA Total Protein Kit (Sigma-Aldrich, USA) based on Peterson's modification of micro Lowry modified method [144].

For gel-based activity (zymogram) analysis, the cells were lysed in non-reducing Laemmli's [145] cracking buffer (40 mM Tris-HCl, pH 6.8, 2% SDS, 4% glycerol, 0.01% Bromophenol Blue) at 50°C for 15 min. The suspension was clarified by centrifugation at 15,000 g for 30 min. For all other applications, protein samples were treated at 100°C in Laemmli's buffer followed by centrifugation at 15,000 rpm for 30 min to remove insoluble cell debris. The protein samples were electrophoretically resolved by 10% or 12% sodium dodecyl sulphate polyacrylamide gels (SDS-PAGE). The gel was poured between a glass and ceramic plate separated by 1 mm spacers. The resolving gel and stacking gel were poured according to details given in Table 2.4. After solidification of acrylamide gel, protein extracts were loaded into the wells and electrophoresis was carried out at 75 V for 30 min followed by 100 V for 2 h in a mini-gel electrophoresis apparatus (Tarsons India Limited, India).

Table 2.4. Composition of polyacrylamide gels.

SL. No.	Ingredient	10% resolving gel	5% stacking gel
1	30% acryl-amide solution	2.5 ml	0.625 ml
2	Tris-Cl 1.5 M	1.875 ml, pH 8.8	1.25 ml, pH 6.8
3	10% SDS	75 µl	50 µl
4	10% Ammonium per sulfate	56.25 µl	37.5 µl
5	TEMED (Tetra-methyl ethylene diamine)	3.75 µl	3.75 µl
6	D/W	2.99 ml	3.033 ml

Post-run, gels were washed in distilled water followed by processing for either Western blotting or zymogram analysis or staining by Coomassie Brilliant Blue (CBB). The gel was stained using CBB G250 and briefly destained with destaining solution I (DS I, Table

2.5) followed by destaining solution II (DS-II, Table 2.5) to minimize the background gel colour and to visualize stained proteins properly. Pre-stained protein markers NEB7708 or Page-ruler plus prestained protein ladder (Thermoscientific India Ltd., India) were used for molecular mass estimation

Table 2.5. Composition of reagents used for protein electrophoresis.

Reagent	Composition
Running buffer	0.3 % Trizma base, 1.44% Glycine, 0.1% SDS.
Destaining solution	I- 50% methanol, 10% acetic acid II- 10% methanol, 2%glycerol, 10% acetic acid.
Coomassie Brilliant blue G250	0.2% CBB G 250 in 40% methanol, 20% acetic acid

2.5 Determination of phosphatase activity

2.5.1 *In vitro* acid/alkaline phosphatase activity by zymogram analysis

Equal amount of proteins in non-reducing Laemmli's buffer were electrophoretically resolved by 10% or 12% SDS-PAGE at 75 V for 30 min followed by 100 V for 2-3 h. After electrophoresis, the gel was rinsed briefly with water to remove surface SDS and renatured using 1% Triton X-100 in 100 mM acetate buffer pH 5.0 (Two washes of 20 min each) for PhoN activity. This was followed by a wash in 100 mM acetate buffer pH 5.0. For PhoK activity staining, the gel was washed 3 times (20 min each wash) with 100 mM Tris-Cl buffer (pH 9.0) to remove SDS and to renature proteins at alkaline pH. The gel was developed using 200 µl of nitroblue tetrazolium chloride/5-bromo-4-chloro-indolyl phosphate (NBT/BCIP) (Roche Diagnostics, Germany 18.75 mg/ml NBT and 9.4 mg/ml BCIP in 67% Dimethyl sulfoxide) mix in 20 ml of appropriate buffer for 2-3 h or overnight (as necessary). The assay was terminated by rinsing the gel in distilled water. Appropriate pre-stained markers were co-electrophoresed with samples for determination of molecular mass.

2.5.2 *In vivo* cell-based acid/alkaline phosphatase activity

Cell associated acid phosphatase activity was estimated by the liberation of *para*-nitro phenol (*p*-NP) from di-sodium *p*-nitrophenyl phosphate (*p*-NPP) as described earlier [146]. Whole cells were suspended in appropriate buffer (1 ml) containing 8.3 mM *p*-NPP and incubated at 37°C for 30 min. The reaction was stopped by addition of 2 ml of 0.2 N NaOH and the amount of *p*-nitro phenol released was spectrophotometrically determined by measuring absorbance at 405 nm. A standard with *p*-NP (product) was also plotted. When required, the pH of assay mixture was varied using following buffers: 100 mM acetate buffer, pH 5.0 or 50 mM MOPS, (pH 7.0 or 9.0), 50 mM Tris-Cl, pH 9.0. The cell-associated phosphatase activity was expressed as nmoles of *p*-NP liberated min^{-1} mg^{-1} bacterial protein. Protein concentration was determined using a protein estimation kit (Bangalore Genei Pvt. Ltd, India).

Phosphatase activity of cells was also assessed in terms of P_i release from β-glycerophosphate (β-GP) substrate. Phosphate release was measured in the buffer supernatant spectrophotometrically by phosphomolybdic acid method [147]. Briefly, cells were suspended in appropriate buffer (50 mM MOPS buffer with pH 7 or 9) (1 ml) containing 8.3 mM β-GP and incubated at 37°C for 30 min followed by phosphate estimation. After 30 min incubation, sample (100-200 µl) from this reaction mixture was used for phosphate estimation. For the estimation of phosphorous, 700 µl of reagent mixture (10% ascorbic acid and 0.42% ammonium molybdate, 1:6, v/v) was added to 300 µl sample. The reaction mixture was mixed properly and incubated at 45^{o}C for 20 min. The amount of phosphomolybdate formed in the reaction was spectrophotometrically estimated at 820 nm. Aqueous solution of KH_2PO_4 was used to obtain standard curve for phosphorous estimation.

2.6 Western Blotting and Immunodetection of PhoK protein

Equal amount of whole cell protein extracts (20-40 µg) or purified PhoK protein (10-20 µg) prepared in Laemmli's cracking buffer (2% SDS, 2 mM dithiothreitol, 4% glycerol, 40 mM Tris-HCl, pH 6.8 and 0.01% bromophenol blue) were resolved by 10% SDS-PAGE. The gel was equilibrated in Transfer buffer (0.125 M Tris base, 0.192 M Glycine, 20% methanol) for 20 min. The proteins were electroblotted on nitrocellulose membrane at 400 mA for 2 h. The blot was processed for immunodetection. Briefly, the blot was placed in an appropriate dilution of the antibody serum in MaNa (0.1M Maleic acid and 0.15 M NaCl) buffer, containing 1% casein suspension, for interaction with primary antibody. After 1 h of incubation, the blot was washed in 100 mM MaNa buffer twice for 20 min each to remove antibody bound non-specifically to the blot. The blot was then incubated in MaNa buffer containing the secondary antibody; alkaline phosphatase conjugated anti-rabbit IgG (Sigma-Aldrich, UK) at 1:10,000 dilution for 1 h. The blot was rinsed in MaNa buffer for 20 min, twice. After equilibration in Tris-NaCl buffer pH 9.0, the blot was processed for colour development using NBT-BCIP (Roche Diagnostics, Germany) as substrate in the same buffer. The colour development reaction was stopped by adding distilled water.

2.7 Determination of surface charge of cells

The surface charge on cells was determined by measuring their zeta potential. Cells were suspended in distilled water or MOPS buffer of specified pH at OD_{600nm} 1.0 and their zeta potential was determined in electrophoretic cell using Zetasizer nano series (Malvern Instruments, UK).

2.8 Uranium precipitation/biosorption assays

Uranyl nitrate solution was prepared as a 100 mM stock solution by dissolving $UO_2(NO_3)_2 \cdot 6H_2O$ (Merck India limited) in double distilled water. To simulate a carbonate

dominated geochemical condition, a stock solution composed predominantly of uranyl carbonate complexes was prepared by addition of 1/10th volume of concentrated solution of ammonium carbonate (~2 M) to 100 mM uranyl nitrate hexahydrate stock solution (final U concentration was 89 mM and carbonate concentration was 214 mM) [113, 148-149]. Formation of carbonate complexes with U was verified by monitoring the absorption spectra of solution in the visible light range between 400-500 nm (Thermoscientific make Unicam UV 300) with specific peaks detected at 434 nm, 448 nm and 464 nm [148-149]. U precipitation assays were carried out with PhoK/PhoN expressing *E. coli* or *D. radiodurans* cells (OD_{600nm}~1) under the following two defined conditions: Geochemical condition 1 (GC 1): 10 mM 3-(N-mopholino) propane sulfonic acid (MOPS, pH 7.0) with uranyl nitrate solution. The final pH attained was 6.8. Geochemical condition 2 (GC 2): 10 mM MOPS (pH 9) containing U solution prepared with ammonium carbonate as explained above. Final pH attained was 9.0. The final concentration of uranium used in the bioprecipitation experiments for GC1 was 1 mM and for GC2 was 1-10 mM. The concentration of carbonate in GC2 in bioprecipitation assay as well as for all further experiments was always 2.4 fold higher than corresponding concentration of U. The pH conditions (6.8 and 9) were optimized for the optimal phosphatase activities for U precipitation.

For bioprecipitation experiments, cells (OD_{600nm}~1-3) were used in a 5 ml reaction mixture containing 1-10 mM U (under either GC1 or GC2) in 10 mM MOPS buffer (pH 7 or 9) and sodium salt of β-glycerophosphate was added as the substrate at specified concentration. The reaction mix was kept at 30° C under static, aerobic conditions for 18 h. The recombinant cells which carried the empty vector (i.e. pRAD1 lacking the *phoN/phoK* genes) were used as a control and were incubated with U under similar conditions as mentioned above. Appropriate controls were also included to ascertain (a) spontaneous chemical precipitation of the metal or sorption to the container surface by excluding cells in

the reaction mix, and (b) biosorption of metal on the cell surface by excluding the substrate, β-glycerophosphate [113]. Aliquots (1 ml) were taken at different time intervals and subjected to centrifugation at 12,000 g for 10 minutes. Residual U in the supernatant or U present in the pellet was estimated using Arsenazo III reagent as described earlier [40]. A 0.1% solution of Arsenazo-III was prepared by dissolving 0.2 g of the reagent (Merck India limited) in 180 ml of 0.01N HCl and 20 ml of absolute ethanol (30 min, stirring) and filtered through Whatman No. 1 filter paper. The samples were acidified (200 µl of 0.01N HCl), followed by the addition of 200 µl of Arsenazo III reagent. The resultant purple colored metal-Arsenazo III complex was estimated spectrophotometrically at 655 nm using uranyl nitrate as the standard. In order to show the correlation between the loss of metal from the supernatant and gain in the pellet, the metal precipitated was also estimated in pellet fraction after digesting the cells with conc. HCl.

For biosorption experiments, the wild-type *D. radiodurans* or *E. coli* (DH5α) cells (OD_{600nm}~1) were suspended in 10 mM MOPS buffer under conditions similar to GC1 or GC2 at 50, 100, 200 and 1000 µM U concentrations. The dry weight corresponding to the optical density of cells used in each experiment was determined and used to calculate mg U biosorbed or precipitated/g dry weight cells. The assay for measuring biosorption would have been complicated by the bioprecipitation phenomenon occurring concomitantly if phosphatase expressing recombinant cells had been employed. Hence only for the biosorption experiments wild type *E. coli* or *D. radiodurans* strains were used.

2.9 Radiation response studies

Early exponential/stationary phase cells of *Deino-PhoK* or *Deino-pRAD1* strains were washed twice with double distilled water and resuspunded in fresh TGY (5 ml) at OD_{600} ~1. The cultures were irradiated at different doses (3-21 kGy) at a dose rate of 4.2 kGy/h (^{60}Co

Gamma Cell 5000 irradiation unit, BARC, India). Vials kept outside the radiation source served as control. Irradiated and control cells were washed, serially diluted and plated in triplicate on TGY/choramphenicol plates. Radioresistance of cells was evaluated by calculating D_{10} dose values. Irradiated cells were also assayed for their PhoK activity. For U precipitation experiments, *Deino-PhoK* cells (OD_{600nm} ~ 1) were exposed to 6 kGy dose of gamma radiation (dose rate: 4.2 kGy/h, ^{60}Co Gamma Cell 5000 irradiation unit, BARC, India) followed by incubation with 1 mM U and 5 mM β-GP at pH 9.0. Unirradiated *Deino-PhoK* cells served as control. The amount of U removed from the supernatant was measured up to 3 h by Arsenazo III reagent.

Survival of *Deinococcus* strains (*Deino-PhoK* or *Deino-pRAD1*) in presence of Caesium (Cs) or strontium (Sr) was checked after 4 h exposure to either (1) uranium, or (2) uranium along with Cs and Sr. Briefly, cells were washed with saline and resuspended (OD_{600nm}~1) into 20 mM uranyl solution (in 10 mM MOPS, pH 9.0) under GC2 with or without 1 mM $CsCl_2$ and 1 mM $SrCl_2$. Appropriate dilutions were plated (3 replicates each) on agar plates which were incubated at 32°C for 48 h to score for colony forming units (CFUs).

2.10 Uranium sensitivity studies

E. coli or *D. radiodurans* cells (wild type or recombinants) were grown in LB broth or TGY respectively, till they reached late exponential phase of growth. Cells were washed twice with double distilled water and suspended (OD_{600nm}~1) in 10 mM MOPS buffer, supplemented with U at 0-1.5 mM under GC1 or at 0-30 mM under GC2 for 4 h. Such U-exposed cells were washed free of uranium containing medium, spotted (10 µl) on corresponding LB/TGY agar plates and growth after incubation of 24 h was recorded. In another set of experiment, cells (resting conditions) were exposed to U as described earlier and such U-exposed cells (OD_{600nm}~0.5) were then inoculated into LB/TGY liquid broth

medium with agitation (150 ± 5 rpm) or plated on LB/TGY agar plates. Growth was assessed by measuring optical density at 600 nm [OD_{600}] or by determining the number of Colony Forming Units (CFU) on LB/TGY agar plates (1.5 % Bacto Agar) after 24 h of incubation (at 37° C) for *E. coli* and after 48 h (at 32° C) of incubation for *D. radiodurans*.

2.11 X-ray diffraction analysis

Powder XRD was performed to identify the nature of bioprecipitated uranium. The cells of *Deino-PhoK, Deino-PhoN* or *Deino-pRAD1* were used to precipitate U under GC1 or GC2. After U precipitation, cells were centrifuged and cell pellet was dried in an oven at 80°C for 4 h. The dried pellet was scrapped off and crushed into fine powder. The powder was subjected to X-ray diffraction analysis employing a Philips analytical X-ray diffractometer (using Ni filtered Cu Kα radiation, Chemistry division, BARC) or high precision Rigaku R-Axis D-max Powder diffractometer using monochromatic Cu-Kα radiation (Solid State Physics Division, BARC**).** The diffraction pattern was recorded from 5 to 70 2θ with a step length of 0.02. The diffraction pattern obtained was compared to known standards in International Centre for Diffraction Data (ICDD) database.

2.12 Fluorimetric analysis

Fluorimetric analysis of uranyl phosphate precipitated by recombinant and control cells was carried out using a fluorescence spectrophotometer (Model FP6500, Jasco Inc, Japan). For qualitative affirmation of precipitated uranyl phosphate, either *Deino-PhoK* and *Deino-pRAD1* cells or beads in which recombinant cells were immobilized were suspended in 10 mM MOPS buffer with 1 mM uranyl carbonate solution and β-GP (5 mM). The cell pellet or beads were exposed to UV (380 nm) after U precipitation and photographed. The supernatant buffer medium was also exposed to UV after removal of beads from the solution. The green fluorescence emanating from uranyl phosphate was visualized. For quantitative

analysis of precipitation, either cells or beads were incubated with U as described above and fluorescence intensity of the solution was monitored using λ_{ex} = 380 nm and λ_{em} = 524 nm over a period of time (0.5- 4 h).

2.13 Transmission Electron Microscopy

PhoN/PhoK-expressing cells (*E. coli* or *D. radiodurans*) which had precipitated U or control (U unchallenged) cells were washed twice with 50 mM cacodylate buffer (pH 7.4) and fixed in a solution (2.5 % glutaraldehyde + 0.5 % Para-formaldehyde) overnight at 4º C. Following three washes with cacodylate buffer, cells were embedded in 2 % noble agar and dehydrated in a graded series of ethanol (30, 60, 75, 90, and 100 %). After the removal of ethanol by treatment with propylene oxide, blocks were subsequently infiltrated with Spurr reagent (Sigma-Aldrich, USA.) and propylene oxide. Blocks were serially incubated in solutions (2 h in each case) containing Spurr reagent and propylene oxide mixed in ratios (v/v), 3:1, 1:3 and 1:1 (v/v propylene oxide: Spurr reagent). The samples were finally infiltrated with Spurr resin for 16 h and incubated at 60ºC for 72 h. Thin sections of samples were prepared with an ultra-microtome (Leica, Germany), placed on 200 mesh formvar-coated copper grids and viewed with the Libra 120 plus TEM (Carl Zeiss, Germany). Both stained (with 1.5 % uranyl acetate) as well as unstained samples were viewed. Altogether 121 fields were observed and the results have been reported for observations seen in more than 85% of the fields visualized for each sample.

2.14 Lyophilization

Overnight grown culture (18 h) (around 1 L) of *Deino-PhoK* or *Deino-PhoNK* cells were centrifuged and cells were given 2 washes of double distilled water. A thick suspension of recombinant cells, was placed in Petri plates, frozen in liquid nitrogen for 5 min and lyophilized without any cryo-protectant overnight in a Lyophilizer (Lyospeed, Genevac, UK)

at 0.07 mbar for 18 h. The lyophilised cells were scraped off from the Petri plate and stored in Eppendorf vials at room temperature without, till further use. Approximately 0.4 mg/ml of lyophilized cells, yielded OD and protein content (15 ± 2 µg/100 µl) equivalent of OD_{600nm} 1. Lyophilized cells were allowed to equilibrate for 5 min in buffer solution before the PhoN/PhoK activity and uranium precipitation assays were carried out.

2.15 Immobilization of cells/protein.

2.15.1 Immobilization of *Deino-PhoK*/*Deino-PhoNK* cells in calcium alginate.

Sodium alginate (2%) was dissolved in hot distilled water (30 ml) with constant stirring. After cooling to room temperature, freshly harvested *Deino-PhoK/Deino-PhoNK* or *Deino-pRAD1* cells (OD_{600}~10) were added to this solution and thoroughly mixed by stirring to form a uniform mixture. This mixture (0.1 % biomass in 2 % sodium alginate) was extruded as droplets in 0.1 M $CaCl_2$ solution through a nozzle. The gel beads (diameter 3.5 ± 0.2 mm) were allowed to cure for 2 h at 4°C and washed thoroughly three times with distilled water. Blank alginate beads (2 % w/v) without cells were also prepared to serve as control. For monitoring uranium removal, beads in which *Deino-PhoK* cells were immobilized were suspended in a 50/100 ml solution (1 mM uranyl carbonate and 5 mM β-GP in 10 mM MOPS buffer pH 9) and the decrease in uranium content of supernatant was monitored by the Arsenazo III reagent. Uranium removal from solution and corresponding gain in beads was also monitored by fluorimetric method as detailed in earlier sections (2.13). Beads in which *Deino-PhoNK* cells were immobilized were incubated with 1 mM U in either MOPS (10 mM, pH 7.0) for GC1 or MOPS (10 mM, pH 9.0) for GC2.

2.15.2 Immobilization of *Deino-PhoK* cells in polyacrylamide gel and U precipitation in flow through system.

For immobilization, 250 mg of lyophilised *Deino-PhoK* cells were used. Fifty ml of 15% polyacrylamide gel (30% Acrylamide bis-acrylamide solution-25 ml, 500 µl of 10%

APS and 500 µl of TEMED) was prepared in distilled water with the aforesaid amount of cells suspended in 10 ml distilled water. The gel was allowed to set at 4°C for 1 h. The gel containing the cells was washed several times in distilled water and then shredded into small pieces using a sieve (8 pores/cm^2). The shredded gel was allowed to swell in distilled water for 5 min. After draining distilled water, the gel was mixed with acid washed sand and filled into the column (125 ml volume). Initially 100 ml MOPS buffer (pH 9.0) was passed through column for equilibration. One litre of U solution (1 mM in 10 mM MOPS buffer, pH 9.0 and 5 mM β-GP) was passed through column over a period of 8 days at an average flow rate of 7 ml/h. U was estimated in the flow-through at regular time intervals and the loading was calculated accordingly.

2.15.3. Immobilization of PhoK on Ni^{+2}-NTA matrix.

Recombinant *E. coli* BL21 pLysS cells carrying the *phoK* gene (EK4, Table 2.1) were grown at 37°C in LB broth containing 50 µg/ml kanamycin and 33 µg/ml chloramphenicol till they attained a OD_{600nm} of 0.6-0.8. PhoK expression was induced by addition of 1 mM isopropyl-β-D-thiogalactopyranoside (IPTG) followed by incubation at 37°C under shaking conditions (180 rpm) for 3-4 h. Cells were harvested (100 ml culture) after 3-4 h of growth and then sonicated (Branson Sonicator, Germany) with total pulse time of 2 min (1 sec ON and 1 sec OFF). The cell-free extracts containing total cellular proteins were obtained by centrifugation at 13,000 rpm for 30 min at 4°C. The cell free lysate (500 µl) was incubated with Ni^{2+}-nitrilotriacetic acid (Ni^{+2}-NTA) matrix (1 ml) for binding of His_6-tagged PhoK for overnight period at 4°C. After binding, matrix was centrifuged at 10,000 rpm for 5 min and lysate was discarded. Matrix slurry was given washes with 5, 10, 15 and 20 mM imidazole (20 min each) so as to remove non-specifically bound protein. The binding of PhoK was ascertained by resolving all samples (lysate, washes and matrix slurry) by 10% SDS-PAGE followed by CBB staining. After binding, activity of PhoK was ascertained by *p*-NPP activity

and zymogram analysis. For *p*-NPP activity, 5 µl control unbound Ni^{+2}-NTA matrix or PhoK bound Ni^{+2}-NTA matrix slurry was used. For zymogram analysis, 20 µl control unbound Ni^{+2}-NTA matrix or PhoK-bound Ni^{+2}-NTA matrix slurry was added to non-reducing cracking buffer.

2.15.4 Uranium precipitation using immobilised PhoK.

For U bioprecipitation assay in batch process, PhoK immobilized Ni^{+2}-NTA matrix was added (100 µl slurry corresponding to around 15 µg protein**)** to 2.5 ml of 1 mM U solution in 10 mM MOPS buffer (pH 9.0) with 5 mM β-GP substrate. U precipitation was monitored up to 5 h. As a control, unbound Ni^{+2}-NTA matrix was used. At regular time intervals, aliquots were withdrawn and centrifuged at 12,000 rpm for 5 min. U removal from supernatant was estimated using Arsenazo III. The same PhoK bound Ni^{+2}-NTA matrix was reused for two more rounds of precipitation. After first round of precipitation, the matrix was subjected to differential centrifugation (2000 rpm for 4 min followed by 12,000 rpm for 10 min) so as to separate heavier Ni^{+2}-NTA matrix first, from precipitated uranyl phosphate. The precipitate was collected in another tube, and matrix was washed with buffer (1 ml 10 mM MOPS, pH 9.0) to remove loosely bound precipitate. This matrix was then used for next round of precipitation.

For column studies, PhoK immobilized Ni^{+2}-NTA matrix (~180 µg protein in 1 ml matrix slurry) was packed in a column (10 ml volume). In first round ~ 200 ml U solution (1 mM U in 10 mM MOPS buffer, pH 9.0 and 5 mM β-GP) was passed through column for 24 h with average flow rate of 10 ml/h. In the second and third round ~150 ml U solution was passed through column. U was estimated in flow-through at regular time intervals and the loading was calculated accordingly. The column was exposed to UV (380 nm) and photographed.

2.16 PhoK inactivation assays

PhoK inactivation/inhibition assays were conducted using *p*-NPP as the substrate. PhoK protein (Ni^{+2}-NTA bound) was incubated at room temperature as well as 4°C for 72 h. At regular time intervals (24 h), 5 µl of matrix slurry was used for *p*-NPP assay (Section 2.5.2). Initial activity before incubation at ambient temperature was taken as 100% and relative activity was calculated as % of initial activity. Inactivation of PhoK was also conducted by treating PhoK (Ni^{+2}-NTA bound) with 0-5 mM U (corresponding concentration of carbonate was 2.4 fold times input U concentration). Briefly, 5 µl PhoK bound Ni^{+2}-NTA matrix slurry was added to 1 ml Tris-Cl buffer (50 mM, pH 9.0) along with 0-5 mM U and 200 µl *p*-NPP (50 mM) was added as substrate. This reaction mixture was incubated for 30 min followed by addition of 0.2 N NaOH to stop the reaction. Absorbance was recorded at 405 nm. Relative activity was calculated as % of activity in the absence of U taken as 100 %.

Chapter 3

Construction of Recombinant *D. radiodurans* strains Expressing Acid/Alkaline Phosphatases for Bioprecipitation of Uranium.

Microbial bioremediation of uranium from acidic-neutral conditions has been studied earlier by many researchers [77, 121, 150] and will continue for gaining insights into relevant mechanistic details. However, bioremediation of uranium from alkaline aqueous solutions remains inadequately explored [113]. Precipitation of U as uranyl phosphate from alkaline solution is rather difficult on account of extremely high solubility of uranyl carbonate complexes at basic pH. Precipitation is feasible only at log (PO^{3-}_4 /CO^{2-}_3) values of >-3 [127]. While it is difficult to achieve such a favourable (PO^{3-}_4/CO^{2-}_3) ratio, an active enzymatic process can generate substantially high localized concentration of inorganic phosphate for precipitation. A *Sphingomonas*, strain BSAR-1, isolated in our laboratory, was shown to possess very high alkaline phosphatase activity. The corresponding gene, designated *phoK*, was cloned into *E. coli* and over-expressed [113]. The recombinant PhoK protein was characterized and its structure was elucidated by X-ray crystallography. PhoK comprised of 559 amino acids and an estimated molecular mass of 59,982 Da [115]. The enzyme was released extracellularly and showed optimum activity at pH 9. The PhoK expressing *Sphingomonas* strain could precipitate uranium, albeit with a low efficiency under alkaline conditions indicating that required (PO^{3-}_4/CO^{2-}_3) ratio could be achieved by PhoK enzyme.

To achieve bioprecipitation of U from alkaline waste under high radiation environment, the *phoK* gene was proposed to be introduced into the extremely radiation resistant bacterium *D. radiodurans*. The recombinant strain expressed high PhoK activity from pH 8-9. However, PhoK activity was drastically reduced in this strain at acidic pH (5-6). Therefore, to enable use of single bacterium which could precipitate U efficiently under both acidic and alkaline conditions, PhoN, a non-specific acidic phosphatase was also introduced in recombinant strain already carrying the *phoK* gene. This chapter describes construction of recombinant *Deinococcus* strains expressing (1) alkaline phosphatase and (2) both acid and alkaline phosphatases, and evaluation of these strains for U precipitation ability.

3.1 Cloning of *phoK* in *E. coli* - *D. radiodurans* plasmid shuttle vector pRAD1

In order to achieve expression of PhoK in *D. radiodurans*, *phoK* gene was cloned in plasmid vector pRAD1 downstream of strong deinococcal promoter P_{groESL}. The *phoN* gene (GenBank Accession no. X59036), encoding a non-specific acid phosphatase from *Salmonella typhimurium*, was cloned into a *Deinococcus*/*E. coli* shuttle plasmid pRAD1 in our laboratory previously (Table 2.2, Fig. 3.1A) [4].

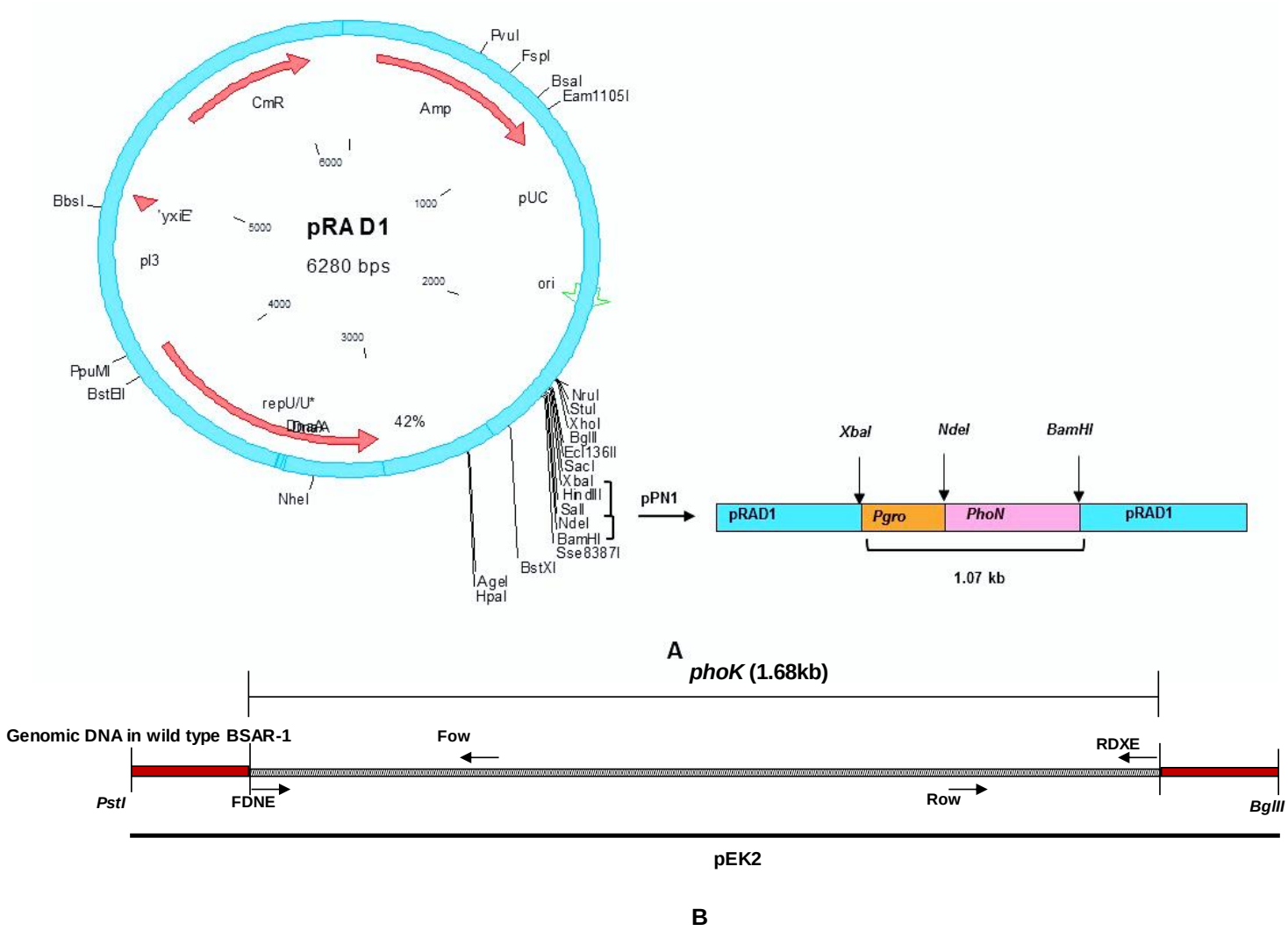

Fig. 3.1. Schematic maps of plasmids (A) pRAD1 and pPN1, and (B) pEK2. Physical map of plasmid pRAD1 depicts the restriction sites used for cloning in plasmid pPN1. Source for schematic map of pEK2 [113].

The plasmid pRAD1 derives its *E. coli*-recognisable part from plasmid pMTL23, which is derivative of pUC18, while the *Deinococcus*-recognisable part of pRAD1 is derived from pUE10, a cryptic plasmid from *D. radiodurans* SARK [151]. The plasmid is maintained in high copy in *E. coli*, while in *Deinococcus* it is present at 7-10 copies per cell. The plasmid pRAD1 contains antibiotic markers ampicillin and chloramphenicol that facilitate selective screening in *E. coli* and *D. radiodurans* respectively. The resulting plasmid pPN1 carried the *phoN* gene downstream of a deinococcal promoter P_{groESL} (Table 2.2, Fig. 3.1A). The *phoK* gene (GenBank accession no EF143994), encoding a novel alkaline phosphatase was cloned from *Sphingomonas* BSAR-1 strain in plasmid vector pBluescriptII SK (+) with its native promoter from BSAR-1, and called pEK2 (Table 2.2) [113]. The *E. coli* strain harbouring pEK2 was called EK2 (Table 2.1, Fig. 3.1B).

The pPN1 plasmid (Fig. 3.1A) was digested with restriction enzymes *NdeI*/*BamHI* and the products were electrophoretically resolved on 1% agarose gel. The digested pPN1 vector band was excised and purified. The *phoK* ORF (1.68 kb) was PCR amplified using primers FDNE and RDBE (Table 2.3) from the plasmid pEK2 (Fig. 3.1B). The *phoK* amplicon was digested using *NdeI*/*BamHI*, and ligated to *NdeI*/*BamHI* digested pPN1 to replace *phoN* ORF (0.81 kb) with *phoK* ORF (Fig. 3.2).

The plasmid pK1 (8.21 kb) thus constructed was transformed into competent *E. coli* DH5α cells (Table 2.1) and transformants were selected on LB agar plates containing carbenicillin (Cb). Individual Cb^r colonies were patched on histochemical agar plates containing Cb, supplemented with PDP and MG for the preliminary screening of transformants with phosphatase activity. Colonies showing green colour due to expression of PhoK were selected for further analysis (Fig. 3.3).

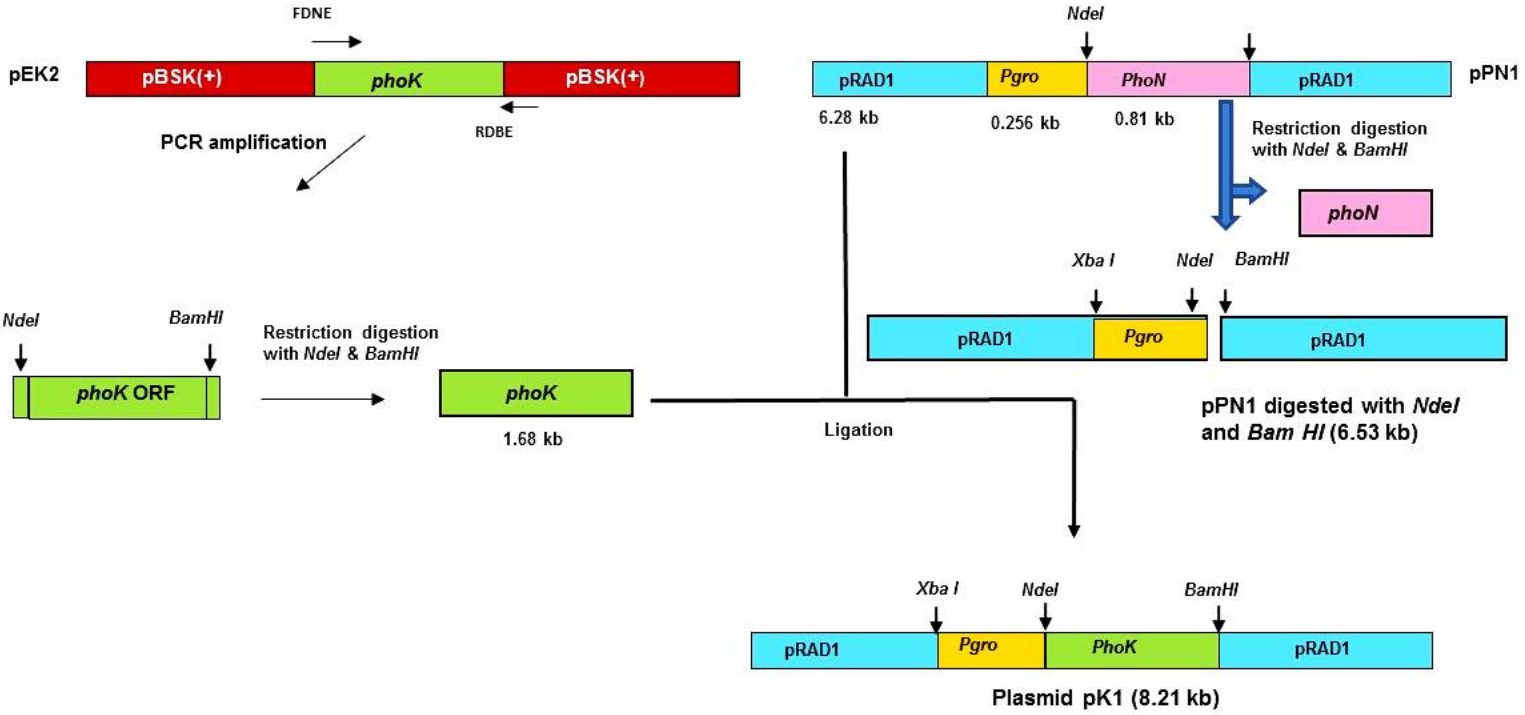

Fig. 3.2. Schematic representation of construction of pK1 plasmid

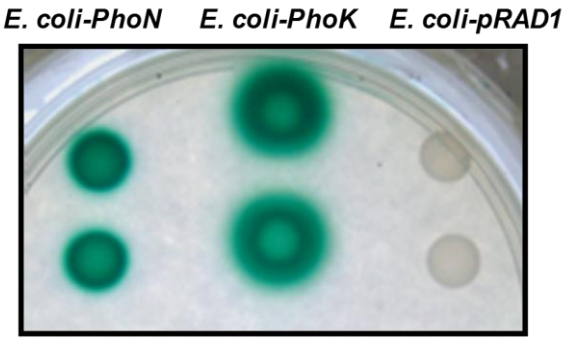

Fig. 3.3. Histochemical screening of *E. coli* transformants on PDP-MG plate. Recombinant *E. coli* cells were grown overnight (18 h) in liquid medium, centrifuged at 10,000 rpm for 2 min. Cell pellet was washed twice with double distilled water. Cell density equivalent to OD_{600nm}~1 (10 µl aliquot) was spotted in duplicate on a modified histochemical plate containing PDP-MG to assess expression and activity of phosphatases.

The recombinant *E. coli* strain carrying plasmid construct pK1 hereafter referred as to *E. coli-PhoK* strain, while the *E. coli* carrying empty pRAD1 plasmid (vector control) is referred as *E. coli-pRAD1* strain whereas the *phoN* carrying *E. coli* strain (Table 2.1) is named *E. coli-PhoN*.

The PhoN/PhoK positive strains appeared as dark green coloured spots due to deposition of methyl green. Unlike green spots of *E. coli-PhoN*, *E. coli-PhoK* showed a green halo extending outside the zone of growth into the medium, suggesting extracellular secretion of the PhoK enzyme, as reported in the parent *Sphingomonas* strain earlier. *E. coli-pRAD1* control cells did not show any green coloured spots and appeared light greyish in colour (Fig. 3.3).

The presence of 1.68 kb *phoK* insert in pK1 was confirmed by restriction digestion with different combinations of enzymes. Upon digestion with *NdeI*/*BamHI*, pK1 released 1.68 kb insert corresponding to *phoK* ORF and 6.28 kb pRAD1 vector (Fig 3.4). When digested with *NdeI* alone, linearized pK1 (8.21 kb) was obtained.

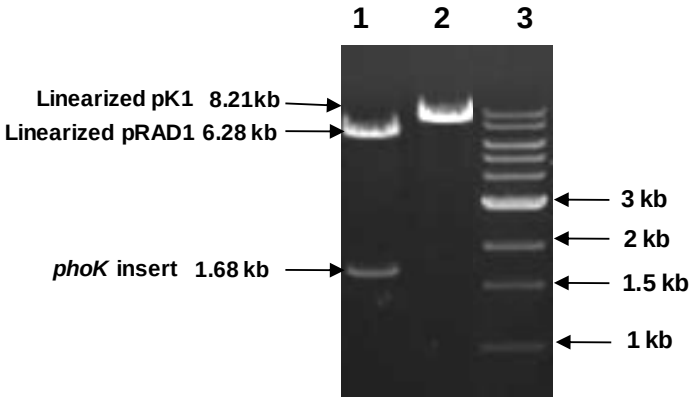

Fig. 3.4. Restriction digestion of plasmid pK1 isolated from *E. coli-PhoK*. The *NdeI/BamHI* digested pK1 (lane 1) was resolved by electrophoresis on 1% agarose gel and compared with pK1 digested with *NdeI* alone (lane 2). Lane 3: 1 kb DNA ladder (NEB).

In order to confirm that there was no modification of the *phoK* gene after cloning in *E. coli*, the nucleotide sequence integrity of *phoK* insert was ascertained by DNA sequencing using P_5 and P_6 vector specific as well as internal primers (F_{ow} and R_{ow}) for *phoK* (Table 2.3). The primer pair P_5 and P_6 was designed in such a way that they would amplify the

inserts present in the multiple cloning sites of pRAD1 plasmid. The primer P_5 binds 54 bp upstream of the multiple cloning start site (MCS); i.e. NruI (Fig. 3.1A) and the primer P_6 binds 58 bp downstream of the BamHI site in pRAD1. The *groESL* promoter and *phoK* ORF sequences obtained from recombinant clone were compared with the respective database sequences using a ClustalW analysis (Fig. 3.5). Such analysis revealed no change in the cloned sequence.

```
GATAACAATTTCACACAGGAAACAGCTATGACCATGATTACGCCAAGCTCGCGAGGCCTC 60
-------------------------TATGACCATGATTACGCCAAGCTCGCGAGGCCTC 34

                                                    XbaI
GAGATCTATCGATGCATGCCATGGTACCCGGGAGCTCGAATTCTAGACATGTTCAGGGAT 120
GAGATCTATCGATGCATGCCATGGTACCCGGGAGCTCGAATTCTAGACATGTTCAGGGAT 94

GGAAGCACGTATTGTCGCCCTACATATATACGTTAAAGCTAACAGCTGGCAAGGGGATAC 180
GGAAGCACGTATTGTCGCCCTACATATATACGTTAAAGCTAACAGCTGGCAAGGGGATAC 154

CCCCATTCCCCGTCCCAGTGCCCCTTGAGCGTCATAGACTCAGATTGTCAGCTTCGGTCA 240
CCCCATTCCCCGTCCCAGTGCCCCTTGAGCGTCATAGACTCAGATTGTCAGCTTCGGTCA 214

GTTGACATTTTTCTTATCGGCGCTCTACCATCCGTGACGGATTGAAGGCGCTGGGCGGGA 300
GTTGACATTTTTCTTATCGGCGCTCTACCATCCGTGACGGATTGAAGGCGCTGGGCGGGA 274

                                                        NdeI
AAAAGCTCGCCGGCACGACTCTCCGCCATTCCATCTCACTCACAGGAGGACCCCATATGT 360
AAAAGCTCGCCGGCACGACTCTCCGCCATTCCATCTCACTCACAGGAGGACCCCATATGT 334

TGAAACACGTCGCCGCTGCCCTGTTGCTCGCCACCGCCATGCCCGTCGTGGCGCAGAGCC 420
TGAAACACGTCGCCGCTGCCCTGTTGCTCGCCACCGCCATGCCCGTCGTGGCGCAGAGCC 394

CGTCGCGCACCGGCATCATCGCCAATAACTGGTTCGACCTCGACGCCAAGCGTGAGGACA 720
CGTCGCGCACCGGCATCATCGCCAATAACTGGTTCGACCTCGACGCCAAGCGTGAGGACA 694
```

Fig 3.5 Alignment of sequence of P_{groESL} + *phoK* from the database with the actual sequence obtained from *E. coli-PhoK* transformant. The sequence shown in different colours depicts: red - Shine-Delgarno sequences; blue - deinococcal *groESL* promoter, green - start codon of *phoK* ORF (GenBank accession no EF143994). Sequence of restriction sites for *XbaI* and *NdeI* are underlined.

3.2 Transformation of plasmid pK1 into *D. radiodurans*

The plasmid pK1 was transformed into *D. radiodurans* cells and transformants were selected on TGY plates containing chloramphenicol (Cm). The recombinant *D. radiodurans* strain carrying plasmid construct pK1 is hereafter referred to as *Deino-PhoK* strain, the *D. radiodurans* carrying empty pRAD1 plasmid (vector control) is henceforth referred to as *Deino-pRAD1* strain while the *phoN*-carrying *D. radiodurans* strain (Table 2.1) is named as *Deino-PhoN*.

The Cm^r transformants were patched on PDP-MG/Cm histochemical plates. *Deino-PhoK* spots appeared intense dark green in colour whereas *Deino-pRAD1* (control cells) showed typical orange coloured spots. In comparison, *Deino-PhoN*, that served as positive control formed light green coloured spots (Fig. 3.6). The intensity of green colour reflected the corresponding phosphatase activity of these strains. The intensity of the green coloured halo surrounding cells was less in recombinant *Deinococcus* cells (Fig. 3.6) as compared to recombinant *E. coli* cells (Fig. 3.3). This could be due to lesser input concentration of methyl green in the plates, higher concentration of methyl green inhibits *Deinococcus* growth.

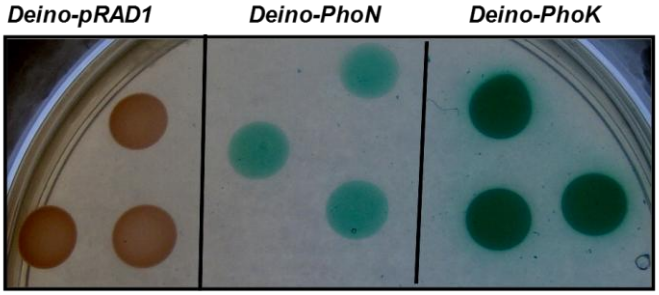

Fig. 3.6. Screening of *Deinococcus* transformed with pK1 on histochemical plate. Recombinant *Deinococcus* cells were grown overnight (18 h) in liquid medium and centrifuged at 10,000 rpm for 2 min. Cell pellet was washed twice with double distilled water. Cell density equivalent to OD_{600nm}~1 was spotted (10 µl) in triplicate on a modified histochemical plate containing PDP-MG to assess expression and activity of phosphatases.

For quick qualitative test of *Deino-PhoK* for expression and extracellular release of phosphatase, spent culture medium was spotted on PDP/MG plates or on *p*-NPP plates. Unlike spent medium of *Deino-pRAD1* cells, spent medium of *Deino-PhoK* cells showed intense green colour when spotted on PDP-MG plates or dark yellow colour on *p*-NPP plates (Fig. 3.7), which confirmed the extracellular secretion of PhoK in *Deinococcus*, similar to parent *Sphingomonas* sp. or in the recombinant *E. coli-phoK*.

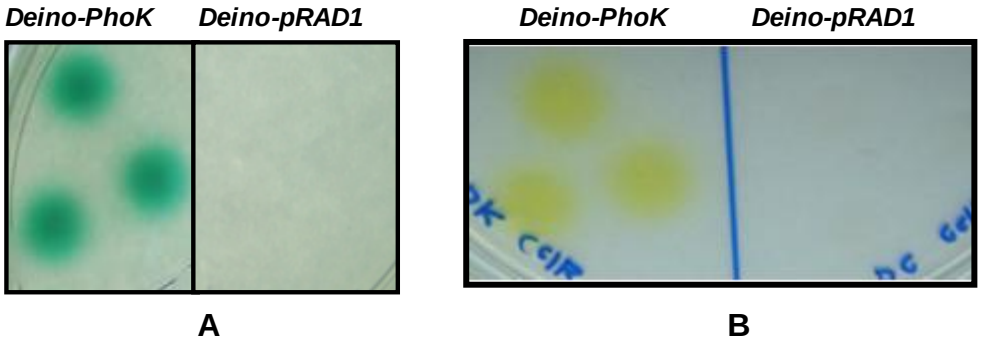

Fig. 3.7. Qualitative affirmation of extracellular secretion of PhoK in recombinant *Deinococcus* strains. Spent culture medium of recombinant *Deinococcus* strains (grown for 18 h) was spotted (10 µl) on PDP-MG (A) or on *p*-NPP plates (B) to visualize green or yellow colour development after 1 h for p-NPP plates and 4 h for PDP-MG plates.

Deino-PhoK (green) and *Deino-pRAD1* (orange) colonies (Fig. 3.6) were subjected to colony PCR (using primers FDNE and RDBE, Table 2.3) to confirm the presence of *phoK* insert in *Deinococcus* (Fig 3.8). The amplified products were resolved on 1% agarose gel. The 1.68 kb *phoK* insert was observed in *Deino-PhoK*, while the control sample had no amplified product (Fig. 3.8).

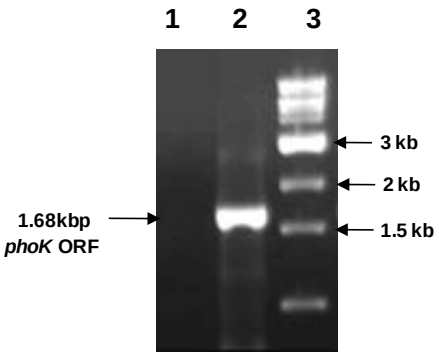

Fig. 3.8. Colony PCR of recombinant *Deinococcus* transformants. Lane 1: *Deino-pRAD1* cells without any PCR product, Lane 2: *Deino-PhoK* showing 1.68 kb *phoK* insert. Lane 3: 1 kb DNA ladder (NEB).

3.3 Expression and activity of PhoK in recombinant strains

3.3.1. *In vivo* cell-associated phosphatase activity

Having qualitatively ascertained the PhoK expression on histochemical plates, cell associated PhoK activity in *Deino-PhoK* or *E. coli-PhoK* cells (grown for 18 h) was determined. Phosphatase activity of all recombinant strains (PhoN/PhoK expressing) was determined using para-nitrophenyl phosphate (*p*-NPP). For *p*-NPP, activity was measured in terms of end product formed (*p*-NP) by determining absorbance spectrophotometrically at 405 nm. The activity was measured for PhoN/PhoK expressing cells at their respective pH optima (Chapter II, section 2.5.2). PhoN-expressing cells were used for comparison between the two phosphatases and as positive control.

In terms of cell-associated activity, *Deino-PhoK* cells showed nearly 3-4 fold higher activity, (as visualised by the intensity of yellow colour) than *E. coli-PhoK* (Fig. 3.9). *E. coli-PhoK* cells showed around 1500 ± 150 units of specific activity, while *Deino-PhoK* showed around ~ 6875 ± 415 units of specific activity (Table 3.1). *E. coli-PhoK* cells showed activity similar to that of *E. coli-PhoN* cells, while *Deino-PhoK* cells showed unexpectedly higher (~35-40 fold) phosphatase activity than *Deino-PhoN* (~170 ± 20 units) cells (Table 3.1).

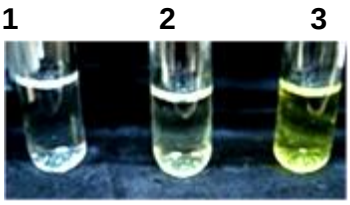

Fig. 3.9. Comparison of cell associated PhoK activity using *p*-NPP as substrate. Whole cells (equivalent to OD_{600}~0.1) were incubated with *p*-NPP for 30 min in Tris-Cl buffer (50 mM, pH 9) and reaction was stopped by 0.2 N NaOH. Difference in intensity of yellow colour is observed in 1: control (No cells, only substrate); 2: *E. coli-PhoK*, 3: *Deino-PhoK*.

Table 3.1 Cell-associated phosphatase activity of different recombinant strains.

Strains	**PhoK/PhoN activity (nmoles p-NP released/min/mg protein)***
E. coli-pRAD1	8 ± 3
E. coli-PhoN	1850 ± 230
E. coli-PhoK	1545 ± 150
Deino-pRAD1	18 ± 5
Deino-PhoN	170 ± 20
Deino-PhoK	6875 ± 415

***** Cell associated phosphatase activity was assayed using *p*-NPP as substrate as explained in legend to Fig. 3.9 and the specific activity was calculated by measuring protein content in cell equivalent used for the assay. For PhoK expressing cells, assay was carried out at pH 9.0, while for PhoN expressing cells assay was carried out at pH 5.0.

Activity of *Deino-PhoK* cells was also determined in terms of P_i release using three different substrates; *p*-NPP, β-GP or phenolphthalein di-phosphate (PDP) (Table 3.2). Phosphate release was measured spectrophotometrically by phosphomolybdic acid method (Chapter II, section 2.5.2) in the supernatant buffer solution after incubation with cells with substrate for 30 min. Activity was measured by using spent medium also (Table 3.2).

Table 3.2 Activity of cells in terms of phosphate hydrolysis from substrate

Substrate used	Activity in terms of P_i release	
	***Deino-PhoK* cells**	**** Spent medium**
p-NPP	3740 ±290	244 ± 25
β-GP	1602 ±45	91 ±15
PDP	3840 ±415	213 ±35

* P_i release measured in terms of nmoles Pi released/min/mg protein.

** P_i release measured in terms of nmoles Pi released/min/ml spent medium.

Deino-PhoK cells showed equivalent activity with *p*-NPP as well as PDP (pH 9.0) while 2-2.5 fold lower activity with β-GP. This was reflected in activity of spent medium too, which lacked cells but contained the extracellularly secreted enzyme. This suggested that the solubility and the rate of uptake of these substrates by PhoK may not be similar. This data confirmed the results from previous studies carried out with purified PhoK using different substrates. In terms of actual application for bioremediation, β-GP would serve as a better substrate as by-product of *p*-NPP or PDP cleavage are pollutants themselves. Therefore, for U precipitation studies β-GP was chosen as the substrate over others.

3.3.2 *In vitro* PhoK activity by zymogram analysis

In gel zymogram assays were carried out with the cell-free extracts of the recombinant cells. In zymogram, both *E. coli-PhoK* and *Deino-PhoK* extracts showed comparable PhoK activity with a major band visualized at ~60 kDa (Fig. 3.10A). Along with this band, multimeric forms of PhoK were also observed on the zymogram. When protein gel was incubated for shorter time (2-3 h) for colour development, monomeric band appeared first, while after prolonged overnight incubation oligomeric bands were observed. Thus, equally active PhoK protein was indeed expressed in both *E. coli-PhoK* and *Deino-PhoK* strains.

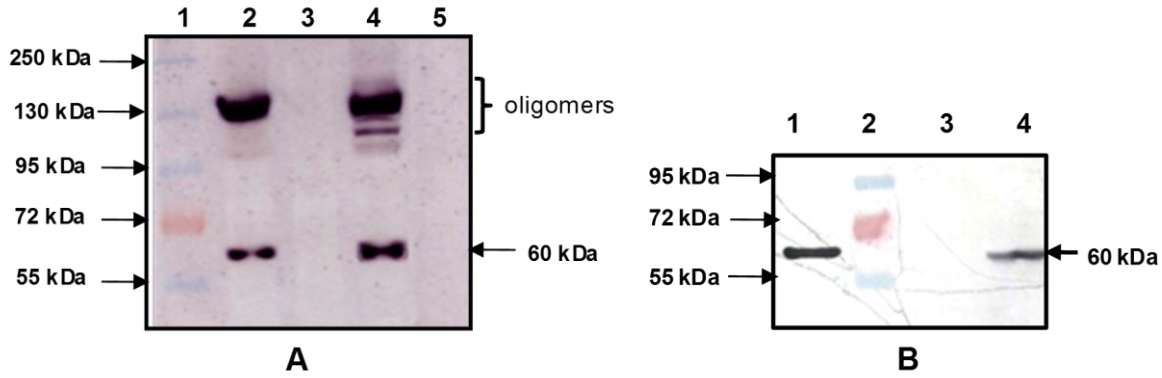

Fig. 3.10. Expression and activity analysis of PhoK. (A) Protein extracts (20 µg) were separated by 10% non-reducing SDS-PAGE and stained for phosphatase activity at pH 9. Lane 1, prestained marker (NEB); lane 2, *E. coli-PhoK*; lane 3, *E. coli-pRAD1*; lane 4, *Deino-PhoK*, and lane 5, *Deino-pRAD1*. (B) Protein extracts (30 µg) from recombinant *Deinococcus* strains were separated by 10% reducing SDS-PAGE and immune-detected using PhoK antiserum. Lane 1, His-tagged purified PhoK protein used as positive control (10 µg); lane 2, prestained NEB marker; lane 3, *Deino-pRAD1* and lane 4, *Deino-PhoK*. PhoK band corresponding to 60 kDa is depicted by arrow.

Expression of PhoK was further confirmed by Western blotting and immune-detection using the PhoK-specific antiserum. Under reducing conditions, the PhoK monomer was detected as a solitary 60 kDa band in *Deino-PhoK* (Fig. 3.10B).

3.4 Optimization of PhoK expression

The bioprecipitation of uranium depends on the phosphatase activity of cells, i.e. higher the phosphatase activity, faster would be the rate of bioprecipitation of uranium. Consequently, if higher phosphatase activity is attained by lesser biomass, higher U loading can be achieved. It was therefore desired to determine the phase of growth wherein the PhoK activity of the cells was maximal.

When cells from similar phase of growth were assayed, *Deino-PhoK* always showed higher phosphatase activity than *E. coli-PhoK* (irrespective of the phase of growth chosen) (Fig. 3.11 and Fig. 3.12). The PhoK activity in both *Deino-PhoK* and *E. coli-PhoK* was low

in lag phase, reached maximal values in the early exponential phase (5 h) and subsequently decreased in the stationary phase. In *Deino-PhoK* cells, the cell-associated PhoK activity during early exponential phase was 2-2.5 times more than lag phase or stationary phase (Fig. 3.12). The AP activity of *Deino-PhoK* and *E. coli-PhoK* cells at early exponential phase of growth (5 h) was 15000 ± 300 and 5800 ± 200 units respectively. In both *Deino-PhoK* and *E. coli-PhoK* enzyme activity was also observed in the spent medium confirming extracellular release of the enzyme. The extracellularly released enzyme accumulated in the medium and maximal activity in the spent medium was observed during the stationary phase.

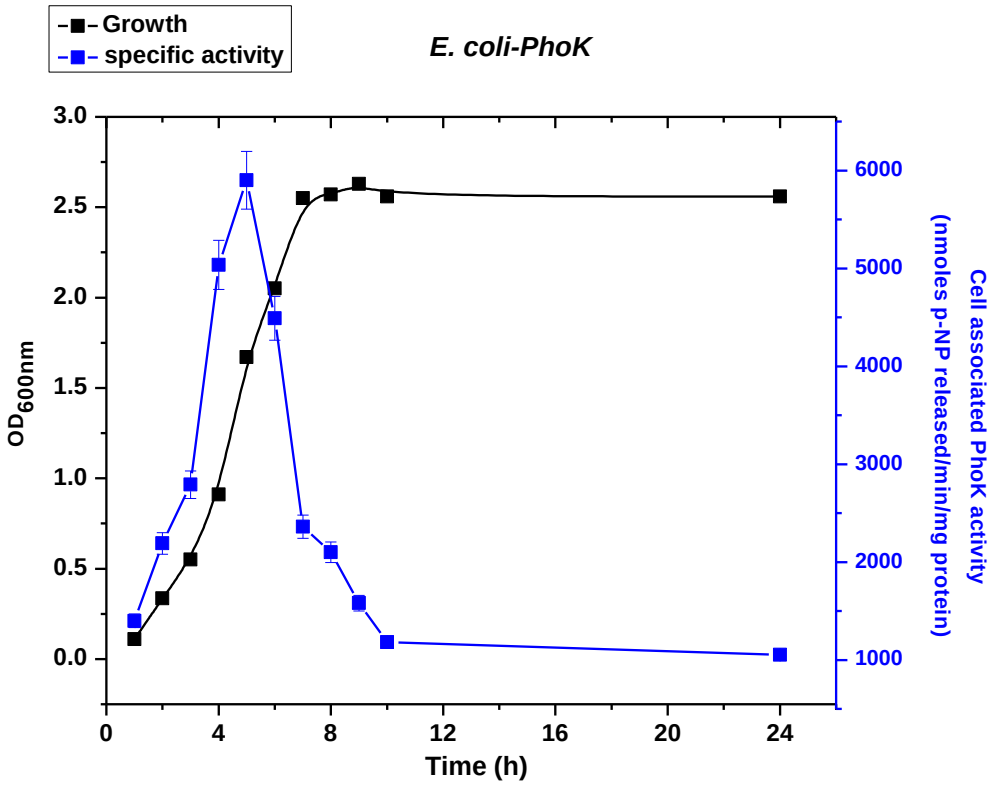

Fig. 3.11. Phosphatase activity as a function of growth in *E. coli-PhoK*. *E. coli-PhoK* cells (18 h grown) were inoculated with initial OD_{600} 0.05 in 100 ml TGY liquid medium supplemented with Cm^3. After every 2 h (up to 24 h), 2 ml aliquot was removed and analysed for growth and the cell-associated PhoK activity. Growth was monitored by measuring OD_{600nm} spectrophotometrically and PhoK activity using *p*-NPP as substrate. The specific activity was calculated by measuring protein content in cell equivalent used for the assay.

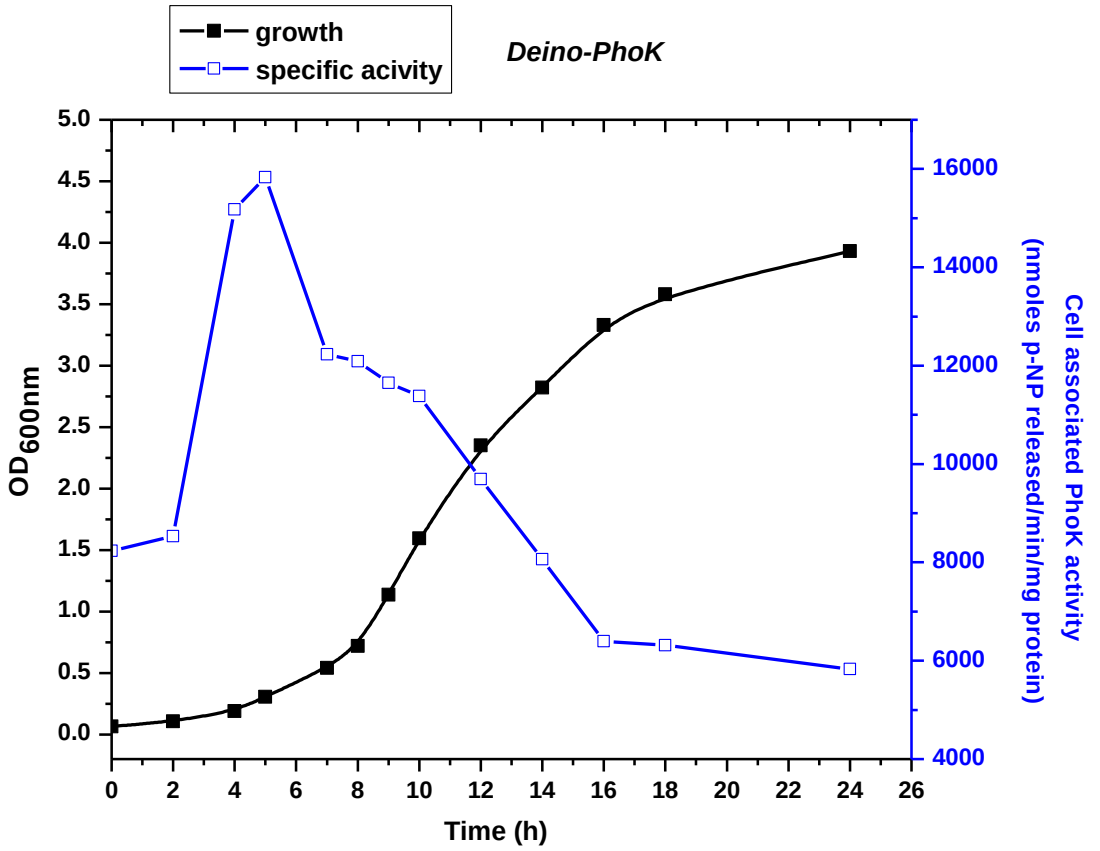

Fig. 3.12. Phosphatase activity as a function of growth in *Deino-PhoK*. *Deino-PhoK* cells (18 h grown) were inoculated with initial OD_{600} 0.05 in 100 ml TGY liquid medium supplemented with Cm^3. After every 2 h (up to 24 h), 2 ml aliquot was removed and analysed for growth and the cell-associated PhoK activity. Growth was monitored by measuring OD_{600nm} spectrophotometrically and PhoK activity using *p*-NPP as substrate. The specific activity was calculated by measuring protein content in cell equivalent used for the assay.

Growth-dependent PhoK activity was determined by *in gel* activity assay too. Cell free protein extracts of *Deino-PhoK* at different phases of growth (lag, early exponential and stationary) were used for zymogram analysis. PhoK activity was visualized as a distinct band around 60 kDa in zymograms. Short-term incubations showed 1.5-2 times higher intensity band in early exponential phase rather than in late exponential (10 h) or stationary phase (24 h) (Fig. 3.13). After prolonged incubation of gel with the substrate, oligomeric forms of PhoK started appearing (Fig. 3.13B) suggesting monomeric form of PhoK might be more active than the oligomeric forms. The formation of bulky multimeric form of PhoK at later stages

(stationary phase) of growth in higher amount might result in drop in cell associated PhoK activity at stationary phase. The zymographic analysis confirmed that the recombinant *Deino-PhoK* cells showed higher PhoK activity in early exponential phase than in the stationary phase of growth.

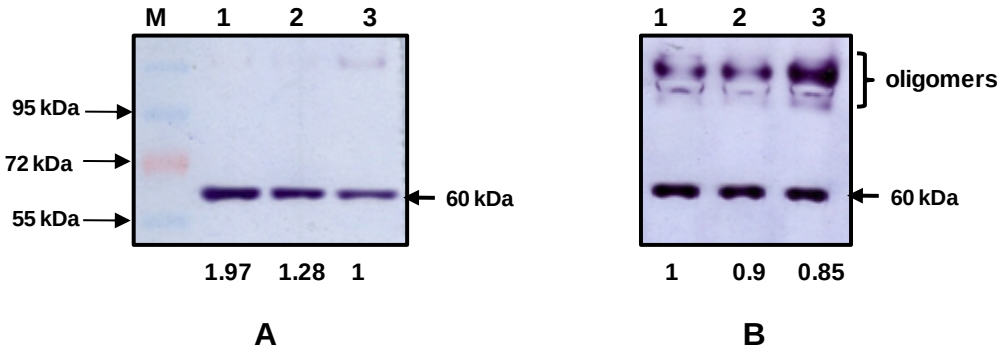

Fig. 3.13. PhoK activity as a function of growth. Protein extracts (10 µg) of *Deino-PhoK* at different stages of growth were resolved by 10% non-reducing SDS-PAGE. Gel was incubated with NBT-BCIP for colour development for (A) 2 h or (B) overnight (18 h). Time points for analysis were lane 1 (5 h); lane 2 (10 h) and lane 3 (24 h). The numbers below the lanes in figure indicate the relative intensity of bands, as determined by densitometry.

3.5 Radiation response of *Deino-PhoK*

D. radiodurans is one of the most radiation resistant organisms known [2]. It has been possible to express foreign genes in *Deinococcus* with no effect on its growth, even at high doses of radiation [2, 137-138, 152]. These were the incentives due to which *Deinococcus* was chosen for bioprecipitation of U employing the PhoN protein earlier [121] and PhoK protein in the present study. Since uranium precipitation is also to be accomplished in high radiation environment, it was important to know if cloning of foreign gene like *phoK* affected the radio-resistance of *Deinococcus*.

3.5.1 Effect of gamma radiation on survival of recombinant *Deino-PhoK*:

The radiation resistance of *Deino-PhoK* was compared with that of *Deino-pRAD1* (Fig. 3.14). The radiation resistance of the recombinant strains was determined in terms of their D_{10} values, which is the does that causes 90% lethality. Both, *Deino-pRAD1* and *Deino-PhoK* showed D_{10} values of around 15.6 kGy, indicating that introduction, expression and activity of *phoK* gene did not alter or compromise the inherent radio-resistance of *D. radiodurans.* Similar results were earlier reported for *Deino-PhoN* which retained its acid phosphatase activity and U precipitation capability even after 6 kGy of γ-irradiation [121].

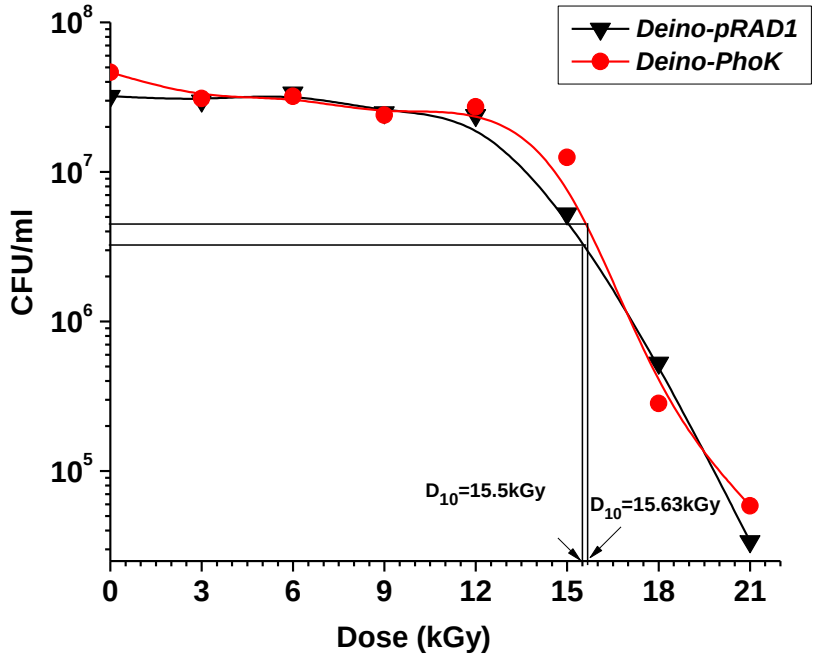

Fig. 3.14. Radioresistance of *Deino-PhoK* strain. Equivalent cells (OD_{600} ~1) of *Deino-PhoK* or *Deino-pRAD1* strains were exposed to different doses of ^{60}Co-gamma radiation (with dose rate of 4.2 kGy/h) and survival was measured in terms of colony forming units (CFU/ml). The calculated D_{10} values are presented in the graph.

3.5.2 Effect on cell associated PhoK activity under radiation stress:

It is also equally essential to determine the stability and activity of PhoK protein in the recombinant *Deino-PhoK* after high doses of gamma radiation. If the PhoK protein should

degrade or get inactivated under high radiation stress, then the strain will not be able to bring about uranium precipitation. Therefore, cell associated PhoK activity of *Deino-PhoK* was determined after exposure to different doses of gamma radiation. *Deino-PhoK* cells (grown till early exponential phase) were exposed to different doses of gamma radiation (3- 21 kGy, with dose rate of 4.2 kGy/h) and the PhoK activity was determined in terms of *p*-NP release. The activity was compared with control (unirradiated) *Deino-PhoK* cells. The cell bound activity of PhoK, assayed immediately after irradiation, remained unaffected up to 12-15 kGy of γ-ray dose (Fig. 3.15). However, beyond 15 kGy, which is the D_{10} value for *Deinococcus*, there was 25-30% decrease in the activity. This shows that PhoK is a robust enzyme and tolerates high radiation doses of 15 kGy. Though cell survival decreases by 90% at this dose, PhoK activity decreases only by 25-30%.

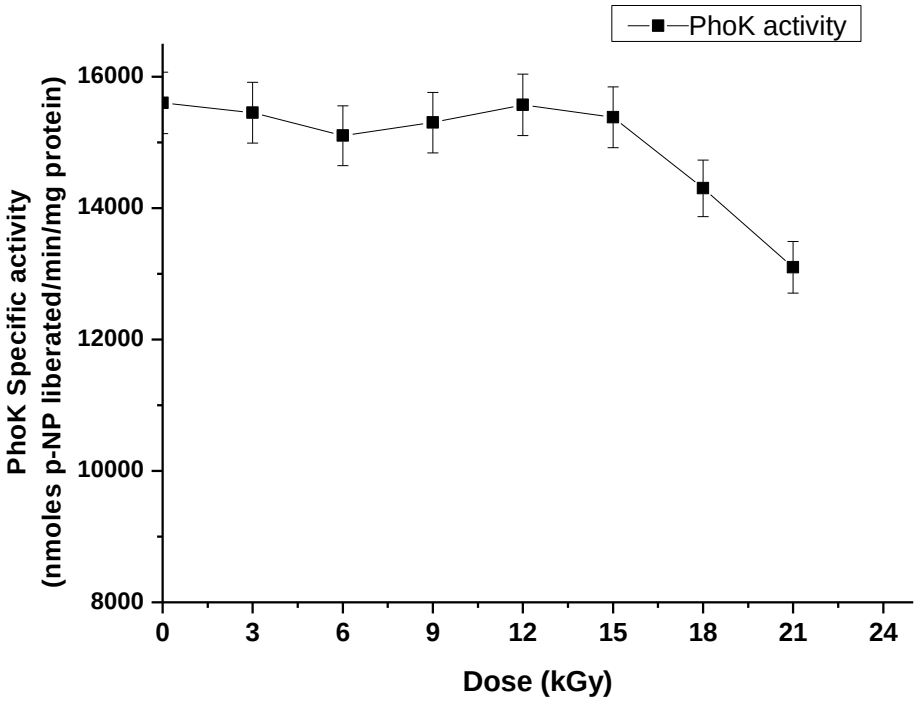

Fig. 3.15. Effect on cell associated PhoK activity after radiation stress. *Deino-PhoK* cells (OD_{600} ~1) were suspended in 10 ml MOPS buffer (10 mM, pH 9.0) and exposed to different doses of ^{60}Co-gamma radiation (with dose rate of 4.2 kGy/h). After every 3 kGy dose, 200 µl aliquot was withdrawn from flask, cells were centrifuged and washed twice with double distilled water and used to determined specific activity using *p*-NPP as substrate.

3.6 Uranium precipitation studies using *Deino-PhoK* cells

3.6.1 Optimization of uranium precipitation conditions

The 3-(N-mopholino) propane sulfonic acid (MOPS) buffer was chosen for U bioprecipitation studies under alkaline conditions (pH 9). It is a structural analogue of MES and contains piperazine ring which is soluble in water. MOPS buffer has a pK_a value of 7.2 and is an excellent buffer for biological systems and biochemical studies. MOPS is a metal-non- interacting buffer, unlike other buffers e.g. bicarbonate, acetate, Tris-Cl, citrate etc, and was selected to ensure that the concentrations of uranium used (1-5 mM) did not alter the pH grossly. This was important since the enzyme mediated precipitation conditions had to be kept optimal. Most importantly, at higher concentrations of U, MOPS did not influence the speciation of the uranyl compounds. This was verified by monitoring the absorption spectra of uranyl which shows specific absorption maxima at 434 nm, 448 nm and 464 nm [148] . In the presence of excess of carbonate ions (with and without MOPS, pH 9.0) the absorption spectra remained identical in the visible light range between 400-500 nm with (Fig. 3.16).

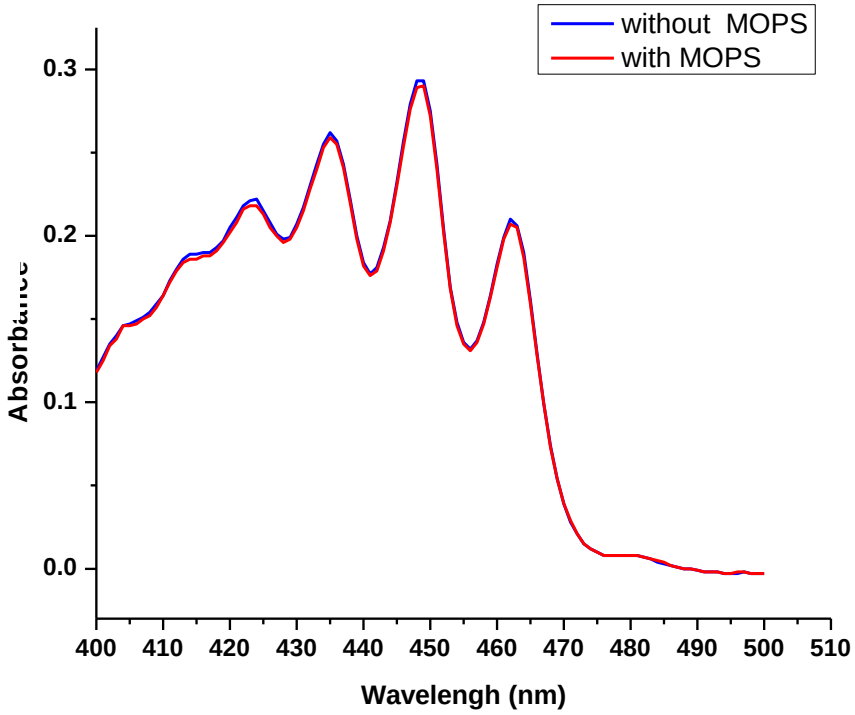

Fig. 3.16. Uranyl ion spectra in the presence or absence of MOPS. Uranyl carbonate (5 mM final concentration) solution was prepared in 10 mM MOPS buffer or in double distilled water separately. Absorbance was recorded spectrophotometrically from 400-500 nm and the presence of peaks at 434 nm, 448 nm and 464 nm was confirmed.

3.6.2 Kinetics of U precipitation by *Deino-PhoK* cells

Early exponential phase (5 h grown) *Deino-PhoK* cells were used to evaluate their U precipitation ability, using either *p*-NPP or β-glycerophosphate (β-GP) as substrates. The U precipitation is brought about by the inorganic phosphate ligand generated via cleavage of an organic phosphate donor (*p*-NPP or β-GP) by the PhoK protein present in the cells. Therefore, the U precipitation capability of recombinant strains depends on the PhoK activities they carry. *Deino-PhoK* cells showed higher inorganic phosphate release with *p*-NPP than with β-GP (Table 3.2). Hence for preliminary study of U precipitation kinetics, both the substrates were employed. Cells were incubated with uranium (1 mM) taken in 10 mM MOPS buffer, pH 9.0, along with 5 mM of phosphate donor substrate. *Deino-pRAD1* cells, used as control, were incubated with U under similar conditions. Other appropriate controls like absence of cells or substrate (β-GP or *p*-NPP) or uranium were maintained to

ascertain that precipitation was indeed mediated by PhoK. U precipitation was monitored, both as metal loss from the supernatant and as metal gain in the pellet, and expressed as % precipitation of input U.

No detectable spontaneous precipitation of uranium occurred in abiotic control solutions where U was incubated with only substrate in the absence of cells. In biotic controls, where cells were incubated with U in the absence of either of the substrate, only 2-3 % U was found to be gained in the pellet and may represent amount of U adsorbed to cells under alkaline conditions (Table 3.3). In *Deino-pRAD1* control cells, U removal was found to be around 2-3%, even after prolonged incubation up to 18 h, thus confirming that the observed precipitation in *Deino-PhoK* strain was indeed PhoK mediated.

Table 3.3 U removal in biotic and abiotic controls.

Time (h)	**% U present**				
	***Deino-pRAD1* (Pellet)**		**Abiotic control (No cells, only U)**		**Substrate control (Cells + U)**
	β-GP	***p*-NPP**	**β-GP**	***p*-NPP**	
0	1.9	2.2	0.05	0.08	2.1
1	2.1	2.1	0.08	0.07	2.5
2	2.4	1.8	0.06	0.1	2.4
3	2.6	2.3	0.1	0.09	2.2
6	2.3	2.5	0.08	0.12	1.8
18	2.5	2.8	0.2	0.1	2.7

Kinetics of U removal from the solution completely matched that of gain in U precipitate in the pellet, confirming one to one correspondence between the two processes. With *p*-NPP, a more rapid precipitation was observed as compared to β-GP at the initial time points of precipitation. *Deino-PhoK* cells could precipitate ~50% uranium within 15 min with *p*-NPP whereas it took nearly 30 min with β-GP (Fig. 3.17). Notwithstanding these initial differences, both the substrates resulted in more than 90 % U precipitation at the end of 2 h.

For bioremediation, β-GP would serve as a better substrate as byproduct of *p*-NPP cleavage is a toxic pollutant. Further studies were, therefore, continued with β-GP as a substrate**.**

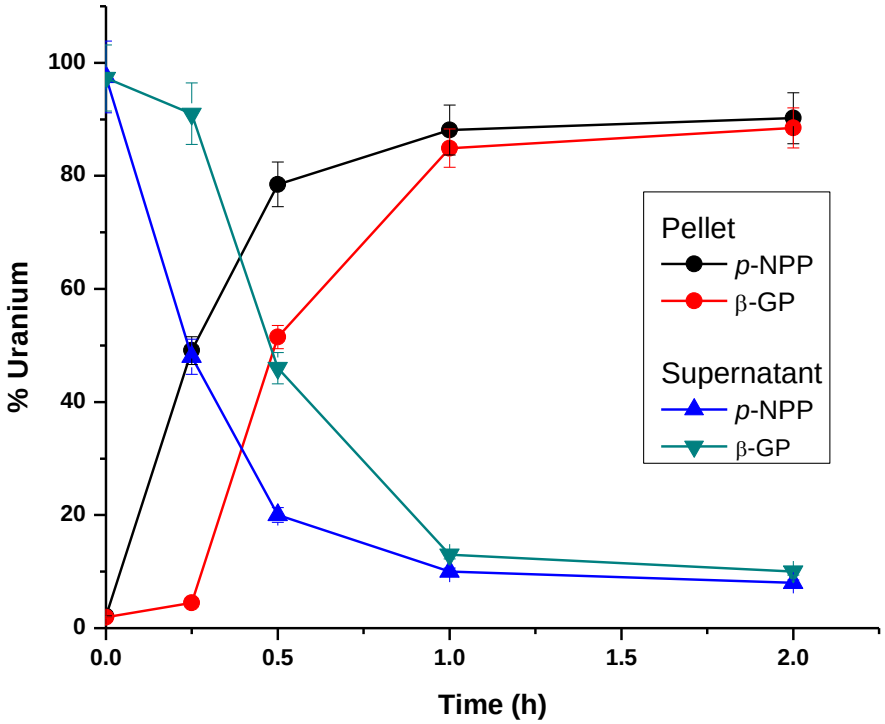

Fig. 3.17 Kinetics of U precipitation by *Deino-PhoK* cells with two different substrates. *Deino-PhoK* cells (OD_{600nm}~1) were incubated with 1 mM U and either *p*-NPP or β-GP (5 mM) as substrate in 10 mM MOPS buffer (pH 9.0) for 2 h. Residual U present in the supernatant and the amount present in the pellet (after digesting the cells with conc. HCl) were estimated by the Arsenazo III reagent.

3.6.3 Uranium precipitation at different concentrations of β-GP

It is essential to optimize the concentration of β-GP required for (a) rapid bioprecipitation of U, and (b) to minimize the cost of the process at the waste site. Therefore, *Deino-PhoK* cells were employed to precipitate 1 mM uranium at different concentrations of β-GP (1-10 mM). The rate of precipitation was found to increase with increasing concentration of β-GP. At 10 mM concentration, U precipitation was most rapid whereas at 1 mM concentration, it was slowest. To achieve more than 90% precipitation it took more than

4 hours at 1 mM concentration of β-GP, whereas at 10 mM concentration the same required around 45 minutes. However, at 3, 5 and 10 mM concentration, maximal precipitation was achieved by 2 hours (Fig. 3.18). Thus, though stoichiometrically 1 mM β-GP was sufficient to bring about precipitation of 1 mM U, 5 mM β-GP was chosen as optimal concentration for rapid precipitation of more than 80 % U within 1 h, in subsequent experiments.

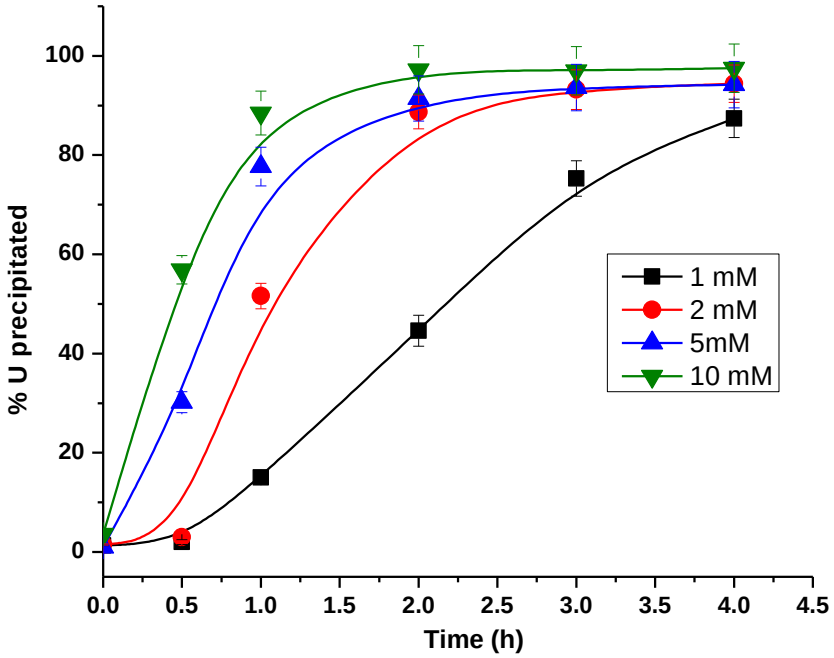

Fig. 3.18 U precipitation by *Deino-PhoK* cells at different input concentrations of substrate (β-GP). *Deino-PhoK* cells (OD_{600} 1) were independently incubated with vials containing 1 mM U with varying concentrations of β-GP under static conditions at 30° C (pH 9.0). U loss from supernatant was measured at different time intervals by Arsenazo III.

3.6.4 Comparison of uranium bioprecipitation by *Deino-PhoK* and *Deino-PhoN* strains.

The U precipitation is brought about by the inorganic phosphate ligand generated by cleavage of an organic phosphate donor by the phosphatase (PhoN/PhoK) present in the cells, and would depend on the phosphatase activities they carry. The relative efficiency of *Deino-PhoK* and *Deino-PhoN* cells to precipitate uranium was found to be very different at 1 mM input U, in accordance with their corresponding phosphatase activity (Fig.3.19) at optimum

pH. *Deino-PhoK* cells could precipitate more than 80% uranium within 2 h whereas *Deino-PhoN* cells could precipitate only 15 % uranium in the same period (Fig. 3.19). To achieve more than 90% precipitation, *Deino-PhoK* cells required only 2 h, whereas *Deino-PhoN* strain required >8 h to achieve the same. The control *Deino-pRAD1* cells adsorbed only 7-8 % of input U (provided as uranyl nitrate) at pH 6.8 and 2-3 % U (provided as uranyl carbonate) at pH 9.0. Maximal U loading (~1 g U/g dry weight) on the biomass was achieved in *Deino-PhoK* cells by 2 h and in *Deino-PhoN* cells only by 18 h.

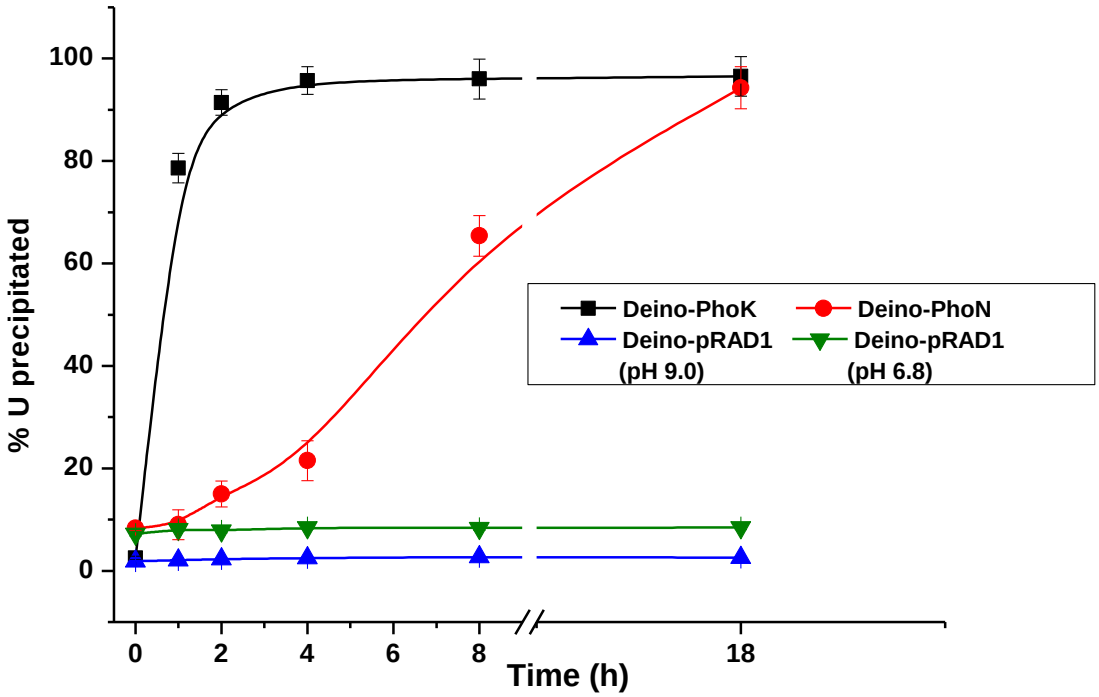

Fig. 3.19 Comparison of uranium bioprecipitation by *Deino-PhoK* and *Deino-PhoN* strains. Equivalent cells (OD_{600} 1) of all three strains were used to precipitate 1 mM U with 5 mM β-GP, respectively at pH 6.8 (*Deino-PhoN*), pH 9.0 (*Deino-PhoK*), and at both pH (*Deino-pRAD1*). U loss from supernatant was measured at different time intervals by Arsenazo III.

3.6.5 Uranium precipitation by *Deino-PhoK* at different input U concentrations

One of the important factors involving metal removal is the concentration of the metal itself. The recombinant *Deino-PhoK* strain was tested for its uranium precipitation ability at

increasing concentrations of input uranium (1-10 mM) (under carbonate abundant conditions at pH 9.0), with correspondingly increasing concentrations of β-GP. The rate of U precipitation increased with increasing concentration of uranium. At 10 mM uranium concentration, cells could precipitate around 60% uranium within 15 minutes, whereas same was achieved in 40 minutes at 2 mM concentration. At all concentrations more than 80% uranium was precipitated within 1 hour (Fig. 3.20). Maximum uranium loading was shown to be 10.7 g of U/ g dry weight cells at 10 mM concentration. Thus *Deino-PhoK* cells proved to be good for U precipitation over a wide range of metal concentration.

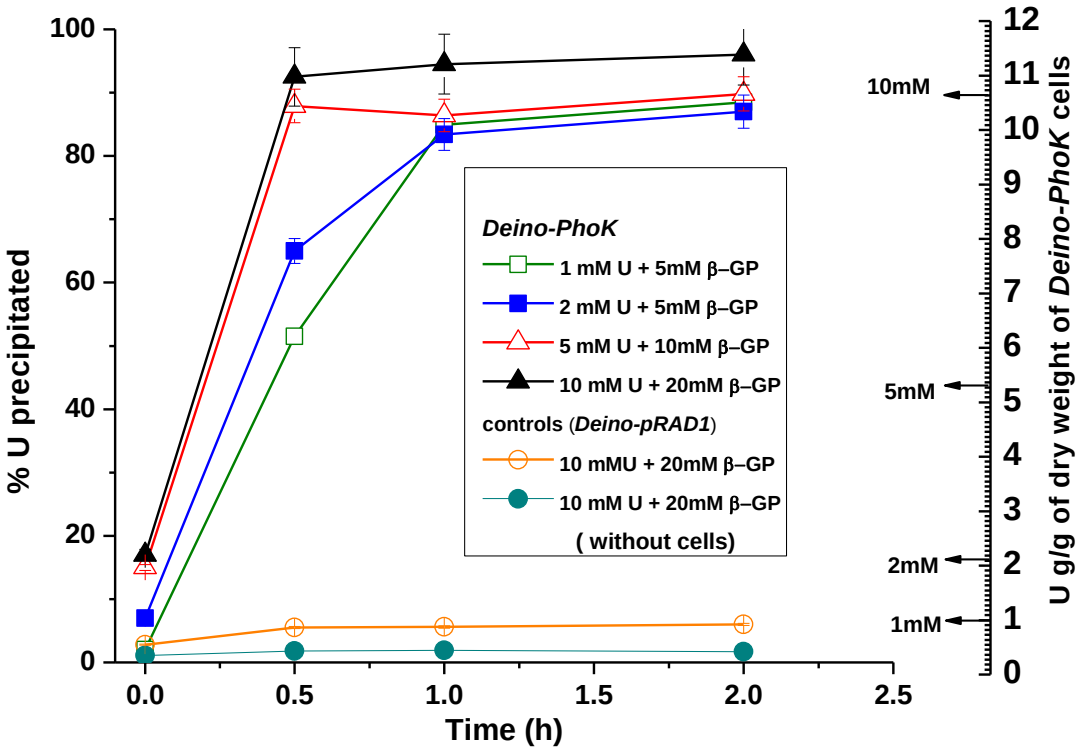

Fig. 3.20. U precipitation by *Deino-PhoK* cells at different input U concentrations. U precipitation (pH 9.0) by *Deino-PhoK* cells (OD_{600} 1) at different input U concentrations and proportionately increasing concentrations of β-GP. Controls containing either no cells (abiotic) (●), or *Deino-pRAD1* (○) cells were also included for comparison.

The main objective of this work was to construct a strain which would be suitable for bioremediation of nuclear waste. Depending on the type of waste, the total radioactivity of such waste solutions may vary from a few Ci/L (in high level liquid waste) to µCi/L (in low level liquid waste). Some of the nuclear wastes contain very high level of radioactivity e.g. aqueous high level liquid waste generated during reprocessing of spent fuel rods. The U powered nuclear plants and nuclear reactors also generate a large volume of intermediate level liquid waste (ILLW) and low level liquid waste (LLW) that is alkaline in nature (pH 8-12), containing residual U (5-20 mM) and other fission products of U e.g. Cs, Sr, Pu etc. which are present in micromolar to millimolar concentrations [4, 153]. *Deino-PhoK* cells showed highest cell associated phosphatase activity as well rapid and efficient U precipitation ability under ambient conditions, among the bacterial strains reported so far. Though PhoK protein seemed to survive and function at high radiation doses, it was of prime importance to evaluate the U precipitation ability of *Deino-PhoK* strain in high radiation environment

3.6.6 U precipitation by *Deino-Pho*K cells post-irradiation.

Early exponential phase cultures of *Deino-PhoK* were irradiated up to 6 kGy following which they were challenged with 1 mM U under alkaline conditions (pH 9). Both irradiated and unirradiated *Deino-PhoK* cells could precipitate uranium from 1 mM solution with similar efficiency (Fig. 3.21). Thus *Deino-PhoK* cells did not compromise their bioprecipitation ability even after exposure to 6 kGy gamma irradiation and has the potential to be used in radioactive nuclear waste.

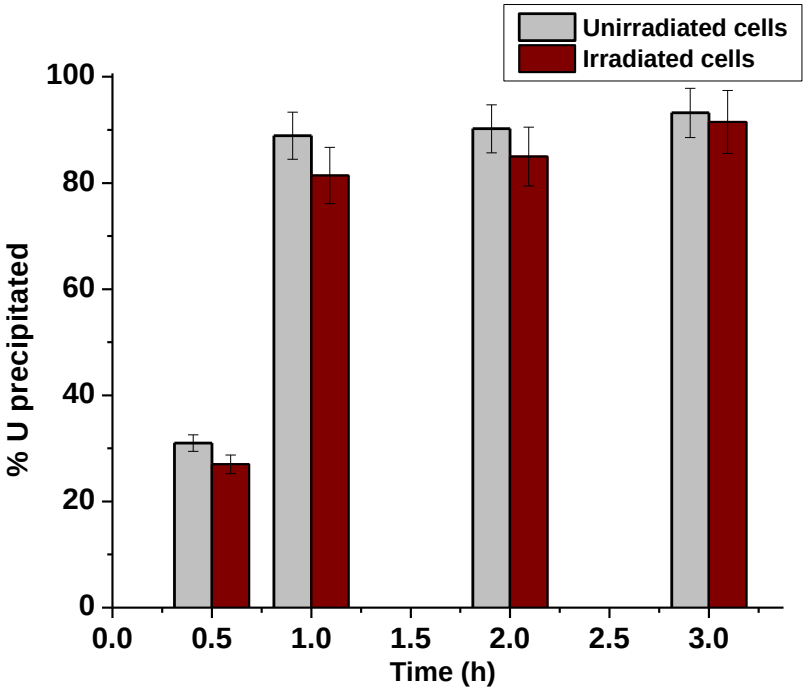

Fig. 3.21 Post irradiation uranium precipitation ability of *Deino-PhoK* cells. *Deino-PhoK* cells (OD_{600nm} ~ 1) were exposed to 6 kGy dose of gamma radiation (dose rate: 4.2 kGy/h, ^{60}Co Gamma Cell 5000 irradiation unit, BARC, India) followed by incubation with 1 mM U and 5 mM β-GP at pH 9.0. Unirradiated *Deino-PhoK* cells served as control. The amount of U removed from the supernatant was measured up to 3 h by Arsenazo III reagent.

Depending on the type of waste, the total radioactivity in waste solutions may vary from a few Ci/L (in high level liquid waste) to µCi/L (in low level liquid waste). The U powered nuclear plants and nuclear reactors also generate a large volume of intermediate level liquid (ILLW) and Low level liquid waste (LLW) which are alkaline in nature (pH 8-12). In the intermediate level radioactive waste or low level liquid waste (pH 8.0-12.0), U concentration lies between 1-5 g/L (4-20 mM) with total radioactivity of ~5–50 Ci/L [4, 153]. Other metals in this waste are radionuclides like Pu, Cs, Sr, Ru etc. which are present in sub milli-molar concentrations. However, the composition and conditions of radioactive waste vary largely from one site to another and full details are rarely published. No utilizable carbon sources are generally available but this may not be a constraint for application of *D.*

radiodurans cells which are highly starvation tolerant [Microbiol. Mol. Biol. Revs. (2011) 7: 133-191]. Therefore, U precipitation of *Deino-PhoK* cells was evaluated in the presence of Cs, Sr and after exposure to 6 kGy dose. *Deino-PhoK* was incubated with U (1 mM) along with Cs and Sr (1 mM each), subjected to 6 kGy dose and evaluated for its ability to precipitate U. Exposure to radiation and/or presence of Sr/Cs had no consequence on the U precipitation ability of the *Deino-PhoK* cells. At the end of 2 h, more than 90% U was precipitated by *Deino-PhoK* (Table 3.4) which is similar to the uranium precipitation ability of *Deino-PhoK* cells (control) in the absence of radiation and/or Cs/Sr metal ions.

Table 3.4- Effect of radiation and heavy metals on U precipitation ability of *Deino-PhoK*

Recombinant strains used	Radiation (6 kGy)	Cs (1 mM)	Sr (1 mM)	U (1 mM)	% U precipitated at the end of 2 h
Deino-PhoK	-	-	-	+	97 %
Deino-PhoK	+	-	-	+	96 %
Deino-PhoK	+	+	+	+	96.5 %
Deino-pRAD1	+	+	+	+	2-3 %

Depending on the content of U and other metals present, the total radiation dose in the effluent (ILLW) may vary from few Grays to several hundred Grays. (For ^{235}U, at a distance of 1 mm, 5 Ci of radioactivity corresponds to a dose of ~336 Gy/h). Taking 25 Ci as a midpoint of 5-50 Ci radioactivity expected to be present in ILLW, the expected dose received in 3 h could be ~ 5 kGy (www.radprocalculator.com). Thus, *Deino-PhoK* may tolerate the adverse conditions likely to be present in ILLW. Also, in view of the fact that resting cells (non-growing) of *Deino-PhoK* perform efficient precipitation and the strain also exhibits adequate tolerance to other metals as well as radiation levels that are likely in ILLW or LLW, the environment prevalent in these wastes may not pose critical problem to the performance of the strain. This suggested the possible use of *Deino-PhoK* in mixed radioactive waste.

3.7 Construction of a recombinant *D. radiodurans* strain co-expressing both acid (PhoN) and alkaline phosphatase (PhoK).

Attempts were made to construct a recombinant *Deinococcus* strain that could address both acidic and alkaline waste and facilitate uranium bioprecipitation using a single bacterial strain. Strains *Deino-PhoN*, constructed earlier for uranium precipitation under acidic conditions [121-122], and *Deino-PhoK*, constructed in this study to precipitate uranium under alkaline conditions, were already available as source of desired genes. Hence, using these strains construction of recombinant *Deinococcus* co-expressing both PhoN and PhoK was undertaken for targeting *Deinococcus* to both acidic and alkaline waste.

The plasmid pK1 (Table 2.3) containing *phoK* gene under deinococcal *groESL* promoter, constructed earlier (Fig. 3.2) was digested with *XhoI-BamHI* and the excised 1.93 kb *phoK* insert was ligated to *XhoI-BglII* digested plasmid pPN1 (Table 2.3) containing *phoN* gene downstream of *groESL* promoter in *XbaI-BamHI* sites (Fig. 3.22). This plasmid, pK2 was first transformed into *E. coli JM109* and then into *Deinococcus radiodurans* R1. Colony PCR and restricting digestion analysis confirmed the presence of correct size of PhoK + PhoN insert (3.2 kb) in the new recombinant plasmid pK2 (Fig.3.22B).

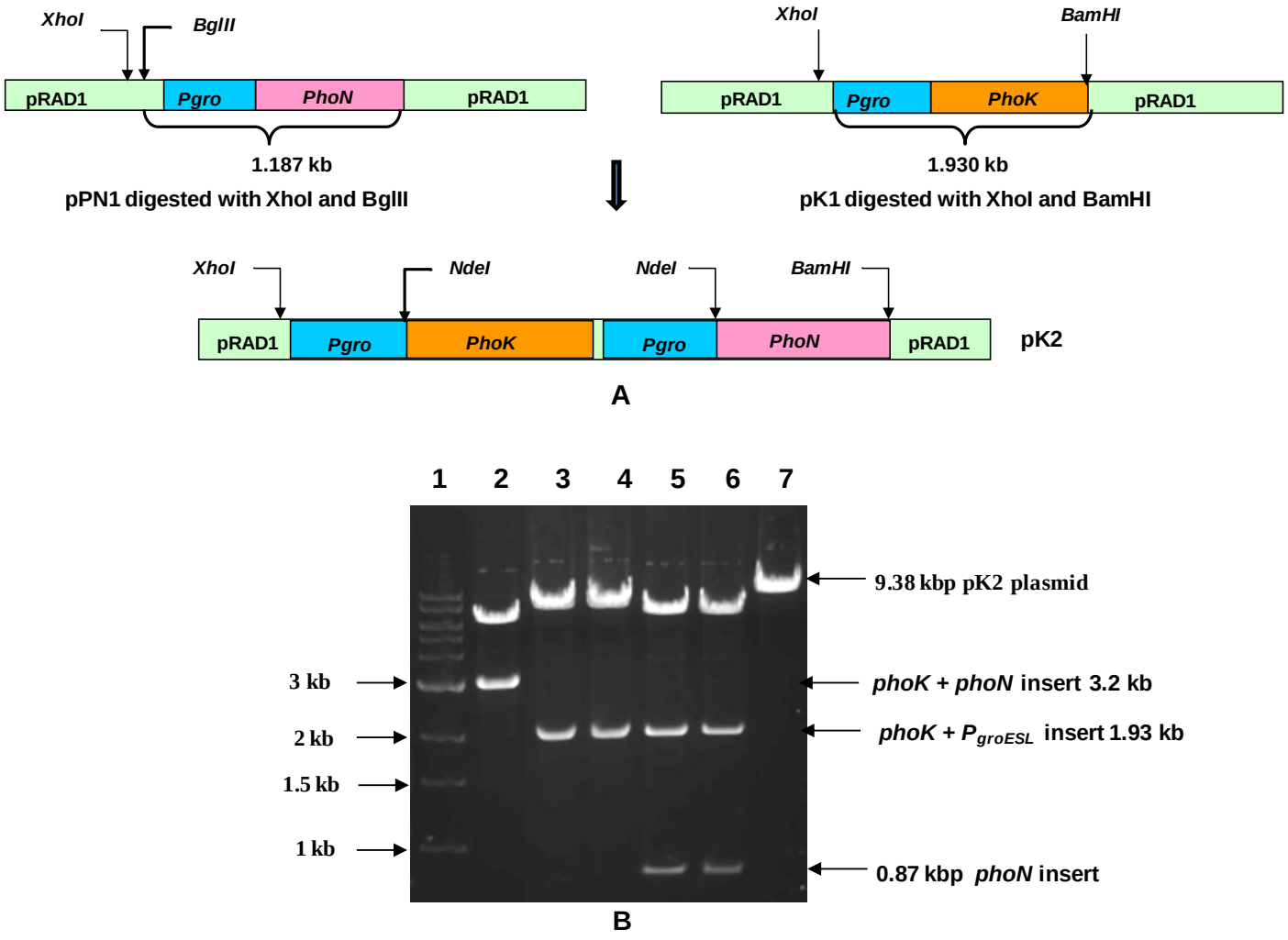

Fig. 3.22 Construction of plasmid pK2. (A) Schematic representation of cloning strategy for plasmid pK2. (B) Restriction digestion of plasmid pK2 isolated from *E. coli***.** The plasmid pK2 was digested with restriction enzymes *XhoI* and *BamHI* (lane 2) or *NdeI* alone (lane 3 and 4) or digested with *Nde*I and *BamHI* (lane 5 and 6) or *XhoI* alone (lane 7) and electrophoretically resolved, along with 1 kb ladder (NEB) (lane 1). The size of various DNA fragments is depicted by arrows.

Recombinant *D. radiodurans* strain carrying both the phosphatase genes *phoK* and *phoN* was hereafter called *Deino-PhoNK*. *Deino-PhoNK* cells were screened on modified histochemical plates in the same manner as *Deino-PhoK* cells (Fig. 3.23). On histochemical plates containing Cm and supplemented with PDP +MG, *Deino-PhoNK* cells showed green

colored spots indicating expression of phosphatases, while *Deino-pRAD1* control cells did not show any green colour.

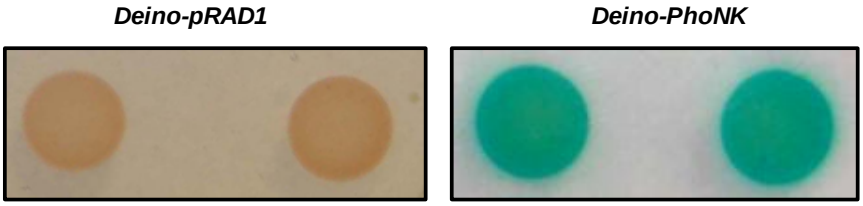

Fig. 3.23 Screening of *Deinococcus* carrying pK2 on histochemical plates. *Deinococcus* cells were grown overnight (18 h) in liquid medium and washed twice with double distilled water. 10 µl (OD_{600nm}~1) was spotted on modified histochemical plate containing PDP-MG to assess expression and activity of phosphatase.

3.8 Phosphatase expression, cell associated enzyme activity and in-gel zymogram assays of *Deino-PhoNK* strain

Presence of cell-associated PhoK and PhoN activities in recombinant *Deino-PhoNK* strain (grown for overnight period for 18 h) was assessed with β-GP (Table 3.5) since for precipitation studies β-GP will be employed as substrate. Activity assays were carried out either in 100 mM acetate buffer (pH 5), or 50 mM MOPS buffer (pH 7), or 50 mM MOPS buffer (pH 9), separately along with appropriate controls. Alkaline phosphatase activity of *Deino-PhoNK* cells was ~788 ± 45 units (pH 9.0), while acid phosphatase activity of *Deino-PhoNK* cells was ~ 80 ± 10 units (pH 5), which were slightly lesser as compared to individual PhoN/PhoK activities in *Deino-PhoN* and *Deino-PhoK* cells. Thus, both the acid and alkaline phosphatases were actively expressed in recombinant *Deino-PhoNK* strain, though the additive effect of expression of both the phosphatases was not reflected in cell associated activities.

Table 3.5. Phosphatase activity of recombinant *Deinococcus* strains in terms of hydrolysis of β-GP

Strains	Cell associated phosphatase Activity* pH 5	pH 7	pH 9
Deino-pRAD1	13.7 ± 1	14.6 ± 1.5	12.8 ± 1
Deino-PhoK	51.6 ± 5	255 ± 15	838.8± 30
Deino-PhoN	103 ±10	67.3 ± 7	36.5 ± 5
Deino-PhoNK	80 ± 10	244 ± 20	788.4 ± 45

***** P_i release measured in terms of nmoles Pi released/min/mg protein

In vitro zymogram analysis was carried out using cell free extracts of the recombinant strain *Deino-PhoNK*, with the activity staining carried out under acidic (pH 5) (Fig. 3.24A) or neutral (7.0) (Fig. 3.24B) or alkaline pH conditions (pH 9) (Fig. 3.24C) separately. Under acidic conditions (pH 5) 27 kDa activity band of PhoN monomer was clearly seen whereas PhoK activity band was not observed, due to loss of PhoK activity at pH 5. Under neutral conditions (pH 7), activity bands corresponding to both 27 kDa PhoN monomer as well 60 kDa PhoK monomer were observed. Under alkaline conditions (pH 9.0) the activity band of 60 kDa PhoK monomer was evident along with reduced activity band of the 27 kDa PhoN monomer, in the *Deino-PhoNK* strain. These results confirmed the expression of active PhoK as well as PhoN proteins in the same recombinant *Deinococcus* strain.

Expression of PhoK in *Deino-PhoNK* strain was further confirmed by Western blotting and immune-detection using anti-PhoK (Fig. 3.25) antibodies. Under reducing conditions, the PhoK monomer was detected at 60 kDa.

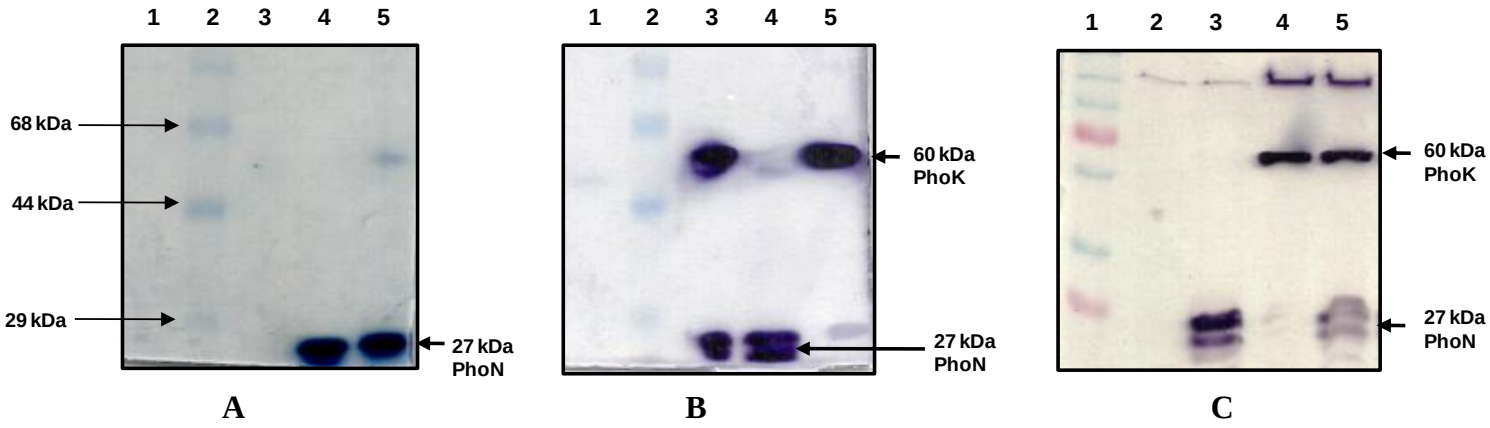

Fig. 3.24 Zymogram analysis of protein extracts (20 µg) of recombinant *Deinococc*us strains. Protein extracts (20 µg) were electrophoretically resolved by non-reducing SDS-PAGE and stained for *in gel* phosphatase activity at (A) pH 5 or (B) pH 7 or (C) pH 9. (A) Lane 1, *Deino-pRAD1*; lane 2, prestained marker; lane 3, *Deino-PhoK*; lane 4, *Deino-PhoN*; lane 5 - *Deino-PhoNK*. (B) Lane 1, *Deino-pPRAD1*; lane 2, prestained marker; lane 3 *Deino-PhoNK*; lane 4, *Deino-phoN*; lane 5, *Deino-PhoK*. (C) Lane 1, prestained marker; lane 2, *Deino-pRAD1*; lane 3, *Deino-PhoN*; lane 4, *Deino-PhoK*; and lane 5. *Deino-PhoNK*.

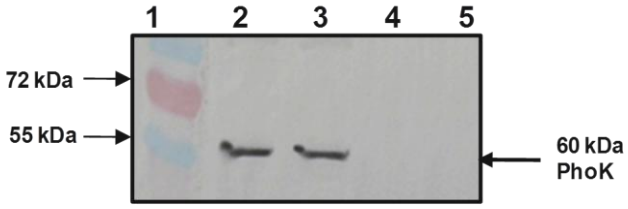

Fig. 3.25 Western blotting and immune-detection with PhoK antiserum. Protein extracts (30 µg) were resolved by 10% reducing SDS-PAGE, electro-blotted and immune-detected using PhoK antiserum. Lane 1, prestained protein marker (NEB); lane 2, *Deino-PhoNK*; lane 3, *Deino-PhoK*, lane 4, *Deino-PhoN* and lane 5, *Deino-pRAD1*. PhoK band corresponding to 60 kDa is depicted by arrow.

. Thus cell associated phosphatase activity, *in vitro* zymogram assays and Western blotting followed by immune-detection; all confirmed that both PhoN and PhoK were expressed, active and functional in the *Deino-PhoNK* strain.

3.9 Evaluation of uranium precipitation by *Deino-PhoNK* strain.

Uranium precipitation ability of *Deino-PhoNK* cells was evaluated under acidic and alkaline pH conditions separately. For U precipitation studies, overnight grown *Deino-PhoNK* cells were used. Though, early exponential phase cells of *Deino-PhoK* strain showed 1.5-2 fold higher specific activity (per mg protein) as compared to overnight grown cells, the cell density is about 9-10 fold lesser in the early exponential phase (OD_{600}~ 0.3-0.4) as compared to overnight grown cells (OD_{600}~3.5-4). Also previous studies with *Deino-PhoN* cells had reported maximal activity in the stationary phase and a higher cell density to achieve bioprecipitation similar to PhoK. Since activity of PhoN itself is very low as compared to PhoK, conditions optimum for PhoN activity was selected.

Uranium precipitation was performed by incubating *Deino-PhoNK* cells in 1 mM uranyl solution at pH 9.0 (OD_{600} ~1) or pH 7 (OD_{600} ~3) separately, along with their corresponding controls. The optimum pH for uranium precipitation with PhoN is 6.8-7. This is due to enhanced protonation of inorganic phosphate at acidic pH, limiting the rate of precipitation at pH 5. The precipitation kinetics shown by *Deino-PhoNK* strain under alkaline conditions displayed >85% uranium precipitation within 3 h which was similar to that shown by *Deino-PhoK* strain treated similarly (Fig. 3.26A). Rate of U precipitation by *Deino-PhoNK* strain near neutral conditions was >80 % precipitation within 6 h, similar to *Deino-PhoN* strain (Fig. 3.26B). At 1 mM input U concentration, *Deino-PhoNK* cells achieved 1.07 g U/g of dry weight of cells under alkaline conditions, which is comparable to *Deino-PhoK* cells showing 1.08 g U/dry weight of cells while under circumneutral conditions (pH 6.8) it showed loading of 0.34 g U/g of dry weight of cells which is comparable to *Deino-PhoN* cells showing ~ 0.35 g of U/g dry weight of cells.

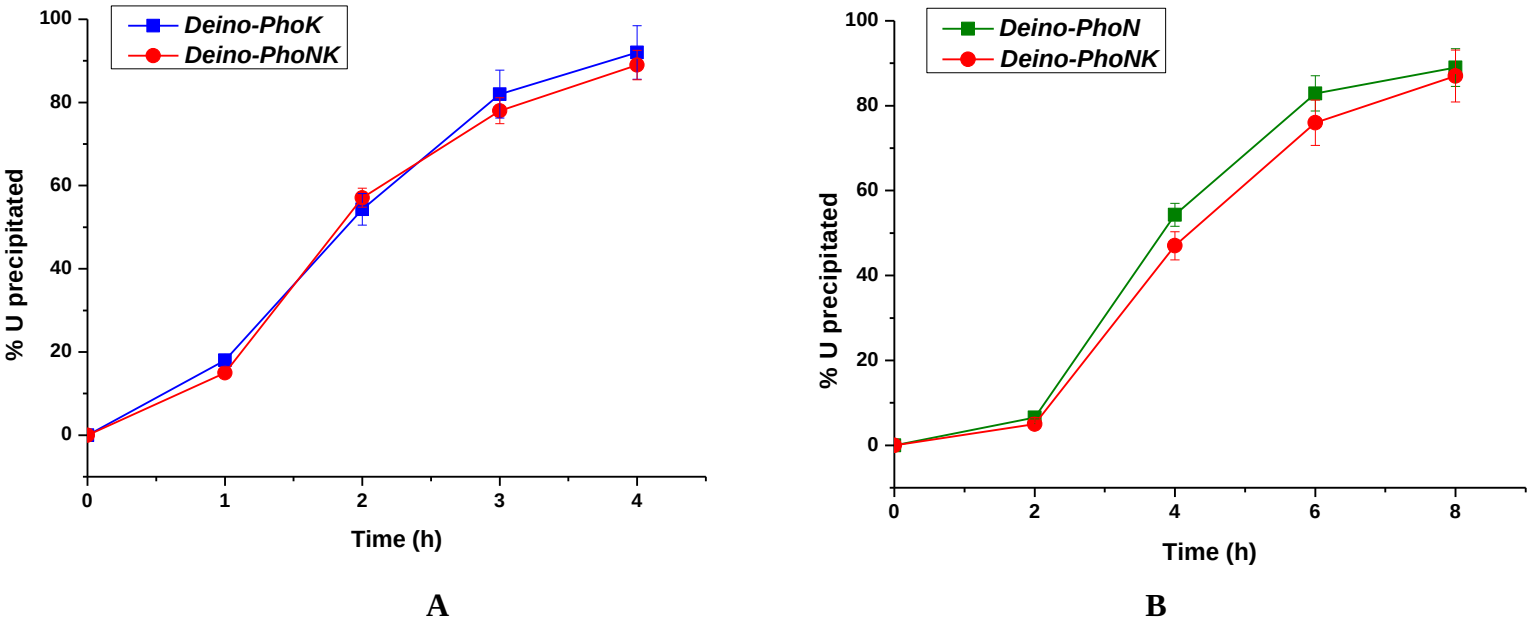

Fig. 3.26 Evaluation of U precipitation by *Deino-PhoNK* cells. (A) *Deino-PhoK* or *Deino-PhoNK* (grown overnight) cells (OD_{600}~1) were in incubated with 1 mM U in 10 mM MOPS, pH 9.0 and U precipitation was monitored up to 4 h. (B) *Deino-PhoN* or *Deino-PhoNK* (grown overnight) cells (OD_{600}~3) were incubated with 1 mM U in 10 mM MOPS (final pH 6.8) and U precipitation was monitored up to 8 h. U was estimated by Arsenazo III.

3.10 Discussion

Major problems with respect to disposal of radioactive waste are its large volume and difficulty in removal of harmful radionuclides and metals (including uranium) that are present in low concentrations. Radioactive waste sites also pose a unique problem since their bioremediation requires radio-resistant organisms which must not only remove metals but also endure such environment [128-129]. The bacterium *Deinococcus radiodurans*, known to survive extreme ionizing radiation stress has been a candidate of choice for many bioremediation studies, since it exhibits remarkable resistance to DNA damage caused by ionizing radiation, desiccation and other stresses [154-155]. *Deinococcus radiodurans* has been engineered for degradation of toluene, and detoxification of Hg and Cr in radioactive

environment [2, 137]. It has also been successfully manipulated to express acid phosphatases (PhoN) from other bacteria to precipitate U from aqueous waste solution. Such recombinant *D. radiodurans* cells exhibited metal precipitation even after being subjected to 6 kGy gamma radiation, unlike *E. coli* cells carrying the same construct [121-122, 136].

Bioprecipitation of U from alkaline waste has not been explored much. Precipitation of U(VI) as uranyl phosphate from alkaline solution is rather difficult on account of extremely high solubility of uranyl carbonate complexes at basic pH. A novel high specific activity alkaline phosphatase, PhoK, was identified by our laboratory recently from *Sphingomonas* sp. strain BSAR-1 [113-114], which could precipitate U under alkaline conditions, albeit with a low efficiency. Bioprecipitation efficiency of PhoK could be enhanced several fold by cloning and over-expressing the *Sphingomonas phoK* gene in *E. coli* [113]. However, utility of this radiosensitive strain remained limited to non-radioactive waste. The present study was undertaken with a view to construct a recombinant bacterial strain capable of bioprecipitation of U from alkaline solution and to impart to it the ability to remove U from both acidic-neutral and alkaline conditions in high radiation environment.

The present study engineered the *phoK* gene from *Sphingomonas* sp. BSAR-1 for overexpression in *E. coli* and *Deinococcus radiodurans* using a strong deinococcal *groESL* promoter [140]. The recombinant strain thus obtained (*Deino-PhoK*) (Fig.3.6) exhibited remarkably high alkaline phosphatase activity (Table 3.1) in comparison to phosphatase activities reported in bacteria earlier (Table 3.6). Cell associated PhoK activity was best seen in the early exponential phase of both *E. coli-PhoK* and *Deino-PhoK* cultures (Fig. 3.11 and 3.12). The important factors for any bioremediation process are a short time for maximal metal removal, wide range of working concentration and a minimum amount of biomass required. *Deino-PhoK* possessed all these attributes i.e. at a relatively low cell density (OD_{600} ~1), these cells could efficiently bioprecipitate over 90% of U within 2 h from 1 mM input U

concentration (Fig 3.19). To achieve same level of precipitation, *Deino-PhoN* cells required 10-fold higher cell density and much longer duration [121]. The *Deino-PhoK* strain worked equally well at higher (10 mM) concentrations of U resulting in loading of as much as 10.7g U/g dry biomass which, to our knowledge, is the highest U loading reported so far.

Table 3.6. Comparison of uranium precipitation ability of various bacterial strains.

Strains	pH conditions for precipitation assay	Specific activity of phosphatase enzyme *	Time (h) required to remove > 90% input U**	Amount of U** precipitated (g U/g of dry biomass)	Reference
Citrobacter N14	7.0	~400	16-18	0.09	[77]
Deino-PhoN	6.8	~170	8-9	0.35	[121-122]
Sphingomonas	9.0	~500	6-7	0.30	[113]
Deino-PhoK	9.0	~15000	< 2	1.07	This study

* Specific activity expressed as nmoles of *p*-NP released/min/mg bacterial protein
** Input uranium concentration at 1 mM.

Some nuclear wastes contain very high level of radioactivity, e.g. aqueous high level liquid waste generated during reprocessing of spent fuel rods. *Deino-PhoK* and also the PhoK protein survived 6 kGy exposure to γ-radiation and continued to function optimally thereafter (Fig 3.15 and 3.21). Also, overexpression of PhoK did not compromise the inherent radioresistance of *Deinococcus* (Fig. 3.14) and cells could efficiently precipitate U even after exposure to high radiation environment (i.e. 6 kGy) (Fig. 3.21). *Deino-PhoK* cells were also indifferent to the presence of other heavy metals like Cs, Sr found in nuclear waste, thus suggesting its potential use for treating waste solutions (Table 3.4).

Finally, to facilitate U bioprecipitation from both acidic and alkaline aqueous waste using a single microbe, the recombinant strain *Deino-PhoNK* that co-expressed both *phoN* and *phoK* genes was constructed (Fig. 3.22). Whole cell phosphatase activity and zymogram assays confirmed that both PhoN and PhoK were not only actively expressed in *Deino-PhoNK* were also optimally active at appropriate pH optima. The U precipitation kinetics in

Deino-PhoNK strain was similar to that shown by *Deinococcus* strains expressing either PhoN or PhoK individually. *Deino-PhoNK* cells achieved 1.07 g U loading/g of dry weight of cells at pH 9, while at pH 6.8 it showed loading of 0.34 g U/g of dry weight of cells at 1 mM input U and 5 mM β-GP.

The use of organic phosphate substrate, though eco-friendly, adds to the cost. U removal is very important for nuclear industry and our environment and hence the necessity to recover this metal from wastes outweighs the cost of β-GP used as substrate. Nevertheless, it would be desirable to make the process more cost effective. The stoichiometry of U and phosphate was found to be 1:1 in the precipitate. Most rapid precipitation was seen with 10 mM β-GP, but even with 1 mM β-GP, over 90% of U could be precipitated with longer incubation period (Fig. 3.18). Also, use of excess β-GP can lead to P_i accumulation and eutrophication of aqueous wastes which needs to be avoided. The economics of the whole process needs to be worked out in terms of shortest time required for maximal precipitation and the cost of substrate utilization while preventing excess phosphate pollution. In waste effluents, no organic phosphate source would be readily available and will need to be added. Macaskie et al, 2010, successfully used another phosphate donor, phytic acid (ubiquitous plant waste), for U precipitation [41]. Alternate easily available, economic and non-polluting P_i donors will need to be found for field application in future.

The studies described in this chapter indicate the potential and utility of *Deino-PhoK* strain for treatment of effluent waste that is alkaline in nature (pH 8-12). Further, construction of *Deino-PhoNK*, co-expressing both the phosphatases, enables the use of a single microbe for treating both acidic-neutral and alkaline effluent solutions. The chemical nature and physical location of precipitated U were characterized using different techniques and the factors affecting its cellular localization are described in the following chapter.

Chapter 4

Characterization and Localization of uranyl phosphate, precipitated by recombinant strains.

The previous chapter described the construction of *Deino-PhoK* for uranium removal from alkaline solutions and U precipitation ability was compared with that of the previously constructed *Deino-PhoN* under acidic-neutral pH conditions. Using appropriate controls, precipitation under both the conditions was shown to be cellular phosphatase (PhoN/PhoK) mediated and substrate (β-GP or *p*-NPP) dependent. Spontaneous precipitation of U or its sorption to containers or cell surface was found to be negligible. In case of PhoN, the precipitate formed was identified to be uranyl phosphate using SEM-EDX and XRD techniques earlier [113, 136]. In all previous studies, PhoN was always evaluated for U bioprecipitation with uranyl nitrate at pH 6.8, and resulted in cell associated precipitate [122, 136]. SEM-EDX analysis of U challenged *Deino-PhoN* cells clearly exhibited cell associated uranyl phosphate precipitate as shown in Fig. 4.1 below.

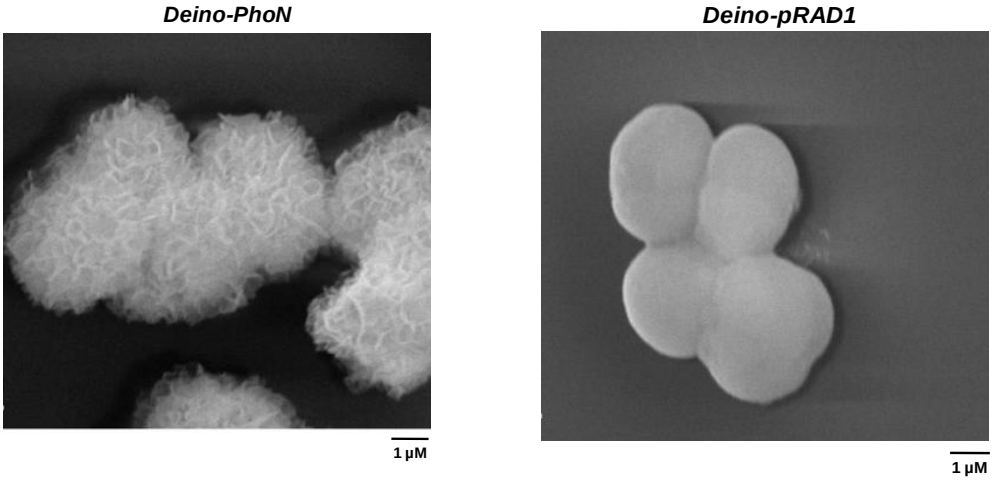

Fig. 4.1. Scanning electron micrograph of *Deino-PhoN* or *Deino-pRAD1* cells after U precipitation (source-Appukutan et al, 2011 [122]). Cells were incubated in a solution containing 10 mM U and 20 mM β-GP for 7 days and cells were visualized by SEM.

In contrast, PhoK was always tested with uranyl carbonate at pH 9.0 in previous as well as this study (Fig. 3.17). The respective uranyl salts for U bioprecipitation studies were used to keep U soluble under the pH conditions optimal for the respective phosphatase activities. The optimum pH for uranium precipitation with PhoN is 6.8-7, while for PhoK it is

8.5-9.0. The other strain, *Deino-PhoNK*, also precipitated U under both the geochemical conditions (pH 6.8 or 9) as both PhoN and PhoK were co-expressed in this strain.

The location of the precipitate in *Deino-PhoN* cells appeared to coincide with the location of PhoN i.e. periplasmic. Uranium speciation is very complex phenomenon and the actual U speciation varies with the pH even for the same salt (e.g. uranyl nitrate or uranyl carbonate). It would, therefore be interesting to know location of the precipitate in *Deino-PhoK* or *Deino-PhoNK* cells under the geochemical conditions employed for the precipitation. Since *Deino-PhoNK*, is proposed to be used at both pH 6.8 as well as pH 9, it would be necessary to understand the dependence of the location of precipitate on U species prevalent under acidic-neutral (pH 6.8) or alkaline (pH 9) conditions employed in this study. This chapter describes experiments which tested both the enzymes (i.e. PhoN/PhoK), with U under both pH conditions, to determine factors governing the precipitation process and its localization. To avoid confusion, the assay conditions are henceforth described as geochemical condition 1 (GC1) and geochemical condition 2 (GC2). GC1 is a carbonate deficient condition at pH 6.8; while GC2 is a carbonate abundant condition at pH 9.0 (Chapter II, section 2.8)

The efficacy of U removal and fate of the metal at the end of the bioremediation process is influenced by the chemical state of U prevalent under the given environmental condition [40]. This chapter describes the physico-chemical characterization of uranyl phosphate (UP), precipitated by the recombinant strains, using XRD and fluorescence analysis under both GC1 and GC2. The phosphatase mediated U bioprecipitation involves formation of crystalline aggregates, which can be visualised well by electron microscopy. Therefore, the transmission electron microscopy was employed as tool to study localization of precipitate (UP) and its interaction with respect to PhoN/PhoK expressing recombinant cells. The effect of aqueous uranyl speciation on cells in terms of U toxicity was also studied.

4.1 Characterization of uranium, precipitated by *Deino-PhoK* cells.

4.1.1 Identification of chemical nature of precipitate by XRD analysis

The identity of chemical species of uranyl phosphate, precipitated by *Deino-PhoK* cells, was confirmed by powder XRD (Chapter II, section 2.10). When compared with standard in database, the XRD pattern of uranium treated *Deino-PhoK* cells was identical to that of uranyl hydrogen phosphate hydrate [$H_2(UO_2)_2(PO_4)_2.8H_2O$]. Data fitting with the ICDD database revealed a match with 16 peaks indicating the precipitated U to be a chemical species CAS NO- 08-296, known as chernikovite (Fig. 4.2A). Uranium treated *Deino-pRAD1* cells (control) did not yield a spectrum (Fig. 4.2B), suggesting the inability of *Deino-pRAD1* to precipitate U and thus confirming the phosphatase-mediated bioprecipitation of U. Expectedly, the XRD pattern of U treated *Deino-PhoK* cells was identical to engineered EK-4 cells [113]. Thus data confirmed the formation of identical crystalline uranyl phosphate by PhoK in *E. coli* as well as in *Deino-PhoK*. The identified uranyl phosphate species, chernikovite or hydrogen meta-autunite is fluorescent when excited by UV light (λ_{ex} 380 nm) and the uranyl phosphate precipitated by EK-4 was shown to be fluorescent earlier.

4.1.2 Fluorimetric analysis of uranyl phosphate precipitate.

To ascertain if the precipitate obtained from *Deino-PhoK* cells possessed the inherent fluorescent properties of chernikovite, *Deino-PhoK* cells were exposed to UV light after U bioprecipitation. After completion of the precipitation assay, cells were subjected to centrifugation, and the cell pellet was exposed to UV light to observe for its fluorescence. This was done to qualitatively ascertain the presence of chernikovite precipitate.

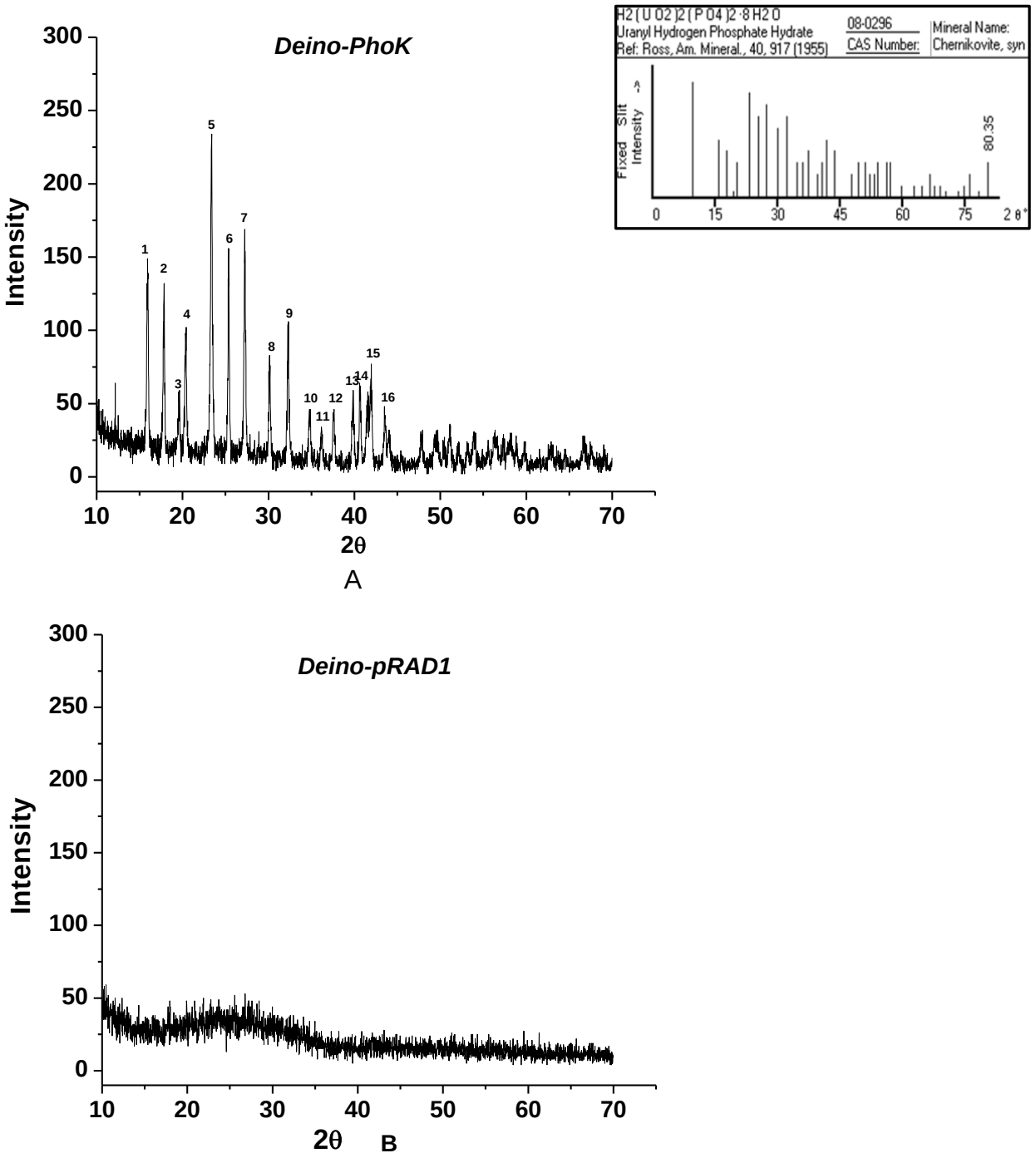

Fig. 4.2. Identity of the precipitated uranium by *Deino-PhoK* cells. Cells (OD_{600nm}~1) of *Deino-phoK* (A) or *Deino-pRAD1* (B) were incubated with 5 mM U and 10 mM β-GP in 10 mM MOPS buffer for 8 h, centrifuged and dried to make fine powder. The powder was subjected to X-ray diffraction analysis employing a Philips analytical X-ray diffractometer (using Ni-filtered Cu Kα radiation, Chemistry division, BARC). The reference spectrum for chernikovite is included.

The nature of the cell pellet was very different in control (*Deino-pRAD1*) and *Deino-PhoK* cells. In case of *Deino-pRAD1* cells where no precipitation was observed, cell pellet remained pinkish in colour, same as the natural pigment colour of *D. radiodurans* (Fig. 4.3A). In *Deino-phoK*, cells displayed a distinct yellowish precipitate of U (marked by arrow) trailing the pink cell pellet (Fig. 4.3B) which showed green coloured fluorescence when exposed to UV light (Fig. 4.3C).

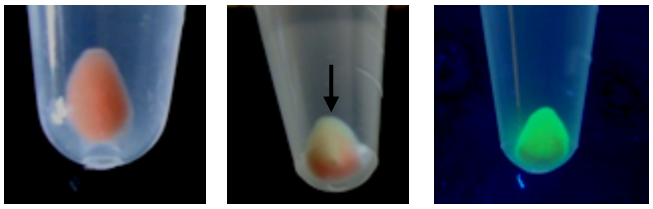

Fig. 4.3. Fluorescence of uranyl phosphate. Cells (OD_{600} 1) of *Deino-pRAD1* (A) or *Deino-PhoK* (B) and (C) were incubated with 1 mM U for 4 h, for bioprecipitation. Cell pellet after precipitation was visually observed under white light (B) or after exposure to UV (C) to ascertain the presence of a fluorescent precipitate.

After qualitative affirmation of the fluorescent uranyl phosphate precipitate, *Deino-PhoK* cells were used for quantitative estimation of U precipitation kinetics. For fluorescence analysis *Deino-PhoK* or *Deino-pRAD1* cells were suspended in U solution along with β-GP and the fluorescence intensity of the cell suspension was monitored over a period of time. During the assay, fluorescence intensity of suspension solution increased up to 2 h after which it remained steady indicating maximal uranium precipitation (Fig. 4.4). No measurable increase in fluorescence was observed in case of *Deino-pRAD1* cell suspension (control) over the same time period. The data correlated very well the colorimetric estimation of

precipitated uranium using Arsenazo III reagent (Fig. 3.17), thus corroborating the earlier results.

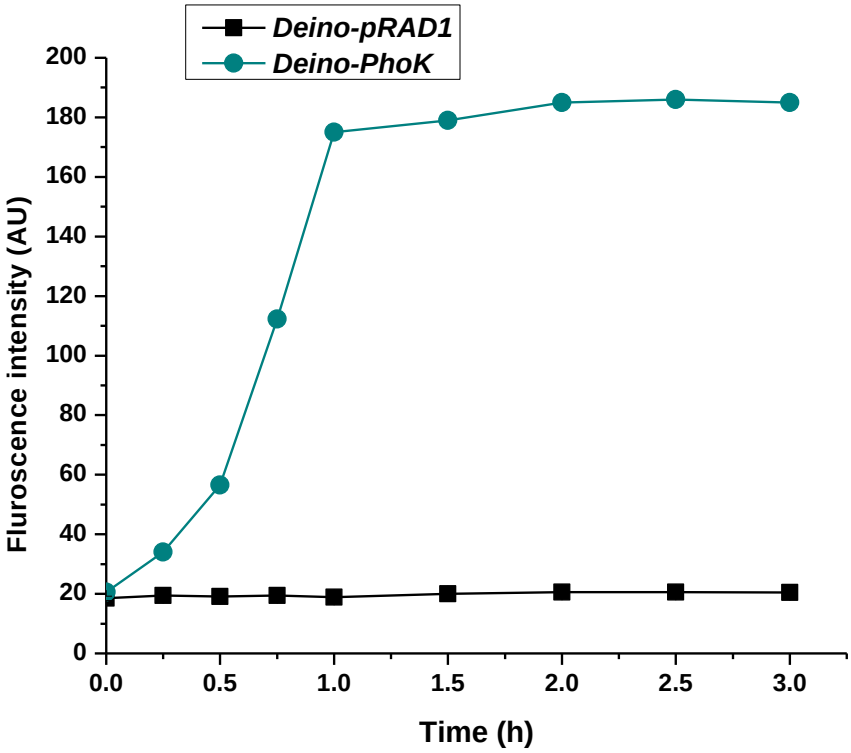

Fig. 4.4 Fluorimetric analysis of bioprecipitation by *Deino-PhoK* cells. *Deino-PhoK* or *Deino-pRAD1* cells (OD_{600nm}~1) were incubated with U with β-GP as substrate (5 mM) in MOPS buffer (10 mM). Fluorescence intensity (in arbitrary units, AU) of the suspension was monitored over a period of time (0.5-4 h) using λ_{ex}=380 nm and λ_{em}=524 nm.

4.2 Electron micrographic visualization and localization of U precipitation

4.2.1 Location of uranyl phosphate precipitate in *Deino-PhoK* cells under GC2

Studies were carried out to understand the localisation of precipitate under two different geochemical conditions employed and factors affecting it. XRD analysis (Fig. 4.2) identified the precipitate as chernikovite when *Deino-PhoK* cells were incubated with U under alkaline conditions (pH 9, GC2). These *Deino-PhoK* cells were then analysed by TEM to understand the nature of localization of precipitate i.e. cell surface associated or extracellular and mechanistic details of the precipitation event. After U precipitation, *Deino-*

PhoK displayed a distinct yellowish precipitate of U trailing the pink cell pellet (Fig. 4.3B). Two phase separation of pellet with *Deino-PhoK* cells is a result of the uranium precipitate settling differentially from the cells, indicative of the formation of free precipitate not associated with cells during bioprecipitation. TEM images of the uranium-treated *Deino-PhoK* and *Deino-pRAD1* cells confirmed the results obtained with the cell pellet. Presence of large, needle like crystals of uranyl phosphate were abundantly visible around *Deino-PhoK* cells incubated with uranium and β-GP (Fig. 4.5A and B). No such crystals or precipitate were observed when the control *Deino-pRAD1* cells were treated with U (Fig. 4.5C), confirming that the precipitation was indeed mediated by PhoK. The crystalline precipitate was also observed in samples which were not stained with uranyl acetate (Fig. 4.5D), demonstrating that it was not an artefact of the uranyl acetate stain which could be precipitated by inorganic phosphate released by PhoK. Additionally, the samples were extensively washed, embedded in resins before sectioning and staining, hence the possibility of uranyl acetate interfering in precipitation was ruled out. Stained images are represented in this figure for their superior quality over unstained images, however, henceforth; all TEM images represented are unstained.

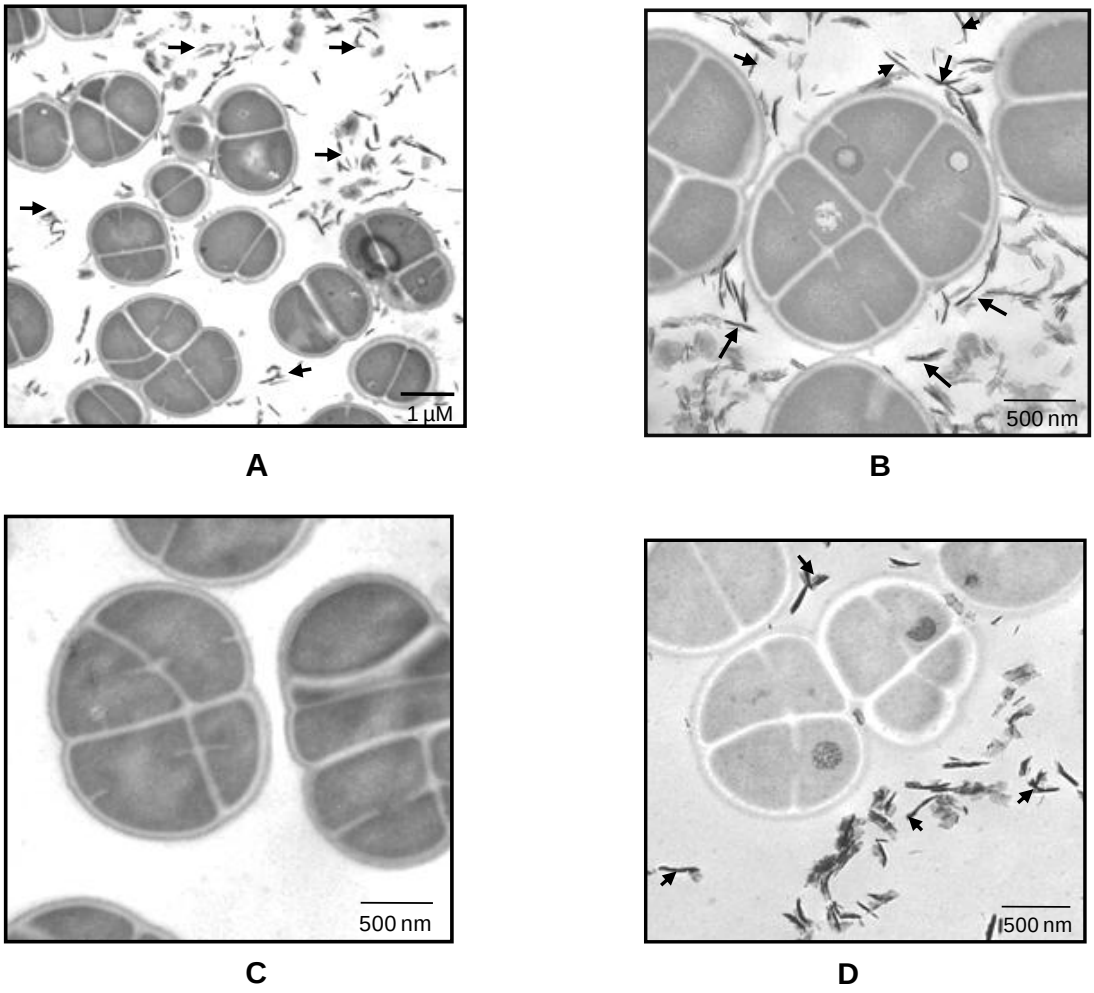

Fig. 4.5 Localization of precipitate in *Deino-PhoK* cells after U precipitation under GC1. *Deino-PhoK* **(A**) or *Deino-pRAD1* cells (OD_{600}~1) **(C)** were incubated with 1 mM U under GC2, in 10 mM MOPS buffer and 5 mM β-GP for 4 h and processed for TEM. Stained (with uranyl acetate) *Deino-PhoK* cells **(A)** lower magnification **(B)** higher magnification as well as unstained images **(D**) are represented and the crystalline extracellular precipitate is depicted by arrows.

4.2.2 Location of uranyl phosphate precipitate in *Deino-PhoN* cells under GC1

Extracellular localisation of precipitate (Fig. 4.5) as observed in case of *Deino-PhoK* cells when incubated with U under GC2 is very distinct from cell bound or cell-surface associated precipitate observed in SEM of *Deino-PhoN* cells under GC1 earlier (Fig. 4.1)

[122]. Also in *Deino-PhoN*, the cell pellet after U precipitation in GC1 was distinct from cell pellet observed with *Deino-PhoK* cells in GC2 (Fig. 4.3B). A homogeneous mix of pink (cells) and yellow (precipitate) colours (Fig 4.6A) was observed in *Deino-PhoN* which was different from *Deino-PhoK* cell which displayed a yellowish precipitate of U trailing the pink cell pellet (Fig. 4.3B). While *Deino-PhoK* showed green coloured fluorescence after precipitation under GC2, no such fluorescence was observed with *Deino-PhoN* after precipitation under GC1.

These *Deino-PhoN* cells when visualised by TEM after precipitation, exhibited exclusively cell surface-bound, spicule-like precipitates (Fig.4.6B). No extracellular precipitate was observed with *Deino-PhoN*. This substantiated the results obtained from earlier SEM analysis of *Deino-PhoN* cells. Absence of precipitate in control *Deino-pRAD1* cells (Fig. 4.6C) when incubated with U under GC1 clearly established the phosphatase mediated precipitation in either pH condition.

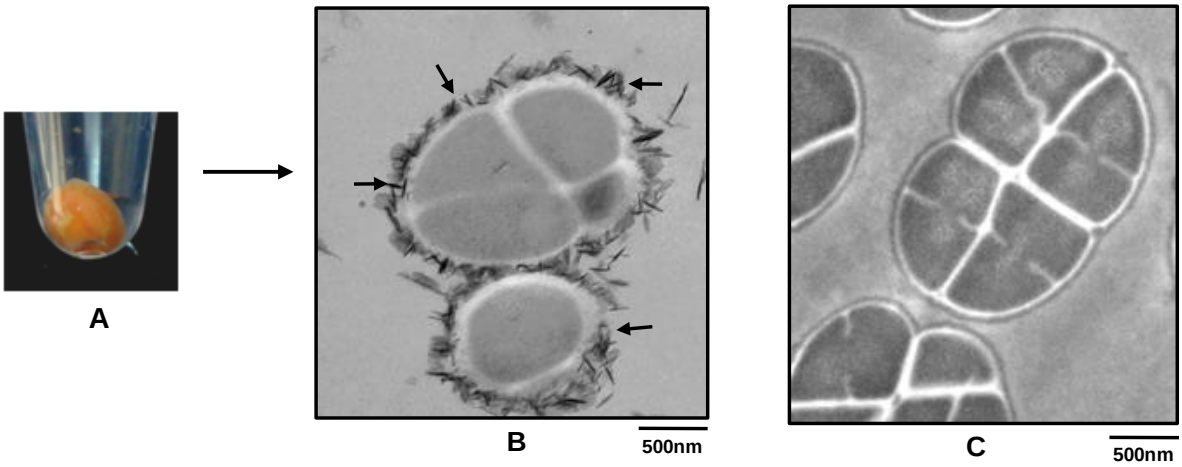

Fig. 4.6 Localization of precipitate in *Deino-PhoN* cells after U precipitation under GC1. *Deino-PhoN* (A) and (B) or *Deino-pRAD1* (C) cells (OD_{600}~1) were incubated with U under acidic-neutral conditions (GC1) for 8 h and cell pellet (A) was processed for TEM. The cell surface associated precipitate is depicted by arrows.

Thus, *Deino-PhoN* displayed cell-associated precipitate under GC1 (Fig. 4.6), whereas *Deino-PhoK* cells showed extracellular precipitation under GC2, in conformity with the known cellular location of the two enzymes. PhoK is known to be secreted extracellularly in addition to being cell-associated, whereas PhoN remains solely contained within cells [113, 121, 136, 156].

The most plausible explanation for the differential localisation of the U precipitate in *Deinococcus* appeared to be the the cellular and extracellular location of PhoN and PhoK enzymes, respectively. However, the geochemical conditions employed for U precipitation for the two strains were also different. Hence geochemical modelling studies using MINTEQ (http://vminteq.lwr.kth.se/download/) were carried out to determine the aqueous U speciation under the two conditions employed [23, 30].

MINTEQ analysis (Table 4.1) showed that under GC1, a carbonate deficient acidic-neutral condition (pH 6.8), U largely formed positively charged uranium hydroxide complexes. In GC1, out of total U species, almost 52% was predicted to form $(UO_2)_2(OH)^{+5}$ and 48% to be $(UO_2)_4(OH)^{+7}$, while only 0.04% was predicted to form negatively charged $(UO_2)_3(OH)^{7-}$. Under GC2, a carbonate abundant alkaline condition (pH 9.0), negatively charged uranyl carbonate/hydroxide complexes predominate. Almost 62% was speculated to be $UO_2(CO_3)_3^{-4}$, while 27% was predicted to be $(UO_2)_3(OH)^{7-}$. Under the precipitation conditions employed in GC2, positively charged uranyl species were almost absent.

Table 4.1 -U speciation in GC1 and GC2, as predicted by MINTEQ modelling.

GC1			GC2		
Component	**% of total concentration (pH 6.8)**	**Species name**	**Component**	**% of total concentration (pH 9.0)**	**Species name**
UO_2^{+2}	0.145	UO_2OH^+	**UO_2^{+2}**	**63.088**	**$UO_2(CO_3)_3^{-4}$**
	0.035	$(UO_2)_2(OH)_2^{+2}$		**26.529**	**$(UO_2)_3(OH)^{7-}$**
	51.899	**$(UO_2)_2(OH)^{+5}$**		**4.252**	**$UO_2(CO_3)_2^{-2}$**
	47.742	**$(UO_2)_4(OH)^{+7}$**		1.741	$(UO_2)_4(OH)^{+7}$
	0.047	$(UO_2)_3(OH)^{7-}$		1.249	$(UO_2)_3(OH)^{+5}$
	0.043	$(UO_2)_3(OH)_4^{+2}$		1.516	$(UO_2)(OH)^{3-}$
	0.109	$UO_2(OH)_2$ (aq)		0.164	$(UO_2)(OH)_2$ (aq)
				0.032	$UO_2(CO_3)$ (aq)
NO_3^{-1}	100	NO_3^{-1}	**CO_3^{-2}**	1.169	CO_3^{-2}
				16.28	HCO_3^-
				0.033	$H_2(CO_3)$ (aq)
				78.86	$UO_2(CO_3)_3^{-4}$
				0.013	$UO_2(CO_3)_3$ (aq)
				3.544	$UO_2(CO_3)_3^{-2}$
				0.062	$NaCO_3^-$(aq)
			NH_4^{+1}	67.012	NH_4^{+1}
				32.98	NH_3 (aq)
MOPS	30.319	MOPS	MOPS	98.652	MOPS
	69.681	H-MOPS (aq)		1.348	H-MOPS (aq)
Na^{+1}	99.974	Na^{+1}	Na^{+1}	99.974	Na^{+1}
	0.022	$NaNO_3$ (aq)		0.015	$NaHCO_3$(aq)
Gly-2-Phosphate	66.77	Gly-2-Phosphate	Gly-2-Phosphate	99.70	Gly-2-Phosphate
	33.23	H-Gly-Phosphate		0.295	H-Gly-Phosphate

GC1: Uranyl nitrate hexahydrate, 1mM; β-glycerophosphate (sodium salt), 5 mM; MOPS, 10 mM, pH 6.8.
GC2: Uranyl nitrate hexahydrate, 1mM; β-glycerophosphate (sodium salt), 5 mM; Ammonium carbonate, 2.4 mM; MOPS, 10 mM, pH 9.

4.2.3 Localisation of uranyl phosphate precipitate on reversing the precipitation conditions for *Deinococcus* expressing PhoN/PhoK.

As described in previous section, U precipitation assays with *Deino-phoN* cells were performed under GC1, where the positively charged uranium hydroxide complexes predominate. On the other hand, assays with *Deino-PhoK* were performed under GC2 where, the negatively charged uranyl carbonate complexes predominate [31] (Table 4.1). Above pH 5, bacterial cell surfaces are mostly negatively charged [157-158]. Therefore, the differential localization of the precipitate could also be governed by the differential aqueous U speciation. To ascertain if specific aqueous uranyl species had a role in determining the site of U precipitation, the assay conditions were reversed.

Deino-PhoN cells were incubated with U under GC2 (pH 9.0), whereas *Deino-PhoK* cells were incubated with U under GC1 (pH 6.8). As the pH conditions employed for precipitation using PhoN/PhoK were not optimum for phosphatase activity, cells were incubated up to 24 h to achieve adequate precipitation. *Deino-phoN* cells precipitated ~ 25 % U in 5 h under GC1, but only 15 % under GC2 over the same time period, in accordance with pH dependence of its activity (Table 3.5). U precipitation by the *Deino-phoK* cells was very rapid in both GCs and over 80 % of U was precipitated by 5 h. However, when incubated for 18 h, both strains showed near-complete removal of U under both GC1 and GC2 (Fig. 4.7). No detectable spontaneous precipitation of uranium occurred in the abiotic control (lacking cells) solution under either GC. Under both GCs, the *Deino-phoK* cells showed higher rate of phosphate hydrolysis, commensurate with its higher specific activity than *Deino-phoN* (Table 3.5), thus accounting for the higher rate of U precipitation shown by the PhoK-expressing cells. In the *Deinococcus* control cells (carrying pRAD1 alone), around 8.5% U was removed from solution under GC1 and about 2.2% was removed under GC2 (Fig. 4.7).

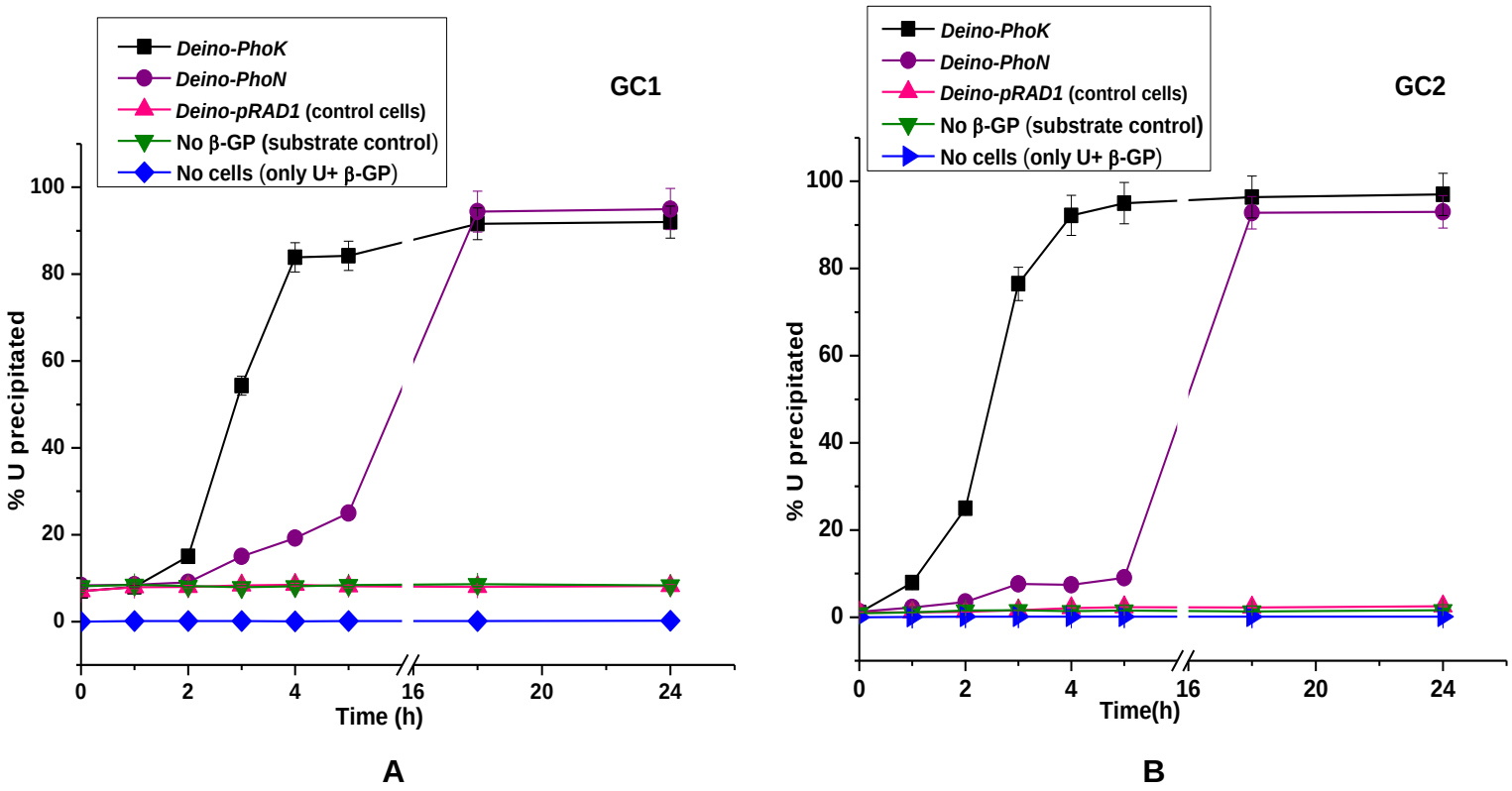

Fig. 4.7 U precipitation by recombinant *Deinococcus* cells under GC1 (A) or GC2 (B). Cells (OD_{600nm}~1) of *Deino-pRAD1*, *Deino-PhoN* or *Deino-PhoK* were used for U bioprecipitation. U removal kinetics was studied using cells incubated in 1 mM U with 5 mM β-glycerophosphate and U remaining in supernatant at various time points was estimated to calculate percent U precipitated.

The differential localisation pattern of precipitate was observed in cell pellet as well in TEM images. Visual examination of cell pellet colour after precipitation under both GC1 and GC2 indicated that regardless of the phosphatase enzyme employed, under GC1 the entire cell pellet turned yellowish while under GC2, a yellow streak of uranyl phosphate, trailed the cell pellet (Fig.4.8A and B). *Deino-PhoN* cells displayed distinct crystals of extracellular precipitate, with little cell surface associated precipitate under GC2 (Fig. 4.8A) which was very different from that shown under GC1 earlier (Fig. 4.6B). In contrast, *Deino-PhoK* cells clearly depicted cell surface bound crystals of uranyl phosphate under GC1, (Fig. 4.8B) which again was very different than formed under GC2 earlier (Fig. 4.5A and B).

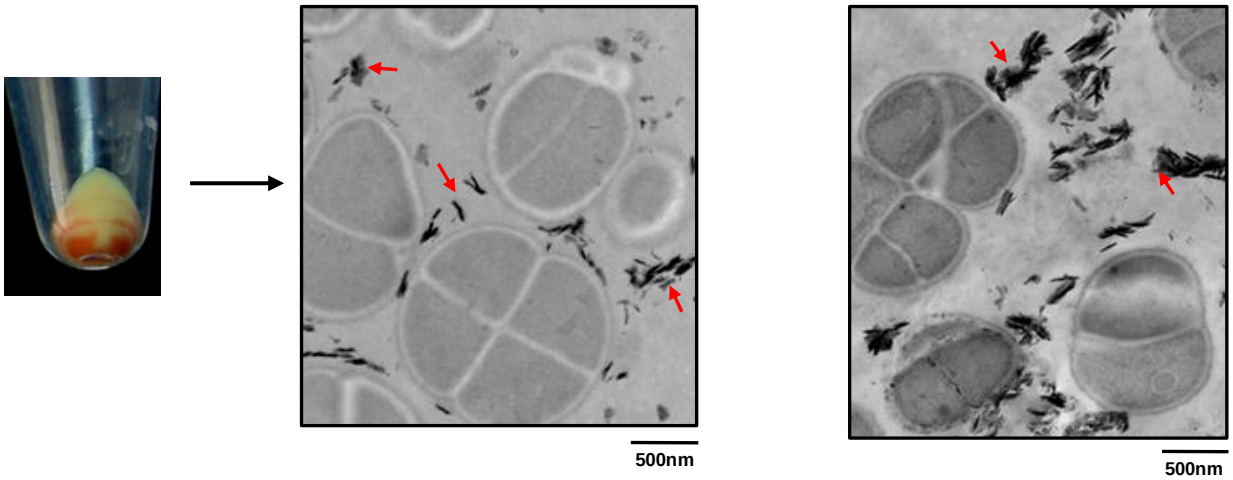

(A) *Deino-PhoN* under GC2

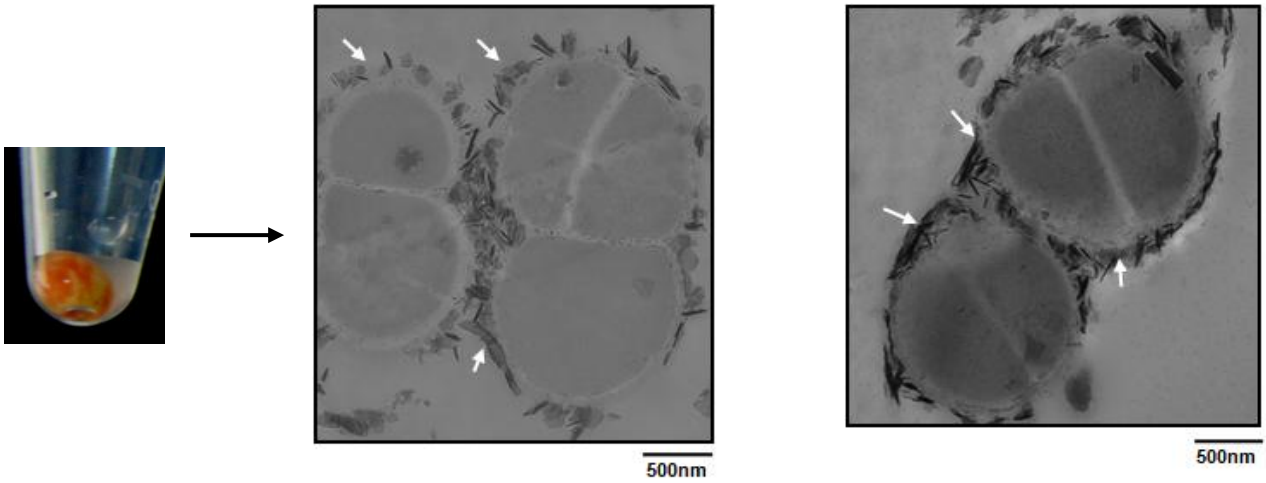

(B) *Deino-PhoK* under GC1

Fig. 4.8 Localization of U precipitate in recombinant *D. radiodurans* cells on reversing the U precipitation conditions. *Deino-PhoN* (A) or *Deino-PhoK* (B) cells (OD_{600}~1) were used for bioprecipitation assay of U (1 mM) under GC1 or GC2. After incubation for 18 h, cells were either subjected to centrifugation to visualize the pellet, or processed for TEM. Two different fields of each sample are presented for TEM.

U precipitation, either in GC1 or GC2 was always decoupled from cell growth in which resting, non-growing cells were used in buffer solution. To make sure that the extracellular/periplasmic location of the two enzymes after incubation under the two different geochemical conditions is not significantly affected by pH, *D. radiodurans* cells expressing

PhoN/PhoK were incubated in buffers of pH 6.8 or 9 for 4 h. Subsequently, the cell-associated and extracellular activities in supernatant were assayed at their respective pH optima (Table 4.2) using *p*-NPP as substrate. Although *Deino-PhoK* releases the enzyme extracellularly (40%), under growing conditions like the parental *Sphingomonas* or *E. coli* strain, EK-4 [113], and also observed in phosphatase activity studies (Table 3.2), negligible extracellular PhoK activity was seen in non-growing, resting cells decoupled from growth. (Table 4.2). At pH 6.8, 90% activity was cell associated while only 10% was extracellular in *Deino-PhoK* (growth decoupled) cells, while at pH 9, 87% activity was cell associated while only 13% was extracellular.

Table 4.2. Cell associated activity* (%) of PhoN/PhoK in *Deinococcus*

Phosphatase	After pre-incubation in pH 6.8	After pre-incubation in pH 9
PhoN	99	98
PhoK	90	87

*****Cells (OD_{600}~1) were incubated in 10 mM MOPS buffer of either pH for 4 h (in absence of U and substrate) and then assayed for phosphatase activity in both the pH.

Data showed that under any given condition, cell associated enzyme activity far exceeded activity in the external buffer solution, which clearly suggests that differential localization of uranyl phosphate precipitate had very little to do with enzyme localization. These data indicated that the differential localisation of U precipitate was not affected by localisation of enzyme but was primarily governed by the aqueous U species predominant under particular GC.

4.3. Confirmation of the uranyl phosphate precipitated under GC1 or GC2 by XRD analysis

Deino-PhoK cells precipitated U under GC2 as fluorescent meta-autunite or chernikovite (4.2A and 4.3C). In previous reports, *Deino-PhoN* cells were shown to precipitate U as uranyl hydrogen phosphate hydrate [136] under GC1. Therefore, XRD spectra for the precipitate generated by the two phosphatases after reversing the GCs were desired to confirm the identity of the precipitated species. XRD analysis of *Deinococcus* expressing PhoN/PhoK was performed after precipitation under both GCs to confirm whether different species of uranyl phosphate precipitate were formed or the precipitated uranyl phosphate species remained the same. XRD analysis of precipitated uranyl phosphate under both the GCs confirmed that the precipitated species remained the same i.e chernikovite, irrespective of GC employed, or phosphatase enzyme used (Fig. 4.9).

Further experiments were performed to ascertain why uranyl phosphate precipitated under GC2 was fluorescent while under GC1 it was not fluorescent. Precipitate obtained under GC2, when shifted to GC1 lost its fluorescence while the precipitate obtained under GC1, if shifted to GC2 exhibited fluorescence (Fig. 4.10) Thus fluorescent property of chernikovite seemed to be dependent on alkaline pH and not observed at acidic/neutral pH.

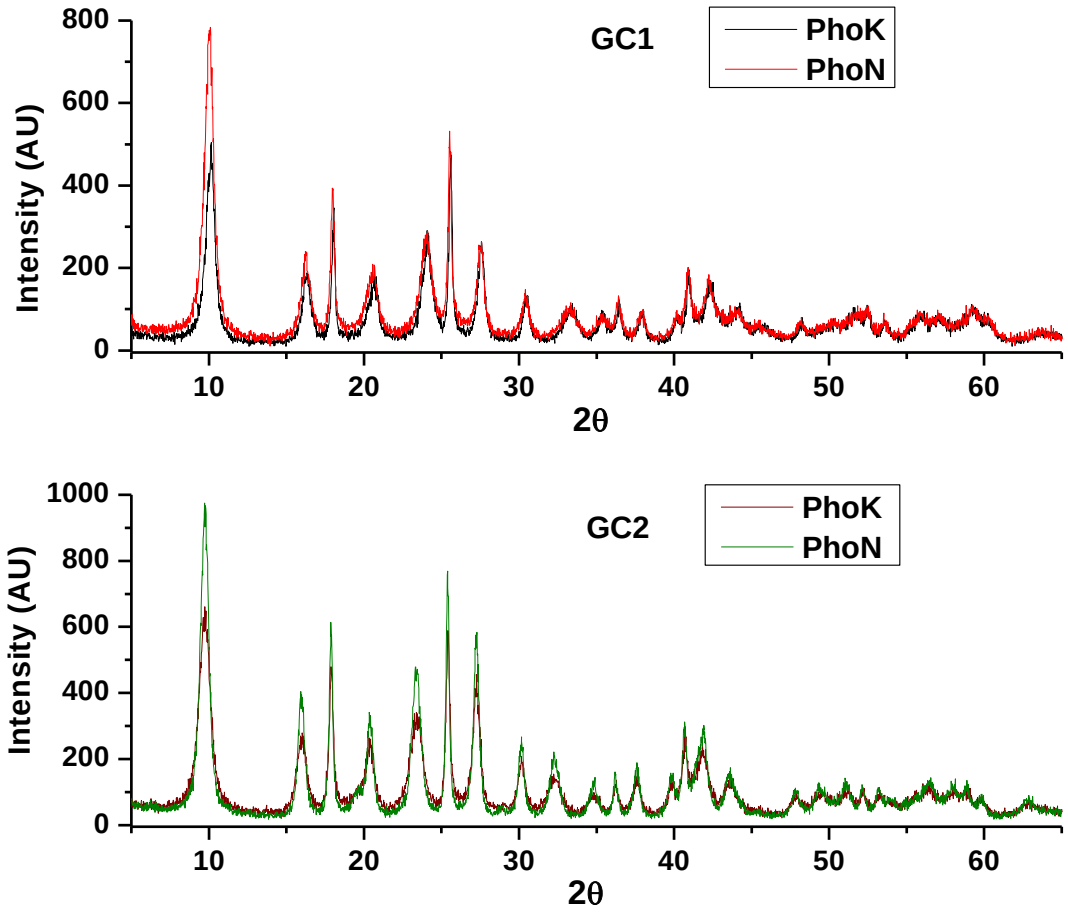

Fig. 4.9 XRD analyses of uranyl phosphate after precipitation under GC1 or GC2. *Deinococcus* (PhoN/PhoK expressing) cells (OD_{600}~1) were incubated with U (5 mM) and 10 mM β-GP under GC1 or GC2 for 18 h. After U precipitation, cells were centrifuged at 12000 rpm for 5 min, and dried at 80°C for 4 h to generate dry powder of biomass which was used for powder XRD analysis [high precision Rigaku R-Axis D-max Powder diffractometer using monochromatic Cu-Kα radiation (Solid State Physics Division, BARC**)].**

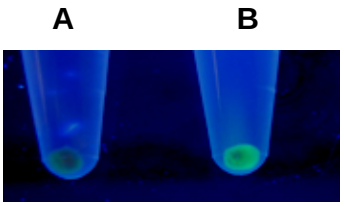

Fig. 4.10. Fluorescence of uranyl phosphate precipitate under GC1 or GC2. *Deino-PhoN* cells (OD_{600}~1) were used to precipitate U under GC1 and exposed to UV light (A). After precipitation, the cell pellet was incubated in 10 mM MOPS buffer pH 9.0 for 2 h and exposed to UV.

4.4 Uranyl phosphate precipitate localization in *E. coli* expressing PhoN/PhoK

To rule out the possibility that effect of aqueous U speciation on localisation of uranyl phosphate precipitate was not *Deinococcus* specific, *E. coli* cells were used for precipitation reactions under similar conditions (GC1 and GC2). Eppendorf tube based separation tests (as in Fig. 4.3 and 4.6) were conducted for *E. coli* cells as well, but the demarcation of precipitate from cells could not be visualized very well (Fig. 4.11). In *D. radiodurans*, as cells show pink colored pigmentation, the separation between the pink cell pellet and the yellow precipitate is distinctly observed. However, as *E. coli* lacks pigmentation, the visual demarcation of yellow precipitate from the creamish colored cells is not distinct as shown below. A slightly larger pellet was observed for *E. coli* cells (*E. coli-PhoK*) which had precipitated uranium, compared to control lacking enzyme (*E. coli-pRAD1*) cells (Fig. 4.11).

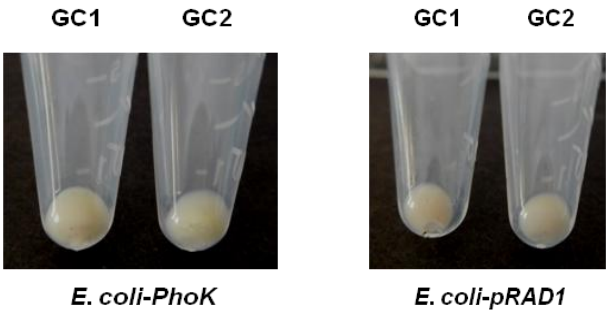

Fig. 4.11 Determination of uranyl phosphate precipitate localization in *E. coli* cells. *E. coli-PhoK* or *E. coli-pRAD1* cells (OD_{600}~1) were used to precipitate U (1 mM) under GC1 or GC2 and cells were centrifuged at 12,000 rpm for 10 min after precipitation. The cell pellet was visually observed to determine the difference in precipitate localization.

TEM analysis with *E. coli* expressing PhoK or PhoN (Fig. 4.12) confirmed the relationship between aqueous U speciation and localization of U precipitate to be in accordance with the results obtained in *D. radiodurans* (Fig. 4.5, 4.6 and 4.8). In *E. coli-pRAD1* control cells, no precipitate was observed (Fig. 4.12A and B) in either GC.

Regardless of the phosphatase employed for precipitation, under GC1 uranyl phosphate precipitate was cell associated (Fig. 4.12A), while under GC2 the precipitate was extracellular (Fig. 4.12B). In *E. coli-phoK* cells, under GC1 the precipitate was evenly bound all over the cell surface (Fig. 4.12A), whereas in *E. coli-phoN* cells, precipitate was found to accumulate at the polar ends (Fig. 4.12A).

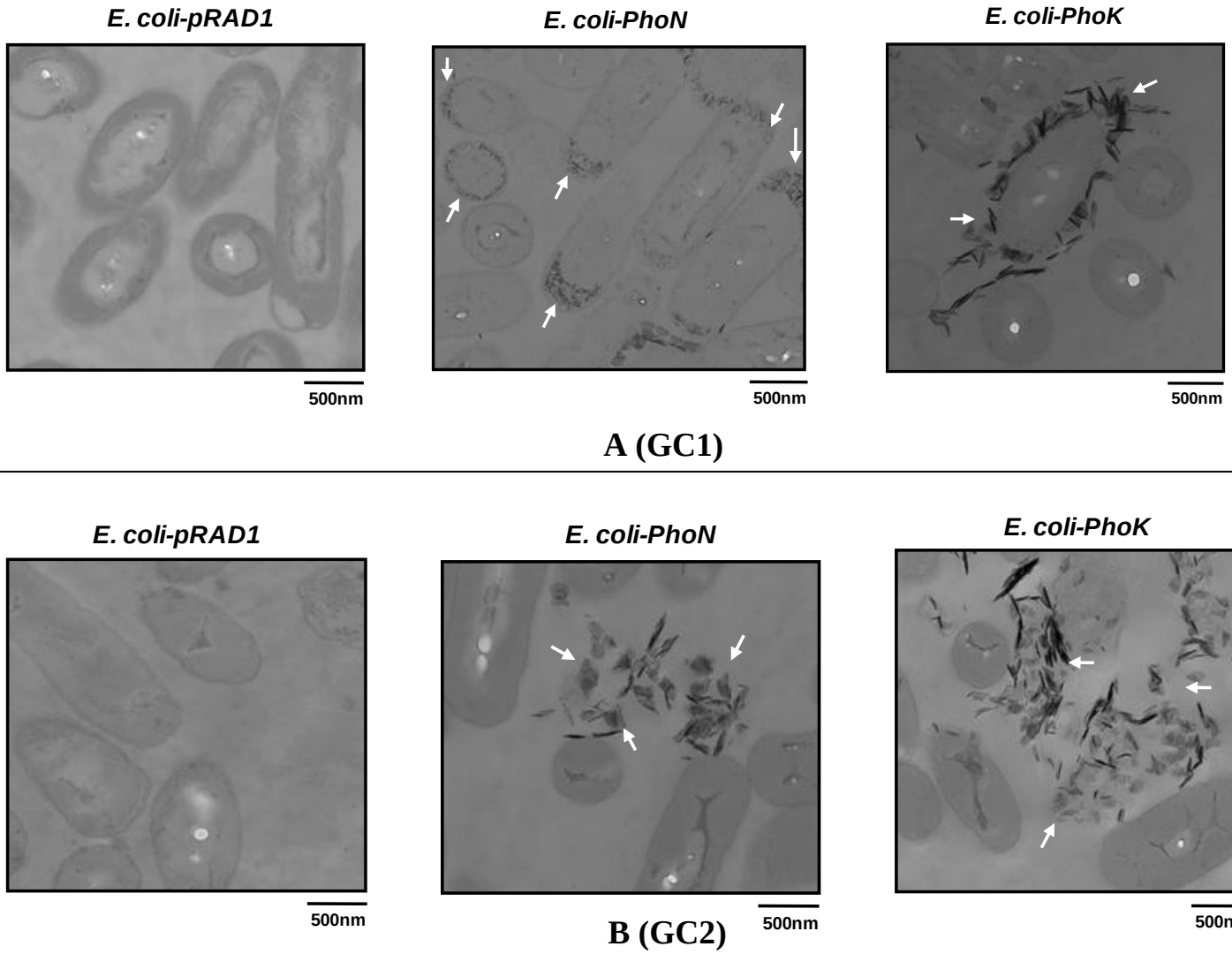

Fig. 4.12 Localization of U precipitate in recombinant *E. coli* cells after U precipitation. Cells (OD_{600nm}~1) of all three strains (*E. coli-pRAD1, E. coli-phoN* or *E. coli-phoK*) were used in U (1 mM) precipitation assays for 18 h under GC1 or GC2 and processed for TEM. Arrows show location of uranyl phosphate precipitate. All samples were unstained.

The results obtained till now indicated that the gross localization pattern of the precipitate is mainly governed by the particular GC employed for precipitation and not by the corresponding phosphatase which drove metal precipitation in both *D. radiodurans* and *E. coli* cells. However, subtle variations, apparently determined by the enzyme localization were also observed. The periplasmic non-specific acid phosphatases are known to concentrate at cell poles in Gram negative bacteria [46, 159-160]. In accordance with this, the *E. coli-phoN* cells under GC1, displayed a periplasmic location of the precipitate at the poles (within the cells). Abundance of PhoN at poles may result in localized high phosphate concentration, leading to periplasmic accumulation of precipitate in *E. coli* (Fig. 4.12A). This is unlike exocellular (but still cell surface-associated) location of precipitate in *E. coli-phoK* under GC1 where the enzyme is released extracellularly and the precipitate is formed with the sorbed U on the external surface of the cell boundary. *Deinococcus* has a multi-layered cell wall with a complex architecture [134], wherein the periplasm is not clearly defined. Further, the U hydroxyl species may not be able to permeate several layers of cell envelope for uranyl hydrogen phosphate to be precipitated inside the cell wall. Thus, while geochemical conditions play a major role in determining the precipitate localization (i.e. cell-associated and extracellular), finer variations may occur due to the different physiological conditions observed in the two bacteria.

4.5 Uranyl phosphate precipitate localization in *Deino-PhoNK*

TEM analysis revealed that when PhoN/PhoK were individually used for precipitation, in *D. radiodurans* or *E. coli*, precipitate localization was based on GC1 or GC2 irrespective of location of corresponding phosphatase. To confirm this, the most appropriate condition would be precipitation carried out by a strain in which both the phosphatases are co-expressed. Therefore, the precipitate localization pattern was evaluated in *Deino-PhoNK* cells.

Deino-NK cells were incubated with U under GC1 or GC2 and cells were processed for TEM after precipitation. Localization of U precipitate was in accordance with the results obtained in *D. radiodurans* and *E. coli* cells individually expressing PhoN/PhoK. Under GC1 (Fig. 4.13A), the precipitate was exclusively cell-associated, whereas under GC2, the precipitate was extracellularly located (Fig. 4.13B). This confirmed the prediction that uranyl phosphate localization is governed by aqueous U species present under particular GC and not by enzyme location.

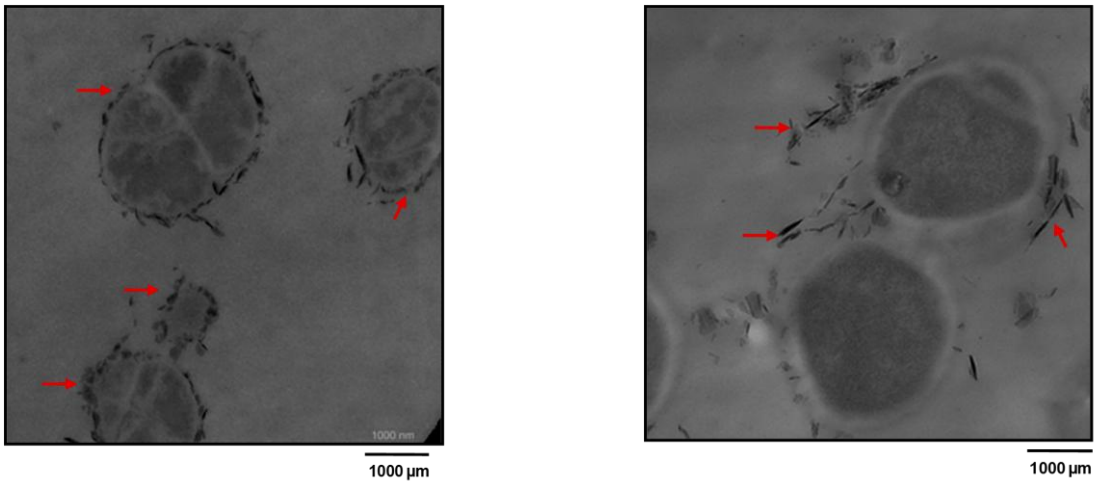

Fig. 4.13 Localization of U precipitate in *Deino-PhoNK* cells after U precipitation under GC1 or GC2. Cells (OD_{600nm}~1) were used in U (1 mM) precipitation assays for 18 h under GC1 or GC2 and processed for TEM. Arrows show location of uranyl phosphate precipitate.

The events leading to localization of precipitate still remain unanswered i.e. whether precipitate is formed first and then attached to cell surface or is U first adsorbed to cell surface, over which further precipitation takes place. To understand this mechanism, biosorption of U was evaluated under GC1 and GC2 with *D. radiodurans* and *E. coli* cells.

4.6 Differential biosorption of uranium under GC1 and GC2

Bacterial cell surfaces generally carry a net negative charge. Since metal binding is usually a result of electrostatic interactions between functional groups present on cell surface and the metal, the zeta potential of wild type *D. radiodurans* and *E. coli* cells was determined. In distilled water, the zeta potential values of the two cell types differed slightly (*D. radiodurans*: -18 mV and *E. coli*: -9.5 mV) but was always found to be negative at and above pH 7. Thus a net negative cell surface charge may have a bearing on metal binding by whole cells. Therefore, it was postulated that the positively charged uranyl hydroxide complexes might get absorbed on cell surfaces in higher amount, resulting in cell-associated metal precipitation while negatively charged uranyl carbonate complexes are likely to be repelled by the cell surface resulting in precipitation away from cell surface in the extracellular space. To test this, biosorption of uranium was tested using *E. coli* and *D. radiodurans* cells in the absence of phosphatases under two GCs. The assays for measuring biosorption would have been complicated by the bioprecipitation phenomenon occurring concomitantly if recombinant phosphatase expressing cells had been employed. Hence, in absence of the phosphatases (wild type cells), these problems were avoided.

For biosorption experiments, the wild-type *D. radiodurans* or *E. coli* (DH5α) cells (OD_{600nm}~1) were suspended in 10 mM MOPS buffer under conditions similar to GC1 and GC2 at U concentrations, 50, 100, 200 and 1000 µM. Dry weight corresponding to the optical density of cells used in each experiment was determined and used to calculated mg U biosorbed or precipitated/g dry weight cells. At all the concentrations of U employed, both organisms showed higher biosorption of U under GC1 than under GC2. For instance, at 1 mM input U concentration under GC1, *D. radiodurans* adsorbed 98 mg U/g dry weight of cells (i.e. 8.3% of the input), whereas *E. coli* cells showed biosorption of 46 mg U/g dry weight of cells (7% of the input) (Fig. 4.14A). In contrast, both organisms adsorbed only 8-12

mg of U/g of dry weight of cells (1-2% of the input) under GC2 (Fig. 4.14B). With increasing concentrations of U, more U is adsorbed onto cells, especially in GC1, till it saturates at 200 µM input U in both the organisms under GC1. In GC1, D. *radiodurans* adsorbed ~ 100 ± 3 mg U/g dry weight of cells at 200 µM as well as at 1000 µM, while *E. coli* adsorbed ~ 58 ± 2 mg U/g dry weight of cells at 200 µM and 44 ± 2 mg U/mg dry weight of cells at 1000 µM. U loading values did not increase further on increasing input U concentration beyond 200 µM indicating bacterial cell surface adsorption is saturated at this U concentration.

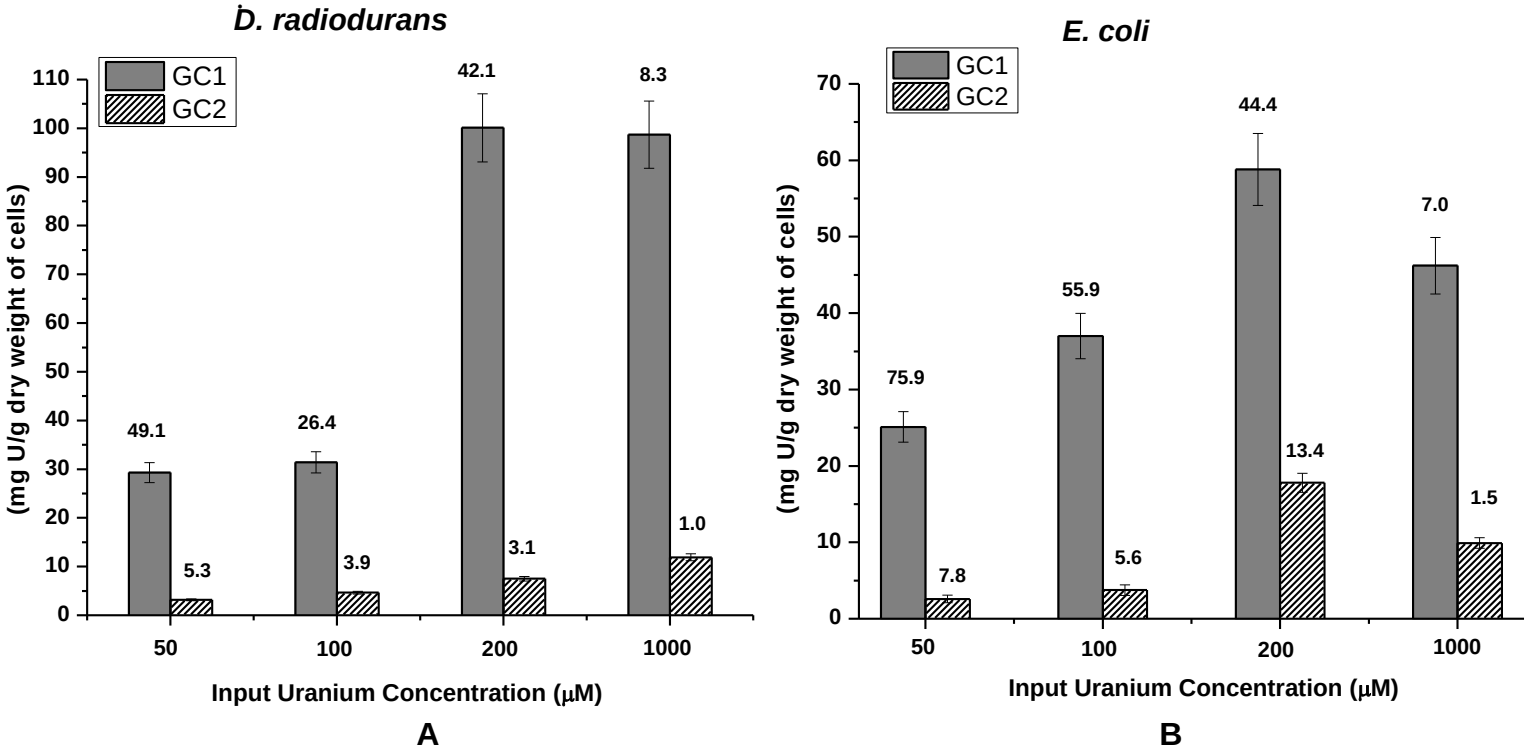

Fig. 4.14 Biosorption of U by *D. radiodurans* and *E. coli*. Wild type *E. coli* or *D. radiodurans* cells (OD_{600nm} ~1) were suspended in 10 mM MOPS buffer containing 50, 100, 200 or 1000 µM U under either GC1 or GC2. Amount of U biosorbed per mg dry weight of cells is reported. Percent U removed is indicated above respective bars.

Thus, greater biosorption of U occurs under GC1 wherein the positively charged hydroxide complexes predominate rather than under GC2 where the negatively charged carbonate/hydroxide complexes of U are prevalent. These results suggest that the aqueous

uranyl species under GC1 are preferentially adsorbed on cell surfaces which in turn may result in cell surface associated precipitation, while negatively charged uranyl complexes are precipitated extracellularly, probably being repelled by the bacterial surface.

4.7 Uranium sensitivity towards *D. radiodurans* and *E. coli*

The results from biosorption experiment showed 5-6 fold higher biosorption of U under GC1 than in GC2 both in *D. radiodurans* and *E. coli*. Reports have shown earlier that U biosorption decreases with increasing pH and increasing carbonate/bicarbonate concentration due to higher complexation of uranyl ion by hydroxides and carbonates [23, 31, 44], which was also observed in our studies (section 4.6). It has also been shown that increasing pH and higher bicarbonate/carbonate concentration exert lower toxicity towards U [23-24, 161-162]. It was observed that in the presence of high concentration of carbonate, bioaccumulation of U was reduced in bacteria, and this led to increased tolerance towards U [30-31, 163]. In order to substantiate this, U toxicity studies were conducted in *D. radiodurans* and *E. coli*.

Cells grown till late exponential growth phase were suspended (OD_{600nm}~1) in 10 mM MOPS buffer, supplemented with U at 0-1.5 mM under GC1 or at 0-25 mM under GC2 for 4 h. Exposure to 1.5 mM U under GC1 (pH 6.8) caused severe loss in cell viability in both *D. radiodurans* and *E. coli* cells (Fig. 4.15). In contrast, survival of cells remained largely unaffected even at 20 mM U under GC2 (Fig. 4.15). In both *Deinococcus* and *E. coli*, only 10 % survival (determined by measuring CFU) was obtained as compared to the control (cells not exposed to U) when incubated (on nutrient agar media) under GC1 at 1.25 mM U, whereas under GC2 growth was unaffected even at 20 mM U (Fig. 4.15).

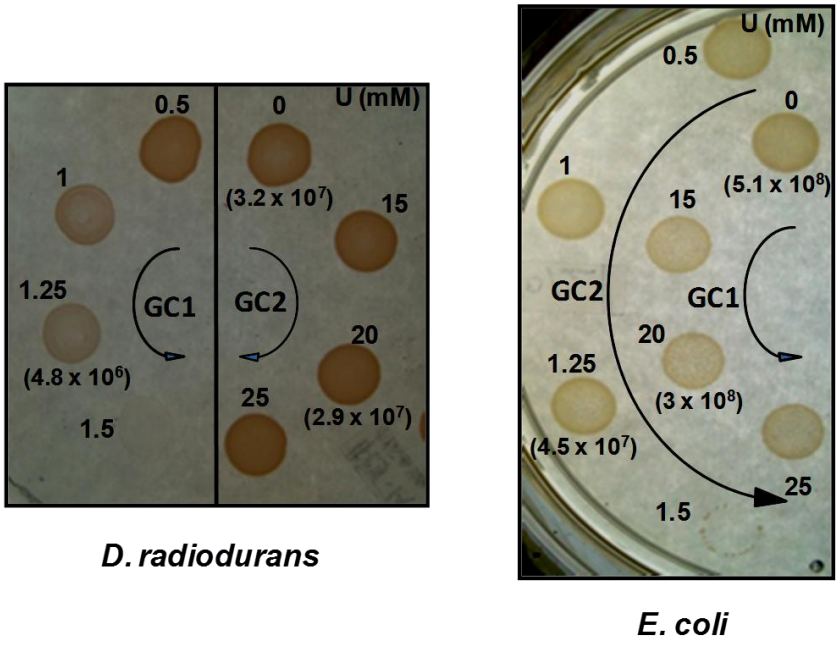

Fig. 4.15 Uranium sensitivity of *D. radiodurans* and *E. coli* under GC1 or GC2. Pre-grown wild type *D. radiodurans* or *E. coli* cells were suspended in buffer solution (10 mM MOPS) containing U under either GC1 (0-1.5 mM) or GC2 (0-25 mM) for 4 h under sterile conditions. Such U-exposed cells were washed free of uranium containing buffer solution, spotted (10 µl) on corresponding LB/TGY agar plates to observe the effect on viability. CFUs obtained after plating are indicated in parentheses

In another set of experiment, cells (resting conditions) were exposed to U (6 h) as described earlier and such U-exposed cells were then inoculated (OD_{600nm}~0.5) into LB/TGY liquid broth medium or plated on LB/TGY agar plates. Growth was assessed by measuring optical density at 600 nm after 18 h or by determining the number of Colony Forming Units (CFU) on agar plates at appropriate temperatures. Growth of cells pre-incubated in U under GC2 remained unaltered as compared to control cells. On the other hand, cells that were pre-incubated in 2 mM U under GC1 did not show growth (Fig. 4.16).

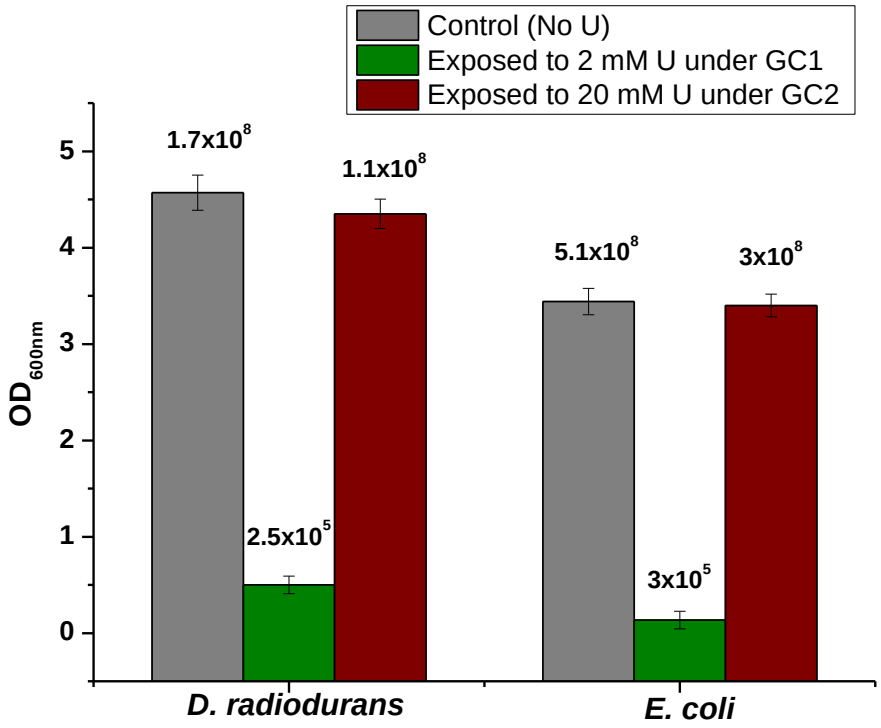

Fig. 4.16 Uranium sensitivity of *D. radiodurans* and *E. coli*. Pre-grown cells were suspended in buffer solution (10 mM MOPS) containing U under either GC1 (0-2 mM) or GC2 (0-20 mM) for 6 h under sterile conditions. Such U-exposed cells were washed free of uranium containing buffer solution, inoculated into liquid broth medium (at 0.5 OD_{600}) and grown for 18 h with agitation (150 ± 5 rpm). CFUs obtained after plating are indicated above the respective bars.

Enzyme-based bioprecipitation can circumvent metal sensitivity by preventing entry and intracellular accumulation of the metal. Thus, phosphatase mediated precipitation is not affected by the high uranium concentration tested (upto 10 mM) in spite of the reported low metal tolerance of *D. radiodurans*. To substantiate this, an experiment was conducted in which actively growing *Deino-pRAD1* (absence of phosphatase) and *Deino-PhoNK* cells were incubated with U under GC1 (2 mM) or GC2 (30 mM) in the presence or absence of β-GP substrate. The concentrations of U were selected based on toxicity effects observed earlier (Fig. 4.15). *Deino-PhoNK* cells were selected as they can express both the phosphatases. *Deino-pRAD1* showed 2 log cycle reduction in survival when incubated with 2 mM U in the

presence or in the absence of β-GP, while *Deino-PhoNK* cells showed similar CFU as compared to control (no U) when β-GP was present, whereas a 2 log cycle reduction in CFU was observed in the absence of β-GP. This suggested that precipitation of U in case of phosphatase positive *Deino-PhoNK* cells increased tolerance towards U aiding advantage to the recombinant strain (Fig. 4.17A and B). On the other hand, *Deino-pRAD1* cells where phosphatase is absent, the presence of β-GP did not confer any advantage to cells and cells showed reduced tolerance. Similar results were obtained with U under GC2, at 30 mM input U (Fig. 4.17B).

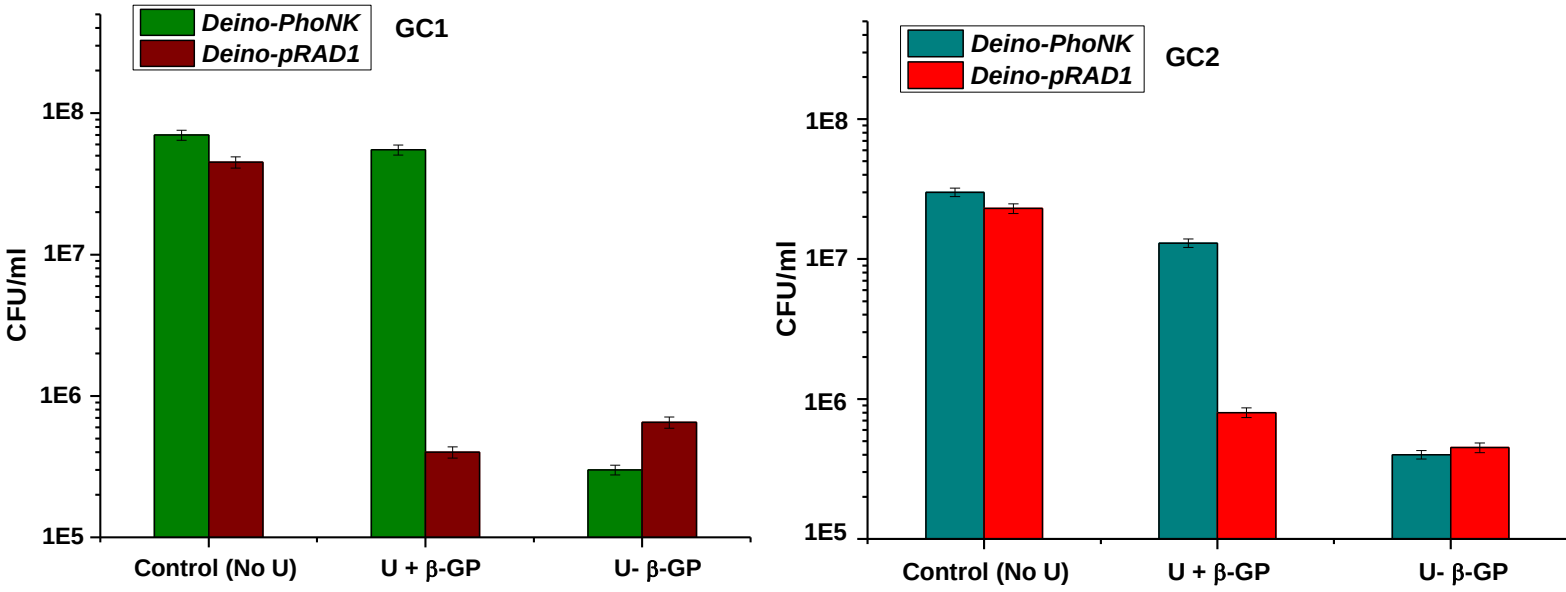

Fig. 4.17 Effect of U toxicity in *Deino-PhoNK* cells under precipitating conditions. *Deino-pRAD1* or *Deino-PhoNK* cells (OD_{600nm} ~0.5) were inoculated in TGY liquid medium containing (A) 2 mM U (GC1) or (B) 30 mM U (GC2) in presence of β-GP (5 mM for GC1 or 60 mM for GC2) or without β-GP. CFUs obtained after 18 h incubation under shaking conditions (150 rpm at 32°C) were recorded.

4.8 Discussion

In this study, a novel alkaline phosphatse, PhoK was cloned and over-expressed in *D. radiodurans* (*Deino-PhoK*). The efficient U precipitation ability of *Deino-PhoK* cells was evaluated and reported in previous chapter. The precipitate characterization studies were conducted to explore on its localization pattern. *Deino-PhoK* cells precipitated U extracellularly. This precipitate was identified as uranyl hydrogen phosphate hydrate [$H_2(UO_2)_2(PO_4)_2.8H_2O$] also, known as chernikovite (Fig. 4.2B), is expected to be fluorescent when excited by UV light. Hence qualitative (Fig. 4.3) and quantitative fluorimetric analysis of uranyl phosphate precipitate was carried out. The results were in conformity with the colorimetric estimation of U (Fig. 4.4). Earlier, PhoN-expressing cells displayed cell associated precipitate which was visualised using SEM. In this study, PhoK-expressing cell (under GC2) showed extracellular precipitation (Fig. 4.5), while PhoN expressing cells showed cell bound precipitation under GC1 as observed by TEM (Fig. 4.6). This was in compliance with the known cellular localization of the two enzymes [113, 121, 136, 156]. The periplasmic or extracellular location of PhoN and PhoK respectively is not a consequence of genetic engineering in alien hosts like *E. coli* or *D. radiodurans*, but is also the natural situation for location and activity of these enzymes in their non-engineered native hosts. The *phoN* gene was cloned from *Salmonella enterica* serovar Typhi wherein it encodes a periplasmic enzyme while *phoK* gene was cloned from *Sphingomonas* sp. strain BSAR-1 wherein it is secreted extracellularly. Since the native localisation/secretion signals have been retained during cloning, the enzymes behave the same way in the new recipient hosts *E. coli* and *D. radiodurans*. Hence, the most plausible explanation for the differential localisation of the U precipitate in *Deinococcus* appeared to be the difference in the cellular and extracellular location of PhoN and PhoK enzymes, respectively. This was also substantiated by the two-phase separation of cell pellet as well as by TEM. Precipitate observed in *Deino-*

phoK cells was unlike in *Deino-phoN* cells where a more uniform mix of cells (pink) and precipitate (yellow) was observed, indicating the presence of cell-associated precipitate (Fig. 4.3B, 4.6A). However, the geochemical conditions employed for U precipitation by the two strains were also different. Hence geochemical modelling studies using MINTEQ were carried out to know the aqueous U speciation under the two conditions employed [23, 30]. MINTEQ modelling studies showed that U mostly formed positively charged complexes under GC1, while uranyl carbonate/hydroxide complexes formed under GC2 were predominantly negatively charged (Table 4.1). Therefore, the present study examined the possible effect of differentially charged aqueous U complexes on precipitate localization under the two GCs employed.

Results showed that under GC1 the precipitate was largely cell associated, whereas under GC2 the precipitate was extracellular with little cell surface association. It was also confirmed that the extracellular/periplasmic location of the two enzymes after incubation under the two different geochemical conditions is not significantly affected by pH. Data showed that under any given condition, cell associated enzyme activity far exceeded activity in the external buffer solution (Table 4.2), which clearly suggested that differential localization of uranyl phosphate precipitate had very little to do with enzyme localization. Further, XRD results showed that the precipitated U species was identical under both the GCs employed, irrespective of the phosphatase used for precipitation (Fig. 4.9). Thus, periplamic (PhoN)/extracellular (PhoK) location of the enzymes [113, 164], which drove metal precipitation, had little role to play in determining whether the precipitate would be cell-associated or extracellular. Identical results were obtained when *E. coli* expressing PhoN/PhoK or *Deino-PhoNK* cells were incubated with U under similar conditions (Fig 4.12 and 4.13).

Phosphatase assays, in absence of uranium, showed that the phosphate liberated was released into the supernatant buffer at pH 6.8 as well as 9 (Table 3.5). Bacterial cells usually carry a net negative surface charge at neutral pH [52-53]. With increase in pH, the negative charge increases due to the increasing deprotonation of the functional groups found on the cell surface. In this study, the differential localisation of the precipitate appears to be governed by the charge-dependent interaction of aqueous U species with the bacterial cell surface. The results indicate that the location of uranyl phosphate precipitate might be a consequence of the earlier event of the differential biosorption of U under the two different geochemical conditions (Fig. 4.14). At pH 6.8 (GC1), U is adsorbed onto the bacterial cell surface, perhaps aided by the positive charge on the uranyl hydroxide aqueous species, which MINTEQ modelling suggests to be most prevalent. This initial complexation on the cell surface forms the nucleation sites, which are further consolidated by the co-deposition of more incoming metal with the outgoing released inorganic phosphate [40, 46, 53-54], resulting in a build-up of polycrystalline metal phosphate precipitate on the cell surface. At pH 9, (GC2), MINTEQ modelling indicated U to be predominantly present as negatively charged uranyl carbonate/hydroxide aqueous complexes. It is difficult to distinguish the decreased biosorption and bioavailability of U due to (a) increasing carbonate concentration in the medium, from (b) repulsion of negatively charged U species from the cell surfaces. However, the low level of U adsorbed onto cell surface seems to be insufficient to consolidate the nucleation sites required for cell-associated precipitation. This leaves the negatively charged uranyl complexes free in the solution resulting in extracellular precipitation of U, upon encountering the phosphate released in the supernatant buffer either by PhoN or PhoK.

The differential toxicity of U under the two geochemical conditions can also be attributed to the above-mentioned phenomenon. U binding to bacterial cell surfaces is

evidently the first step towards obtaining cellular access, which subsequently causes disruption of metabolic processes, eventually leading to lethality [15, 23]. The predominantly negatively charged aqueous complexes of U formed under GC2 are repelled by bacterial cell surface, making it difficult for U to acquire sufficient proximity to cells to cause significant damage. On the other hand, the predominantly positively charged aqueous U species formed under GC1 would allow U to interact with cells resulting in higher toxicity, as evidenced in this study (Fig. 4.15 and Fig. 4.16). This substantiates earlier reports that U biosorption decreases with increasing pH and increasing carbonate/bicarbonate concentration due to higher complexation of uranyl ion by hydroxides and carbonates [23, 31, 44]. U toxicity studies have been reported earlier in native strains isolated from waste contaminated sites; however, U toxicity in *Deinococcus* and *E. coli* is reported only in few studies. *Deinococcus* was shown to be sensitive to 80 ppm (i.e. 0.34 mM) uranyl nitrate at pH 4.0 [165]. A subsequent study reported *Deinococcus* to tolerate 2.5 mM uranyl nitrate, while *E. coli* to tolerate 2.8 mM U [166] but this was when cells were actively growing. No data on the toxicity of U under alkaline conditions (at pH 9.0) to *Deinococcus* or *E. coli* are available in the literature. The experiment shown in Fig. 4.15 and 4.16 were performed in buffer for 4 h in the absence of nutrients, which do not support active cell growth. In our studies we report for the first time that at pH 9.0 exposure to 20 mM U did not decrease survival of *Deinococcus* or *E. coli*.

U precipitation by recombinant *Deino-PhoK/Deino-PhoNK* cells does not require actively growing cells and is essentially de-coupled from growth. In typical precipitation assays, we used resting, non-growing cells and assays were performed in solutions devoid of any nutrient medium. Hence, the low heavy metal tolerance of *D. radiodurans* cells may not be a serious issue in nutrient deficient waste environment. Also enzyme-based bioprecipitation can circumvent this handicap by preventing entry and intracellular

accumulation of the metal. Thus, the issue of metal sensitivity can be avoided by PhoN/PhoK mediated uranium bioprecipitation (Fig. 4.17).

This chapter provides illustrative insights into the interaction of U complexes with bacterial cell surface. The work demonstrates the effect of aqueous speciation of U on microbial cell surface by visualizing localization pattern of uranyl phosphate precipitate. This study shows that, unlike biosorption (which has limited capacity and is often reversible) or bioaccumulation (which depends on the metabolic activity and metal toxicity), U species can be efficiently precipitated and removed from effluent solution by employing phosphatases. The cell associated precipitation of metal under GC1 has advantages of easy downstream processing by simple gravity based settling down of metal loaded cells compared to cumbersome separation techniques [46-47]. With this notion and in light of the fact that the uranium precipitate localization is determined primarily by aqueous uranium speciation, the results from this study are of relevance to effluent treatment using such cells.

Chapter 5

Uranium precipitation by lyophilized or immobilised recombinant *Deinococcus* strains.

The main objective of this study was to develop a system for uranium bioprecipitation from radioactive waste solutions. The present study was undertaken with a view to construct a recombinant bacterial strain capable of bioprecipitation of U from alkaline solution and also to construct a separate strain that could remove U from both acidic-neutral or alkaline conditions in high radiation environment. Previous chapters described cloning and over-expression of a novel alkaline phosphatase, PhoK, in radioresistant *D. radiodurans* to obtain *Deino-PhoK*, and co-expression of both PhoN and PhoK in *D. radiodurans* to generate a strain *Deino-PhoNK*. The recombinant strains exhibited efficient bioprecipitation ability under acidic/alkaline conditions. The precipitated uranyl phosphate species was subsequently characterized using different analytical techniques. The precipitated U and its cellular location were characterized using TEM and the factors affecting its localization were described. These studies on uranyl phosphate precipitate suggested that localization of precipitate is governed by aqueous uranyl speciation and not by location of corresponding phosphatase used for precipitation.

Though, recombinant *Deinococcus* strains showed superior U removal ability and potential for use in effluent waste treatment, in terms of actual application in waste, many factors need to be considered and assessed. Further improvements in uranium bioprecipitation using such cells were therefore sought in terms of (a) lyophilisation and (b) immobilization of cells and the subsequent use of these cells to evaluate U precipitation.

Lyophilisation, also known as freeze drying, is widely used in food industries, microbial culture collection centres etc., in which dehydration process is typically used to preserve perishable material or make the material more convenient for transport. Lyophilized substance may be stored at room temperature without refrigeration [167]. Use of lyophilized cells can offer a better mode of application in bioremediation studies as it converts biomass into dry powder, thereby increasing the ease of handling storage and transport, and further

extending the product shelf life. Few studies have earlier reported use of lyophilized biomass for successful bioprecipitation of cadmium and uranium [47, 122-123]. In actual waste solutions, the conditions would be unfavourable for cells to grow and produce more PhoN/PhoK enzymes on a continuous basis. Once lyophilized, cells can be stored and used whenever needed thus reducing the cost of producing cells frequently. Therefore, lyophilization of *Deino-PhoK* and *Deino-PhoNK* cells was attempted and their U precipitation ability was evaluated.

For the bioremediation of effluent waste, use of freely suspended biomass has several disadvantages, such as storage and maintenance of biomass stability, separation of suspended biomass from the treated effluent, regeneration of used biomass etc. [168]. In contrast, use of immobilized biomass over freely suspended biomass for uranium removal from effluent waste is advantageous in terms of increased mechanical strength, higher cell density, resistance to chemical environment, easy separation of cells from effluents and high biomass loading/performance. Immobilization is the caging of cell or enzyme in a distinct support or matrix. The support or matrix on which the enzymes are immobilized allows the exchange of medium containing substrate or effectors or inhibitor molecules. The practice of immobilization of cells is very old and the first immobilized enzyme was amino acylase of *Aspergillus oryzae* for the production of L-amino acids in Japan [169]. Immobilization technology is widely used in many industries like production of antibiotics, amino acids, beverages, food industry, textile industries etc. In view of above characteristics, it was considered desirable to explore the potential of immobilized *Deinococcus* cells and PhoK enzyme for uranium removal, in a column-based flow-through system.

5.1. Lyophilisation of *Deino-phoK* cells.

Though early exponential phase cells of *Deino-PhoK* strain showed 1.5-2 fold higher specific activity as compared to overnight grown (18 h) cells, the cell density is about 9-10 fold lesser in early exponential phase (OD_{600}~ 0.3-0.4) as compared to overnight grown cells (OD_{600}~3.5-4). In terms of actual application for large volumes of waste solutions, higher cell mass would be needed. Therefore, in order to economise the process, in terms of time, effort and cost, stationary phase cells were used for lyophilisation, as described in Chapter 2. The dried powder (approximately 1.2 g from 1 L overnight grown culture) of lyophilized cells was stored in vials at room temperature up to 2.5 years. These cells were used to determine their alkaline phosphatase activity and uranium precipitation ability.

5.1.1. Effect of lyophilization on survival of the recombinant *Deino-PhoK* cells.

Microbial cell survival during lyophilization is dependent on many factors, such as the strain used, age of culture, use of cryo-protectant etc. Survival of *Deino-PhoK* strain was measured in terms of CFU/ml, before and after lyophilization. Lyophilized cells when suspended in water rapidly formed a uniform suspension. Fresh and lyophilized cells equivalent in terms of cell density (OD_{600}~1) were plated onto TGY/Cm plates. Lyophilized *Deino-PhoK* cells retained nearly 84% viability when tested immediately after lyophilisation. However, after 6 months of storage, cells completely lost viability (Table 5.1).

D. radiodurans being a highly desiccation tolerant organism, was expected to retain viability immediately after lyophilization. However, loss in viability would not be an issue as long as the cells retained the PhoK activity and U precipitation ability. U precipitation by the recombinant *Deino-PhoK* cells, (as described in previous chapters) implied that it does not require actively growing cells and is essentially de-coupled from growth. In U precipitation assays, resting, non-growing cells were used and assays were performed in solutions devoid of any nutrient medium. Therefore, non-viable but PhoK-active lyophilized cells would serve

best in terms of application as they negate and circumvent the risk of horizontal gene transfer and environmental and biosafety issues relevant to application of genetically engineered organisms.

Table 5.1. Viability of lyophilized *Deino-PhoK* cells.

Cells used	**CFU/ml**
Fresh cells	$8.9 \pm 0.7 \times 10^7$
Lyophilized cells (stored for)	
1 day	$7.45 \pm 0.5 \times 10^7$
6 months	Nil

5.1.2. Alkaline phosphatase activity of lyophilized cells.

Although lyophilization is a form of drying by which there is minimum damage to the cells, some loss of activity is often seen. Also as cells were not viable beyond 6 months after lyophilization, it was important to determine the PhoK activity in order to use them for bioprecipitation. PhoK activity for fresh as well as lyophilized cells was determined using *p*-NPP as substrate, immediately after lyophilization and after every 6 months up to 2.5 years. If activity was compared using equal OD cells, lyophilized cells showed PhoK activity comparable to that of fresh *Deino-PhoK* cells even after storage up to 1.5 years. However, the activity was reduced by 15-20% beyond 1.5 years storage (Table 5.2). If the comparison was based on equal protein, the specific activity of lyophilized cells appeared to be slightly higher than fresh cells. This is because the protein content in lyophilized cells is slightly reduced in storage as they are metabolically inactive. Thus, lyophilization did not have any adverse effect and increased the shelf life of *Deino-PhoK* cells, while retaining PhoK activity.

Table 5.2. Alkaline phosphatase activity of lyophilized *Deino-PhoK* cells

Cells	**OD_{405nm}**	**PhoK Specific Activity (nmoles *p*-NP released/min/mg protein)**
Fresh cells	0.865 ± 0.03	3960 ± 185
Lyophilized cells (stored up to)		
1 day	0.845 ± 0.025	4513 ± 296
6 months	0.838 ± 0.03	4476 ± 187
12 months	0.801 ± 0.015	4667 ± 248
18 months	0.790 ± 0.022	4603 ± 280
2 years	0.741 ± 0.01	4318 ± 205
2.5 years	0.685 ± 0.013	3659 ± 175

5.1.3 Uranium precipitation ability of lyophilized *Deino-PhoK* cells.

Fresh and lyophilized *Deino-PhoK* cells (OD_{600}~1) were incubated with 1 mM U (under GC2) and their uranium precipitation was monitored up to 4 h. Although lyophilized *Deino-PhoK* cells exhibited slightly higher specific activity, U precipitation occurred equally efficiently in both fresh and lyophilized cells. Lyophilized cells could precipitate more than 90% uranium within 4 h which was comparable to precipitation shown by fresh cells (Fig. 5.1). U precipitation by lyophilized *Deino-PhoK* cells stored up to 2.5 years was slightly slower as compared to fresh cells, but nonetheless achieved more than 90% precipitation in 4 h. Lyophilized cells showed higher U loading as compared to fresh cells, in terms of equivalent protein used for precipitation at 1 mM input U (GC2). Fresh cells showed 1.428 ± 0.08 g U loading/g of PhoK protein, while lyophilized cells showed 2.03 ± 0.1 U loading/g of PhoK protein. The prime advantage of using lyophilized cells would thus be for long term storage at room temperature with negligible loss of activity and higher U loading capacity**.**

Thus, lyophilisation preserved the PhoK activity as well as uranium precipitation ability of *Deino-PhoK* cells, even after storage up to 2.5 years at room temperature.

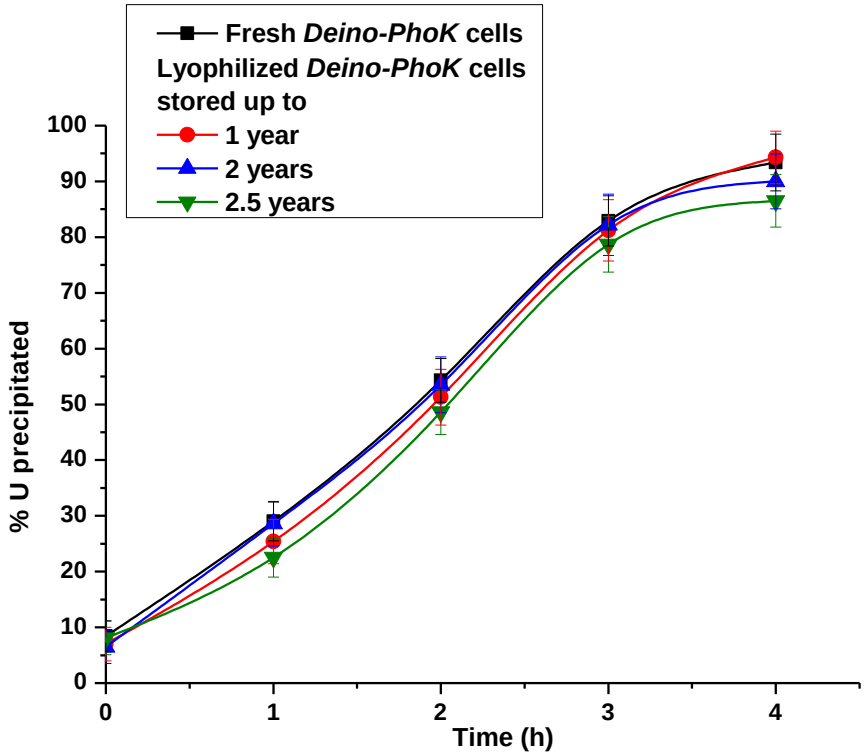

Fig. 5.1 U precipitation by lyophilized *Deino-PhoK* cells. Fresh and lyophilized cells (OD_{600}~1) were incubated with 1 mM U in 10 mM MOPS buffer (pH 9.0) with 5 mM β-GP for 4 h. Aliquots were removed at specific time intervals, centrifuged at 12,000 rpm for 5 min, and U was estimated in the supernatant by Arsenazo III method.

5.2 Lyophilisation of *Deino-PhoNK* cells

Previous chapter (Chapter III) described uranium precipitation ability of *Deino-PhoNK* cells evaluated under GC1 and GC2 separately. The precipitation kinetics shown by *Deino-PhoNK* strain under GC1 or GC2 was similar to *Deinococcus* expressing PhoN or PhoK independently (Fig. 3.26). The *Deino-PhoNK* cells were also subjected to lyophilisation and used to determine their PhoN/PhoK activity as well as U precipitation ability.

5.2.1 Phosphatase activity of lyophilized *Deino-PhoNK* cells.

PhoN/PhoK activity of fresh as well as lyophilized cells was determined by measuring inorganic phosphate release from β-GP. Lyophilized cells retained nearly 92-95% PhoN/PhoK activity as compared to fresh cells, at all the three pH conditions tested, i.e. pH 5,

pH 7 and pH 9, when stored up to 1 year (Table 5.3). Thus lyophilisation increased shelf life of recombinant *Deino-PhoNK* cells and did not have any deleterious effect on the either PhoN or PhoK activity.

Table 5.3. **PhoN/PhoK activity of lyophilized *Deino-PhoNK* cells**

Deino-PhoNK cells used	Amount of P_i released (nmoles/µg protein)		
	pH 5	pH 7	pH 9
Fresh cells	516 ±7	1614 ± 10	5650 ±25
Lyophilized	484 ± 5	1517 ± 10	5972 ± 20

5.2.2. Uranium precipitation ability of lyophilized *Deino-PhoNK* cells

Fresh and lyophilized *Deino-PhoNK* cells were evaluated for U (1 mM) precipitation ability at acidic (GC1) or alkaline pH (GC2) separately. Lyophilized *Deino-PhoNK* cells (OD_{600}~3) showed slightly slower U precipitation initially as compared to fresh cells, however it was comparable at the end of 4 h. At the end of 8 h, both lyophilized and fresh cells showed more than 90% precipitation (Fig. 5.2A). In terms of U loading, lyophilized *Deino-PhoNK* cells precipitated 0.648 ± 0.05 g U/g protein equivalent in 8 h at 1 mM input U under GC1, while fresh cells precipitated ~ 0.510 ± 0.07 g of U/g of protein equivalent in same time at same U concentration. Under GC2, lyophilized cells showed similar precipitation kinetics as compared to fresh cells. Lyophilized cells (OD_{600}~1) showed more than 80% precipitation of U within 3 h similar to shown by fresh cells (Fig. 5.2B). In terms of U loading, lyophilized *Deino-PhoNK* cells precipitated 1.94 ± 0.06 g U/g protein equivalent, while fresh cells precipitated ~ 1.52 ± 0.06 g of U/g of protein equivalent at 1 mM input U in 4 h. Thus lyophilisation was able to maintain PhoN/PhoK activity as well as uranium precipitation ability of recombinant *Deino-PhoNK* cells.

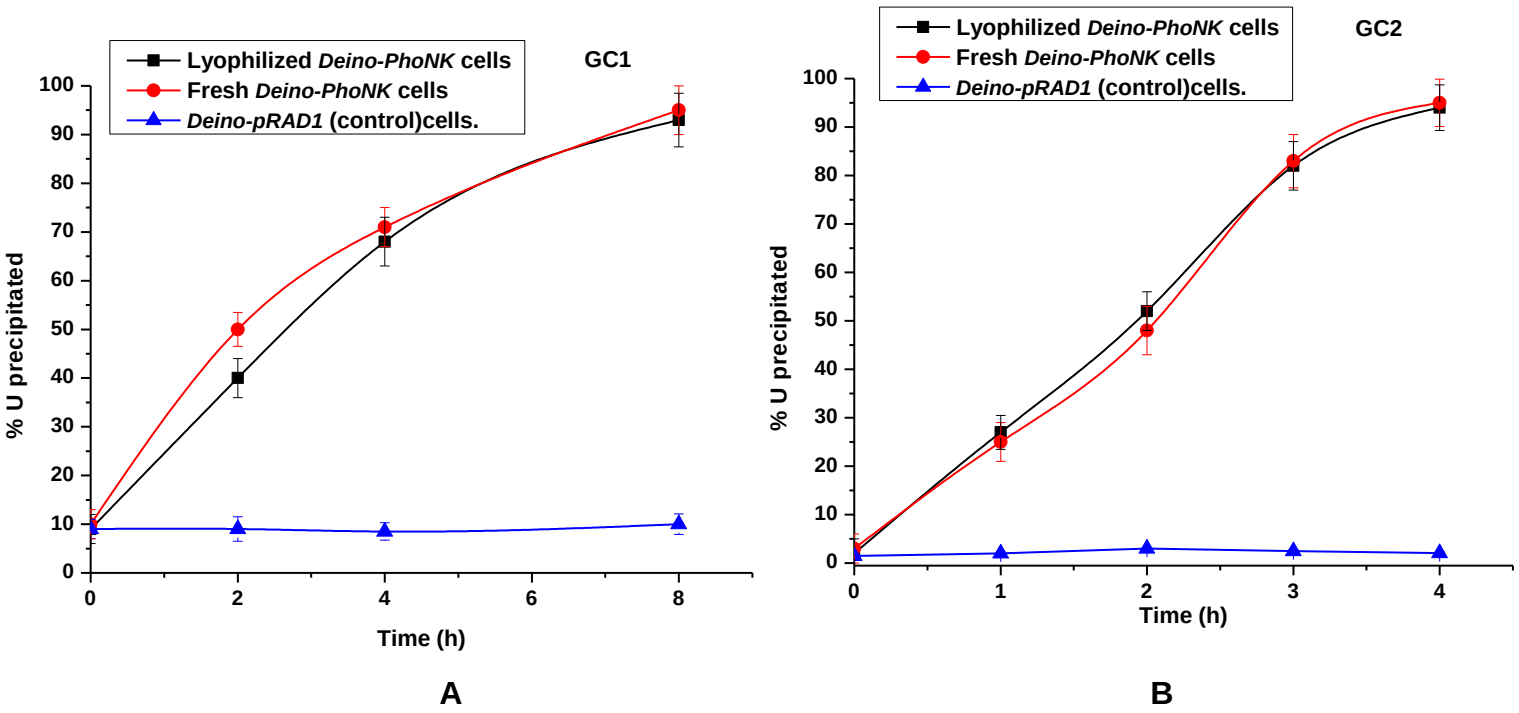

Fig. 5.2. U Precipitation by lyophilized *Deino-PhoNK* cells under GC1 or GC2. Fresh or lyophilized *Deino-PhoNK* cells (OD_{600}~3) were incubated with U (1 mM) in 10 mM MOPS with 5 mM β-GP as substrate (final pH 6.8) for 8 h under GC1. For GC2, cells (OD_{600}~1) were incubated with U (1 mM) in 10 mM MOPS with 5 mM β-GP as substrate (final pH 9) for 4 h. U removal at different time intervals was measured from supernatant using Arsenazo III reagent**.**

5.3 Immobilization of *Deino-PhoK*/*Deino-PhoNK* cells and evaluation of their uranium precipitation ability:

Localization pattern of uranyl phosphate precipitate revealed that important factor governing precipitate localization, i.e. cell-associated or extracellular, was the aqueous uranyl species predominant under the particular geochemical condition (Chapter IV). Under GC1, the precipitate was cell surface associated while under GC2, it was extracellular, irrespective of phosphatase (PhoN/PhoK) employed for precipitation or uranyl salt used. Under GC1, the cell bound precipitate makes cells heavy causing them to settle down, thus facilitating easy recovery of the precipitated U without centrifugation. However, the uranyl phosphate,

precipitated under GC2 by PhoK expressing cells remained extracellular and required centrifugation for complete recovery. In order to achieve more convenient and easier separation of uranyl phosphate precipitate from the bulk volume, bioprecipitation was attempted with immobilized *Deino-PhoK* and *Deino-PhoNK* cells.

A widely used technique for cell immobilization is cell entrapment, in which the living cells are contained in a polymeric matrix which is porous enough to allow the diffusion of substrate to the cells and of products away from the cells. The entrapment technique of cell immobilization is simple and causes no harm to cells [170-171]. Materials that have been successfully used for cell entrapment include agar, agarose, alginate, k-carrageenan, polyacrylamide, polyurethane, cellulose, collagen, chitin, chitosan, etc. [172-173]. For immobilization of *Deino-PhoK*/*Deino-PhoNK* cells, calcium alginate was selected. Most of the polymers used for entrapment are also known to bind metal ions strongly [43]. Ca-alginate immobilized biomass was found to be most suitable due to its easy immobilization at room temperature and having a long stability of more than 2 months under the experimental conditions, as also reported previously for uranium biosorption by fungal biomass [174]. Suitability of other immobilizing matrices have been tested earlier and Ca-alginate was found to be most appropriate for batch studies [175-176]. Ca-alginate immobilized *Scenedesmus quadricauda* was used for biosorption of Cu(II), Zn(II) and Ni(II) [176]. Ca-alginate immobilization has also been reported to enhance cadmium uptake potential of *Trametes versicolor* mycelia in batch system [177]. Therefore, Ca-alginate was selected as suitable immobilization matrix for immobilization studies.

5.3.1 U precipitation using immobilized *Deino-PhoK* cells in batch process.

Freshly harvested *Deino-PhoK* or *Deino-pRAD1* cells were immobilized in Ca-alginate beads, as described in Chapter 2. Blank alginate beads (2 % w/v) without cells were

also prepared and used as control. To confirm that immobilisation of cells has not altered their phosphatase activity and substrate is well accessible even after entrapment in beads, *p*-NPP assay of beads was carried out, in the same way as for the free cells. Test and control beads were incubated in MOPS buffer for 3 h and activity in beads as well as in the supernatant were assayed. Beads were incubated in the assay mixture with substrate for 30 min. For supernatant, activity in 100 µl volume was estimated. After 30 min, beads were removed and 0.2 N NaOH was added to assay mixture. OD of assay mixture was recorded spectrophotometrically at 405 nm (Table 5.4).

Table 5.4. The *p*-NPP activity of *Deino-PhoK* cells after immobilization into beads

Sample	*p*-NPP activity (nmoles *p*-NP liberated/min)	
	Beads	Supernatant
Deino-PhoK	5.32 ± 0.15	0.51 ± 0.08
Deino-pRAD1	0.025 ± 0.013	NA

Thus, PhoK activity was largely retained in the cells even after entrapment in beads. Negligible extracellular PhoK activity was observed when beads were incubated in buffer in conformity with the results obtained when free cells (non-growing) were incubated in buffer (Table 4.2).

The beads were tested for U bioprecipitation under alkaline conditions (GC2) similar to conditions employed for free biomass of *Deino-PhoK* cells. Blank beads when incubated with U, showed 8-9% U loss from supernatant, indicating the amount of U adsorbed by Ca-alginate itself. In U solution where no beads were incubated, there was only 0.1-0.2% loss of U from supernatant. Beads immobilized with *Deino-PhoK* could remove ~90% uranium from

1 mM solution within 2 h (Fig. 5.3), whereas control beads immobilized with *Deino-pRAD1* cells could remove only 8-9 % uranium even after prolonged exposure (Fig. 5.3).

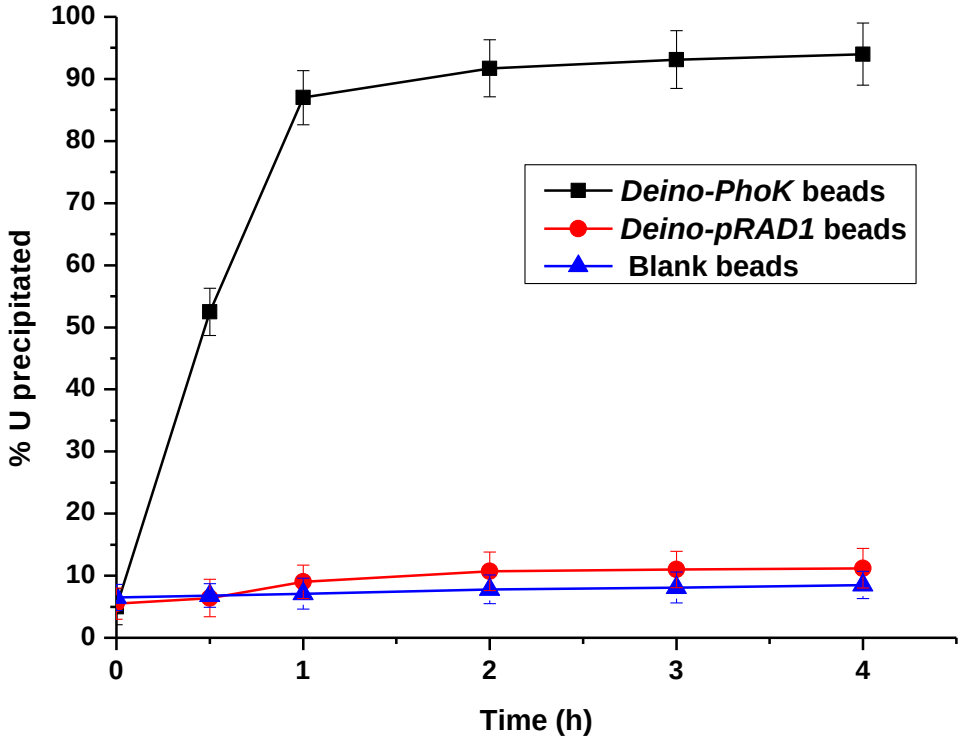

Fig 5.3. U precipitation by immobilized *Deino-PhoK* cells. Equal number (100) of calcium alginate beads without cells (blank beads) or containing immobilized *Deino-PhoK* or *Deino-pRAD1* cells were suspended in uranium solution (1 mM U in 10 mM MOPS buffer, pH 9.0 with 5 mM β-GP under GC2) and U removal was monitored as decrease in uranium content from supernatant up to 4 h.

In chapter IV, the inherent fluorescent property of uranyl phosphate precipitate (chernikovite) was used for qualitative and quantitative estimation of precipitation (Figs. 4.3 and 4.4). Similarly, spectrofluorimetric analysis of precipitation by beads was also carried out. On exposure to UV light (380 nm), a bright green fluorescence, indicating the presence of chernikovite, was seen only in *Deino-PhoK* beads (Fig. 5.4A) but not in *Deino-pRAD1* (control cells) beads (Fig.5.4B). Supernatant buffer medium after removal of beads, when

exposed to UV light, did not show green coloured fluorescence in either *Deino-PhoK* or *Deino-pRAD1* (Fig. 5.4C).

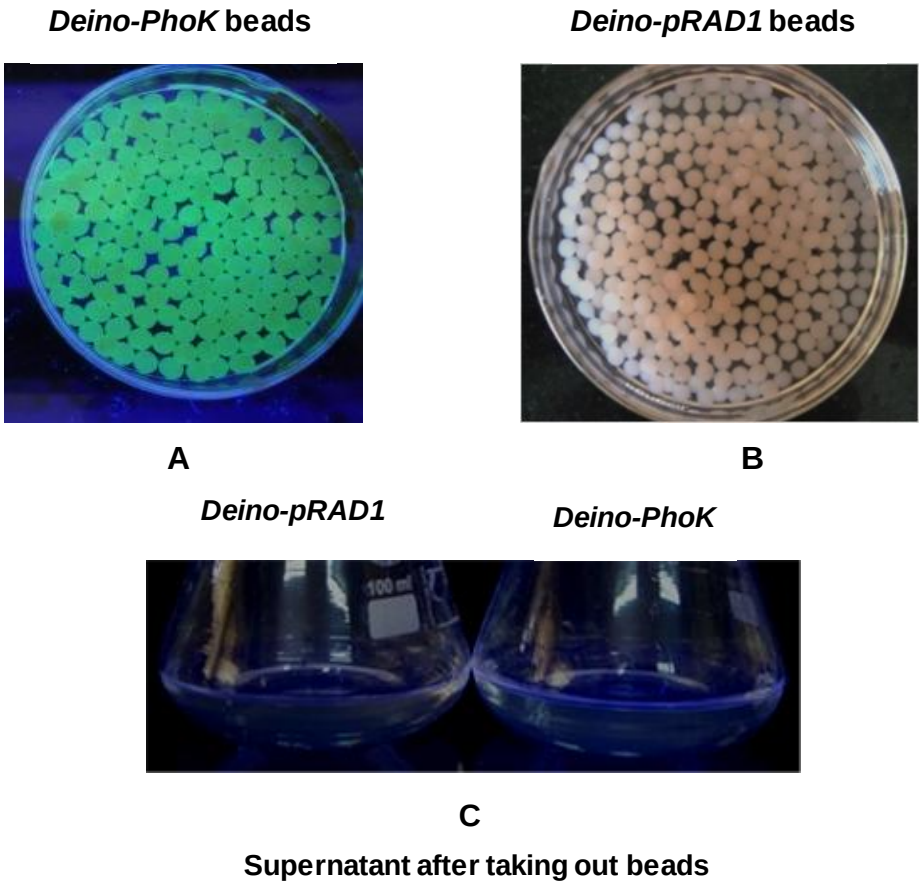

Fig. 5.4. Qualitative affirmation of uranyl phosphate in beads. Calcium alginate beads containing immobilized *Deino-PhoK* cells **(A)** or *Deino-pRAD1* cells **(B)** were incubated with 1 mM U as described in legend to Fig. 5.4 for 4 h. The beads were removed from the solution, exposed to UV (380 nm) and photographed. The supernatant buffer medium was also exposed to UV after removal of beads from the solution. The green fluorescence emanating from chernikovite entrapped inside beads is observed in (A) but not in (B) or (C).

The beads were then analysed spectrofluorimetrically for quantitative estimation. The *Deino-PhoK* beads showed increase in fluorescence up to 2 h after which it remained steady. When the supernatant (after removal of beads) was analysed similarly, no significant increase

in fluorescence was observed up to 4 h (Fig. 5.5), clearly establishing confinement of precipitate to the beads.

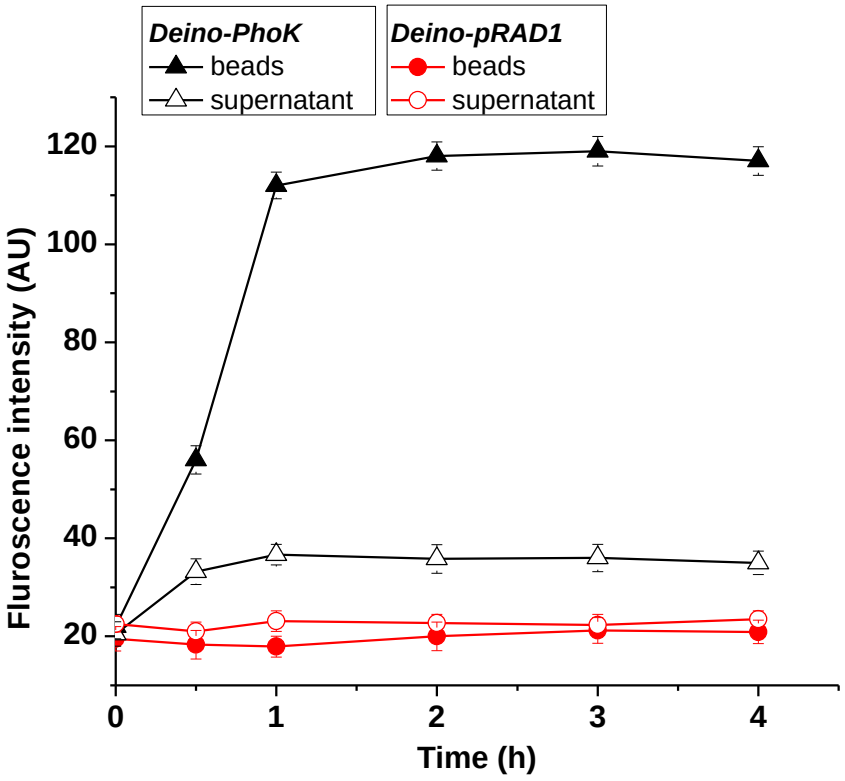

Fig. 5.5 Spectrofluorimetric analysis of bioprecipitation by recombinant cells immobilized in beads. *Deino-PhoK* or *Deino-pRAD1* cells were immobilised into beads and evaluated for U precipitation as described in Fig. 5.4. Ten beads were removed from solution at each time intervals and their fluorescence intensity (in arbitrary units, AU) was measured in a spectrofluorimeter over a period of time (0-4 h) using λ_{ex}=380 nm and λ_{em}=524 nm.

This was in contrast to fluorescence pattern observed with whole cell suspension (Fig. 4.4) wherein fluorescence increases over time, while in case of beads it does not change in the supernatant. Thus, precipitate is indeed entrapped into beads which settled down to the floor of the flask. The beads could be easily separated from solution just by decanting supernatant in another container, thus facilitating easy separation and recovery of the bioprecipitated uranium. The beads showed ~ 0.5 g of U loading/g of biomass dry weight at 1 mM input U concentration.

5.3.2. U precipitation by calcium alginate immobilized *Deino-PhoNK* cells in batch process.

Lyophilized *Deino-PhoNK* cells were also immobilised into calcium alginate beads, similar to *Deino-PhoK* cells, and the beads were used for U precipitation under GC1 or GC2 separately. Under GC1 blank beads (beads without cells) or *Deino-pRAD1* beads, showed about 80% U removal from solution (Table 5.5), whereas under GC2, only 7-8% U was removed (Fig. 5.4) with control beads. This might be because of adsorption of U to the beads. It was demonstrated in previous chapter that; U is adsorbed in higher amount to the cell surface under GC1 than under GC2 (Section 4.6). In Ca-alginate, due to presence of reactive carboxylic groups of alginate, considerable U is also adsorbed directly to the beads. Hence U precipitation was tested only under GC2, with *Deino-PhoNK* cells. *Deino-PhoNK* cells immobilised into beads showed >90% U precipitation within 3 h (Fig. 5.6) at 1 mM U input concentration, similar to that shown by *Deino-PhoK* cells (Fig. 5.3). The beads also showed green coloured fluorescence on exposure to UV and settled well at the bottom of flask in a short time.

Table 5.5. U removal (%) in control Ca-alginate beads under GC1

Time (h)	Blank beads (No cells)	*Deino-pRAD1* beads
0	72.3 ± 3	75 ± 3
1	75.4 ± 2	78.6 ± 2
2	78.2 ± 4	80 ± 4
3	81.6 ± 3	81.5 ± 3
4	82 ± 2	80.5 ± 2

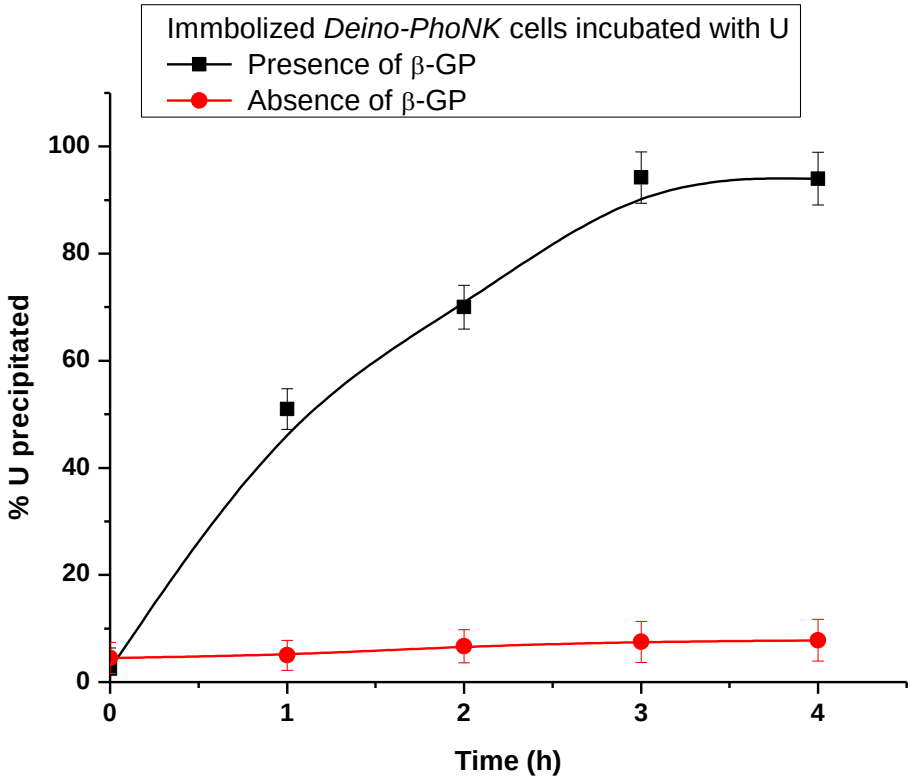

Fig 5.6. U precipitation by immobilized *Deino-PhoNK* cells under GC2. Equal number (100) of calcium alginate beads in which *Deino-PhoNK* cells were immobilized, were suspended in uranium solution (1 mM U in 10 mM MOPS buffer, pH 9.0) with and without β-GP substrate and U removal was monitored as decrease in uranium content from supernatant up to 4 h.

5.3.3. U bioprecipitation by calcium alginate immobilized *Deino-PhoK* cells in a column

U bioprecipitation in large-scale application can be handicapped by operational limitations in batch process. A column based approach for U bioprecipitation provides the advantage of a continuous flow system wherein input U can be passed through the column, such that U is retained while the U depleted solution comes out in the flow-through. Also high loading values can be attained in column based process. Hence U bioprecipitation was attempted in column-based flow-through process under GC2.

For preliminary studies and standardization of procedure for column studies, blank beads (No cells) and *Deino-pRAD1* cells immobilized into beads were used as a control. Blank beads were packed in a column (125 ml volume). About 500 ml uranyl carbonate (1

mM) solution along with substrate (5 mM β-GP) was passed through column at a flow rate of 10 ml/h for 24 h. Though, negligible U loss was observed (8-9%) in the eluted solution, it was observed that after few hours, beads started swelling (Fig. 5.7). Also, due to pressure built up inside the column, beads started moving in the direction against the flow of U solution and after overnight period, most of the beads were broken. As calcium alginate beads could not withstand pressure in the column, further studies were attempted using polyacrylamide gel as a matrix.

Before passing U solution **After passing U solution**

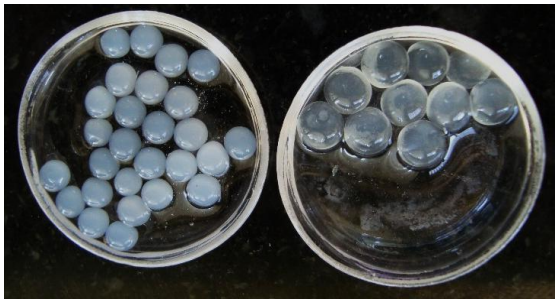

Fig. 5.7. Standardization of procedure for column studies. U solution (1 mM) in 10 mM MOPS buffer (pH 9.0) and 5 mM β-GP was passed through a column packed with blank Ca-alginate beads (without cells) for 24 h and beads observed subsequently.

Previous studies have reported use of polyacrylamide gels to immobilize cells and subsequent use in column studies. In our laboratory, lyophilized *Deino-PhoN* cells immobilized in polyacrylamide gel have been used to precipitate U in column studies under GC1 [122] with loading of 0.73 g of U/g of dry biomass achieved in 8 days. Hence it was desired to immobilize *Deino-PhoK* cells in polyacrylamide gel.

Lyophilized cells of *Deino-PhoK* (250 mg) were immobilized into polyacrylamide gels and tested in a continuous flow-through system as described earlier (Chapter 2, Section 2.14.2). The uranium metal concentration in the flow through was reduced by 80-90% of the input uranium concentration on an average. The rate of uranium precipitation was similar for

3-4 days, when up to 600 ml U solution was passed through column, following which the rate started to decrease due to clogging of the column. At the end of 8 days, around 1L of the uranyl carbonate solution had passed through the column resulting in uranium loading of 0.85 g/g dry weight (Fig. 5.8). At the end of the experiment the column packed with recombinant cells turned from pink to yellow due to substantial deposition of uranyl phosphate (Fig. 5.8A and B).

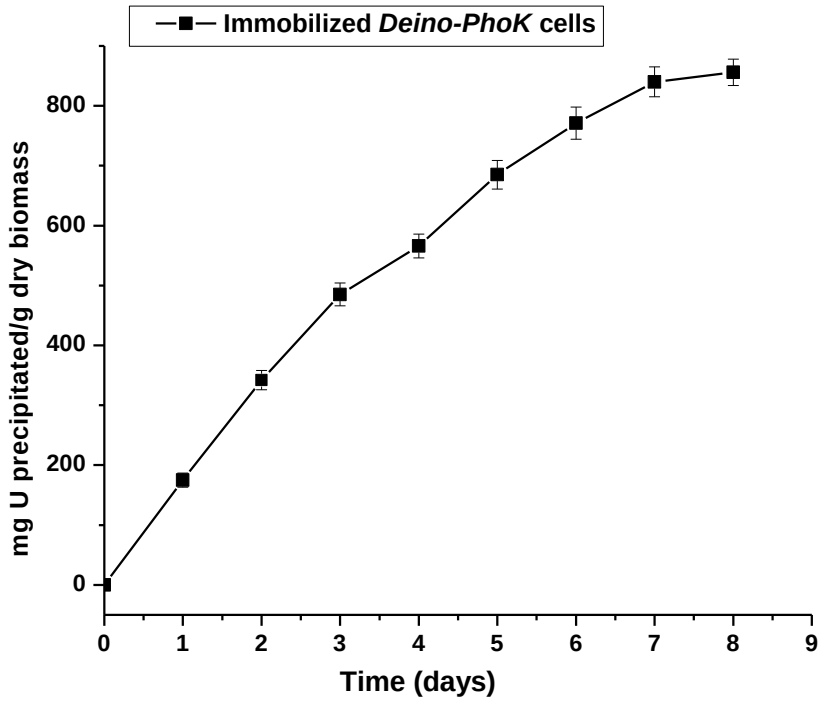

Fig. 5.8. U precipitation by immobilised *Deino-PhoK* cells in column. Lyophilized *Deino-PhoK* cells (250 mg) immobilised in a polyacrylamide gel were packed in column (125 ml volume). One litre of U solution (1 mM in 10 mM MOPS buffer, pH 9.0 and 5 mM β-GP, under GC2) was passed through column over a period of 8 days at an average flow rate of 7 ml/h. U was estimated in the flow-through at regular time intervals and the loading was calculated accordingly.

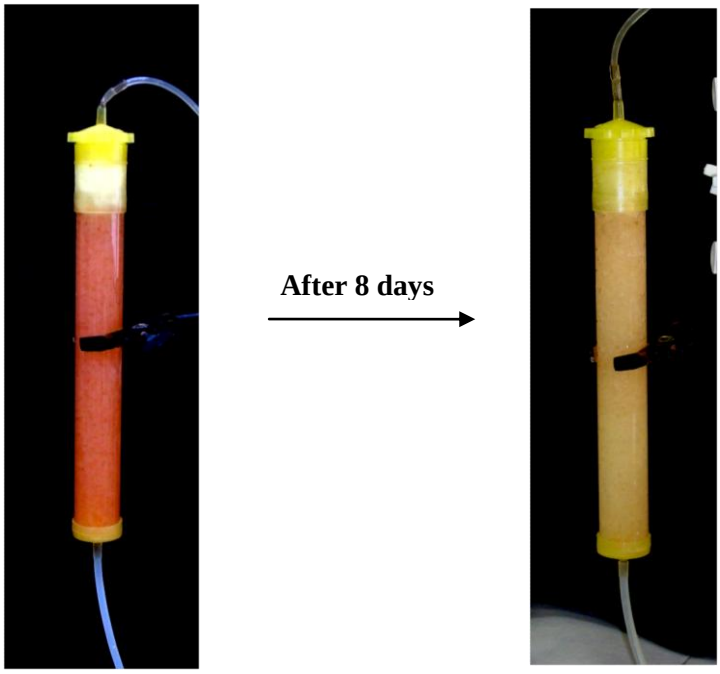

Fig. 5.9 Uranium precipitation by immobilized *Deino-PhoK* cells in continuous flow through system. U precipitation was monitored in column flow-through, as explained in the legend to Fig. 5.9. Column of *Deino-PhoK* cells immobilized in polyacrylamide gel, before the start of the experiment (A) and at the end of the experiment (B) showing distinct change in colour due to deposition of uranyl phosphate precipitate.

5.4. Use of immobilised PhoK protein in column-based U bioprecipitation

Previous sections described immobilisation of whole cells into Ca-alginate or polyacrylamide gel matrix and use of these cells in either batch or column process. The potential of cell-based flow-through system appeared to be seriously limited due to clogging of the column by the precipitate formed. Also to achieve high loading capacity of U, higher biomass was required (~250 mg). Therefore, to achieve high U loading values while avoiding the problem of clogging, one solution thought was use of immobilised PhoK protein instead of whole cells. Immobilised cells are bulky and occupy large volume, whereas purified protein due to its smaller size can be efficiently packed in column. The prime advantage of

using PhoK protein over cells would be its high specific activity, which may facilitate judicious use of substrate. A very small amount of protein can achieve efficient U precipitation as compared to whole cells. PhoK protein immobilization was attempted in Ni-NTA (Ni^{+2}-nitrilotriacetic acid) affinity matrix and U precipitation was evaluated using immobilised PhoK in batch and column process.

5.4.1 Immobilisation of PhoK and its activity

Recombinant PhoK (His_6-tagged) over-expressing BL21 *E. coli* cells (EK-4, Table 2) were used for immobilisation of PhoK on Ni-NTA matrix. The cell free lysate was incubated with Ni-NTA matrix for binding of PhoK to matrix. After binding, matrix slurry was given washes with 5, 10, 15 and 20 mM imidazole so as to remove non-specifically bound proteins (Fig. 5.10).

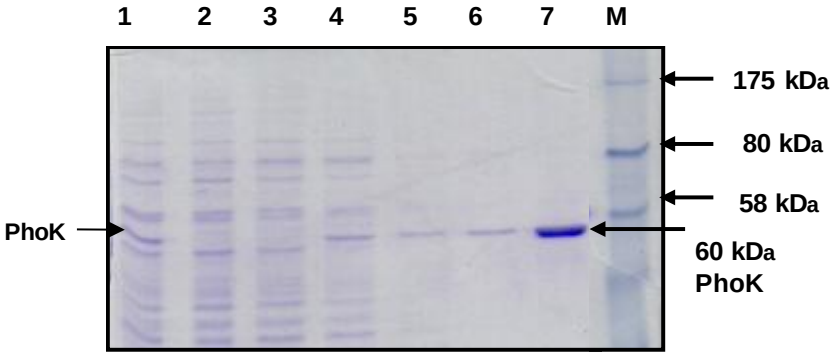

Fig. 5.10. Binding of PhoK on Ni^{+2}-NTA matrix. EK-4 cell free lysate (800 µl) was incubated with Ni^{+2}-NTA matrix slurry (250 µl) for 6 h and given washes with 5, 10, 15 and 20 mM imidazole (20 min each). After final wash matrix was stored at 4°C for further use. Lane 1, EK-4 cell free extract before incubation with Ni^{+2}-NTA; lane 2, EK-4 cell free extract after incubation with Ni^{+2}-NTA; lanes 3-6, wash with 5, 10, 15 and 20 mM imidazole respectively; lane 7, added to PhoK bound to Ni^{+2}-NTA (eluted from 20 µl matrix slurry in non-reducing cracking buffer); lane M, pre-stained protein marker.

The binding of PhoK was ascertained by *p*-NPP activity (Table 5.6) and zymogram analysis (Fig. 5.11). For this, 5 µl control, unbound Ni^{+2}-NTA matrix and PhoK bound Ni^{+2}-NTA matrix slurry was used. Control matrix slurry showed negligible *p*-NPP activity, whereas PhoK immobilised Ni^{+2}-NTA matrix showed very high activity of 8.2 ± 0.5 nanomoles of *p*-NP liberated/min. In terms of specific activity (per mg protein), this corresponds to ~24,000 ± 145 units of PhoK/min/mg protein.

Table 5.6. Activity of PhoK immobilized on Ni^{+2}-NTA matrix

Sample	PhoK Activity (nmoles of *p*-NP released/min)
Control (PhoK unbound Ni^{+2}-NTA matrix)	0.02 ± 0.05
PhoK immobilized on Ni^{+2}-NTA	8.2 ± 0.65

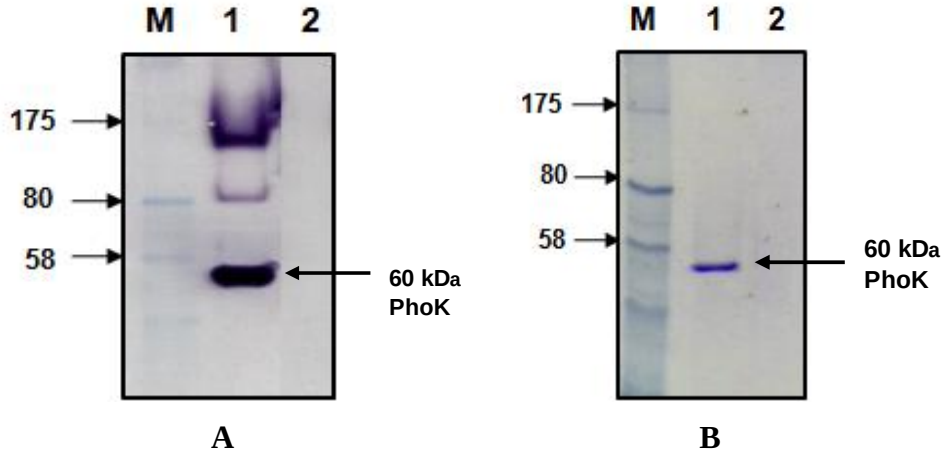

Fig. 5.11. Zymogram analysis of immobilized PhoK. (A) PhoK bound (0.375 µg,) Ni^{+2}-NTA slurry (20 µl) was incubated with non-reducing cracking buffer for 20 min to extract protein and electrophoretically resolved by 10% non-reducing SDS-PAGE to stain for *in gel* phosphatase activity at pH 9.0. Lane M, prestained protein marker; lane 1, PhoK immobilized on Ni^{+2}-NTA; lane 2, unbound Ni^{+2}-NTA matrix (control) (B) Coomassie brilliant blue stained gel as loading control.

5.4.2 U precipitation by immobilised PhoK in batch process

For U bioprecipitation assay in batch process, PhoK immobilized Ni^{+2}-NTA matrix (100 µl slurry carrying ~15 µg protein) was added to 2.5 ml of 1 mM U solution under GC2. As a control, unbound Ni^{+2}-NTA matrix was used. More than 95% precipitation of U was observed within 3 h in case of PhoK immobilized on Ni^{+2}-NTA matrix. The same matrix was reused for two more rounds of precipitation. After first round of precipitation, the matrix was subjected to differential centrifugation so as to separate heavier Ni^{+2}-NTA matrix first, from precipitated uranyl phosphate. The precipitate was collected in another tube, and matrix was washed with buffer to remove loosely bound precipitate. This matrix was then used for next round of precipitation. In second round, precipitation was slightly slower, ~60% at the end of 2 h and 83% within 5 h, compared to the first round where more than 80% U was precipitated in 2 h. For third time use of matrix, only 10-15 % precipitation was observed up to 5 h. In control (unbound Ni^{+2}-NTA matrix) only 2-3% U removal was observed (Fig. 5.12).

If U precipitation is compared in terms of loading capacities, Ni^{+2}-NTA bound PhoK showed 30 µg of U/µg of PhoK protein in the first round and 21 µg of U/µg of PhoK in the second round at the end of 2 h. In the third round only 0.74 µg of U/µg of PhoK was precipitated over same time period. However, ~ 32 µg of U/µg of PhoK was precipitated at the end of 5 h in second round and ~7 µg of U/µg PhoK in the third round.

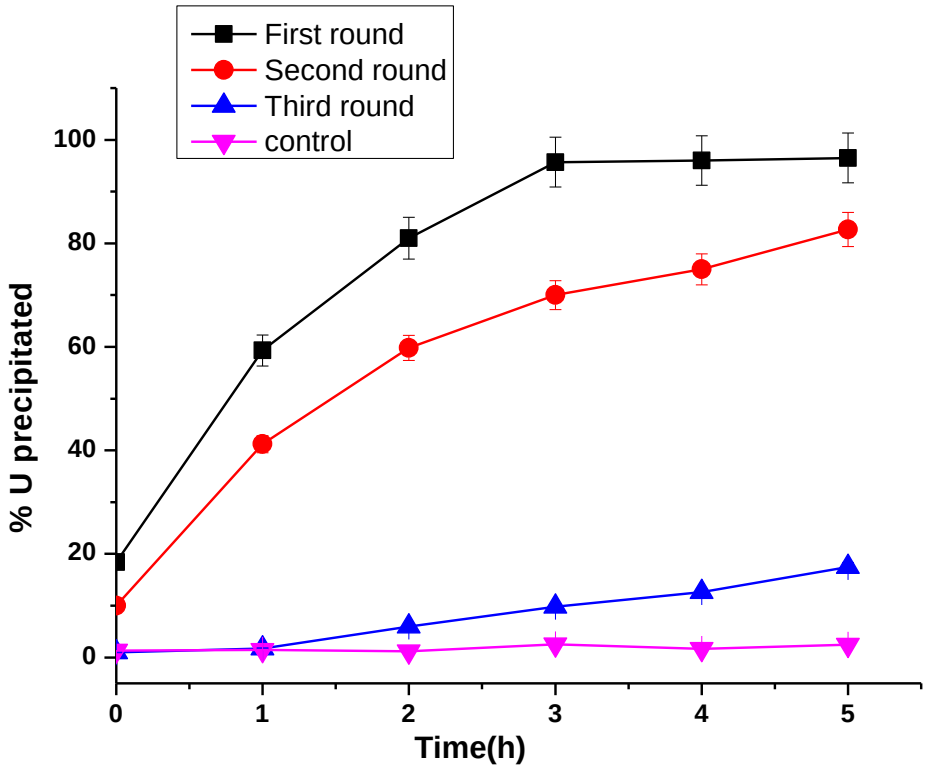

Fig. 5.12. U bioprecipitation using PhoK immobilized on Ni^{+2}-NTA in batch process. PhoK immobilized Ni^{+2}-NTA matrix (corresponding to ~15 µg protein per 100 µl Ni^{+2}-NTA slurry) was added to 2.5 ml of 1 mM U solution (in 10 mM MOPS buffer, pH 9.0 and 5 mM β-GP) under GC2 and incubated for 5 h. Unbound Ni^{+2}-NTA matrix was used as a control. At regular time intervals, aliquots were withdrawn and centrifuged at 12000 rpm for 5 min. U removal from supernatant was estimated using Arsenazo III.

5.4.3 U precipitation by immobilised PhoK in continuous flow through process

For column studies, 1 ml Ni^{+2}-NTA matrix (PhoK immobilised) was packed in small column (volume-10 ml) and 200 ml uranyl solution (1 mM input concentration) solution was passed through it for 24 h. In first round, more than 90% U was precipitated in the column and eluted solution contained only 8-9% of input U. This precipitated U was then eluted out in 0.2 M carbonate – bicarbonate buffer with 80% efficiency. In first round, ~ 40 mg U was precipitated by using 180 µg protein, corresponding to U loading of ~220 ± 10 µg U/µg PhoK protein. In terms of loading capacity, continuous flow through system do have advantage over batch process. U loading capacity for column in first round was ~ 220 ± 10

µg of U/µg of PhoK which was 7-8 times higher as compared to batch process (Table 5.7). In the second round 150 ml U solution was passed achieving 87% U precipitation. Approximately 31 mg U precipitated in second round, corresponding to a U loading of 175 ± 10 µg U/µg PhoK protein. However, in third round, only 8-9 % U precipitation was observed due to loss of PhoK activity.

The higher U loading values obtained in column process is the consequence of higher amount of input metal passed through the column on continuous basis. In the batch process, if the amount of input metal is increased, it might also achieve higher U loading as the protein used in both the processes is equally efficient. The column showed intense green coloured fluorescence (due to accumulation of uranyl phosphate in first and second round of precipitation) when exposed to UV light, thus qualitatively indicating precipitation of U (Fig. 5.13) inside the column.

Table 5.7 Comparison* of U precipitation in batch verses column process using immobilised PhoK protein

PhoK-bound Ni^{+2}-NTA matrix used for U precipitation	**U precipitated (µg U/µg PhoK protein) after each round**		
	I	**II**	**III**
Column process	220 ± 10	175 ± 10	2.9 ± 0.5
Batch process (2 h)	30 ± 1.5	21 ± 1	0.75 ± 0.1

* Compared with respect to amount of PhoK protein required (µg) to achieve U loading

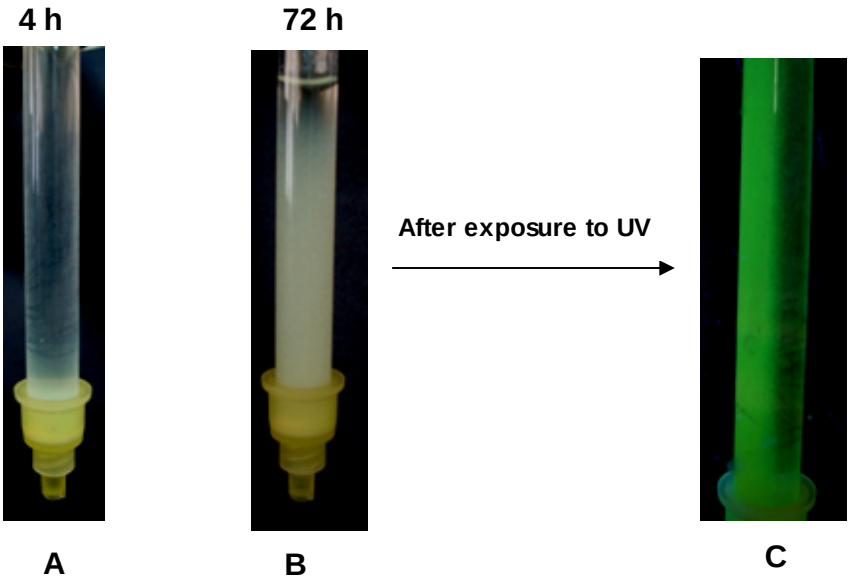

Fig. 5.13. U bioprecipitation using PhoK immobilized on Ni^{+2}-NTA in a column. PhoK immobilized Ni^{+2}-NTA matrix (~ 180 µg protein in 1 ml matrix slurry) was packed in a column (10 ml volume). In first round ~ 200 ml U solution (1 mM U in 10 mM MOPS buffer, pH 9.0 and 5 mM β-GP) was passed through column for 24 h at an average flow rate of 10 ml/h. In the second and third round ~150 ml U solution was passed through column. U was estimated in flow-through at regular time intervals and the loading was calculated accordingly. After third round. the column was exposed to UV (380 nm) and photographed. The green fluorescence emanating from chernikovite is observed in (C).

Although U precipitation with PhoK immobilized on Ni-NTA showed impressive U loading capacities, in both batch and column process, matrix showed poor U precipitation in the third time reuse. The *p*-NPP activity of PhoK was measured and found to drop drastically by 97% in the third round. While the initial PhoK activity was ~ 24,000 ± 145 units, at the end of 72 h after third round of precipitation it was reduced to ~720 ± 25 units. Generally purified proteins are more prone to inactivation due to small variations in environmental milieu. Therefore, the activity of purified PhoK was assayed when kept at room temperature and at 4°C separately. At room temperature, after 24 h, activity of purified PhoK was reduced to 33 ± 5%, while only 9-10% decrease in activity was observed when stored at 4°C for 72 h

(Table 5.8). The substantial decrease in the U precipitation ability thus seems to be a result of inactivation of PhoK due to prolonged incubation at room temperature and exposure to U.

Table 5.8. Activity of PhoK when stored at room temperate and at 4°C

Time (h)	Activity of PhoK (nmoles p-NP liberated/min) when stored at	
	Room temperature	4°C
0	8.80 ± 0.4	8.91 ± 0.55
24	3.03 ± 0.25	8.41 ± 0.45
48	2.57 ± 0.3	8.62 ± 0.5
72	2.12 ± 0.45	8.1 ± 0.65

As purified PhoK was in direct contact with U, intoxication of PhoK by U might also result in reduced activity. Therefore, PhoK activity was assayed in presence of U at different input concentrations. It was observed that activity of purified PhoK was reduced to 40-45%, in the presence of 1 mM U under GC2 and declined slowly thereafter up to 5 mM (Fig. 5.14).

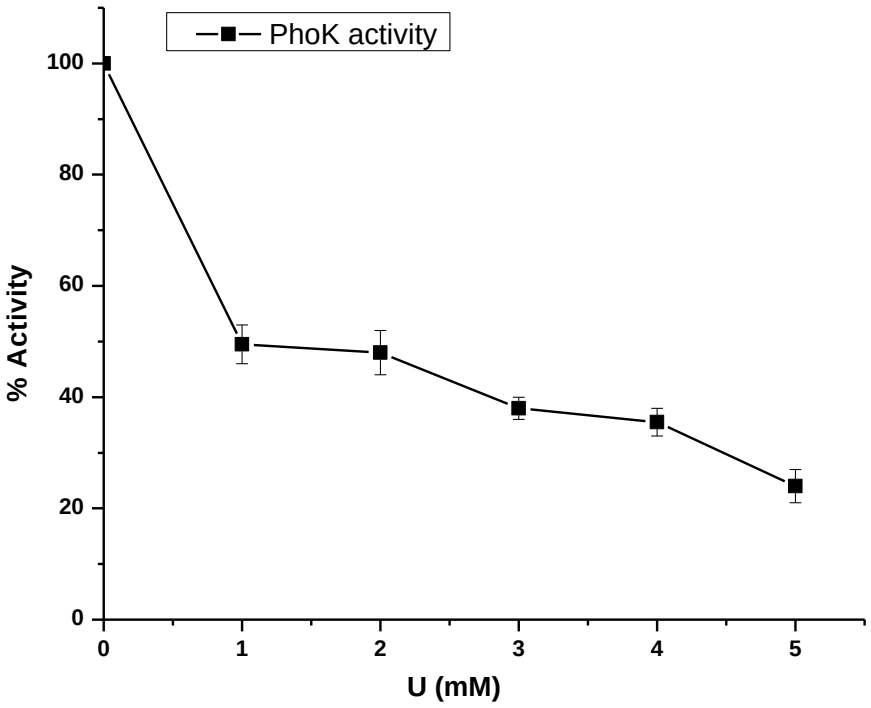

Fig. 5.14. **Effect of U on PhoK activity.** Activity of PhoK immobilized on Ni-NTA was determined in the presence of U (1-5 mM) under GC2. Five µl of matrix was incubated with *p*-NPP substrate (8.3 mM) along with increasing concentrations of U (1-5 mM) for 30 min and the reaction was stopped by 0.2 N NaOH. Absorbance at 405 nm was measured spectrophotometrically. Relative activity was calculated as % of activity in the absence of U taken as 100 %.

Thus distinct loss of PhoK activity and subsequent decrease in U precipitation might be the result of precipitation carried out at room temperature or due to toxicity of U to purified PhoK.

5.5 Discussion

Previous chapters described efficient bioprecipitation abilities of recombinant *Deino-PhoK* and *Deino-PhoNK* cells. Further improvement of the recombinant cells, aimed at their application in bioprecipitation of U from nuclear waste was achieved through lyophilization and immobilization. With respect to actual application in bioremediation, it would be desirable to increase the shelf life and ease of handling of the strains. Thus lyophilisation was

attempted with recombinant *Deinococcus* strains. Lyophilization of *Deino-PhoK* or *Deino-PhoNK* cells had the following beneficial consequences: (1) reduced the bulk volume and converted the biomass into a dry powdered form, thereby increasing the ease of handling, storage, transport and application, (2) preserved the PhoN/PhoK activity and uranium precipitation ability of cells for application in a batch process or in a flow through system, and (3) significantly extended the shelf life of the product in terms uranium precipitation capability for more than 1 year when stored at room temperature (Fig. 5.1 and 5.2). Further, cells lost their viability post lyophilisation while still exhibiting PhoK activity and U precipitation ability. This is desirable in view of the apprehensions prevalent about the use and release of genetically engineered strains in the environment.

Results from previous chapter indicated that under GC1, the cell bound precipitate makes cells heavy causing them to settle down, thus facilitating easy recovery of the precipitated U without centrifugation, compared to extracellular free precipitate. However, the uranyl phosphate, precipitated under GC2 by PhoN/PhoK expressing cells remained extracellular and required centrifugation for complete recovery. In order to achieve easier separation of uranyl phosphate precipitate from the bulk volume, bioprecipitation was attempted with *Deino-PhoK* and *Deino-PhoNK* cells immobilized in calcium alginate beads. These beads could remove ~ 90% U from 1 mM solution within 2 h. On exposure to UV, these beads showed bright green coloured fluorescence while the supernatant buffer medium did not (Fig. 5,3, 5.4 and 5.6) indicating that the precipitate was entirely entrapped into beads. The beads settled down to the floor of the flask quickly and could be easily harvested to facilitate separation and recovery of the bioprecipitated U. The beads precipitated ~ 0.5 g of U /g of dry weight of biomass at 1 mM input U concentration under GC2 in batch process.

6. A column based approach for U bioprecipitation provides the advantage of a continuous flow system for removal and recovery of U. Whole cells of *Deino-PhoK* were

immobilized (acrylamide) and tested for their U precipitation (input concentration 1 mM) in column process under GC2. Although, U loading was higher in column process (0.85 g U/g of dry biomass) as compared to batch process (0.5 g U/ g of dry biomass), the time required to achieve this loading was rather long (Fig. 5.8 and 5.9). In flow-through process, 0.85 g U loading was achieved over 8 days of continuous flow of U solution, while in batch process, 0.5 g U loading could be achieved within 4 h. Also, the potential of flow-through system appears to be seriously limited due to clogging of the column by the precipitate formed.

Immobilization of the His-tagged PhoK was attempted using Ni^{+2}-NTA (Ni^{+2}-nitrilotriacetic acid) affinity matrix and tested in batch process as well as in column studies to overcome the problem of clogging. PhoK immobilized on Ni^{+2}-NTA matrix was able to precipitate more than 90% U in batch process within 3 h when input U was 1 mM (GC2) with impressive loading capacities (Fig. 5.12). In column studies, 220 µg U/µg of PhoK was precipitated in the first round while 175 µg was precipitated in second round, which is approximately 8 fold higher per unit enzyme than in the batch process (Table 5.7). The precipitated U could be eluted out in 0.2 M carbonate – bicarbonate buffer with 80 % efficiency. However, in the third round negligible U was precipitated (8-9% only) due to loss of PhoK activity. Prolonged incubation of PhoK at room temperature and with uranyl ion inhibited purified PhoK. When kept at room temperature for 24 h, activity of purified PhoK was reduced to 33±5% (Table 5.8), while incubation in the presence of 1 mM U under GC2 reduced the activity of purified PhoK to 40-45% (Fig. 5.14). These results suggest that though Ni-NTA based U precipitation exhibited impressive loading capacities, whole cells are superior in terms of actual application for effluent waste treatment, since purified enzyme is prone to inactivation at room temperature as well as to poisoning of its activity by U.

Thus, use of immobilized whole cells in batch process appeared to be the most appropriate, in terms of actual application in waste solutions. Batch process appears to be superior over a column-based flow-through system in terms of (a) time required, (b) extent of uranium removal, and (c) no problem of clogging. A simple set-up, easy downstream processing and rapid uranium precipitation, distinctly make the batch process the preferred mode of operation for PhoK mediated uranium precipitation. Further, continuous flow-through operation may require setting up of additional independent facility with columns, pumps, etc. which may contribute to additional cost and pose additional containment requirement for radioactive waste treatment. In batch process, the existing facility of delay /waste tanks can be used for easy application of the lyophilized powder. Also, batch operation provides better process control over the system, which is a priority while handling radioactive waste.

Chapter 6

Summary and Conclusions

This study was conceived to develop genetically engineered bacteria expressing an alkaline phosphatase, PhoK or co-expressing both acid (PhoN) and alkaline phosphatases (PhoK), aimed at U bioprecipitation from both acidic-neutral as well as alkaline solutions. The radioresistant organism, *D. radiodurans*, was chosen as a host for expression of phosphatases, since it is well suited for remediation of radioactive waste. The salient findings of the study are summarized below:

- In order to enable bioprecipitation of U from alkaline waste solutions, *phoK* gene, encoding a novel alkaline phosphatase, was cloned from *Sphingomonas* into radioresistant organism *D. radiodurans*.
- The recombinant strain, *Deino-PhoK* exhibited remarkably high alkaline phosphatase specific activity (~6500 units) in comparison to phosphatase activities reported in bacteria earlier. Cell associated PhoK activity was best seen in the early exponential phase of both recombinant *E. coli-PhoK* and *Deino-PhoK* cultures.
- *Deino-PhoK* cells efficiently precipitated uranium. U precipitation was assessed under two different geochemical conditions (GCs): (a) GC1; a carbonate deficient condition with uranyl nitrate (1-2 mM) at final pH 6.8. (b) GC2; a carbonate abundant condition, with uranyl carbonate at pH 9.0. In both the GCs, β-GP was used as substrate in appropriate concentration.
- At a relatively low cell density (OD_{600} ~1), *Deino-PhoK* cells could efficiently bioprecipitate over 90% of U within 2 h from 1 mM input U concentration under GC2. To achieve same level of precipitation, *Deino-PhoN*, constructed earlier, required 6-fold higher cell density and much longer duration (~ 6-8 h) under GC1.
- The *Deino-PhoK* strain worked equally well at higher (10 mM) concentrations of U under GC2, resulting in high loading of U as 10.7g U/g dry biomass.

- The stoichiometry of U and phosphate was found to be 1:1 in the precipitate. Most rapid U precipitation using *Deino-PhoK* cells was seen under GC2 with 10 mM β-GP (> 90% precipitation in 45 min), but even with 1 mM β-GP, over 80% of U could be precipitated with longer incubation period (4-5 h). For subsequent experiments, 5 mM β-GP was used when input U concentration was 1 mM.
- *Deino-PhoK* cells as also the PhoK protein survived up to 6 kGy exposure to γ-radiation and continued to function optimally thereafter. Also, overexpression of PhoK did not compromise the inherent radioresistance of *Deinococcus* and cells could grow efficiently precipitate U even after exposure to high radiation environment up to 6 kGy dose.
- *Deino-PhoK* cells were also indifferent to the presence of other heavy metals found in nuclear waste such as like Cs, Sr, thus suggesting possible use of the strain for treating waste solutions like intermediate level waste or low level waste.
- To facilitate U bioprecipitation from both acidic and alkaline aqueous waste using a single microbe, the recombinant strain *Deino-PhoNK* co-expressing both *phoN* and *phoK* genes was constructed. Whole cell phosphatase activity and zymogram assays confirmed that both PhoN and PhoK phosphatases actively expressed in *Deino-PhoNK* and were optimally active at appropriate pH optima.
- The U precipitation kinetics in *Deino-PhoNK* strain was similar to that shown by *Deinococcus* strains expressing either PhoN or PhoK individually. *Deino-PhoNK* cells achieved 1.07 g U loading/g of dry weight of cells under GC2 (at the end of 4 h), while under GC1 it showed loading of 0.34 g U/g of dry weight of cells at 1 mM input U and 5 mM β-GP (at the end of 8 h).

- X-ray diffraction (XRD) and fluorescence analysis identified the uranyl phosphate species precipitated by *Deino-PhoK* cells under GC2 as uranyl hydrogen phosphate hydrate, $H_2(UO_2)_2(PO_4)_2.8H_2O$ also known as chernikovite (meta-autunite).
- In conformity with known characteristics of chernikovite, the precipitate exhibited intense green fluorescence which showed excellent qualitative and quantitative correspondence with the colorimetric data on U bioprecipitation under GC2.
- *Deino-PhoK* cells, when incubated with U under GC1, clearly showed a cell associated precipitate like the *Deino-PhoN* cells treated similarly. Interestingly, *Deino-PhoN* cells when incubated with U under GC2 exhibited extracellular precipitation. Identical results were observed with recombinant *E. coli* strains, individually expressing PhoN/PhoK phosphatases.
- XRD analysis of uranyl phosphate, precipitated by both the enzymes, PhoN or PhoK under both geochemical conditions, confirmed that the precipitated uranyl phosphate species remained the same i.e. chernikovite, irrespective of pH or phosphatase enzyme used.
- TEM analysis revealed that the cell-bound or extracellular location of the precipitate was determined not by the location of the corresponding enzyme (PhoN-periplasmic or PhoK-extracellular) or the uranyl salt (nitrate or carbonate) used, but by the uranyl species prevalent under particular GC. Thus precipitate was cell surface associated under GC1 and extracellular under GC2.
- MINTEQ modelling predicted that U mostly formed positively charged complexes under GC1, while negatively charged uranyl carbonate complexes are formed under GC2.
- Four-Five folds more U was found to be adsorbed on to cell surface under GC1 than under GC2 from 1 mM U solution. U removal from solution by absorption was found

to be 8.5% under GC1 and only about 2.2% under GC2. Differential adsorption of uranyl ions to cell surface also resulted in differential U toxicity to cells under the two GCs employed. Only 10 % growth was obtained at 1.25 mM input U concentration under GC1, while pre-exposure of cells even at 20 mM U under GC2 cell growth was unaffected. Thus, U was far less inhibitory under GC2.

- Under both GC1 and GC2, the phosphatase expressing cells could survive at inhibitory concentration of U (2 mM for GC1, 30 mM for GC2), while phosphatase negative cells did not show any growth after exposure to these U concentrations. Thus, the issue of metal sensitivity can be avoided by PhoN/PhoK mediated U bioprecipitation.
- Lyophilized dry powder of both *Deino-PhoK* and *Deino-PhoNK* cells fully retained phosphatase activity as well as U precipitation ability at ambient temperature for >1 year during storage and facilitated easy recovery of precipitated metal with the biomass. Thus, lyophilization significantly extended the shelf life of the product, and increased the ease of handling, storage, transport and application.
- To achieve easier separation of uranyl phosphate precipitate from the bulk volume, bioprecipitation was attempted with *Deino-PhoK* and *Deino-PhoNK* cells immobilized in calcium alginate beads. These beads could remove ~ 90% U from 1 mM solution within 2 h.
- Immobilized *Deino-PhoK* cells in beads were evaluated for U precipitation in a batch versus flow-through process. Although, U loading was higher in column process (0.85 g U/g of dry biomass) as compared to batch process (0.5 g U/ g of dry biomass), the time required to achieve this loading was rather long (8 days) in flow-through process, compared to batch process (4 h). The potential of flow-through system appears to be seriously limited due to rapid clogging of the column by the precipitate formed.

- Immobilization of the His-tagged PhoK enzyme was attempted using Ni^{+2}-NTA (Ni^{+2}-nitrilotriacetic acid) affinity matrix and compared for U precipitation in batch process or in flow-through system. Ni^{+2}-NTA based U precipitation exhibited impressive loading capacities (30 µg U/µg PhoK protein) compared to immobilized cells (0.5 g U/ g of dry biomass). However, purified enzyme was prone to inactivation at room temperature as well as to poisoning of activity by U indicating cells are superior in terms of actual application for effluent waste treatment.

References

[1] I.M.I. Salman H. Abbas1, Tarek M. Mostafa3, Abbas H. Sulaymon4, Biosorption of Heavy Metals: A Review, Journal of Chemical Science and Technology, 3 (2014) 74-102.

[2] H. Brim, S.C. McFarlan, J.K. Fredrickson, K.W. Minton, M. Zhai, L.P. Wackett, M.J. Daly, Engineering *Deinococcus radiodurans* for metal remediation in radioactive mixed waste environments, Nature Biotechnology, 18 (2000) 85-90.

[3] B.W. Brook, C.J. Bradshaw, Key role for nuclear energy in global biodiversity conservation, Conservation Biology, 29 (2015) 702-712.

[4] K. Raj, K.K. Prasad, N.K. Bansal, Radioactive waste management practices in India, Nuclear Engineering and Design, 236 (2006) 914-930.

[5] IAEA, Management of low and intermediate level radioactive wastes with regard to their chemical toxicity, in: IAEA-TECDOC-1325, International atomic energy agency Austria, (2002) 1-77.

[6] IAEA, In situ leaching of uranium: Technical, environmental and ecomomic aspects IAEA-TECDOC-492, (1989).

[7] IAEA, Analysis of Uranium Supply to 2050, in, IAEA, Viena, Austria, (2001) 1-103.

[8] D. Lunt, P. Boshoff, M. Boylett, Z. El-Ansary, Uranium extraction: The key process drivers, Journal of the Southern African Institute of Mining and Metallurgy, 107 (2007) 419-426.

[9] E.A. Santos, A.C.Q. Ladeira, Recovery of uranium from mine waste by leaching with carbonate-based reagents, Environmental Science and Technology, 45 (2011) 3591-3597.

[10] D.H. Underhill, Developments in uranium resources, production, demand and the environment, IAEA- TECDOC-1425, (1999) 25-41.

[11] D.C. Seidel, Extracting Uranium from its ores, IAEA bulletin, 23 (1978) 24-28.

[12] D.P.a.A.K.S. P.K. Tamrakar, Study of leaching characteristics on low grade uranium ore of bagjata mine Proceedings of the XI International Seminar on Mineral Processing Technology (MPT-2010), 2426 (2010) 666-672.

[13] IAEA, Developments in uranium resources, production, demand and the environment, in: I. 92–0–112904–1 (Ed.), IAEA, Vienna, Austria, 2005.

[14] IAEA, The long term stabilization of uranium mill tailings, IAEA-TECDOC-1403, (2004).

[15] S. Choudhary, P. Sar, Uranium biomineralization by a metal resistant *Pseudomonas aeruginosa* strain isolated from contaminated mine waste, Journal of Hazardous Materials, 186 (2011) 336-343.

[16] L. Zavodska, Environmental chemistry of uranium, Health Education Journal, 1418-7108.

[17] W.H.O organisation, Uranium in drinking water, WHO/SDE/WSH/03.04/118, (2005).

[18] M.A. Moss, McCurdy, R.F., Dooley, K.C., Givner, M.L., Dymond, L.C., Slayter, J.M., & Courneya, M.M. Savory, J. (Ed). Uranium in drinking water - report on clinical studies in Nova Scotia., Chemical toxicology and clinical chemistry of metals. Proceedings of 2. international conference 02 (1983).

[19] Y.D. La Touche, D.L. Willis, O.I. Dawydiak, Absorption and Biokinetics of U in Rats Following an Oral Administration of Uranyl Nitrate Solution, Health Physics, 53 (1987) 147-162.

[20] A. Krestou, D. Panias, Uranium (VI) speciation diagrams in the $UO_2^{2+}/CO_3^{2-}/H_2O$ system at 25° C, European Journal of Mineral Processing & Environmental Protection, 4 (2004).

[21] M.L. Zamora, B.L. Tracy, J.M. Zielinski, D.P. Meyerhof, M.A. Moss, Chronic Ingestion of Uranium in Drinking Water: A Study of Kidney Bioeffects in Humans, Toxicological Sciences, 43 (1998) 68-77.

[22] A. Tapia-Rodríguez, A. Luna-Velasco, J. Field, R. Sierra-Alvarez, Toxicity of Uranium to Microbial Communities in Anaerobic Biofilms, Water Air Soil Pollut, 223 (2012) 3859-3868.

[23] M.R. VanEngelen, E.K. Field, R. Gerlach, B.D. Lee, W.A. Apel, B.M. Peyton, UO_2^{2+} speciation determines uranium toxicity and bioaccumulation in an environmental *Pseudomonas* sp. isolate, Environmental Toxicology and Chemistry, 29 (2010) 763-769.

[24] M.R. VanEngelen, R.K. Szilagyi, R. Gerlach, B.D. Lee, W.A. Apel, B.M. Peyton, Uranium Exerts Acute Toxicity by Binding to Pyrroloquinoline Quinone Cofactor, Environmental Science & Technology, 45 (2011) 937-942.

[25] Y. Suzuki, T. Suko, Geomicrobiological factors that control uranium mobility in the environment: Update on recent advances in the bioremediation of uranium-contaminated sites, Journal of Mineralogical and Petrological Sciences, 101 (2006) 299-307.

[26] G. Echevarria, M.I. Sheppard, J. Morel, Effect of pH on the sorption of uranium in soils, Journal of Environmental Radioactivity, 53 (2001) 257-264.

[27] Y. Suzuki, J.F. Banfield, Geomicrobiology of uranium, Reviews in Mineralogy and Geochemistry, 38 (1999) 393-432.
[28] S.J. Markich, Uranium Speciation and Bioavailability in Aquatic Systems: An Overview, The Scientific World Journal, 2 (2002).
[29] R. Finch, T. Murakami, Systematics and paragenesis of uranium minerals, Reviews in Mineralogy and Geochemistry, 38 (1999) 91-179.
[30] D.A. Carvajal, Y.P. Katsenovich, L.E. Lagos, The effects of aqueous bicarbonate and calcium ions on uranium biosorption by *Arthrobacter* G975 strain, Chemical Geology, 330–331 (2012) 51-59.
[31] D. Gorman-Lewis, P.E. Elias, J.B. Fein, Adsorption of aqueous uranyl complexes onto *Bacillus subtilis* cells, Environmental Science and Technology, 39 (2005) 4906-4912.
[32] M.J. Beazley, Nonreductive biomineralization of uranium (VI) as a result of microbial phosphatase activity, (2009).
[33] V. Pekárek, M. Benešová, A study on uranyl phosphates—I: Sorption properties of uranyl hydrogen phosphate, Journal of Inorganic and Nuclear Chemistry, 26 (1964) 1743-1751.
[34] V. Pekárek, V. Veselý, A study on uranyl phosphates—II sorption properties of some 1- to 4-valent cations on uranyl hydrogen phosphate heated to various temperatures, Journal of Inorganic and Nuclear Chemistry, 27 (1965) 1151-1158.
[35] P. Rajendran, J. Muthukrishnan, P. Gunasekaran, Microbes in heavy metal remediation, Indian journal of experimental biology, 41 (2003) 935-944.
[36] G.M. Gadd, Metals, minerals and microbes: geomicrobiology and bioremediation, Microbiology, 156 (2010) 609-643.
[37] R.J. Martinez, M.J. Beazley, P.A. Sobecky, Phosphate-Mediated Remediation of Metals and Radionuclides, Advances in Ecology, (2014).
[38] A. Malik, Metal bioremediation through growing cells, Environment International, 30 (2004) 261-278.
[39] M.F.AbdEl-Sabour, Remediation and bioremediation of uranium contaminated soils, Electronic journal of environmental, agriculture and food chemistry, 6 (2007) 2009-2013.
[40] L. Newsome, K. Morris, J.R. Lloyd, The biogeochemistry and bioremediation of uranium and other priority radionuclides, Chemical Geology, 363 (2014) 164-184.
[41] J.R. Lloyd, D.R. Lovley, L.E. Macaskie, Biotechnological Application of Metal-reducing Microorganisms, in: Advances in Applied Microbiology, Academic Press, 2003, pp. 85-128.

[42] C. Acharya, P. Chandwadkar, S.K. Apte, Interaction of uranium with a filamentous, heterocystous, nitrogen-fixing cyanobacterium, *Anabaena torulosa*, Bioresource Technology, 116 (2012) 290-294.
[43] K. Akhtar, A.M. Khalid, M.W. Akhtar, M.A. Ghauri, Removal and recovery of uranium from aqueous solutions by Ca-alginate immobilized *Trichoderma harzianum*, Bioresource Technology, 100 (2009) 4551-4558.
[44] F. Morcillo, M.T. Gonźalez-M̃unoz, T. Reitz, M.E. Romero-Gonźalez, J.M. Arias, M.L. Merroun, Biosorption and biomineralization of U(VI) by the marine bacterium *Idiomarina loihiensis* MAH1: Effect of background electrolyte and pH, PLoS ONE, 9 (2014).
[45] G.M. Gadd, Biosorption: critical review of scientific rationale, environmental importance and significance for pollution treatment, Journal of Chemical Technology & Biotechnology, 84 (2009) 13-28.
[46] L.E. Macaskie, K.M. Bonthrone, P. Yong, D.T. Goddard, Enzymically mediated bioprecipitation of uranium by a *Citrobacter* sp.: A concerted role for exocellular lipopolysaccharide and associated phosphatase in biomineral formation, Microbiology, 146 (2000) 1855-1867.
[47] L.E. Macaskie, B.C. Jeong, M.R. Tolley, Enzymatically accelerated biomineralization of heavy metals: Application to the removal of americium and plutonium from aqueous flows, FEMS Microbiology Reviews, 14 (1994) 351-367.
[48] M. Barlett, H. Moon, A. Peacock, D. Hedrick, K. Williams, P. Long, D. Lovley, P. Jaffe, Uranium reduction and microbial community development in response to stimulation with different electron donors, Biodegradation, 23 (2012) 535-546.
[49] B.J. Converse, T. Wu, R.H. Findlay, E.E. Roden, U(VI) Reduction in Sulfate-Reducing Subsurface Sediments Amended with Ethanol or Acetate, Applied and Environmental Microbiology, 79 (2013) 4173-4177.
[50] J.R. Lloyd, Microbial reduction of metals and radionuclides, FEMS Microbiology Reviews, 27 (2003) 411-425.
[51] E. Remoudaki, A. Hatzikioseyian, M. Tsezos, Metabolically Mediated Metal Immobilization Processes for Bioremediation.
[52] M. Van Loosdrecht, J. Lyklema, W. Norde, G. Schraa, A. Zehnder, Electrophoretic mobility and hydrophobicity as a measured to predict the initial steps of bacterial adhesion, Applied and Environmental Microbiology, 53 (1987) 1898-1901.

[53] S. French, D. Puddephatt, M. Habash, S. Glasauer, The dynamic nature of bacterial surfaces: Implications for metal-membrane interaction, Critical Reviews in Microbiology, 39 (2013) 196-217.
[54] S. Langley, T. Beveridge, Effect of O-side-chain-lipopolysaccharide chemistry on metal binding, Applied and Environmental Microbiology, 65 (1999) 489-498.
[55] N. Das, R. Vimala, P. Karthika, Biosorption of heavy metals—an overview, Indian journal of Biotechnology, 7 (2008) 159-169.
[56] R. Singh, B.B. Prasad, Trace metal analysis: selective sample (copper II) enrichment on an AlgaSORB column, Process Biochemistry, 35 (2000) 897-905.
[57] P. Kotrba, L. Dolečková, V. de Lorenzo, T. Ruml, Enhanced Bioaccumulation of Heavy Metal Ions by Bacterial Cells Due to Surface Display of Short Metal Binding Peptides, Applied and Environmental Microbiology, 65 (1999) 1092-1098.
[58] H. Pan-Hou, M. Kiyono, H. Omura, T. Omura, G. Endo, Polyphosphate produced in recombinant *Escherichia coli* confers mercury resistance, 2002.
[59] L. Andrade, C.N. Keim, M. Farina, W.C. Pfeiffer, Zinc detoxification by a cyanobacterium from a metal contaminated bay in Brazil, Brazilian Archives of Biology and Technology, 47 (2004) 147-152.
[60] N. Renninger, R. Knopp, H. Nitsche, D.S. Clark, J.D. Keasling, Uranyl precipitation by *Pseudomonas aeruginosa* via controlled polyphosphate metabolism, Applied and Environmental Microbiology, 70 (2004) 7404-7412.
[61] N. Perdrial, N. Liewig, J.-E. Delphin, F. Elsass, TEM evidence for intracellular accumulation of lead by bacteria in subsurface environments, Chemical Geology, 253 (2008) 196-204.
[62] T. Sousa, A.-P. Chung, A. Pereira, A.P. Piedade, P.V. Morais, Aerobic uranium immobilization by *Rhodanobacter* A2-61 through formation of intracellular uranium-phosphate complexes, Metallomics, 5 (2013) 390-397.
[63] Webb, McGinness, S. Lappin, Metal removal by sulphate-reducing bacteria from natural and constructed wetlands, Journal of Applied Microbiology, 84 (1998) 240-248.
[64] H. Boukhalfa, G.A. Icopini, S.D. Reilly, M.P. Neu, Plutonium(IV) Reduction by the Metal-Reducing Bacteria *Geobacter metallireducens* GS15 and *Shewanella oneidensis* MR1, Applied and Environmental Microbiology, 73 (2007) 5897-5903.
[65] N. Anaganti, B. Basu, A. Gupta, D. Joseph, S.K. Apte, Depletion of reduction potential and key energy generation metabolic enzymes underlies tellurite toxicity in *Deinococcus radiodurans*, Proteomics, 15 (2015) 89-97.

[66] J.R. Lloyd, P. Yong, L.E. Macaskie, Enzymatic recovery of elemental palladium by using sulfate-reducing bacteria, Applied and Environmental Microbiology, 64 (1998) 4607-4609.
[67] J.D. Wall, L.R. Krumholz, Uranium reduction, Annu. Rev. Microbiol., 60 (2006) 149-166.
[68] R.B. Payne, D.M. Gentry, B.J. Rapp-Giles, L. Casalot, J.D. Wall, Uranium reduction by *Desulfovibrio desulfuricans* strain G20 and a cytochrome c3 mutant, Applied and Environmental Microbiology, 68 (2002) 3129-3132.
[69] J.K. Fredrickson, H.M. Kostandarithes, S.W. Li, A.E. Plymale, M.J. Daly, Reduction of Fe(III), Cr(VI), U(VI), and Tc(VII) by *Deinococcus radiodurans* R1, Applied and Environmental Microbiology, 66 (2000) 2006-2011.
[70] M.J. Beazley, R.J. Martinez, S.M. Webb, P.A. Sobecky, M. Taillefert, The effect of pH and natural microbial phosphatase activity on the speciation of uranium in subsurface soils, Geochimica et Cosmochimica Acta, 75 (2011) 5648-5663.
[71] J. Istok, J. Senko, L.R. Krumholz, D. Watson, M.A. Bogle, A. Peacock, Y.-J. Chang, D.C. White, In situ bioreduction of technetium and uranium in a nitrate-contaminated aquifer, Environmental Science & Technology, 38 (2004) 468-475.
[72] K.H. Williams, P.E. Long, J.A. Davis, M.J. Wilkins, A.L. N'Guessan, C.I. Steefel, L. Yang, D. Newcomer, F.A. Spane, L.J. Kerkhof, Acetate availability and its influence on sustainable bioremediation of uranium-contaminated groundwater, Geomicrobiology Journal, 28 (2011) 519-539.
[73] R.T. Anderson, H.A. Vrionis, I. Ortiz-Bernad, C.T. Resch, P.E. Long, R. Dayvault, K. Karp, S. Marutzky, D.R. Metzler, A. Peacock, Stimulating the in situ activity of *Geobacter* species to remove uranium from the groundwater of a uranium-contaminated aquifer, Applied and Environmental Microbiology, 69 (2003) 5884-5891.
[74] A.L. N'Guessan, H.A. Vrionis, C.T. Resch, P.E. Long, D.R. Lovley, Sustained removal of uranium from contaminated groundwater following stimulation of dissimilatory metal reduction, Environmental Science & Technology, 42 (2008) 2999-3004.
[75] J. Lloyd, C. Pearce, V. Coker, R. Pattrick, G. Van Der Laan, R. Cutting, D. Vaughan, M. Paterson-Beedle, I. Mikheenko, P. Yong, Biomineralization: linking the fossil record to the production of high value functional materials, Geobiology, 6 (2008) 285-297.
[76] S. Glasauer, S. Langley, T.J. Beveridge, Intracellular iron minerals in a dissimilatory iron-reducing bacterium, Science, 295 (2002) 117-119.

[77] L.E. Macaskie, R.M. Empson, A.K. Cheetham, C.P. Grey, A.J. Skarnulis, Uranium bioaccumulation by a *Citrobacter* sp. as a result of enzymically mediated growth of polycrystalline HUO_2PO_4, Science, 257 (1992) 782-784.

[78] C. Boswell, R. Dick, H. Eccles, L. Macaskie, Phosphate uptake and release by *Acinetobacter johnsonii* in continuous culture and coupling of phosphate release to heavy metal accumulation, Journal of Industrial Microbiology and Biotechnology, 26 (2001) 333-340.

[79] C.D. Boswell, R.E. Dick, L.E. Macaskie, The effect of heavy metals and other environmental conditions on the anaerobic phosphate metabolism of *Acinetobacter johnsonii*, Microbiology, 145 (1999) 1711-1720.

[80] K. Benzerara, J. Miot, G. Morin, G. Ona-Nguema, F. Skouri-Panet, C. Férard, Significance, mechanisms and environmental implications of microbial biomineralization, 343 (2011) 160-167.

[81] M.L. Merroun, S. Selenska-Pobell, Bacterial interactions with uranium: an environmental perspective, Journal of Contaminant Hydrology, 102 (2008) 285-295.

[82] L. Macaskie, B. Jeong, M. Tolley, Enzymically accelerated biomineralization of heavy metals: application to the removal of americium and plutonium from aqueous flows, FEMS Microbiology Reviews, 14 (1994) 351-368.

[83] D.M. Wellman, K.M. Gunderson, J.P. Icenhower, S.W. Forrester, Dissolution kinetics of synthetic and natural meta-autunite minerals, $X_{3-n}^{(n)+}[(UO_2)(PO_4)]_2 \cdot xH_2O$, under acidic conditions, Geochemistry, Geophysics, Geosystems, 8 (2007).

[84] M. Paterson-Beedle, J. Readman, J. Hriljac, L. Macaskie, Biorecovery of uranium from aqueous solutions at the expense of phytic acid, Hydrometallurgy, 104 (2010) 524-528.

[85] R.A. Thomas, L. Macaskie, Biodegradation of tributyl phosphate by naturally occurring microbial isolates and coupling to the removal of uranium from aqueous solution, Environmental Science & Technology, 30 (1996) 2371-2375.

[86] E.M. du Plessis, J. Theron, L. Joubert, T. Lotter, T.G. Watson, Characterization of a Phosphatase Secreted by *Staphylococcus aureus* Strain 154, a New Member of the Bacterial Class C Family of Nonspecific Acid Phosphatases, Systematic and Applied Microbiology, 25 (2002) 21-30.

[87] J.B. Vincent, M.W. Crowder, B.A. Averill, Hydrolysis of phosphate monoesters: a biological problem with multiple chemical solutions, Trends in Biochemical Sciences, 17 (1992) 105-110.

[88] J.B. Bliska, K. Guan, J.E. Dixon, S. Falkow, Tyrosine phosphate hydrolysis of host proteins by an essential Yersinia virulence determinant, Proceedings of the National Academy of Sciences, 88 (1991) 1187-1191.

[89] T.J. Reilly, D.L. Chance, A.L. Smith, Outer Membrane Lipoprotein e (P4) of *Haemophilus influenzae* Is a Novel Phosphomonoesterase, Journal of bacteriology, 181 (1999) 6797-6805.

[90] A.D. Gutu, K.J. Wayne, L.-T. Sham, M.E. Winkler, Kinetic Characterization of the WalRKSpn (VicRK) Two-Component System of *Streptococcus pneumoniae*: Dependence of WalKSpn (VicK) Phosphatase Activity on Its PAS Domain, Journal of bacteriology, 192 (2010) 2346-2358.

[91] N. U. Gandhi, S. B. Chandra, A comparative analysis of three classes of bacterial non-specific acid phosphatases and archaeal phosphoesterases: evolutionary perspective, Acta Informatica Medica, 20 (2012) 167-173.

[92] M.C. Thaller, S. Schippa, G.M. Rossolini, Conserved sequence motifs among bacterial, eukaryotic, and archaeal phosphatases that define a new phosphohydrolase superfamily, Protein Science, 7 (1998) 1647-1652.

[93] G. Satta, R. Pompei, G. Grazi, G. Cornaglia, Phosphatase activity is a constant feature of all isolates of all major species of the family *Enterobacteriaceae*, Journal of clinical microbiology, 26 (1988) 2637-2641.

[94] G. Basnakova, E.R. Stephens, M.C. Thaller, G.M. Rossolini, L.E. Macaskie, The use of *Escherichia coli* bearing a *phoN* gene for the removal of uranium and nickel from aqueous flows, Applied Microbiology and Biotechnology, 50 (1998) 266-272.

[95] M.C. Thaller, S. Schippa, A. Bonci, S. Cresti, G.M. Rossolini, Identification of the gene (aphA) encoding the class B acid phosphatase/phosphotransferase of *Escherichia coli* MG1655 and characterization of its product, FEMS microbiology letters, 146 (1997) 191-198.

[96] J. Pond, C. Eddy, K. Mackenzie, T. Conway, D. Borecky, L. Ingram, Cloning, sequencing, and characterization of the principal acid phosphatase, the phoC^{+} product, from *Zymomonas mobilis*, Journal of bacteriology, 171 (1989) 767-774.

[97] M. Kasahara, A. Nakata, H. Shinagawa, Molecular analysis of the *Salmonella typhimurium phoN* gene, which encodes nonspecific acid phosphatase, Journal of bacteriology, 173 (1991) 6760-6765.

[98] M.C. Thaller, F. Berlutti, S. Schippa, G. Lombardi, G.M. Rossolini, Characterization and sequence of PhoC, the principal phosphate-irrepressible acid phosphatase of *Morganella morganii*, Microbiology, 140 (1994) 1341-1350.
[99] W. Uerkvitz, Periplasmic nonspecific acid phosphatase II from *Salmonella typhimurium* LT2. Crystallization, detergent reactivation, and phosphotransferase activity, Journal of Biological Chemistry, 263 (1988) 15823-15830.
[100] W. Uerkvitz, C.F. Beck, Periplasmic phosphatases in *Salmonella typhimurium* LT2. A biochemical, physiological, and partial genetic analysis of three nucleoside monophosphate dephosphorylating enzymes, Journal of Biological Chemistry, 256 (1981) 382-389.
[101] K.C. Bloch, R. Nadarajah, R. Jacobs, Chryseobacterium meningosepticum: An Emerging Pathogen Among Immunocompromised Adults Report of 6 Cases and Literature Review, Medicine, 76 (1997) 30-41.
[102] G. Schenk, M.L. Korsinczky, D.A. Hume, S. Hamilton, J. DeJersey, Purple acid phosphatases from bacteria: similarities to mammalian and plant enzymes, Gene, 255 (2000) 419-424.
[103] P. Nalini, P. Ellaiah, T. Prabhakar, G. Girijasankar, Microbial alkaline phosphatases in bioprocessing, Int. J. Curr. Microbiol. App. Sci, 4 (2015) 384-396.
[104] J.L. Millán, Alkaline Phosphatases: Structure, substrate specificity and functional relatedness to other members of a large superfamily of enzymes, Purinergic Signal, 2 (2006) 335-341.
[105] B. Wanner, Gene regulation by phosphate in enteric bacteria, Journal of cellular biochemistry, 51 (1993) 47-54.
[106] M. Yamada, K. Makino, M. Amemura, H. Shinagawa, A. Nakata, Regulation of the phosphate regulon of *Escherichia coli*: analysis of mutant phoB and phoR genes causing different phenotypes, Journal of bacteriology, 171 (1989) 5601-5606.
[107] R.A. Bradshaw, F. Cancedda, L.H. Ericsson, P.A. Neumann, S.P. Piccoli, M.J. Schlesinger, K. Shriefer, K.A. Walsh, Amino acid sequence of *Escherichia coli* alkaline phosphatase, Proceedings of the National Academy of Sciences, 78 (1981) 3473-3477.
[108] J.E. Coleman, Structure and mechanism of alkaline phosphatase, Annual review of biophysics and biomolecular structure, 21 (1992) 441-483.
[109] A. Pantazaki, A. Karagiorgas, M. Liakopoulou-Kyriakides, D. Kyriakidis, Hyperalkaline and thermostable phosphatase in *Thermus thermophilus*, Applied biochemistry and biotechnology, 75 (1998) 249-259.

[110] T. Park, J.-H. Lee, H.-K. Kim, H.-S. Hoe, S.-T. Kwon, Nucleotide sequence of the gene for alkaline phosphatase of *Thermus caldophilus* GK24 and characteristics of the deduced primary structure of the enzyme, FEMS microbiology letters, 180 (1999) 133-139.

[111] S. Mori, M. Okamoto, M. Nishibori, M. Ichimura, J. Sakiyama, H. Endo, Purification and characterization of alkaline phosphatase from *Bacillus stearothermophilus*, Biotechnology and applied biochemistry, 29 (1999) 235-239.

[112] S. Pandey, R. Banik, Extractive fermentation for enhanced production of alkaline phosphatase from *Bacillus licheniformis* MTCC 1483 using aqueous two-phase systems, Bioresource technology, 102 (2011) 4226-4231.

[113] K.S. Nilgiriwala, A. Alahari, A.S. Rao, S.K. Apte, Cloning and overexpression of alkaline phosphatase PhoK from *Sphingomonas* sp. strain BSAR-1 for bioprecipitation of uranium from alkaline solutions, Applied and Environmental Microbiology, 74 (2008) 5516-5523.

[114] K.S. Nilgiriwala, S.C. Bihani, A. Das, V. Prashar, M. Kumar, J.L. Ferrer, S.K. Apte, M.V. Hosur, Crystallization and preliminary X-ray crystallographic analysis of PhoK, an extracellular alkaline phosphatase from *Sphingomonas* sp. BSAR-1, Acta Crystallographica Section F: Structural Biology and Crystallization Communications, 65 (2009) 917-919.

[115] S.C. Bihani, A. Das, K.S. Nilgiriwala, V. Prashar, M. Pirocchi, S.K. Apte, J.L. Ferrer, M.V. Hosur, X-ray structure reveals a new class and provides insight into evolution of alkaline phosphatases, PLoS ONE, 6 (2011).

[116] A. Torriani, From cell membrane to nucleotides: the phosphate regulon in *Escherichia coli*, Bioessays, 12 (1990) 371-376.

[117] F.M. Hulett, E.E. Kim, C. Bookstein, N.V. Kapp, C.W. Edwards, H.W. Wyckoff, *Bacillus subtilis* alkaline phosphatases III and IV. Cloning, sequencing, and comparisons of deduced amino acid sequence with Escherichia coli alkaline phosphatase three-dimensional structure, Journal of Biological Chemistry, 266 (1991) 1077-1084.

[118] A.S. Wilkins, Physiological factors in the regulation of alkaline phosphatase synthesis in *Escherichia coli*, Journal of bacteriology, 110 (1972) 616-623.

[119] L.E. Macaskie, A.C.R. Dean, Cadmium Accumulation by a *Citrobacter* sp, Microbiology, 130 (1984) 53-62.

[120] M. Paterson-Beedle, L. Macaskie, C. Lee, J. Hriljac, K. Jee, W. Kim, Utilisation of a hydrogen uranyl phosphate-based ion exchanger supported on a biofilm for the removal of cobalt, strontium and caesium from aqueous solutions, Hydrometallurgy, 83 (2006) 141-145.

[121] D. Appukuttan, A.S. Rao, S.K. Apte, Engineering of *Deinococcus radiodurans* R1 for bioprecipitation of uranium from dilute nuclear waste, Applied and Environmental Microbiology, 72 (2006) 7873-7878.
[122] D. Appukuttan, C. Seetharam, N. Padma, A.S. Rao, S.K. Apte, PhoN-expressing, lyophilized, recombinant *Deinococcus radiodurans* cells for uranium bioprecipitation, Journal of Biotechnology, 154 (2011) 285-290.
[123] C. Seetharam, S. Soundarajan, A.C. Udas, A.S. Rao, S.K. Apte, Lyophilized, non-viable, recombinant *E. coli* cells for cadmium bioprecipitation and recovery, Process Biochemistry, 44 (2009) 246-250.
[124] R.J. Martinez, M.J. Beazley, M. Taillefert, A.K. Arakaki, J. Skolnick, P.A. Sobecky, Aerobic uranium (VI) bioprecipitation by metal-resistant bacteria isolated from radionuclide- and metal-contaminated subsurface soils, Environmental Microbiology, 9 (2007) 3122-3133.
[125] E.S. Shelobolina, H. Konishi, H. Xu, E.E. Roden, U (VI) sequestration in hydroxyapatite produced by microbial glycerol 3-phosphate metabolism, Applied and Environmental Microbiology, 75 (2009) 5773-5778.
[126] M.L. Merroun, M. Nedelkova, J.J. Ojeda, T. Reitz, M.L. Fernández, J.M. Arias, M. Romero-González, S. Selenska-Pobell, Bio-precipitation of uranium by two bacterial isolates recovered from extreme environments as estimated by potentiometric titration, TEM and X-ray absorption spectroscopic analyses, Journal of Hazardous Materials, 197 (2011) 1-10.
[127] Z. Zheng, J. Wan, X. Song, T.K. Tokunaga, Sodium meta-autunite colloids: Synthesis, characterization, and stability, Colloids and Surfaces A: Physicochemical and Engineering Aspects, 274 (2006) 48-55.
[128] M.J. Daly, Engineering radiation-resistant bacteria for environmental biotechnology, Current Opinion in Biotechnology, 11 (2000) 280-285.
[129] D. Prakash, P. Gabani, A.K. Chandel, Z. Ronen, O.V. Singh, Bioremediation: A genuine technology to remediate radionuclides from the environment, Microbial Biotechnology, 6 (2013) 349-360.
[130] J.R. Battista, Against all odds: The survival strategies of *Deinococcus radiodurans*, in, 1997, pp. 203-224.
[131] D. Slade, M. Radman, Oxidative stress resistance in *Deinococcus radiodurans*, Microbiology and Molecular Biology Reviews, 75 (2011) 133-191.
[132] M.M. Cox, J.R. Battista, *Deinococcus radiodurans*—the consummate survivor, Nature Reviews Microbiology, 3 (2005) 882-892.

[133] T. Pavkov-Keller, S. Howorka, W. Keller, Chapter 3 - The Structure of Bacterial S-Layer Proteins, in: H. Stefan (Ed.) Progress in Molecular Biology and Translational Science, Academic Press, 2011, pp. 73-130.

[134] H. Rothfuss, J.C. Lara, A.K. Schmid, M.E. Lidstrom, Involvement of the S-layer proteins Hpi and SlpA in the maintenance of cell envelope integrity in *Deinococcu*s *radiodurans* R1, Microbiology, 152 (2006) 2779-2787.

[135] K.S. Makarova, L. Aravind, Y.I. Wolf, R.L. Tatusov, K.W. Minton, E.V. Koonin, M.J. Daly, Genome of the extremely radiation-resistant bacterium *Deinococcus radiodurans* viewed from the perspective of comparative genomics, Microbiology and Molecular Biology Reviews, 65 (2001) 44-79.

[136] C.S. Misra, D. Appukuttan, V.S.S. Kantamreddi, A.S. Rao, S.K. Apte, Recombinant *D. radiodurans* cells for bioremediation of heavy metals from acidic/neutral aqueous wastes, Bioengineered Bugs, 3 (2012) 44-48.

[137] C.C. Lange, L.P. Wackett, K.W. Minton, M.J. Daly, Engineering a recombinant *Deinococcus radiodurans* for organopollutant degradation in radioactive mixed waste environments, Nature Biotechnology, 16 (1998) 929-933.

[138] H. Brim, J.P. Osborne, H.M. Kostandarithes, J.K. Fredrickson, L.P. Wackett, M.J. Daly, *Deinococcus radiodurans* engineered for complete toluene degradation facilitates Cr(VI) reduction, Microbiology, 152 (2006) 2469-2477.

[139] C.-S. Liao, L.-C. Chen, B.-S. Chen, S.-H. Lin, Bioremediation of endocrine disruptor di-n-butyl phthalate ester by *Deinococcus radiodurans* and *Pseudomonas stutzeri*, Chemosphere, 78 (2010) 342-346.

[140] R. Meima, M.E. Lidstrom, Characterization of the minimal replicon of a cryptic *Deinococcus radiodurans* SARK plasmid and development of versatile Escherichia coli-D. radiodurans shuttle vectors, Applied and Environmental Microbiology, 66 (2000) 3856-3867.

[141] M.L. Riccio, G.M. Rossolini, G. Lombardi, A. Chiesurin, G. Satta, Expression cloning of different bacterial phosphatase-encoding genes by histochemical screening of genomic libraries onto an indicator medium containing phenolphthalein diphosphate and methyl green, Journal of Applied Microbiology, 82 (1997) 177-185.

[142] J. Sambrook, E.F. Fritsch, T. Maniatis, Molecular cloning, Cold spring harbor laboratory press New York, 1989.

[143] E. Lennon, K.W. Minton, Gene fusions with lacZ by duplication insertion in the radioresistant bacterium *Deinococcus radiodurans*, Journal of Bacteriology, 172 (1990) 2955-2961.

[144] G.L. Peterson, A simplification of the protein assay method of Lowry et al. which is more generally applicable, Analytical biochemistry, 83 (1977) 346-356.
[145] U.K. Laemmli, Cleavage of structural proteins during the assembly of the head of bacteriophage T4, Nature, 227 (1970) 680-685.
[146] P. Bolton, A. Dean, Phosphatase synthesis in *Klebsiella* (*Aerobacter*) *aerogenes* growing in continuous culture, Biochem. J, 127 (1972) 87-96.
[147] B.N. Ames, [10] Assay of inorganic phosphate, total phosphate and phosphatases, in: V.G. Elizabeth F. Neufeld (Ed.) Methods in Enzymology, Academic Press, 1966, pp. 115-118.
[148] A. Francis, C. Dodge, J. Gillow, H. Papenguth, Biotransformation of uranium compounds in high ionic strength brine by a halophilic bacterium under denitrifying conditions, Environmental Science & Technology, 34 (2000) 2311-2317.
[149] C. Acharya, D. Joseph, S. Apte, Uranium sequestration by a marine cyanobacterium, *Synechococcus elongatus* strain BDU/75042, Bioresource technology, 100 (2009) 2176-2181.
[150] M.J. Beazley, R.J. Martinez, P.A. Sobecky, S.M. Webb, M. Taillefert, Uranium biomineralization as a result of bacterial phosphatase activity: Insights from bacterial isolates from a contaminated subsurface, Environmental Science and Technology, 41 (2007) 5701-5707.
[151] C.I. Masters, K.W. Minton, Promoter probe and shuttle plasmids for *Deinococcus radiodurans*, Plasmid, 28 (1992) 258-261.
[152] H. Brim, A. Venkateswaran, H.M. Kostandarithes, J.K. Fredrickson, M.J. Daly, Engineering *Deinococcus geothermalis* for bioremediation of high-temperature radioactive waste environments, Applied and Environmental Microbiology, 69 (2003) 4575-4582.
[153] T.P. Valsala, A. Joseph, N.L. Sonar, M.S. Sonavane, J.G. Shah, K. Raj, V. Venugopal, Separation of strontium from low level radioactive waste solutions using hydrous manganese dioxide composite materials, Journal of Nuclear Materials, 404 (2010) 138-143.
[154] J.R. Battista, Against all odds: the survival strategies of *Deinococcus radiodurans*, Annual review of microbiology, 51 (1997) 203-224.
[155] A. Venkateswaran, S.C. McFarlan, D. Ghosal, K.W. Minton, A. Vasilenko, K. Makarova, L.P. Wackett, M.J. Daly, Physiologic determinants of radiation resistance in *Deinococcus radiodurans*, Appl Environ Microbiol, 66 (2000) 2620-2626.
[156] S. Kulkarni, A. Ballal, S.K. Apte, Bioprecipitation of uranium from alkaline waste solutions using recombinant *Deinococcus radiodurans*, Journal of Hazardous Materials, 262 (2013) 853-861.

[157] W.W. Wilson, M.M. Wade, S.C. Holman, F.R. Champlin, Status of methods for assessing bacterial cell surface charge properties based on zeta potential measurements, Journal of Microbiological Methods, 43 (2001) 153-164.

[158] O.M. Lage, J. Bondoso, J.A.M. Catita, Determination of zeta potential in *Planctomycete*s and its application in heavy metals toxicity assessment, Archives of Microbiology, 194 (2012) 847-855.

[159] B.C. Jeong, C. Hawes, K.M. Bonthrone, L.E. Macaskie, Localization of enzymically enhanced heavy metal accumulation by *Citrobacter* sp. and metal accumulation in vitro by liposomes containing entrapped enzyme, Microbiology, 143 (1997) 2497-2507.

[160] M.A. Nesmeyanova, I.M. Tsfasman, A.L. Karamyshev, N.E. Suzina, Secretion of the overproduced periplasmic PhoA protein into the medium and accumulation of its precursor in phoA-transformed *Escherichia coli* strains: involvement of outer membrane vesicles, World Journal of Microbiology & Biotechnology, 7 (1991) 394-406.

[161] R.K. Sani, B.M. Peyton, A. Dohnalkova, Toxic effects of uranium on *Desulfovibrio desulfuricans* G20, Environmental Toxicology and Chemistry, 25 (2006) 1231-1238.

[162] P.M. Sepulveda-Medina, Y.P. Katsenovich, D.M. Wellman, L.E. Lagos, The effect of bicarbonate on the microbial dissolution of autunite mineral in the presence of gram-positive bacteria, Journal of Environmental Radioactivity, 144 (2015) 77-85.

[163] C. Fortin, L. Dutels, J. Garnier-Laplace, Uranium complexation and uptake by a green alga in relation to chemical speciation: The importance of the free uranyl ion, Environmental Toxicology and Chemistry, 23 (2004) 974-981.

[164] L.D. Kier, R. Weppelman, B.N. Ames, Resolution and purification of three periplasmic phosphatases of *Salmonella typhimurium*, Journal of bacteriology, 130 (1977) 399-410.

[165] Y. Suzuki, J.F. Banfield, Resistance to, and accumulation of, uranium by bacteria from a uranium-contaminated site, Geomicrobiology Journal, 21 (2004) 113-121.

[166] C.E. Ruggiero, H. Boukhalfa, J.H. Forsythe, J.G. Lack, L.E. Hersman, M.P. Neu, Actinide and metal toxicity to prospective bioremediation bacteria, Environmental Microbiology, 7 (2005) 88-97.

[167] C.A. Morgan, N. Herman, P. White, G. Vesey, Preservation of micro-organisms by drying; a review, Journal of microbiological methods, 66 (2006) 183-193.

[168] Y. Liu, H. Xu, S.-F. Yang, J.-H. Tay, A general model for biosorption of Cd^{2+}, Cu^{2+} and Zn^{2+} by aerobic granules, Journal of Biotechnology, 102 (2003) 233-239.

[169] T. Sato, Optical resolution of racemic amino acids by aminoacylase, Industrial application of immobilized biocatalysts, 3-14.

[170] J.A. Trelles, C.W. Rivero, Whole Cell Entrapment Techniques, in: M.J. Guisan (Ed.) Immobilization of Enzymes and Cells: Third Edition, Humana Press, Totowa, NJ, 2013, pp. 365-374.

[171] A. Tripathi, J.S. Melo, S.F. D'Souza, Uranium (VI) recovery from aqueous medium using novel floating macroporous alginate-agarose-magnetite cryobeads, Journal of hazardous materials, 246–247 (2013) 87-95.

[172] T.S. Chung, K.-C. Loh, S.K. Goh, Development of cellulose acetate membranes for bacteria immobilization to remove phenol, Journal of applied polymer science, 68 (1998) 1677-1688.

[173] P. Yang, M. Wang, Entrapment of microbial cells for wastewater treatment, Wastewater treatment by immobilized cells, (1990) 45-77.

[174] K. Akhtar, M.W. Akhtar, A.M. Khalid, Removal and recovery of uranium from aqueous solutions by *Trichoderma harzianum*, Water research, 41 (2007) 1366-1378.

[175] G. Kostov, M. Angelov, I. Mihaylov, D. Poncelet, Mechanical properties of Ca-alginate beads for ethanol fermentation with immobilized yeast, (2010).

[176] G. Bayramoğlu, M.Y. Arıca, Construction a hybrid biosorbent using *Scenedesmus quadricauda* and Ca-alginate for biosorption of Cu (II), Zn (II) and Ni (II): kinetics and equilibrium studies, Bioresource technology, 100 (2009) 186-193.

[177] M.Y. Arıca, Y. Kaçar, Ö. Genç, Entrapment of white-rot fungus *Trametes versicolor* in Ca-alginate beads: preparation and biosorption kinetic analysis for cadmium removal from an aqueous solution, Bioresource technology, 80 (2001) 121-129.

Journal of Hazardous Materials 262 (2013) 853–861

Contents lists available at ScienceDirect

Journal of Hazardous Materials

journal homepage: www.elsevier.com/locate/jhazmat

Bioprecipitation of uranium from alkaline waste solutions using recombinant *Deinococcus radiodurans*

Sayali Kulkarni, Anand Ballal, Shree Kumar Apte*

Molecular Biology Division, Bhabha Atomic Research Centre, Mumbai 400085, India

HIGHLIGHTS

- *Deinococcus radiodurans* was genetically engineered to overexpress alkaline phosphatase (PhoK).
- *Deino-PhoK* bioprecipitated U efficiently over a wide range of input U concentration.
- A maximal loading of 10.7 g U/g of biomass at 10 mM input U was observed.
- Radioresistance and U precipitation by *Deino-PhoK* remained unaffected by γ radiation.
- Immobilization of *Deino-PhoK* facilitated easy separation of precipitated U.

ARTICLE INFO

Article history:
Received 6 March 2013
Received in revised form 5 September 2013
Accepted 24 September 2013
Available online xxx

Keywords:
Deinococcus radiodurans
Bioprecipitation
Uranium
Alkaline solutions

ABSTRACT

Bioremediation of uranium (U) from alkaline waste solutions remains inadequately explored. We engineered the *phoK* gene (encoding a novel alkaline phosphatase, PhoK) from *Sphingomonas* sp. for overexpression in the radioresistant bacterium *Deinococcus radiodurans*. The recombinant strain thus obtained (*Deino-PhoK*) exhibited remarkably high alkaline phosphatase activity as evidenced by zymographic and enzyme activity assays. *Deino-PhoK* cells could efficiently precipitate uranium over a wide range of input U concentrations. At low uranyl concentrations (1 mM), the strain precipitated >90% of uranium within 2 h while a high loading capacity of around 10.7 g U/g of dry weight of cells was achieved at 10 mM U concentration. Uranium bioprecipitation by *Deino-PhoK* cells was not affected in the presence of Cs and Sr, commonly present in intermediate and low level liquid radioactive waste, or after exposure to very high doses of ionizing radiation. Transmission electron micrographs revealed the extracellular nature of bioprecipitated U, while X-ray diffraction and fluorescence analysis identified the precipitated uranyl phosphate species as chernikovite. When immobilized into calcium alginate beads, *Deino-PhoK* cells efficiently removed uranium, which remained trapped in beads, thus accomplishing physical separation of precipitated uranyl phosphate from solutions. The data demonstrate superior ability of *Deino-PhoK*, over earlier reported strains, in removal of uranium from alkaline solutions and its potential use in bioremediation of nuclear and other waste.

1. Introduction

Uranium (U) has a worldwide demand for use as a fuel in nuclear power plants. Large amount of uranium-containing radioactive waste is generated from activities such as uranium mining and extraction, fuel fabrication, reactor operation, spent fuel reprocessing and its disposal. Depending on the process used for its extraction (i.e. acidic or alkaline leaching), U mining generates large quantities of dilute acidic or alkaline waste [1,2]. Alkaline leaching of U, considered to be a more selective process than acid leaching, is employed when the carbonate content of the U ore is more than 2% [3]. The use of sodium or ammonium carbonate solutions in alkaline leaching generates carbonate complexes of U, such as $\left[UO_2(CO_3)_2^{2-}\right]$ and $\left[UO_2(CO_3)_3^{4-}\right]$ that are highly soluble at alkaline pH [4], consequently giving rise to dilute U-containing alkaline waste that is dumped as mill tailings. Depending on the type of waste, the total radioactivity of such waste solutions may vary from a few Ci/L (in high level liquid waste) to μCi/L (in low level liquid waste). The U powered nuclear plants and nuclear reactors also generate a large volume of intermediate level liquid waste (ILLW) and low level liquid waste (LLW) that is alkaline in nature (pH 8–12), and contains residual U (5–20 mM) and other μM–mM amounts of fission products such as Cs, Sr, Pu etc. [5,6]. Uranium in such waste, on account of its high solubility, can find its way to the ground water and soil and can contaminate them. Hence, it is of particular importance to efficiently remove U from alkaline waste solutions.

* Corresponding author. Tel.: +91 22 25595342; fax: +91 22 25505326.
E-mail addresses: aptesk@barc.gov.in, sksmbd@barc.gov.in (S.K. Apte).

0304-3894/$ – see front matter © 2013 Elsevier B.V. All rights reserved.
http://dx.doi.org/10.1016/j.jhazmat.2013.09.057

Bioremediation of U waste by microbes offers a good alternative to physiochemical methods in terms of in situ applicability and high efficiency at rather low concentration of the metal ion. The main processes that are currently employed in uranium bioremediation are (a) enzymatic metal bioreduction of soluble U(VI) to sparingly soluble U(IV) [7–10] (b) biosorption on cell surface, biopolymers or dead biomass [11,12], and (c) bioprecipitation of U(VI) with ligands such as inorganic phosphate [13–16]. Among these, enzymatic bioprecipitation of heavy metals as metal phosphates using microbial phosphatases is particularly attractive and is considered to be a promising new approach for bioremediation of uranium. In contrast to reduced uranium minerals such as uraninite [U(IV)] that have a tendency to reoxidise back to the more soluble U(VI), uranium phosphate precipitates [U(VI)] are not susceptible to changes in oxidation states and therefore represent a long term stable sink for uranium in contaminated environments [17]. Many studies have shown successful bioprecipitation of uranium and other heavy metals (e.g. cadmium) from acidic wastes using bacterial acid phosphatases. Naturally occurring bacteria expressing phosphatases such as *Citrobacter* sp. [18,19], *Bacillus* sp. [20], *Rahnella* sp. [16], *Pseudomonas* sp. [21] have been reported for bioremediation of heavy metals like cadmium and uranium in acidic to neutral pH range.

Microbial phosphatases can be efficiently expressed into suitable hosts and these genetically engineered microbes can be employed for bioremediation of heavy metals [22–25]. However, radiosensitivity of microbes e.g. *Citrobacter*, *Escherichia coli* or *Sphingomonas* often limits their bioremediation capabilities in radioactive waste. Radiation resistant bacteria which can remediate these metals are better choices to address these wastes [26,27]. The bacterium *Deinococcus radiodurans*, known to survive extreme ionizing radiation stress [28] has been a candidate of choice for many such bioremediation studies. It has been shown that *Deinococcus* could grow continuously in the presence of chronic radiation exposure of 60 Gy/h with no effect on its growth or ability to express foreign genes [29]. Use of engineered *D. radiodurans* for bioremediation of a mixed radioactive waste to detoxify mercury and toluene has been reported earlier [30]. A *Deinococcus*, engineered to degrade toluene, was also able to facilitate Cr (VI) reduction under radioactive conditions [31]. PhoN (non-specific acid phosphatase) expressing *Deinococcus* (*Deino-PhoN*) could survive and efficiently precipitate uranium even after exposure to high radiation doses (6 kGy) at acidic to neutral pH, whereas a recombinant PhoN overexpressing *E. coli* failed to do so [32,33]. In batch process, *Deino-PhoN* cells could precipitate uranium from a concentration range of (0.5–20 mM) resulting in maximum loading of 5.7 g U/g dry weight of cells at 20 mM input concentration in 17 days [32].

Although, U bioprecipitation from acidic to neutral conditions has received considerable attention, bioprecipitation of U from alkaline waste remains relatively unexplored so far. Precipitation of uranium as uranyl phosphate from alkaline solution is rather difficult on account of extremely high solubility of uranyl carbonate complexes at basic pH. Precipitation is feasible only at log $\left(PO_4^{-3}/CO_3^{-2}\right)$ values of >−3 [34]. While it is chemically difficult to achieve such a favorable $\left(PO_4^{-3}/CO_3^{-2}\right)$ ratio, an active enzymatic process can generate a high localized concentration of inorganic phosphate for precipitation. Recently, our laboratory identified a novel alkaline phosphatase enzyme, PhoK, having very high specific activity from a *Sphingomonas* sp. [35–37]. This *Sphingomonas* strain could precipitate uranium, albeit with a low efficiency, under alkaline conditions indicating that the required $\left(PO_4^{-3}/CO_3^{-2}\right)$ ratio for U precipitation could be achieved by this enzyme.

To extend bioremediation capability of PhoK to high radiation environments, the *phoK* gene was introduced into the radioresistant bacterium *D. radiodurans*. The resulting recombinant strain (*Deino-PhoK*) exhibited high PhoK activity and bioprecipitated U from alkaline solutions containing wide range of input U concentrations. The *Deino-PhoK* cells remained functional even after exposure to high radiation dose and achieved a U loading of ~10.7 g U/g of dry weight of cells at 10 mM input U concentration.

2. Materials and methods

2.1. Bacterial strains and growth conditions

Bacterial strains, primers and plasmids used in this study are listed in Table 1. *D. radiodurans* strain R1 was grown aerobically in TGY (1% Bacto-Tryptone, 0.1% glucose, and 0.5% yeast extract) liquid medium at 32 °C ± 1 °C with agitation (180 ± 5 rpm). *E. coli* DH5α cells were grown in Luria-Bertani (LB) medium at 37 °C ± 1 °C under agitation (180 ± 5 rpm). Bacterial growth was assessed by measuring optical density at 600 nm [OD_{600}] or by determining the number of CFU on TGY agar plates (1.5% Bacto Agar) after 48 h of incubation in the case of *D. radiodurans* and on LB agar plates after 24 h of incubation in case of *E. coli*.

The antibiotic concentrations used were 100 μg/ml of carbenicillin for *E. coli* and 3 μg/ml of choramphenicol for *D. radiodurans* transformants. For screening of PhoK-expressing recombinants, LB/TGY media were supplemented with phenolphthalein diphosphate (PDP, 1 mg/ml) and methyl green (MG, at 50 μg/ml for *E. coli* or at 5 μg/ml for *Deinococcus* transformants) to obtain histochemical plates [38].

2.2. Cloning of phoK in D. radiodurans/E. coli shuttle vector pRAD1

The *phoK* gene was cloned downstream of a strong deinococcal promoter P_{groESL} in a *D. radiodurans*/*E. coli* shuttle vector pRAD1 [39]. The *phoK* ORF (1.68 kb) was PCR amplified using primers FDNE and RDBE (Table 1) from the plasmid construct isolated from strain EK-2 ([35], Table 1). The *phoN* gene (encoding non specific acid phosphatase) was excised out from plasmid pPN1 with restriction enzymes NdeI and BamHI and was replaced with the identically digested *phoK* PCR product. This new plasmid construct (pK1, Table 1) was transformed into *E. coli DH5α* cells and transformants were patched on histochemical agar plates containing PDP and MG. Colonies that appeared green were picked up and subjected to colony PCR (using primers FDNE and RDBE) to confirm the presence of *phoK* insert. Restriction analysis with appropriate enzymes and DNA sequencing (with primers P_5, P_6, F_{ow} and R_{ow}, Table 1) was performed to ascertain to accuracy of the cloned *phoK* in pK1. The plasmid, pK1 was subsequently transformed into *D. radiodurans* and resulting transformants were selected on TGY/chloramphenicol histochemical plates. Green colored *Deinococcus* transformants were picked up for further analysis.

2.3. PhoK expression, enzyme activity and zymogram assays

Cell based PhoK and PhoN activity of recombinant cells was determined with the substrate *para*-nitro phenyl phosphate (*p*-NPP), as described earlier [22,35] and expressed as *n*moles of *para*-nitrophenol (*p*-NP) liberated per min per mg of total protein. Activity assay was carried out in 100 mM acetate buffer (pH 5) for *Deino-PhoN* cells or 50 mM Tris–Cl buffer (pH 9) for *Deino-PhoK* cells. *In gel* zymogram assay was carried out with cell extracts obtained by treating cells with 2X non-reducing cracking buffer as described earlier [22], followed by electrophoretic resolution on 10% SDS-PAGE and activity staining with nitro-blue-tetrazolium chloride/5-bromo-4-chloro-3-indolyl phosphate (NBT/BCIP, Roche

Table 1
Bacterial strains, plasmids and primers used in this study.

Strains, plasmids and primers	Description	Source, reference or comment
Strains		
E. coli DH5α	F⁻ *recA41 endA1 gyrA96 thi-1 hsdr17*(r^{K-} m^{K+}) *supE44 relAλ lacU169*	Lab collection
EK2	*E. coli* DH5α containing a 3-kb PstI-BglII fragment from BSAR-1 in PstI/BamHI sites of the pBluescriptII SK(−) vector	[35]
E.coli-pPN1	*E. coli* DH5α containing plasmid pPN1	[22]
Deino-PhoN	*Deinococcus radiodurans R1* containing plasmid construct pPN1	[22]
E.coli-PhoK	*E. coli* DH5α containing plasmid construct pK1	This study
Deino-PhoK	*Deinococcus radiodurans R1* containing plasmid construct pK1	This study
E.coli-pRAD1	*E. coli* DH5α containing shuttle vector plasmid pRAD1	This study
Deino-pRAD1	*Deinococcus radiodurans R1* containing shuttle vector plasmid pRAD1	This study
Plasmids		
pEK 2	pBSK(−) containing a 3-kb PstI-BglII fragment from *Sphingomonas* sp. *BSAR-1* in PstI/BamHI sites	[35]
pPN1	pRAD1 containing *S. enterica* serovar Typhi *phoN* gene with deinococcal *groESL* promoter	[22]
pRAD1	*E. coli-D. radiodurans* shuttle vector; Ap^r Cm^r; 6.28 kb	[39]
pK1	pRAD1 containing *Sphingomonas* sp. *phoK* gene tagged downstream of deinococcal *groESL* promoter	This study
Primers		
P_5	5′GGAGCGGATAACAATTTCACACA	
P_6	5′AACGCGGCTGCAAGAATGGTA	
F_{ow}	5′CCAGTTATTGGCGATGATGCC	
R_{ow}	5′GGAGCCTGATCCAGGAAGCG	
DAG-f	5′GCCTCTAGACATGTTCAG (XbaI)	
FDNE	5′GGAATTCCATATGTTGAAACACGTCGCCGCTGCC (NdeI)	
RDBE	5′CGCGGATCCTTACTGCCCGGCGCAGCTGTCGTCCCTTG (Bam HI)	

Note: The underlined sequence in the primer corresponds to the restriction site indicated in the parenthesis.

chemicals, Germany) [35]. For Western blotting, protein extracts obtained by treating cells with 2X cracking buffer (Laemmli's sample buffer) were electrophoretically resolved on 10% SDS-PAGE and electroblotted on to a nitrocellulose membrane. The PhoK-specific antiserum was raised in rabbits immunized with the purified His-tagged PhoK at a commercial facility (Merck, India) and was employed as primary antibody (1:5000 dilution, incubated with blot for 1 h). The secondary antibody used was anti-rabbit IgG-conjugated to alkaline phosphatase (Roche Chemicals, Germany) and the blot was developed using NBT/BCIP.

2.4. Uranium precipitation assay

Uranium precipitation was performed as described previously [35] with certain modifications. *Deino-PhoK* cells ($OD_{600nm} \sim 1\ ml^{-1}$) were incubated with 5 mM 3-(*N*-mopholino) propane sulfonic acid (MOPS) buffer (5 ml, pH 9.0) along with appropriate concentration of β-glycerophosphate (β-GP) with 1–10 mM uranyl carbonate and kept at 30 °C under static conditions. *Deino-pRAD1* cells were used as control and were incubated with U under similar conditions as mentioned above. Other appropriate controls like absence of substrate (β-GP or *p*-NPP) or uranium were maintained to ascertain that precipitation was indeed mediated by PhoK as described earlier [35]. Aliquots were taken at different time intervals and subjected to centrifugation at 12,000 g for 10 min. Residual uranium in the supernatant or U in the pellet was estimated using Arsenazo III reagent as described [40]. Metal precipitation was expressed as % precipitation of input U. U precipitation with the *Deino-PhoN* was performed by incubating cells ($OD_{600nm} \sim 1\ ml^{-1}$) in a solution containing 1 mM uranyl nitrate (5 mM acetate buffer, pH 5.0).

2.5. Uranium sensitivity and radiation response of Deino-PhoK

Survival of *Deinococcus* strains (Wild-type *D. radiodurans* R1, *Deino-PhoK* and *Deino-pRAD1*) was checked after 4 h exposure to uranium, or uranium along with Cs and Sr. Briefly, cells ($OD_{600nm} \sim 1\ ml^{-1}$) were washed with saline and resuspended into 20 mM uranyl carbonate solution (in 5 mM MOPS, pH 9.0) with or without 1 mM $CsCl_2$ and 1 mM $SrCl_2$. Appropriate dilutions were plated (three replicates each) on agar plates which were incubated at 32 °C and colony forming units (CFUs) were recorded after 48 h. In parallel, cells ($OD_{600nm} \sim 1\ ml^{-1}$) were also inoculated in TGY medium in the absence or the presence of uranyl carbonate (1 or 2 mM) and turbidity (OD_{600nm}) of cultures was recorded after 16 h of incubation at 32 °C.

For radiation response studies, early exponential phase cultures of *Deino-PhoK* and *Deino-pRAD1* were washed twice and resuspended in fresh TGY (5 ml) at an OD_{600nm} of 3.0. The cultures were irradiated at different doses (3–21 kGy) at a dose rate of 4.2 kGy/h (^{60}Co Gamma Cell 5000 irradiation unit, BARC, India). Vials kept outside the radiation source served as control. Irradiated and control cells were washed, serially diluted and plated in triplicate on TGY/choramphenicol plates. Radioresistance of cells was evaluated by calculating D_{10} dose values [22]. Irradiated cells were also assessed for their PhoK activity and uranium precipitation ability as described earlier.

2.6. X-ray diffraction and fluorimetric analyses

Uranium-treated *Deino-PhoK* and *Deino-pRAD1* cells were dried in glass petri plates at 60 °C for 3 h. The dried pellet was crushed into a fine powder and subsequently subjected to XRD analysis employing a Philips analytical X-ray diffractometer (using Ni filtered Cu *K*α radiation). The diffraction pattern was collected from 10° to 70° 2θ. The data fitting were performed as described in ICDD database. For fluorescent analysis *Deino-PhoK* or *Deino-pRAD1* cells were suspended in uranyl carbonate solution along with β-GP and fluorescence intensity of this solution was monitored using λ_{ex} = 380 nm and λ_{em} = 524 nm (Jasco FP-6500 spectrofluorimeter) over a period of time (0.5–4 h).

2.7. Transmission electron microscopy

Uranium-treated *Deino-PhoK* and *Deino-pRAD1* (control) cells were washed twice with 50 mM cacodylate buffer (pH 7.4) and fixed in a solution (2.5% glutaraldehyde + 0.5% *para*-formaldehyde) overnight at 4 °C. Following three washes with cacodylate buffer,

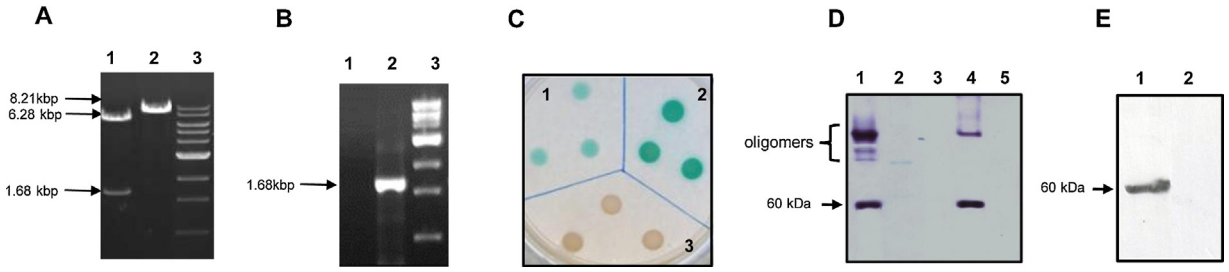

Fig. 1. Cloning and overexpression of PhoK in *D. radiodurans*. (A) Restriction digestion of pK1 isolated from *E. coli*, with NdeI and BamHI (lane 1) or NdeI alone (lane 2), followed by electrophoretic resolution along with 1 kbp ladder (NEB) (lane 3). (B) Colony PCR of *D. radiodurans* transformants with primers FDNE and RDBE: Lane 1, *Deino-pRAD1* (control cells); lane 2, *Deino-PhoK* and lane 3, 1 kbp ladder (NEB). (C) Screening of *Deinococcus* transformants on histochemical plates: 1, *Deino-PhoN*; 2, *Deino-PhoK* and 3, *Deino-pRAD1*. (D) Zymographic analysis of protein extracts (20 μg) at pH 9.0: Lane 1, *Deino-PhoK*; lane 2, prestained marker (NEB); lane 3, *Deino*-pRAD1; lane 4, *E. coli-PhoK* and lane 5, *E. coli-pRAD1*. (E) Western blotting and immunodetection of PhoK in protein extracts (20 μg) from *Deino-PhoK* (lane 1) or *Deino-pRAD1* (lane 2). The 60 kDa PhoK band is indicated by an arrow. (For interpretation of the references to color in this figure legend, the reader is referred to the web version of this article.).

cells were embedded in 2% noble agar and dehydrated in a graded series of ethanol (30%, 60%, 75%, 90%, and 100%). After removal of ethanol by treatment with propylene oxide, blocks were subsequently infiltrated with spurr reagent on incubation with 1:3, 3:1 and 1:1 (v/v propylene oxide: spurr reagent) for 2 h each. The samples were finally infiltrated with spurr resin for 16 h and embedded in it by incubation at 60 °C for 72 h. Thin sections of samples were prepared with a microtome (Leica, Germany), stained with 1.5% uranyl acetate, placed on 200 mesh formvar-coated copper grids and viewed with the Libra 120 plus Transmission Electron Microscope (Carl Zeiss). Samples were also viewed without staining with uranyl acetate.

2.8. Immobilization of cells in calcium alginate beads

Sodium alginate (2%) was dissolved in hot distilled water (30 ml) with constant stirring. On cooling to room temperature, freshly harvested *Deino-PhoK* or *Deino-pRAD1* cells were added to this solution and thoroughly mixed by stirring to form a uniform mixture. This mixture (0.1% biomass in 2% sodium alginate) was extruded as droplets in 0.1 M $CaCl_2$ solution through a nozzle. The gel beads (diameter 3.5 ± 0.2 mm) were allowed to cure for 2 h at 4 °C and washed thoroughly three times with distilled water. Blank alginate beads (2% w/v) without cells were also prepared. For monitoring uranium removal, beads were suspended in a 50 ml solution (1 mM

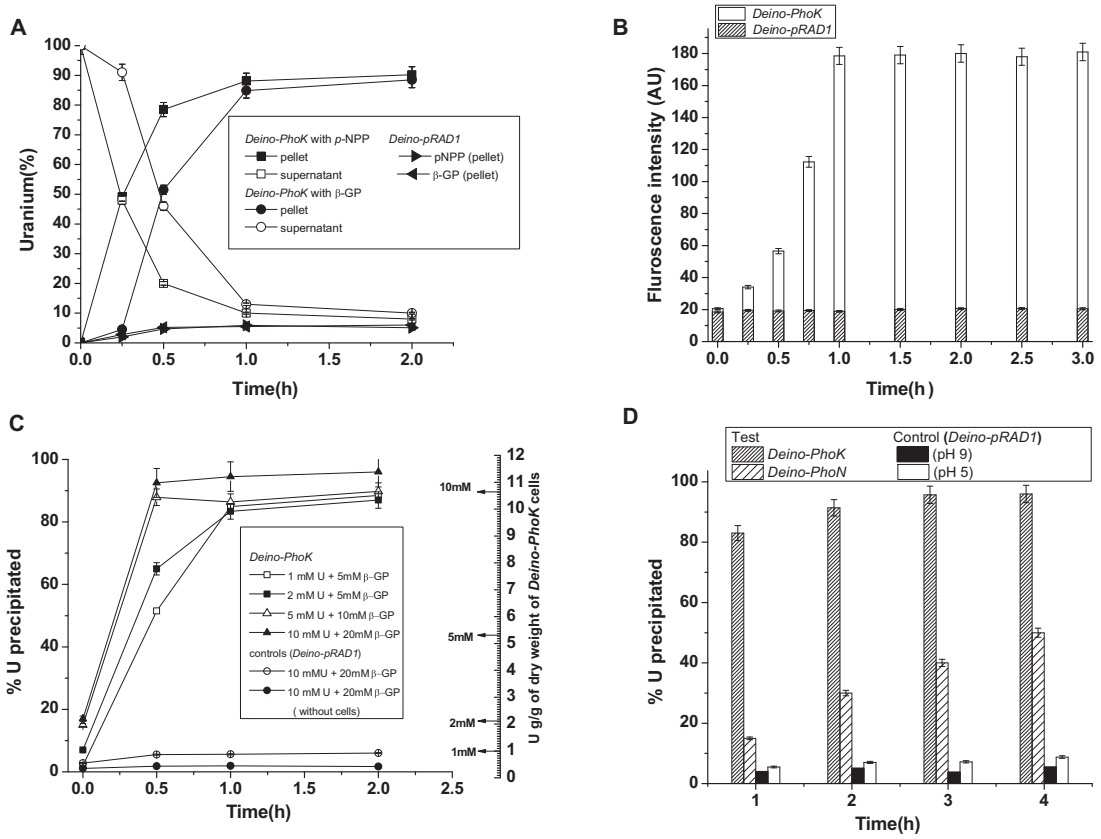

Fig. 2. Uranium bioprecipitation by *Deino-PhoK*. (A) Bioprecipitation assays were conducted using equal number ($OD_{600nm} \sim 1\ ml^{-1}$) of *Deino-PhoK* or *Deino-pRAD1* with either *p*-NPP or β-GP as substrate (5 mM). Residual U present in the supernatant and the amount of U present in the pellet was estimated by the Arsenazo III reagent (B) Bioprecipitation assay was conducted with *Deino-PhoK* or *Deino-pRAD1* cells. Fluorescence intensity (in arbitrary units, AU) of the suspension was monitored over a period of time. (C) Uranium precipitation by *Deino-PhoK* cells at different concentrations of uranyl carbonate and appropriate concentration of β-GP. Controls containing either no cells (•) or *Deino-pRAD1* (○) cells were also included for comparison. (D) Comparison of uranium bioprecipitation by *Deino-PhoK*, *Deino-PhoN* and *Deino-pRAD1* strains. Equivalent cells of all three strains were used in the assays as mentioned in materials and methods. *Deino-pRAD1* cells incubated at pH 5.0 or pH 9.0 served as respective control in both the cases.

Table 2
Phosphatase activity of different strains*.

Strains	Specific activity**
Deino-pRAD1	18 ± 5
Deino-PhoK	15,000 ± 1000
Deino-PhoN	200 ± 10
E.coli-PhoK	4500 ± 200

* At their optimum pH values (pH 9.0 for PhoK and pH 5.0 for PhoN).
** *n* moles of *p*-NP liberated/min/mg of total cellular protein.

uranyl carbonate and 5 mM β-GP in 5 mM MOPS buffer pH 9) and the decrease in uranium content of supernatant was monitored by the Arsenazo III reagent. Uranium removal from solution and corresponding gain in beads was also monitored by fluorimetric method as detailed in earlier sections. The *Deino-PhoK* beads (uranium treated and untreated) were also dried at 60 °C for 4 h and the amount of uranium loaded was calculated by estimating gain in dry weight of beads.

3. Results and discussion

3.1. Heterologous expression of PhoK in D. radiodurans and analysis of phosphatase activity

The *phoK* gene was cloned downstream of a strong deinococcal promoter P_{groESL} in a *D. radiodurans*/*E. coli* shuttle vector, pRAD1 to obtain the recombinant plasmid, pK1. The presence of 1.68 kbp PhoK insert in pK1 was confirmed by restriction digestion of pK1 (Fig. 1A) and the nucleotide sequence integrity of *phoK* insert was ascertained by DNA sequencing (data not included). The plasmid, pK1, was transformed into *D. radiodurans* R1 to obtain the strain *Deino-PhoK*. The presence of *phoK* in *Deino-PhoK* was confirmed by colony PCR employing *phoK*-specific primers (Fig. 1B). On histochemical plates (pH 7), *Deino-PhoK* cells appeared as intense dark green colored spots whereas *Deinococcus* carrying pRAD1 (control cells), showed typical orange colored spots. In comparison *Deino-PhoN*, a recombinant *D. radiodurans* expressing a non-specific acid phosphatase, PhoN, [22] that served as positive control formed light green colored spots (Fig. 1C). The intensity of green color reflects the corresponding phosphatase activity of these strains.

When assayed on zymogram, cell free extracts of *Deino-PhoK* and *E. coli-PhoK* both showed an activity band of 60 kDa corresponding to the expected PhoK monomer and also several high molecular mass activity bands suggesting PhoK oligemerization in both the strains (Fig. 1D). Expression of PhoK in *Deino-PhoK* was further confirmed by Western blotting and immunodetection using PhoK-specific antiserum (Fig. 1E). Under reducing conditions, the PhoK monomer was immunodetected as a solitary 60 kDa band.

Deino-PhoK cells showed 4–5 fold higher activity than *E. coli-PhoK* (*E. coli* transformed with pK1) and unexpectedly 75-fold higher activity than *Deino-PhoN* cells with *para*-nitrophenyl phosphate (*p*-NPP) as substrate (Table 2).

3.2. Deino-PhoK efficiently precipitates U from alkaline solutions

Deino-PhoK cells were assessed for their uranium precipitation ability using either *p*-NPP or β-glycerophosphate (β-GP) as substrates. With *p*-NPP, a more rapid precipitation was observed as compared to β-GP at the initial time points of precipitation. *Deino-PhoK* cells could precipitate ~50% uranium within 15 min with *p*-NPP whereas it took nearly 30 min with β-GP as substrate (Fig. 2A). Notwithstanding these initial differences, both the substrates resulted in more than 90% U precipitation at the end of 2 h. In waste effluents, no organic phosphate source would be readily available and will need to be added. Macaskie et al., successfully used another phosphate donor, phytic acid (ubiquitous plant waste), for U precipitation [41]. Alternate easily available, economic and non pollutant P_i donors will need to be found for field application.

PhoK is known to precipitate uranyl carbonate to metautunite [chernikovite, $H_2(UO_2)_2(PO_4)_2{\cdot}8H_2O$] which fluoresces green upon exposure to UV. During the assay, fluorescence intensity of supernatant solution increased up to 2 h after which it remained steady indicating maximal uranium precipitation (Fig. 2B). No measurable increase in fluorescence was observed in case of *Deino-pRAD1* cells (control) over the same time period. The data correlated very well the colorimetric estimation of precipitated uranium (Fig. 2A). Uranium was also estimated from the cell pellet and results showed that metal loss from the supernatant fraction correlated very well with increase in U in the pellet fraction (Fig. 2A).

Deino-PhoK cells were tested for their uranium precipitation ability under different concentrations of input uranium (1, 2, 5 and 10 mM). At all concentrations tested; more than 80% uranium was precipitated within 1 h. In case of control cells only 5–6% uranium precipitation was seen even after prolonged exposure (Fig. 2C).

The relative efficiency of *Deino-PhoK* and *Deino-PhoN* to precipitate uranium was found to be very different. *Deino-PhoK* cells could precipitate more than 80% uranium within 1 h whereas *Deino-PhoN* cells could precipitate only 10% uranium in the same period (Fig. 2D). To achieve more than 90% precipitation, *Deino-PhoK* cells required only 2 h, whereas *Deino-PhoN* could precipitate only 50% U even after 4 h of incubation with uranium. The control *Deino-pRAD1* cells could precipitate only 5–6% of input U (Fig. 2D) in both the conditions tested (i.e. pH 5.0 or pH 9.0).

The important factors for any bioremediation process are the time required for maximal metal removal, the range of working concentration and the minimum amount of biomass required. *Deino-PhoK* possessed all these attributes. At a relatively low cell density ($OD_{600nm} \sim 1\ ml^{-1}$), these cells could efficiently bioprecipitate over 90% of input U within 1 h. To achieve same level of precipitation, *Deino-PhoN* cells required 10 fold higher cell density and much longer time [20]. *Deino-PhoK* cells showed highest phosphatase activity as well as a very rapid U removal ability compared to those reported by earlier studies (Table 3). The uranium loading capacity of *Deino-PhoK* was found to be 10.7 g U/g dry weight of cells (with input U concentration of 10 mM), which to our knowledge, is the highest reported so far.

Table 3
Comparison of uranium bioprecipitation ability of *Deino-PhoK* with earlier reported strains.

Strains	pH conditions for precipitation assay	Specific activity of enzyme (phosphatase) *	Time (h) required to remove >90% input U**	Amount of uranium** precipitated (mg U/g of dry biomass)***	Reference
Citrobacter N14	5.0	~400	16–18	91	[19,23]
Deino-PhoN	6.8	~200	8	214	[22]
Sphingomonas	9.0	~500	6–7	306	[35]
Deino-PhoK	9.0	~15,000	<2	1070	This study

* Specific activity expressed as *n*moles of *p*-NP released/min/mg bacterial protein.
** At acidic/neutral pH, uranyl nitrate was employed while at alkaline pH conditions uranyl carbonate was employed in typical precipitation assays.
*** Input uranium concentration at 1 mM.

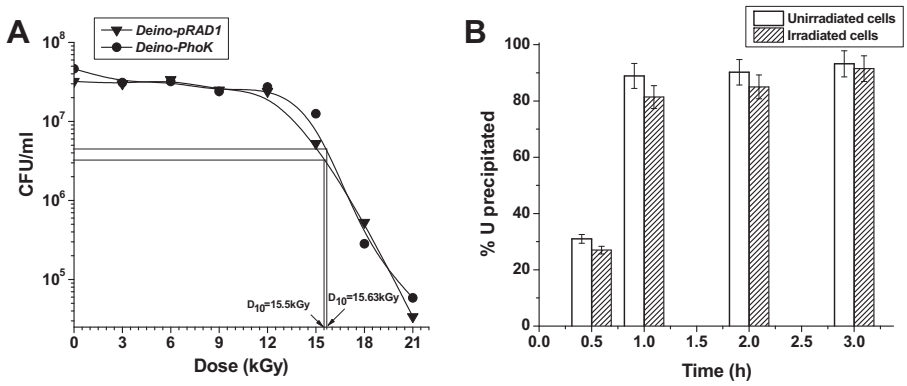

Fig. 3. Radioresistance and post irradiation uranium precipitation ability of *Deino-PhoK* cells. (A) *Deino-PhoK* or *Deino-pRAD1* cells were exposed to different doses of ^{60}Co-gamma radiation. Survival was measured in terms of the number of CFUs/ml and the calculated D_{10} dose is shown (B) *Deino-PhoK* cells (5 ml of $OD_{600nm} \sim 1\ ml^{-1}$) were exposed to 6 kGy dose of gamma radiation followed by incubation with 1 mM uranyl carbonate and 5 mM β-GP at pH 9.0. Unirradiated *Deino-PhoK* cells served as control. The amount of U removed from the supernatant was measured over a period of time by the Arsenazo III reagent.

3.3. *Deino-PhoK can function in environments similar to LLW/ILLW.*

The common components of LLW/ILLW, in addition to U, include other metals such as Pu, Cs, Sr, etc. which are present in sub-millimolar concentrations. *Deinococcus* cells (wild-type *D. radiodurans* R1, *Deino-PhoK* or *Deino-pRAD1*) showed no loss of survival (data not shown) on exposure to 1–20 mM uranyl carbonate or to 1 mM $CsCl_2$ and 1 mM $SrCl_2$ for 4 h. However, when cells were grown in TGY medium containing 1 or 2 mM uranyl carbonate, a 50–60% reduction in growth was observed (data not included). Thus, toxicity of uranyl carbonate becomes apparent only when *Deinococcus* cells are grown in nutrient rich media. However, metal sensitivity to U, Cs, Sr, etc. may not be an issue in nutrient deficient alkaline waste solutions.

Radiation resistance of recombinant *Deino-PhoK* and *Deino-pRAD1* strains was determined by evaluating their D_{10} dose values (i.e. the dose that causes 90% cell death and allows only 10% survival). Both control and *Deino-PhoK* cells showed similar D_{10} values of around 15.5 kGy (Fig. 3A). *Deino-PhoK* cells exposed to a wide range of gamma radiation dose (3–15 kGy) showed no change in their PhoK activity (data not included). When exposed to 6 kGy dose of ^{60}Co gamma radiation, both irradiated and unirradiated *Deino-PhoK* cells could precipitate uranium from 1 mM uranyl carbonate solution with similar efficiency (Fig. 3B).

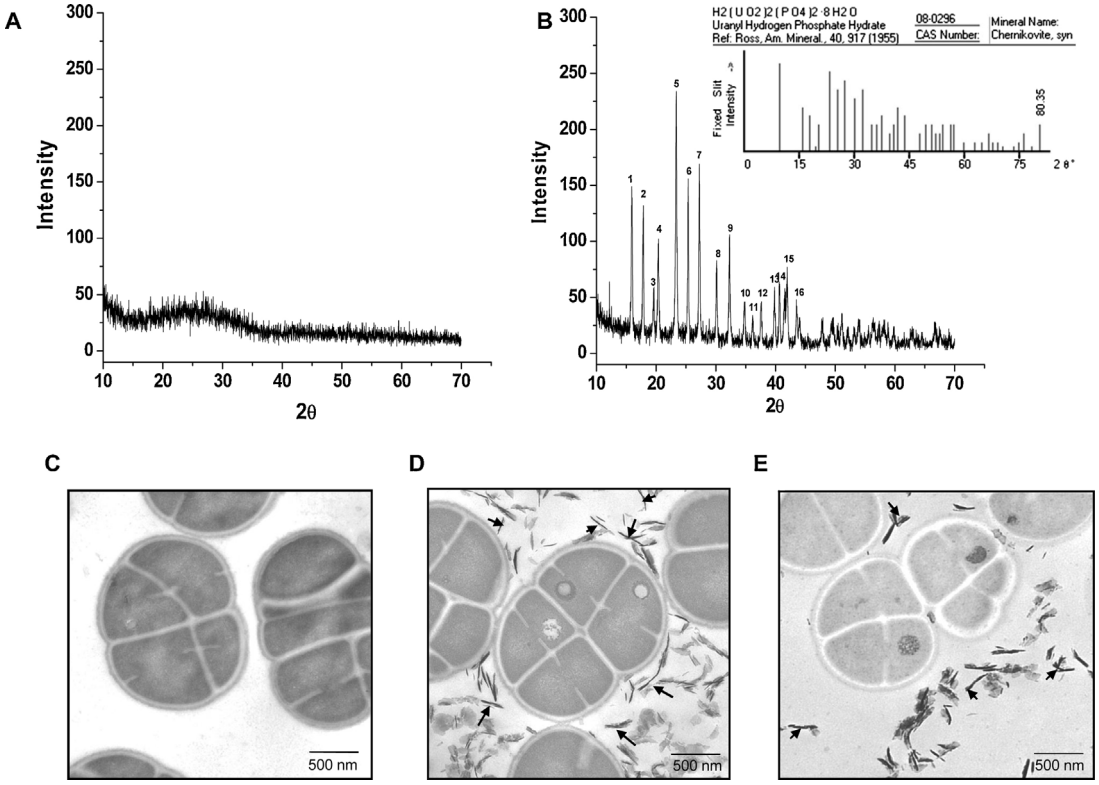

Fig. 4. Identity and localization of the bioprecipitated uranium. XRD spectra of uranium treated cells, incubated with 1 mM uranyl carbonate in 5 mM MOPS buffer with 5 mM β-GP for 2 h (A) *Deino-pRAD1* (control) cells or (B) *Deino-PhoK* cells. (C–E) Transmission electron micrographs of *Deinococcus* cells incubated with 1 mM uranyl carbonate in 5 mM MOPS buffer with 5 mM β-GP for 2 h. *Deino-pRAD1* cells (C), *Deino-PhoK* cells stained with uranyl acetate (D) or unstained *Deino-PhoK* cells (E) are shown and the crystalline extracellular precipitate is depicted by arrows.

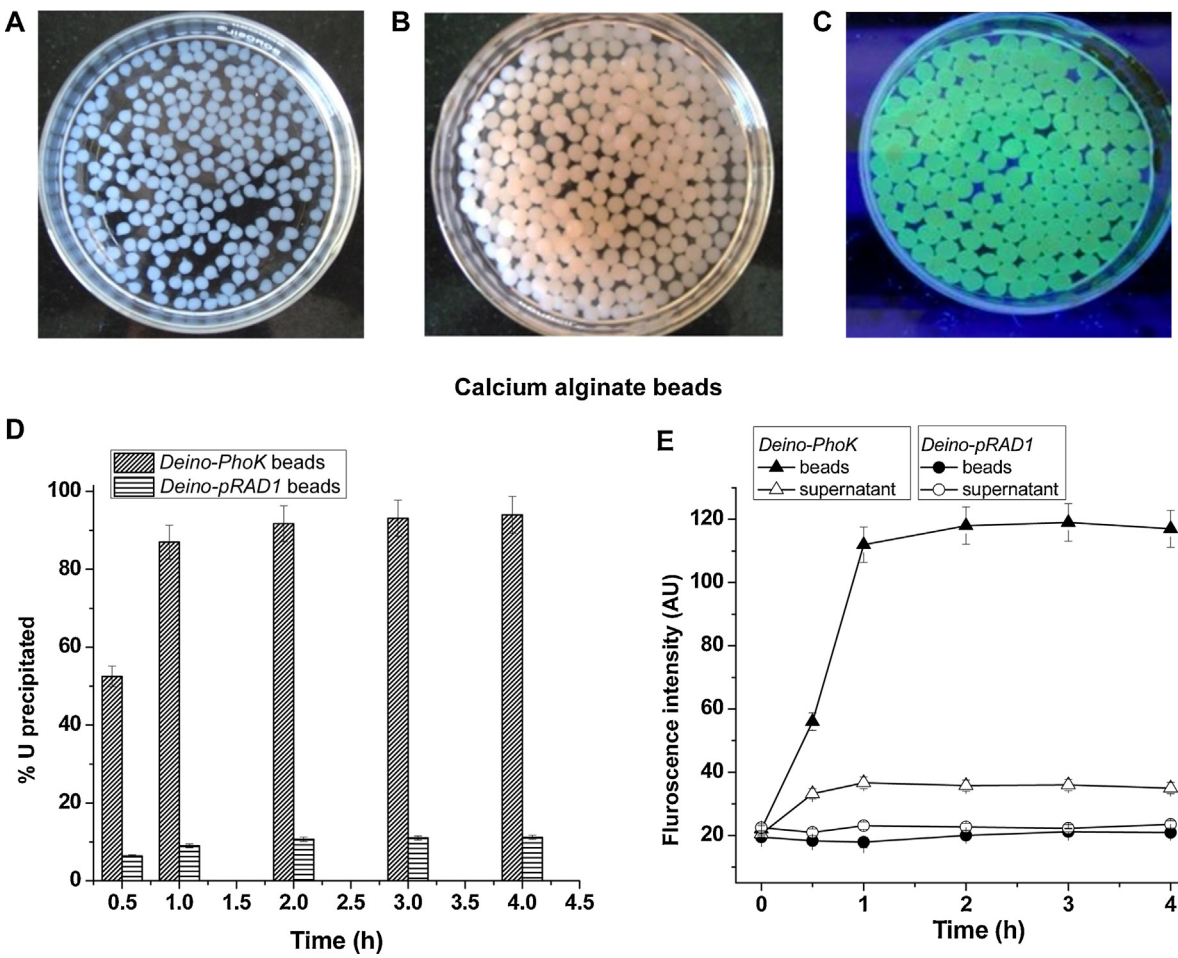

Fig. 5. U precipitation by immobilized *Deino-PhoK* cells. Calcium alginate beads without cells (blank beads) (A) or containing immobilized *Deino-pRAD1* cells (B) or *Deino-PhoK* cells (C) were incubated in a solution (1 mM uranyl carbonate in 5 mM MOPS buffer with 5 mM β-GP) for 4 h. The beads were removed from the solution, exposed to UV (312 nm) and photographed. The green fluorescence emanating from chernikovite entrapped inside beads is observed in (C). (D) Uranium precipitation with *Deino-PhoK* or *Deino-pRAD1* cells immobilized in calcium alginate beads. Equal number (1 0 0) of above mentioned beads were suspended in uranium solution (1 mM) and U removal was monitored as decrease in uranium content from supernatant up to 4 h (E) *Deino-PhoK* or *Deino-pRAD1* beads were evaluated for U precipitation in assay as described in (D). Ten beads were removed from solution at regular time intervals and their fluorescence intensity (in arbitrary units, AU) measured. The fluorescence intensity of the supernatant at corresponding intervals of time was monitored in a spectrofluorimeter. (For interpretation of the references to color in this figure legend, the reader is referred to the web version of this article.).

Thus expression of PhoK did not compromise the inherent radioresistance or the bioprecipitation ability of *Deinococcus*, and the *Deino-PhoK* strain could function in environment typical of LLW/ILLW.

3.4. The precipitated uranyl phosphate species, chernikovite, is extracellular in nature

XRD analysis of uranium loaded *Deino-PhoK* cells showed the presence of uranyl hydrogen phosphate hydrate $[H_2(UO_2)_2(PO_4)_2{\cdot}8H_2O]$. Data fitting with the ICDD database revealed a match with 16 peaks indicating the precipitated U to be a chemical species CAS no.—08-296 (Fig. 4B). Uranium treated *Deino-pRAD1* cells did not yield a spectrum (Fig. 4A) suggesting inability of *Deino-pRAD1* to precipitate U. TEM images of uranium-treated *Deino-PhoK* and *Deino-pRAD1* cells are shown in the Fig. 4. Presences of large, abundant needle like crystals of uranyl phosphate were visible around *Deino-PhoK* cells treated with uranium (Fig. 4D). These crystalline structures were also observed in samples which were not stained with uranyl acetate (Fig. 4E), confirming the precipitation is indeed mediated by PhoK. No such crystals or precipitate were observed when control *Deino-pRAD1* cells were treated with uranyl carbonate and stained with uranyl acetate (Fig. 4C).

3.5. Precipitated U is entrapped in beads containing immobilized Deino-PhoK

The *Deino-PhoN* cells when loaded with sufficient uranyl phosphate settle to the bottom of the container and can be easily collected to recover uranium from them [22]. However, the uranyl phosphate precipitated by *Deino-PhoK* remained extracellular (Fig. 4D and E) and required centrifugation for complete recovery. In order to achieve easier separation uranyl phosphate precipitate from the bulk volume, bioprecipitation was attempted with *Deino-PhoK* cells immobilized in calcium alginate beads.

Freshly harvested *Deino-PhoK* cells were immobilized in Ca–alginate beads and employed to remove uranium from test solutions. On exposure to UV light (312 nm), a bright green fluorescence, indicating the presence of chernokovite, was seen only in *Deino-PhoK* beads (Fig. 5C) but not in blank or *Deino-pRAD1* (control cells) beads (Fig. 5A and B). These *Deino-PhoK* beads showed increase in fluorescence up to 2 h after which it remained steady. These beads could remove ~90% uranium from 1 mM solution within 2 h as estimated by the Arsenazo III method

(Fig. 5D), whereas control beads, immobilized with *Deino-pRAD1* cells could remove only 8–9% uranium even after prolonged exposure (Fig. 5D). When the supernatant (after removal of beads) was analyzed fluorimetrically, no significant increase in fluorescence was observed up to 4 h (in contrast to whole cell suspension) thus indicating that precipitate is indeed entrapped into beads (Fig. 5E). The beads settled down to the floor of the flask and could be easily harvested to facilitate separation and recovery of the bioprecipitated uranium. The beads showed ~0.5 g of U loading/g of dry weight of biomass at 1 mM input U concentration.

4. Conclusions

The alkaline phosphatase (PhoK) was overexpressed in the radioresistant bacterium *D. radiodurans* (*Deino-PhoK*) for bioprecipitation of U from dilute alkaline solutions. This recombinant strain (1) possessed very high phosphatase activity, (2) precipitated U very rapidly and efficiently under ambient conditions even after exposure to high doses of radiation, (3) functioned over a wide range of U concentration and in the presence of other metals (Cs, Sr, etc.) commonly present in LLW/ILLW, and (4) displayed an impressive high U loading capacity, 10.7 g U/g dry weight. These features make *Deino-PhoK* an excellent candidate for U bioremediation from alkaline nuclear and other waste solutions. Immobilization of *Deino-PhoK* accomplished easy separation of precipitated uranyl phosphate from bulk solutions.

Acknowledgments

The authors thank Ms. Alka Gupta and Ms. Namrata Jadhav, MBD, BARC, for TEM analysis, Mr. Deepak Tyagi and Dr. Salil Verma, Chemistry Division, BARC for XRD studies and Ms. Chitra Seetharam Misra, MBD, BARC for valuable suggestions during preparation of the manuscript.

References

[1] D.C. Seidel, Extracting uranium from its ores, IAEA Bull. 23 (1978) 24–28.
[2] D.H. Underhill, Uranium production in the commonwealth of independent states, China and Mangolia, in: Developments in Uranium Resources, Production, Demand and Environment, IAEA, 1999, pp. 25–41, IAEA—TECDOC—1425.
[3] E.A. Santos, A.C.Q. Ladeira, Recovery of uranium from mine waste by leaching with carbonate-based reagents, Environ. Sci. Technol. 45 (2011) 3591–3597.
[4] M.C. Duff, D.B. Hunter, D.T. Hobbs, S.D. Fink, Z. Dai, J.P. Bradley, Mechanisms of strontium and uranium removal from high-level radioactive waste simulant solution by the sorbent monosodium titanate, Environ. Sci. Technol. 38 (2004) 5201–5207.
[5] K. Raj, K.K. Prasad, N.K. Bansal, Radioactive waste management practices in India, Nucl. Eng. Des. 236 (2006) 914–930.
[6] T.P. Valsala, A. Joseph, N.L. Sonar, M.S. Sonavane, J.G. Shah, K. Raj, V. Venugopal, Separation of strontium from low level radioactive waste solutions using hydrous manganese dioxide composite materials, J. Nucl. Mater. 404 (2010) 138–143.
[7] B.J. Converse, T. Wu, R.H. Findlay, E.E. Roden, U(VI), Reduction in sulfate-reducing subsurface sediments amended with ethanol or acetate, Appl. Environ. Microbiol. 79 (2013) 4173–4177.
[8] K.H. Williams, J.R. Bargar, J.R. Lloyd, D.R. Lovley, Bioremediation of uranium-contaminated groundwater: a systems approach to subsurface biogeochemistry, Curr. Opin. Biotechnol. 24 (2013) 489–497.
[9] D.R. Lovley, E.J.P. Phillips, Reduction of uranium by *Desulfovibrio desulfuricans*, Appl. Environ. Microbiol. 58 (1992) 850–856.
[10] M. Barlett, H. Moon, A. Peacock, D. Hedrick, K. Williams, P. Long, D. Lovley, P. Jaffe, Uranium reduction and microbial community development in response to stimulation with different electron donors, Biodegradation 23 (2012) 535–546.
[11] C. Acharya, D. Joseph, S.K. Apte, Uranium sequestration by a marine cyanobacterium, *Synechococcus elongatus* strain BDU/75042, Bioresour. Technol. 100 (2009) 2176–2181.
[12] K. Akhtar, A.M. Khalid, M.W. Akhtar, M.A. Ghauri, Removal and recovery of uranium from aqueous solutions by Ca–alginate immobilized *Trichoderma harzianum*, Bioresour. Technol. 100 (2009) 4551–4558.
[13] M.L. Merroun, M. Nedelkova, J.J. Ojeda, T. Reitz, M.L. Fernández, J.M. Arias, M. Romero-González, S. Selenska-Pobell, Bio-precipitation of uranium by two bacterial isolates recovered from extreme environments as estimated by potentiometric titration, TEM and X-ray absorption spectroscopic analyses, J. Hazard. Mater. 197 (2011) 1–10.
[14] S. Choudhary, P. Sar, Uranium biomineralization by a metal resistant *Pseudomonas aeruginosa* strain isolated from contaminated mine waste, J. Hazard. Mater. 186 (2011) 336–343.
[15] M. Nedelkova, M.L. Merroun, A. Rossberg, C. Hennig, S. Selenska-Pobell, Microbacterium isolates from the vicinity of a radioactive waste depository and their interactions with uranium, FEMS Microbiol. Ecol. 59 (2007) 694–705.
[16] R.J. Martinez, M.J. Beazley, M. Taillefert, A.K. Arakaki, J. Skolnick, P.A. Sobecky, Aerobic uranium(VI) bioprecipitation by metal-resistant bacteria isolated from radionuclide- and metal-contaminated subsurface soils, Environ. Microbiol. 9 (2007) 3122–3133.
[17] K. Benzerara, J. Miot, G. Morin, G. Ona-Nguema, F. Skouri-Panet, C. Férard, Significance, mechanisms and environmental implications of microbial biomineralization, C.R. Geosci. 343 (2011) 160–167.
[18] L.E. Macaskie, K.M. Bonthrone, P. Yong, D.T. Goddard, Enzymically mediated bioprecipitation of uranium by a *Citrobacter* sp.: a concerted role for exocellular lipopolysaccharide and associated phosphatase in biomineral formation, Microbiology 146 (2000) 1855–1867.
[19] L.E. Macaskie, R.M. Empson, A.K. Cheetham, C.P. Grey, A.J. Skarnulis, Uranium bioaccumulation by a *Citrobacter* sp. as a result of enzymically mediated growth of polycrystalline HUO_2PO_4, Science 257 (1992) 782–784.
[20] M.J. Beazley, R.J. Martinez, P.A. Sobecky, S.M. Webb, M. Taillefert, Uranium biomineralization as a result of bacterial phosphatase activity: insights from bacterial isolates from a contaminated subsurface, Environ. Sci. Technol. 41 (2007) 5701–5707.
[21] N. Renninger, R. Knopp, H. Nitsche, D.S. Clark, J.D. Keasling, Uranyl precipitation by *Pseudomonas aeruginosa* via controlled polyphosphate metabolism, Appl. Environ. Microbiol. 70 (2004) 7404–7412.
[22] D. Appukuttan, A.S. Rao, S.K. Apte, Engineering of *Deinococcus radiodurans* R1 for bioprecipitation of uranium from dilute nuclear waste, Appl. Environ. Microbiol. 72 (2006) 7873–7878.
[23] G. Basnakova, E.R. Stephens, M.C. Thaller, G.M. Rossolini, L.E. Macaskie, The use of *Escherichia coli* bearing a *phoN* gene for the removal of uranium and nickel from aqueous flows, Appl. Microbiol. Biotechnol. 50 (1998) 266–272.
[24] C. Seetharam, S. Soundarajan, A.C. Udas, A.S. Rao, S.K. Apte, Lyophilized, nonviable, recombinant *E. coli* cells for cadmium bioprecipitation and recovery, Process Biochem. 44 (2009) 246–250.
[25] D. Appukuttan, K.S. Nilgiriwala, C. Misra, S.K. Apte, Natural recombinant bacteria for bioremediation of uranium from acidic/alkaline aqueous solutions in high radiation environment, J. Biotechnol. 150S (2010) 53.
[26] M.J. Daly, Engineering radiation-resistant bacteria for environmental biotechnology, Curr. Opin. Biotechnol. 11 (2000) 280–285.
[27] D. Prakash, P. Gabani, A.K. Chandel, Z. Ronen, O.V. Singh, Bioremediation: a genuine technology to remediate radionuclides from the environment, Microb. Biotechnol. 6 (2013) 349–360.
[28] J.R. Battista, Against all odds: the survival strategies of *Deinococcus radiodurans*, Annu. Rev. Microbiol. 51 (1997) 203–224.
[29] C.C. Lange, L.P. Wackett, K.W. Minton, M.J. Daly, Engineering a recombinant *Deinococcus radiodurans* for organopollutant degradation in radioactive mixed waste environments, Nat. Biotechnol. 16 (1998) 929–933.
[30] H. Brim, S.C. McFarlan, J.K. Fredrickson, K.W. Minton, M. Zhai, L.P. Wackett, M.J. Daly, Engineering *Deinococcus radiodurans* for metal remediation in radioactive mixed waste environments, Nat. Biotechnol. 18 (2000) 85–90.
[31] H. Brim, J.P. Osborne, H.M. Kostandarithes, J.K. Fredrickson, L.P. Wackett, M.J. Daly, Deinococcus radiodurans engineered for complete toluene degradation facilitates Cr(VI) reduction, Microbiology 152 (2006) 2469–2477.
[32] D. Appukuttan, C. Seetharam, N. Padma, A.S. Rao, S.K. Apte, PhoN-expressing, lyophilized, recombinant *Deinococcus radiodurans* cells for uranium bioprecipitation, J. Biotechnol. 154 (2011) 285–290.
[33] C.S. Misra, D. Appukuttan, V.S.S. Kantamreddi, A.S. Rao, S.K. Apte, Recombinant *D. radiodurans* cells for bioremediation of heavy metals from acidic/neutral aqueous wastes, Bioeng. Bugs 3 (2012) 44–48.
[34] Z. Zheng, J. Wan, X. Song, T.K. Tokunaga, Sodium meta-autunite colloids: synthesis, characterization, and stability, Colloids Surf., A: Physicochem. Eng. Aspects 274 (2006) 48–55.
[35] K.S. Nilgiriwala, A. Alahari, A.S. Rao, S.K. Apte, Cloning and overexpression of alkaline phosphatase PhoK from *Sphingomonas* sp. strain BSAR-1 for bioprecipitation of uranium from alkaline solutions, Appl. Environ. Microbiol. 74 (2008) 5516–5523.
[36] K.S. Nilgiriwala, S.C. Bihani, A. Das, V. Prashar, M. Kumar, J.L. Ferrer, S.K. Apte, M.V. Hosur, Crystallization and preliminary X-ray crystallographic analysis of PhoK, an extracellular alkaline phosphatase from *Sphingomonas* sp. BSAR-1, Acta Crystallogr., Sect. F: Struct. Biol. Cryst. Commun. 65 (2009) 917–919.
[37] S.C. Bihani, A. Das, K.S. Nilgiriwala, V. Prashar, M. Pirocchi, S.K. Apte, J.L. Ferrer, M.V. Hosur, X-ray structure reveals a new class and provides insight into evolution of alkaline phosphatases, PLoS One 6 (2011) e22767.
[38] M.L. Riccio, G.M. Rossolini, G. Lombardi, A. Chiesurin, G. Satta, Expression cloning of different bacterial phosphatase-encoding genes by histochemical

screening of genomic libraries onto an indicator medium containing phenolphthalein diphosphate and methyl green, J. Appl. Microbiol. 82 (1997) 177–185.
[39] R. Meima, M.E. Lidstrom, Characterization of the minimal replicon of a cryptic *Deinococcus radiodurans* SARK plasmid and development of versatile *Escherichia coli–D. radiodurans* shuttle vectors, Appl. Environ. Microbiol. 66 (2000) 3856–3867.
[40] J.S. Fritz, E.C. Bradford, Detection of thorium and uranium, Anal. Chem. (U.S.) 30 (1958) 1021–1022.
[41] M. Paterson-Beedle, J.E. Readman, J.A. Hriljac, L.E. Macaskie, Biorecovery of uranium from aqueous solutions at the expense of phytic acid, Hydrometallurgy 104 (2010), 524-258.

zam01616/zam7338d16z | xppws | S=1 | 7/1/16 | 19:07 | 4/C Fig: 1,2,3,6 | ArtID: 00728-16 | NLM: research-article | CE: CNV-as

Editor: Liu | Section: Environmental Microbiology | Designation: T

AMERICAN SOCIETY FOR MICROBIOLOGY | Applied and Environmental Microbiology

Interaction of Uranium with Bacterial Cell Surfaces: Inferences from Phosphatase-Mediated Uranium Precipitation

AQ: au Sayali Kulkarni,[a,b] Chitra Seetharam Misra,[a] Alka Gupta,[a] Anand Ballal,[a,b] Shree Kumar Apte[a,b]

AQ: aff Molecular Biology Division, Bhabha Atomic Research Centre, Mumbai, India[a]; Homi Bhabha National Institute, Anushaktinagar, Mumbai, India[b]

ABSTRACT

Deinococcus radiodurans **and** ***Escherichia coli*** **expressing either PhoN, a periplasmic acid phosphatase, or PhoK, an extracellular alkaline phosphatase, were evaluated for uranium (U) bioprecipitation under two specific geochemical conditions (GCs): (i) a carbonate-deficient condition at near-neutral pH (GC1), and (ii) a carbonate-abundant condition at alkaline pH (GC2). Transmission electron microscopy revealed that recombinant cells expressing PhoN/PhoK formed cell-associated uranyl phosphate precipitate under GC1, whereas the same cells displayed extracellular precipitation under GC2. These results implied that the cell-bound or extracellular location of the precipitate was governed by the uranyl species prevalent at that particular GC, rather than the location of phosphatase. MINTEQ modeling predicted the formation of predominantly positively charged uranium hydroxide ions under GC1 and negatively charged uranyl carbonate-hydroxide complexes under GC2. Both microbes adsorbed 6- to 10-fold more U under GC1 than under GC2, suggesting that higher biosorption of U to the bacterial cell surface under GC1 may lead to cell-associated U precipitation. In contrast, at alkaline pH and in the presence of excess carbonate under GC2, poor biosorption of negatively charged uranyl carbonate complexes on the cell surface might have resulted in extracellular precipitation. The toxicity of U observed under GC1 being higher than that under GC2 could also be attributed to the preferential adsorption of U on cell surfaces under GC1. This work provides a vivid description of the interaction of U complexes with bacterial cells. The findings have implications for the toxicity of various U species and for developing biological aqueous effluent waste treatment strategies.**

IMPORTANCE

The present study provides illustrative insights into the interaction of uranium (U) complexes with recombinant bacterial cells overexpressing phosphatases. This work demonstrates the effects of aqueous speciation of U on the biosorption of U and the localization pattern of uranyl phosphate precipitated as a result of phosphatase action. Transmission electron microscopy revealed that location of uranyl phosphate (cell associated or extracellular) was primarily influenced by aqueous uranyl species present under the given geochemical conditions. The data would be useful for understanding the toxicity of U under different geochemical conditions. Since cell-associated precipitation of metal facilitates easy downstream processing by simple gravity-based settling down of metal-loaded cells, compared to cumbersome separation techniques, the results from this study are of considerable relevance to effluent treatment using such cells.

Bioremediation strategies, such as bioreduction (1–3), biosorption (4–8), bioaccumulation (9, 10), and bioprecipitation (5, 11, 12, 13), have been studied for their potential to immobilize U AQ: A from solutions. There is also a large body of work on microbial interactions with uranium relevant to environmental *in situ* bioremediation. The efficacy of U removal and fate of the metal at the end of the waste solution treatment are influenced by the chemical state of U prevalent under the given condition. U forms aqueous species as a result of complexation with ligands under different pH conditions (14). In open atmospheric systems, under oxygenic conditions, and with pH values lower than 3, U(VI) is present exclusively in the form of hexavalent uranyl cation, UO_2^{2+}, which is the most bioavailable form of U (15, 16). Circumneutral pH favors the formation of positively charged uranyl hydroxide, $[(UO_2)_3(OH)]^{5+}$, or $[(UO_2)_4(OH)]^{+7}$complexes that are transformed to negatively charged ones at higher pH (pH 8 to 9). However, under strongly alkaline conditions, negatively charged uranyl-carbonate complexes, like $[UO_2(CO_3)_2]^{2-}$ and $[UO_2(CO_3)_3]^{4-}$, predominate (17–19). It is important to understand how these different U species interact with bacterial cellular surfaces, especially for designing biological wastewater treatment systems. However, studies evaluating the effect of aqueous U speciation have been largely limited to biosorption, bioaccumulation, and bioreduction (9, 15, 16, 20).

Among the biological mechanisms involved in metal remediation, enzymatic bioprecipitation of heavy metals as metal phosphates is particularly attractive and is considered to be a promising approach for biological treatment of U effluents due to its high efficiency (14, 21). Bioprecipitation of metals as phosphates is mediated by phosphatases that cleave a phosphomonoester substrate (such as β-glycerophosphate) to release the phosphate moiety, which in turn precipitates heavy metals, such as U, Cd, Ni, Am, etc., from solutions (22, 23). Phosphatases are ubiquitous

Received 4 March 2016 Accepted 30 May 2016

Accepted manuscript posted online 10 June 2016

Citation Kulkarni S, Misra CS, Gupta A, Ballal A, Apte SK. 2016. Interaction of uranium with bacterial cell surfaces: inferences from phosphatase-mediated uranium precipitation. Appl Environ Microbiol 82:000–000. doi:10.1128/AEM.00728-16.

Editor: S.-J. Liu, Chinese Academy of Sciences

Address correspondence to Shree Kumar Apte, aptesk@barc.gov.in.

TABLE 1 Bacterial strains used in this study

Strain	Description	Source or reference
E. coli DH5α	F$^-$ *recA41 endA1 gyrA96 thi-1 hsdr17*(r_K^- m_K^+) *supE44 relA* λ*lacU169*	Lab collection
D. radiodurans R1	Wild-type strain	Lab collection
E. coli(pPN1)	*E. coli* DH5α containing plasmid pPN1 (*phoN* ORF, GenBank accession no. X59036, in plasmid pRAD1 under P_{groESL} promoter)[a]	Appukutan et al. (30)
E. coli(pK1)	*E. coli* DH5α containing plasmid construct pK1 (*phoK* ORF, GenBank accession no. AY764287, in plasmid pRAD1 under P_{groESL} promoter)	Nilgiriwala et al. (32); Kulkarni et al. (11)
E. coli(pRAD1)	*E. coli* DH5α containing shuttle vector plasmid pRAD1	Kulkarni et al. (11)
D. radiodurans(pPN1)	*D. radiodurans* R1 containing plasmid construct pPN1	Appukutan et al. (30)
D. radiodurans(pK1)	*D. radiodurans* R1 containing plasmid construct pK1	Kulkarni et al. (11)
D. radiodurans(pRAD1)	*D. radiodurans* R1 containing shuttle vector plasmid pRAD1	Appukutan et al. (30); Kulkarni et al. (11)

[a] ORF, open reading frame.

among prokaryotes that catalyze dephosphorylation of various substrates by hydrolysis of phosphoester or phosphoanhydride bonds (24, 25). Traditionally, phosphatases are broadly categorized as acid or alkaline phosphatases, based on the pH required for their optimum activity. Phosphatases play a crucial role in supporting microbial nutrition by releasing the assimilable phosphate from the organic source (24, 26). Phosphatases are either secreted outside the plasma membrane, where they are released in a soluble form, or retained as membrane-bound proteins. Phosphatases enable the release of inorganic phosphate (P_i) and organic by-products that can be transported across the membrane, thus providing cells with essential nutrients (25).

As uranyl phosphate precipitate is highly insoluble, it can serve as a long-term stable sink for U immobilization (27, 28), thus making phosphatase-mediated bioprecipitation a very attractive strategy for treating nuclear waste. In recent years, our laboratory has explored the ability of phosphatase-expressing recombinant bacterial cells to bioprecipitate U and other heavy metals from solutions (29). The PhoN enzyme from *Salmonella enterica* serovar Typhimurium (encoded by the *phoN* gene, GenBank accession no. X59036), a nonspecific acid phosphatase, was overexpressed in the Gram-positive radioresistant bacterium *Deinococcus radiodurans* [*D. radiodurans*(pPN1)], as well as in the Gram-negative bacterium *Escherichia coli* [*E. coli*(pPN1)] to achieve phosphatase-mediated bioprecipitation of U from acidic to neutral solutions (pH 6.8) (30, 31). In view of its phenomenal radioresistance, *D. radiodurans* was the organism of choice for its potential use in U bioprecipitation from nuclear effluents. Similarly, the *phoK* gene (GenBank accession no. AY764287), encoding a novel alkaline phosphatase from *Sphingomonas* sp. strain BSAR-1, was also introduced into both *D. radiodurans* [*D. radiodurans*(pK1)] and *E. coli* [*E. coli*(pK1)]. PhoN and PhoK show good activity between pH 5 and 7 and pH 7 and 9, respectively. PhoK-expressing recombinants were shown to efficiently bioprecipitate U under carbonate-abundant conditions from alkaline solutions (11, 32). The crystalline precipitate formed by PhoN-/PhoK-expressing cells was identified as uranyl hydrogen phosphate by X-ray diffraction (XRD) analysis (11, 29, 32). Such crystalline aggregates of uranyl phosphate can be easily visualized by electron microscopy (11, 31).

The present study exploits the use of transmission electron microscopy to determine the effect of aqueous uranyl species predominant under two different geochemical conditions (GC) on the spatial distribution of the uranyl phosphate precipitate formed around *D. radiodurans* and *E. coli* cell surfaces. The information generated dissects the nature of interaction of U with bacterial cell surfaces under the given conditions and further indicates how these factors affect metal toxicity.

MATERIALS AND METHODS

Bacterial strains, growth conditions, and expression of phosphatases. The bacterial strains used in this study are listed in Table 1. *Deinococcus radiodurans* strain R1 was grown aerobically in TGY (1% Bacto-tryptone, 0.1% glucose, and 0.5% yeast extract) liquid medium at 32°C ± 1°C with agitation (180 ± 5 rpm). *E. coli* DH5α cells were grown in Luria-Bertani (LB) medium at 37°C ± 1°C under agitation (180 ± 5 rpm). The antibiotic concentrations used for recombinant strains were 100 μg/ml of carbenicillin for *E. coli* and 3 μg/ml of chloramphenicol for *D. radiodurans*. Screening for the phosphatase-positive colonies was carried out on LB or TGY agar medium supplemented with 1 mg/ml phenolphthalein diphosphate (PDP) and methyl green (MG) at 50 μg/ml for *E. coli* or at 5 μg/ml for *D. radiodurans* transformants. T1

Determination of phosphatase activities. PhoK and PhoN activities of the recombinant cells were determined in terms of P_i release from β-glycerophosphate (β-GP) substrate. Briefly, *D. radiodurans*(pK1), *D. radiodurans*(pPN1), and *D. radiodurans*(pRAD1) (Table 1) cells (optical density at 600 nm [OD_{600}], ~0.1) were suspended in 50 mM MOPS (morpholinepropanesulfonic acid) buffer (1 ml) either at pH 6.8 or 9, and 200 μl of 50 mM β-GP substrate was added, followed by incubation at 37°C for 30 min. Phosphate released in the supernatant was spectrophotometrically measured by the phosphomolybdic acid method (33). Protein concentration in equivalent cells was estimated by using Sigma total protein kit (Sigma-Aldrich, USA), based on Peterson's modification of the micro-Lowry method (34). Phosphatase activity was expressed as nanomoles of P_i released per minute per milligram of total cellular protein. AQ: B

Uranium precipitation/biosorption assays. Uranyl nitrate solution was prepared as a 100 mM stock solution by dissolving $UO_2(NO_3)_2{\cdot}6H_2O$ (Merck India Ltd.) in double-distilled water. To simulate a carbonate-dominated geochemical condition, a stock solution composed predominantly of uranyl carbonate complexes was prepared by the addition of a 1/10th volume of saturated ammonium carbonate to a 100 mM uranyl nitrate hexahydrate stock solution (final U concentration, 89 mM; carbonate concentration, 214 mM) (32, 35, 36). The formation of carbonate complexes with U was verified by monitoring the absorption spectra of solution in the visible light range between 400 and 500 nm (300 UV Unicam; Thermo Scientific) with specific peaks at 434 nm, 448 nm, and 464 nm (35, 36). U precipitation assays were carried out with PhoK/PhoN-expressing *E. coli* or *D. radiodurans* cells (OD_{600}, ~1) under the following two defined conditions: (i) geochemical condition 1 (GC 1) (carbonate-deficient condition; 10 mM MOPS [pH 7.0] with uranyl nitrate solution; final pH, 6.8); (ii) geochemical condition 2 (GC 2) (carbonate-abundant condition; 10 mM MOPS [pH 9] and U solution prepared with ammo-

AQ: C

nium carbonate, as explained above; final pH, 9.0). The concentration of carbonate in GC2 in all assays was always 2.4-fold higher than the U concentration used, i.e., the carbonate-to-U ratio of 2.4 was always maintained. The pH conditions (6.8 and 9) were optimized for the optimal phosphatase activity for U precipitation. The bioprecipitation assays were carried out at a U concentration of 1 mM and the sodium salt of β-glycerophosphate at a 5 mM concentration. The reaction mixture was subsequently kept at 30°C under static aerobic conditions for 18 h. The recombinant cells which carried the empty vector (i.e., pRAD1 lacking the *phoN*

AQ: D

or *phoK* gene) were used as a control and were incubated with U under conditions similar to those mentioned above. The inability of these control cells to precipitate U confirmed the role of PhoK/PhoK in U precipitation and also ruled out spontaneous metal precipitation. An abiotic control (lacking cells) was also included. Aliquots (1.5 ml) were taken at different time intervals and subjected to centrifugation at 12,000 × *g* for 10 min. Residual U in the supernatant or U present in the pellet was estimated using Arsenazo III reagent, as described earlier (37). For biosorption experiments, the wild-type *D. radiodurans* or *E. coli* (DH5α) cells (OD_{600}, ~1) were suspended in 10 mM MOPS buffer for 10 min under conditions similar to those of GC1 and GC2 at U concentrations of 50, 100, 200, and 1,000 μM. In GC2, the carbonate concentration was 2.4-fold-higher than that of U. The dry weight corresponding to the optical density of cells used in each experiment was determined and used to calculate the milligrams of U biosorbed or precipitated per gram (dry weight) of cells.

Transmission electron microscopy and X-ray diffraction analysis. PhoN- or PhoK-expressing cells which had precipitated U or control cells were washed twice with 50 mM cacodylate buffer (pH 7.4) and fixed in a solution (2.5% glutaraldehyde and 0.5% *para*-formaldehyde) overnight at 4°C. Following three washes with cacodylate buffer, cells were embedded in 2% noble agar and dehydrated in a graded series of ethanol (30, 60, 75, 90, and 100%). After the removal of ethanol by treatment with propylene oxide, blocks were subsequently infiltrated with Spurr resin and propylene oxide (Sigma Aldrich) in ratios of 1:3, 1:1, and 3:1 (vol/vol) for 2 h in each case. The samples were finally infiltrated with Spurr resin for 16 h and then embedded by incubation at 60°C for 72 h. Thin sections of samples were prepared with an ultramicrotome (Leica, Germany), placed on 200-mesh Formvar-coated copper grids, and viewed with the Libra 120 Plus TEM (Carl Zeiss). Both stained (with 1.5% uranyl acetate) and unstained samples were viewed. Altogether, 121 fields were observed, and the results have been reported for observations seen in more than 85% of the fields visualized for each sample.

For X-ray diffraction analysis (XRD), the cells of *D. radiodurans*(pK1) and *D. radiodurans*(pPN1) after U precipitation were dried in an oven at 80°C for 4 h. The dried pellet was scraped and crushed into a fine powder. The powder was subjected to X-ray diffraction analysis using a high-precision Rigaku R-Axis D-max powder diffractometer using monochromatic Cu-Kα radiation (Solid State Physics Division [SSPD], Bhabha Atomic Research Centre [BARC], India). The diffraction pattern was recorded at 2θ, from 5° to 70°, with a step length of 0.02. The diffraction pattern obtained was compared to known standards in the International Centre for Diffraction Data (ICDD) database.

Uranium toxicity experiments. *E. coli* or *D. radiodurans* was grown in LB or TGY liquid medium, respectively, until late-exponential phase of growth. Cells were washed twice with double-distilled water and suspended (OD_{600}, ~1) in 10 mM MOPS buffer, supplemented with U at 0 to 2 mM under GC1 or at 0 to 25 mM under GC2 for 4 h. Such U-exposed cells were washed free of uranium-containing medium, spotted (10 μl) on corresponding agar plates for the visual examination of growth or plated on agar plates to determine CFU, and growth after incubation of 24 h was recorded. In another set of experiments, cells (under resting conditions) were exposed to U, as described earlier, and such U-exposed cells (OD_{600}, ~0.5) were then inoculated into LB or TGY liquid broth medium with agitation (150 ± 5 rpm) or plated on LB or TGY agar plates. Growth was assessed by measuring the optical density at 600 nm (OD_{600}) or by determining the CFU on agar plates (1.5% Bacto agar) after 24 h of incubation at 37°C for *E. coli* and after 48 h of incubation at 32°C for *D. radiodurans*.

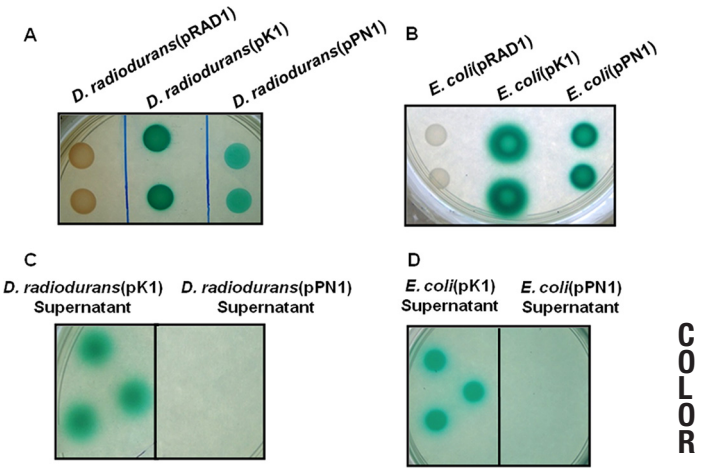

COLOR

FIG 1 Phosphatase expression and secretion. Spotting of recombinant *D. radiodurans* (A) and *E. coli* (B) cells (10 μl; OD_{600}, ~1) to assess expression and activity of phosphatases, or of spent medium (10 μl) to identify extracellular secretion of PhoK in *D. radiodurans* (C) and *E. coli* (D) on modified histochemical plate containing PDP-MG (pH 7.0).

Statistical analysis and thermodynamic modeling. Each experiment was repeated three times. The reported values are the means of the results from three replicates from a representative experiment, and the error bars correspond to 95% confidence intervals. Aqueous U speciation under GC1 or GC2 was determined using Visual MINTEQ version 3.1 (http://vminteq.lwr.kth.se/download/) (9, 17).

RESULTS

PhoN is a cell-associated phosphatase, whereas PhoK is secreted extracellularly. On histochemical (PDP-MG) plates (38) the recombinant cells expressing PhoN or PhoK appeared as intense green spots, whereas the control cells (carrying the empty vector pRAD1) showed no such color (Fig. 1A and B). Compared to the *D. radiodurans* cells expressing PhoN, PhoK-bearing strains formed darker green spots due to the higher specific activity of the phosphatase enzyme. In recombinants expressing PhoK (but not PhoN), a green halo extended outside the zone of growth into the medium, confirming the extracellular secretion of the PhoK enzyme reported earlier (Fig. 1A and B) (32). The spent medium from cultures was separated by centrifugation and spotted on PDP-MG plates. Unlike the spent medium of *D. radiodurans*(pPN1) or *E. coli*(pPN1) cells, the spent medium of *D. radiodurans*(pK1) (Fig. 1C) or *E. coli*(pK1) (Fig. 1D) cells showed intense green color, demonstrating extracellular secretion of the PhoK enzyme.

F1

***D. radiodurans*(pPN1) cells show cell surface-associated precipitation under GC1, while *D. radiodurans*(pK1) cells exhibit extracellular precipitation under GC2.** *D. radiodurans*(pPN1) and *D. radiodurans*(pK1) cells were used in U precipitation assays under GC1 and GC2, respectively. The GCs were selected for optimal U precipitation by the two enzymes employed, i.e., final pH 6.8 for the acid phosphatase PhoN, and pH 9.0 for the alkaline phosphatase PhoK. As reported earlier, the PhoK is a much higher-specific-activity enzyme than PhoN (at their respective pH optima) (11). *D. radiodurans*(pPN1) cells precipitated ~25% U in 5 h under GC1 but only 15% under GC2

TABLE 2 Hydrolysis of β-glycerophosphate by recombinant *Deinococcus radiodurans* strains

Cells used	P_i release from β-GP (nmol/min/mg of total cellular protein)[a]	
	pH 6.8	pH 9
D. radiodurans(pK1)	270.6 ± 2.5	931.8 ± 5
D. radiodurans(pPN1)	32.1 ± 0.5	6.0 ± 0.5
D. radiodurans(pRAD1)	2.2 ± 0.1	0.49 ± 0.05

[a] P_i release was measured in the buffer supernatant. Values reported are means with standard errors.

over the same time period (Fig. 2A), in accordance with pH dependence of its activity (Table 2). U precipitation by the *D. radiodurans*(pK1) cells was very rapid in both GCs, and more than 80% of U was precipitated by 5 h. However, when incubated for 18 h, both strains showed near-complete removal of U under both GC1 and GC2 (Fig. 2A). No detectable spontaneous precipitation of uranium occurred in the abiotic control (lacking cells) solution under either GC. Under both GCs, the *D. radiodurans*(pK1) cells showed a higher rate of phosphate hydrolysis than *D. radiodurans*(pPN1), commensurate with the higher specific activity of *D. radiodurans*(pPN1) (Table 2), thus accounting for the higher rate of U precipitation shown by the PhoK-expressing cells. In the *D. radiodurans* control cells (carrying pRAD1 alone), around 8.5% U was removed from the solution under GC1, and about 2.2% was removed under GC2 (Fig. 2A). XRD analysis identified that the U precipitate formed under all experimental conditions was chernikovite, a uranyl hydrogen phosphate, $H_2(UO_2)_2(PO_4)_2{\cdot}8H_2O$ (Fig. 2B).

In the control cells [*D. radiodurans*(pRAD1)], where no precipitation was observed, the cell pellet displayed a pinkish color typical of *D. radiodurans* under both GCs (Fig. 3A and B). In *D. radiodurans*(pPN1) the cell pellet was a mix of pink (cells) and

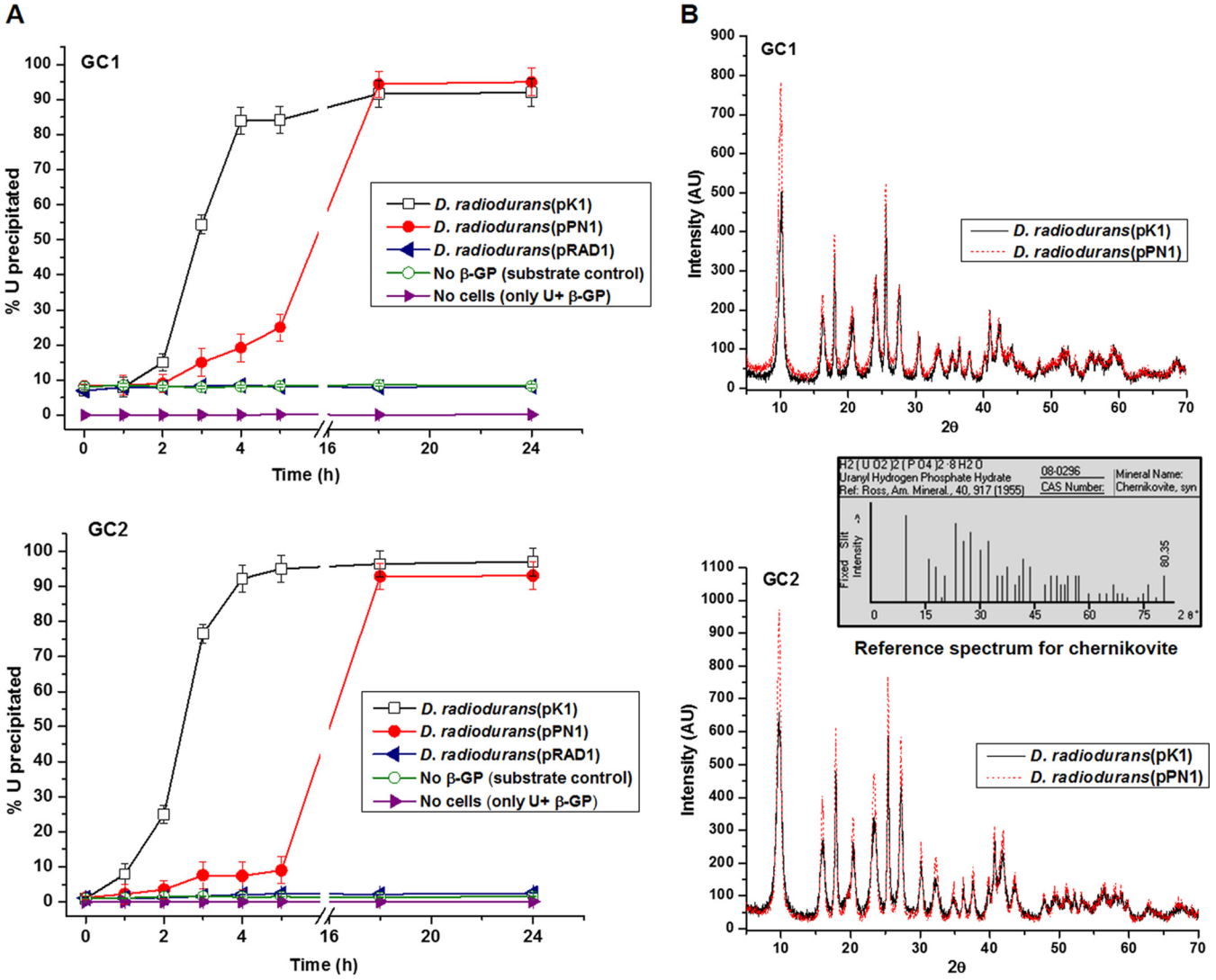

COLOR

FIG 2 Uranium bioprecipitation using *D. radiodurans* and confirmation of precipitate as uranyl hydrogen phosphate under GC1 or GC2. (A) Cells (OD_{600}, ~1) of *D. radiodurans*(pRAD1), *D. radiodurans*(pPN1), or *D. radiodurans*(pK1) were used for U bioprecipitation. U removal kinetics was studied using cells incubated in 1 mM U with 5 mM β-glycerophosphate, and the percent metal removed from the supernatant is shown. (B) XRD spectra of cells incubated with 5 mM U and 10 mM β-glycerophosphate for 18 h. The reference spectrum for chernikovite is also included.

zam01616/zam7338d16z | xppws | S=1 | 7/1/16 | 19:07 | 4/C Fig: 1,2,3,6 | ArtID: 00728-16 | NLM: research-article | CE: CNV-as

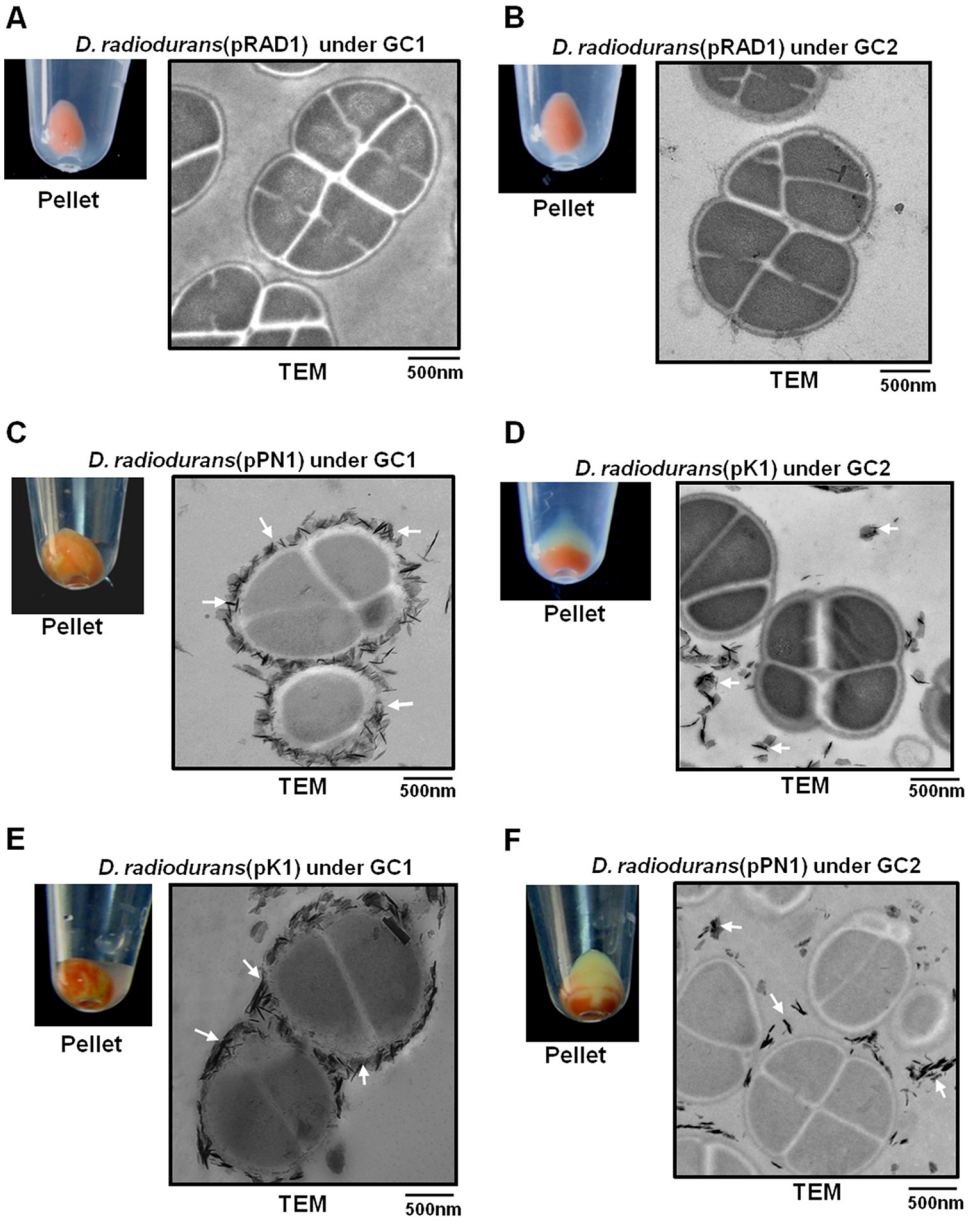

COLOR

FIG 3 Localization of U precipitate in recombinant *D. radiodurans* cells after U precipitation. *D. radiodurans*(pRAD1), *D. radiodurans*(pPN1), or *D. radiodurans*(pK1) cells were used for bioprecipitation assay of U (1 mM) under GC1 or GC2. After incubation for 18 h, the cells were either subjected to centrifugation to visualize the pellet or processed for TEM. (A, B, and D) Electron micrographs from uranyl acetate-stained samples are shown. The U precipitate is indicated by arrows.

AQ: H

yellow (precipitate) (Fig. 3C). Interestingly, *D. radiodurans*(pK1) cells displayed a distinct yellowish precipitate of U trailing the pink cell pellet (Fig. 3D).

Both the geochemical results and the TEM analysis showed that U did not precipitate from solution in the control under either of the GCs, clearly establishing the phosphatase enzyme-mediated precipitation of U (Fig. 3A and B). *D. radiodurans*(pPN1) cells under GC1 formed cell surface-bound spicule-like precipitates (Fig. 3C). In contrast, *D. radiodurans*(pK1) cells under GC2 showed extracellular U precipitation exterior to the cell surface (Fig. 3D).

Uranyl phosphate precipitate is mostly cell bound under GC1, whereas under GC2, it is extracellular. To ascertain if the aqueous uranyl species predominant under a particular geochemical condition indeed govern the precipitate location, the assay conditions were reversed. *D. radiodurans*(pPN1) cells were incubated with U under GC2, whereas *D. radiodurans*(pK1) cells were incubated with U under GC1. Visual examination of the cell pellet color after precipitation indicated that regardless of the phosphatase enzyme employed or its location, under GC1, the entire cell pellet turned yellowish (Fig. 3E), while under GC2, a yellow streak of uranyl phosphate trailed the pink cell pellet (Fig. 3D and F). TEM images of *D. radiodurans*(pK1) cells clearly showed cell surface-bound crystals under GC1, along with sparse presence of extracellular precipitate (Fig. 3E). In contrast, *D. radiodurans*(pPN1) cells displayed

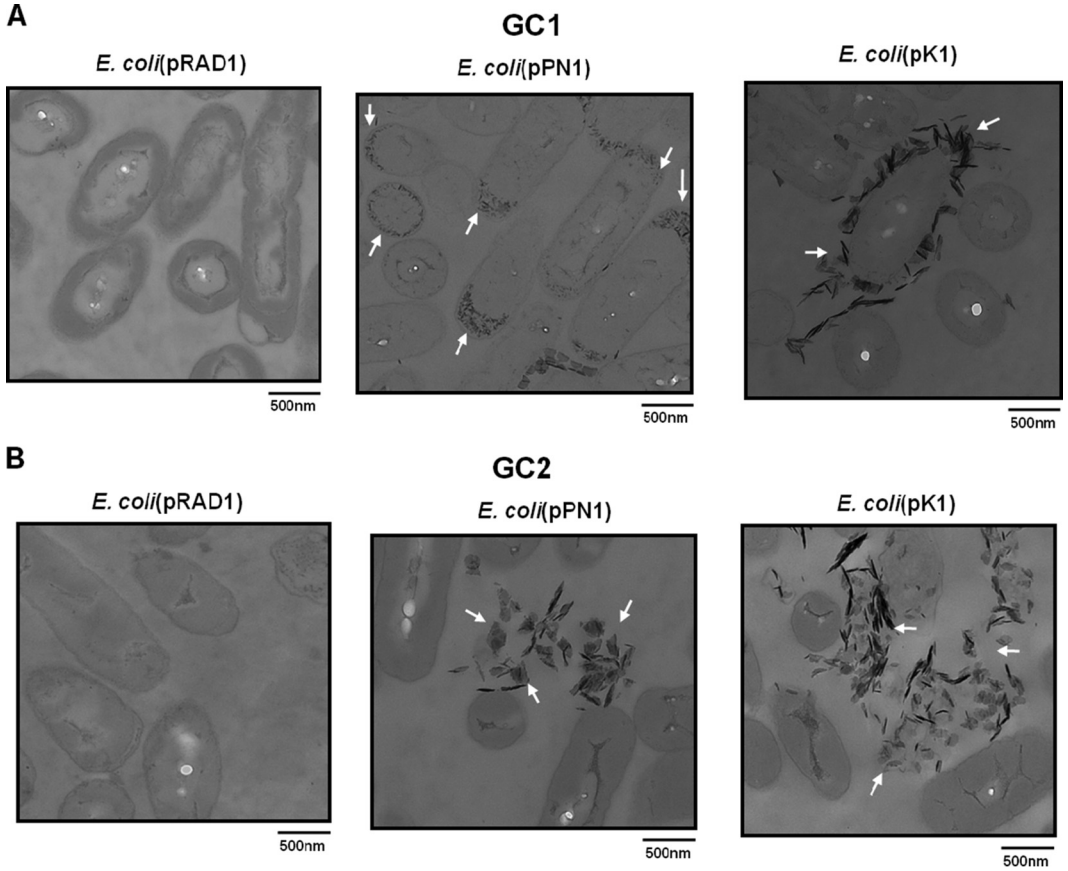

FIG 4 TEM analysis of recombinant *E. coli* cells after U precipitation. Cells (OD_{600}, ~1) of all three strains [*E. coli*(pRAD1), *E. coli*(pPN1), ~~or~~ *E. coli*(pK1)] were used in U (1 mM) precipitation assays for 18 h under GC1 (A) or GC2 (B) and processed for TEM. Arrows show the locations of uranyl phosphate precipitate.

distinct extracellular uranyl phosphate crystals, with little cell surface-associated precipitate under GC2 (Fig. 3F).

The nature of the aqueous uranyl species predominant under a particular GC determines the eventual localization of U precipitate in *E. coli*. Similar experiments performed with *E. coli* expressing PhoK or PhoN (Fig. 4) confirmed the relationship between aqueous U speciation and localization of U precipitate to be in accordance with the results obtained in *D. radiodurans* (Fig. 3). In the *E. coli*(pRAD1) control cells, no precipitate was observed (Fig. 4A and B). Regardless of the phosphatase employed for precipitation, under GC1, uranyl phosphate precipitate was cell associated (Fig. 4A), while under GC2, the precipitate was extracellular (Fig. 4B). In *E. coli*(pK1) cells under GC1, the precipitate was evenly bound all over the cell surface (Fig. 4A), whereas in *E. coli*(pPN1) cells, the precipitate was located in the periplasmic space at the polar ends (Fig. 4A).

Amount of uranium adsorbed by bacterial cells is higher under GC1 than GC2. The amount of U adsorbed onto the wild-type bacterial cells lacking the PhoN/PhoK enzymes was monitored under either GC1 or GC2. At all the concentrations of U employed, both organisms showed higher biosorption of U under GC1 than under GC2. For instance, at a concentration of 1 mM input U under GC1, *D. radiodurans* adsorbed 98 mg of U/g (dry weight) of cells (i.e., 8.3% of the input U), whereas *E. coli* cells showed biosorption of 46 mg of U/g (dry weight) of cells (7% of the input U) (Fig. 5A and B). In contrast, both organisms adsorbed only 8 to 12 mg of U/g (dry weight) of cells (1 to 2% of the input U) under GC2 (Fig. 5A and B). Geochemical modeling studies using the MINTEQ software showed that under GC1, U largely formed positively charged uranium hydroxide complexes, while under GC2, the negatively charged uranyl carbonate-hydroxide complexes predominated (Table 3). Thus, greater biosorption of U occurs under GC1, where the positively charged hydroxide complexes predominate, rather than under GC2, where the negatively charged carbonate-hydroxide complexes of U are prevalent.

Complexation of uranyl ions at alkaline pH decreases their toxicity to bacteria. Exposure to 1.5 mM U under GC1 (pH 6.8) caused severe loss in cell viability in both *D. radiodurans* and *E. coli* cells, as visualized by a spot experiment (Fig. 6A). In contrast, the survival of cells remained largely unaffected even at 20 mM U under GC2 (Fig. 6A). In both *D. radiodurans* and *E. coli*, only 10% survival (determined by measuring CFU) was obtained compared to the control (cells not exposed to U) when incubated (on nutrient agar medium) under GC1 at 1.25 mM U, whereas under GC2, growth was unaffected even at 20 mM U (Fig. 6A). In a separate experiment, *D. radiodurans* and *E. coli* cells were exposed to 2 mM U under GC1 or 20 mM U under GC2 for 4 h and then inoculated (OD_{600}, ~0.5) in liquid nutrient medium without U. Growth of cells preincubated in U under GC2 remained unaltered compared to the control cells. On the other hand, cells that were preincubated in 2 mM U under GC1 did not show growth (Fig. 6B).

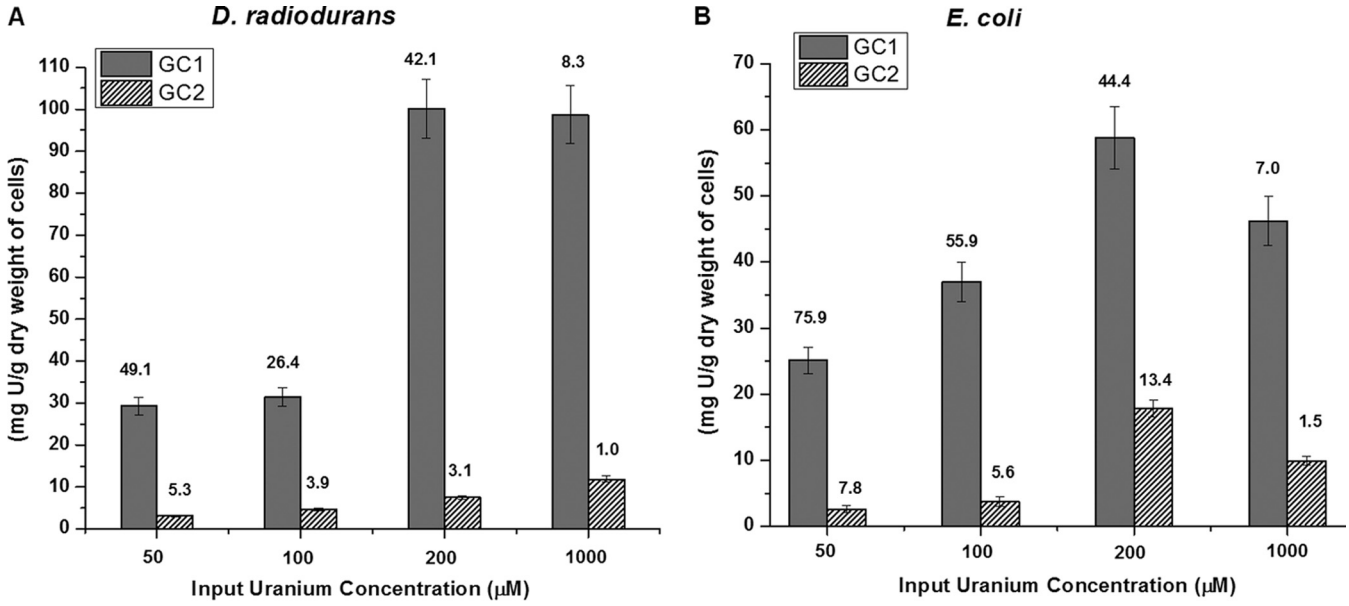

FIG 5 Biosorption of U by *D. radiodurans* and *E. coli*. Wild-type *E. coli* or *D. radiodurans* cells (OD_{600}, ~1) were suspended in 10 mM MOPS buffer containing 50, 100, 200, or 1,000 μM U under either GC1 or GC2. Under GC2, the carbonate concentration was always 2.4 times higher than the U concentration used. The amount of U biosorbed per milligrams (dry weight) of cells is reported. The percent U removed is indicated by numbers above the respective bars.

DISCUSSION

Bacterial phosphatases can be efficiently expressed in appropriate host systems and effectively utilized to precipitate heavy metals, such as U, from effluents. Earlier, our laboratory expressed two different phosphatases (PhoK/PhoN) in *E. coli* and *D. radiodurans* and demonstrated the U removal potential of these engineered recombinant strains (11, 29–32) from solutions. PhoN-expressing cells (in GC1) formed cell-bound uranyl phosphate precipitates

TABLE 3 U speciation in GC1 and GC2, as predicted by MINTEQ modeling[a]

	GC1		GC2	
Component	% of total concn (pH 6.8)	Species name	% of total concn (pH 9.0)	Species name
UO_2^{2+}	0.145	UO_2OH^+	63.088	$UO_2(CO_3)_3^{4-}$
	0.035	$(UO_2)_2(OH)_2^{2+}$	26.529	$(UO_2)_3(OH)^{7-}$
	51.899	$(UO_2)_2(OH)^{5+}$	4.252	$UO_2(CO_3)_2^{2-}$
	47.742	$(UO_2)_4(OH)^{7+}$	1.741	$(UO_2)_4(OH)^{7+}$
	0.047	$(UO_2)_3(OH)^{7-}$	1.249	$(UO_2)_3(OH)^{5+}$
	0.043	$(UO_2)_3(OH)_4^{2+}$	1.516	$(UO_2)(OH)^{3-}$
	0.109	$UO_2(OH)_2$ (aq)[b]	0.164	$(UO_2)(OH)_2$ (aq)
			0.032	$UO_2(CO_3)$ (aq)
NO_3^{1-}	100	NO_3^{1-}		
CO_3^{2-}			1.169	CO_3^{2-}
			16.28	HCO_3^-
			0.033	$H_2(CO_3)$ (aq)
			78.86	$UO_2(CO_3)_3^{4-}$
			0.013	$UO_2(CO_3)_3$ (aq)
			3.544	$UO_2(CO_3)_3^{2-}$
			0.062	$NaCO_3^-$ (aq)
NH_4^{1+}			67.012	NH_4^{1+}
			32.98	NH_3 (aq)
MOPS	30.319	MOPS	98.652	MOPS
	69.681	H-MOPS (aq)	1.348	H-MOPS (aq)
Na^{1+}	99.974	Na^{1+}	99.974	Na^{1+}
	0.022	$NaNO_3$ (aq)	0.015	$NaHCO_3$(aq)
Gly-2-phosphate	66.77	Gly-2-phosphate	99.70	Gly-2-phosphate
	33.23	H-Gly-phosphate	0.295	H-Gly-phosphate

[a] GC1, 1 mM uranyl nitrate hexahydrate, 5 mM β-glycerophosphate (sodium salt), and 10 mM MOPS (pH 6.8); GC2, 1 mM uranyl nitratehexahydrate, 5 mM β-glycerophosphate (sodium salt), 2.4 mM ammonium carbonate, and 10 mM MOPS (pH 9).
[b] aq, aqueous.

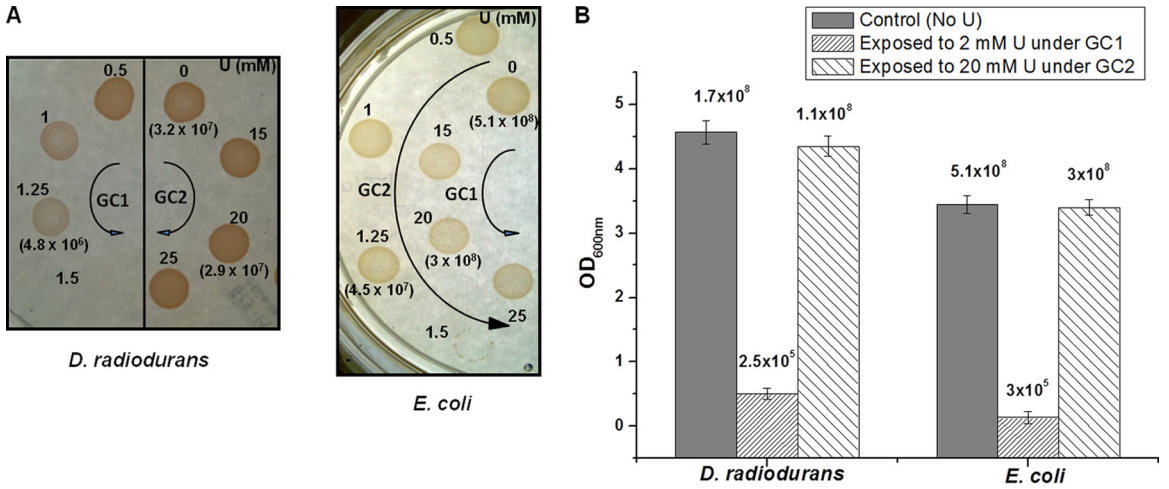

FIG 6 Uranium sensitivity of *D. radiodurans* and *E. coli*. Pregrown wild-type *D. radiodurans* or *E. coli* cells were suspended in U under either GC1 or GC2 for 4 h under sterile conditions. In GC2, the carbonate concentration was 2.4 times higher than the U concentration used. The uranium-exposed cells were either spotted (10 μl) on LB or TGY agar plates for visual examination of growth or plated on agar plates to determine CFU (A) or inoculated into liquid broth medium (at OD_{600} of 0.5) and grown for 18 h (B). The CFU obtained after plating are indicated in parentheses.

(Fig. 3), whereas PhoK-expressing cells (in GC2) generated extracellular uranyl phosphate precipitates, in conformity with the known cellular localization of the two enzymes (11, 29, 30, 32) (Fig. 3). This was substantiated by both TEM analysis and the nature of the cell pellet formed upon centrifugation of the assay mixture. The two-phase separation of the pellet in *D. radiodurans*(pK1) cells under GC2 resulted from extracellular U precipitation that was not associated with cells, while a more uniform mixture of cells (pink) and precipitate (yellow) was observed in *D. radiodurans*(pPN1) cells under GC1, indicating the presence of cell-associated precipitate.

A possible explanation for the differential localization of the U precipitate appeared to be the difference in the location of PhoN and PhoK enzymes. In addition to being cell associated, PhoK was secreted extracellularly by both *D. radiodurans* and *E. coli*, whereas PhoN remained solely contained within cells of both bacteria (Fig. 1). Alternatively, localization of the precipitate may be governed by uranium speciation. MINTEQ modeling studies showed that U mostly formed positively charged complexes under GC1, while the uranyl carbonate-hydroxide complexes formed under GC2 were predominantly negatively charged (Table 3). Therefore, the present study examined the possible effect of differentially charged aqueous U complexes on precipitate localization under the two GCs employed. The results showed that under GC1, the precipitate was largely cell associated, whereas under GC2, the precipitate was extracellular, with little cell surface association (Fig. 3 and 4). XRD results showed that the precipitated U phase was identical (chernikovite) under both GCs employed (Fig. 2B). Thus, the location of the enzymes had little role to play in determining whether the precipitate would be cell associated or extracellular.

Phosphatase assays, in the absence of uranium, show that the liberated phosphate is released into the supernatant buffer at pH 6.8 and 9 (Table 2). Bacterial cells usually carry a net negative surface charge at neutral pH (39, 40). With an increase in pH, the negative charge increases due to the increasing deprotonation of the functional groups found on the cell surface. In this study, the differential localization of the precipitate appears to be governed by the charge-dependent interaction of aqueous U species with the bacterial cell surface. The results indicate that the location of uranyl phosphate precipitate might be a consequence of the earlier event of the differential biosorption of U under the two different geochemical conditions. At pH 6.8 (GC1, in the absence of excess carbonate), U is adsorbed onto the bacterial cell surface, perhaps aided by the positive charge on the uranyl hydroxide aqueous species, which MINTEQ modeling suggests to be most prevalent. This initial complexation on the cell surface forms the nucleation sites, which are further consolidated by the codeposition of more incoming metal with the outgoing released inorganic phosphate (14, 40, 41), resulting in a build-up of polycrystalline metal phosphate precipitate on the cell surface (Fig. 3 and 4). At pH 9 (GC2, under carbonate-abundant conditions), MINTEQ modeling indicated U to be predominantly present as negatively charged uranyl carbonate-hydroxide aqueous complexes. It is difficult to distinguish the decreased biosorption and bioavailability of U due to (i) increasing carbonate concentration in the medium from the (ii) repulsion of negatively charged U species from the cell surfaces. However, the low level of U adsorbed onto the cell surface seems to be insufficient to consolidate the nucleation sites required for cell-associated precipitation. This probably leaves the negatively charged uranyl complexes free in the solution, resulting in extracellular precipitation of U upon encountering the phosphate released in the supernatant buffer either by PhoN or PhoK.

While the gross localization pattern of the precipitate seemed to be largely decided by the GC, subtle variations, apparently determined by the enzyme localization, were also observed. The periplasmic nonspecific acid phosphatases are known to concentrate at cell poles in Gram-negative bacteria (41–43). In accordance with this, the *E. coli*(pPN1) cells under GC1 displayed a periplasmic location of the precipitate at the poles (within the cells). The abundance of PhoN at the poles may result in localized sites of high phosphate concentration, leading to periplasmic accumulation of precipitate in *E. coli* (Fig. 4). This is unlike the exocellular (but still cell surface-associated) location of the pre-

cipitate in *E. coli*(pK1) under GC1, where the enzyme is released extracellularly and the precipitate is formed with the sorbed U on the external surface of the cell boundary. *Deinococcus* has a multilayered cell wall with a complex architecture (44), wherein the periplasm is not clearly defined. Further, the U hydroxyl species may not be able to permeate several layers of the cell envelope for uranyl hydrogen phosphate to be precipitated inside the cell wall. Thus, while geochemical conditions play a major role in determining the precipitate localization (i.e., cell associated and extracellular), finer variations may occur due to the different physiological conditions observed in the two bacteria.

The differential toxicity of U under the two geochemical conditions can also be attributed to the above-mentioned phenomenon. Binding of U to bacterial cell surfaces is evidently the first step toward obtaining cellular access, which subsequently causes the disruption of metabolic processes, eventually leading to lethality (9, 17). The predominantly negatively charged aqueous complexes of U formed under GC2 are repelled by the bacterial cell surface, making it difficult for U to acquire sufficient proximity to cells to cause significant damage. The presence of excess carbonate under such conditions may further decrease U availability to cells. On the other hand, the predominantly positively charged aqueous U species formed under GC1 would allow U to interact with cells, resulting in higher toxicity, as evidenced in this study (Fig. 6A and B). Also, increasing concentrations of uranium in GC1 lead to increased toxicity; however, there was no threshold concentration of uranium at which toxicity occurred in GC2 up to 25 mM U. Very likely, this was because under GC2, the carbonate concentration at each U concentration increased proportionally with the uranium concentration, thus continually limiting the amount of biosorption and, consequently, toxicity. These results also substantiate earlier reports that U biosorption decreases with increasing pH and increasing carbonate/bicarbonate concentration due to the higher complexation of uranyl ion by hydroxides and carbonates (9, 18, 45). It has also been shown that increasing pH and higher bicarbonate/carbonate concentration exert lower toxicity (46–48), as in the presence of high carbonate concentration, bioaccumulation of U is reduced in bacteria, consequently leading to increased U tolerance (17, 18, 49).

The present study has provided illustrative insights into the interaction of U complexes with bacterial surfaces by imaging the location of the uranyl phosphate precipitates. Using recombinant bacterial strains expressing phosphatases, this work demonstrates the effect of aqueous speciation of U on its interaction with cell surfaces and on the eventual cellular/extracellular localization of the precipitated uranyl phosphate. The efficacy of recombinant strains expressing PhoN and PhoK in uranium removal from solutions has already been established, with the *D. radiodurans*(pK1) strain being much more efficient (11, 23, 29–32). This study shows that, unlike biosorption (which has limited capacity and is often reversible) or bioaccumulation (which depends on metabolic activity and toxicity of metal), U species can be efficiently precipitated and removed from effluent solution by employing phosphatases. The cell-associated precipitation of metal has the advantages of easy downstream processing by simple gravity-based settling down of metal-loaded cells, compared to cumbersome separation techniques (22, 41). With this notion and in light of the fact that localization of the uranium precipitate is determined primarily by aqueous uranium speciation, the results from this study are of relevance to effluent treatment using such cells. *D. radiodurans*(pK1) is an efficient strain, on account of the high specific activity of PhoK phosphatase over a wider pH range, and can be used under GC1 to obtain cell-associated precipitation. Under GC2, PhoK immobilized in a suitable matrix would be an appropriate choice for metal recovery.

ACKNOWLEDGMENTS

S.K.A. thanks the Department of Science and Technology, India, for the award of the Sir J. C. Bose National Fellowship and the Department of Atomic Energy for the award of the Raja Ramanna Fellowship. We gratefully acknowledge the XRD analysis of samples by Chitra Radhakrishan, and Rajul R. Choudhury, Solid State Physics Division, BARC, and technical help provided by Namrata Waghmare in TEM analysis.

AQ: G

REFERENCES

1. **Converse BJ, Wu T, Findlay RH, Roden EE.** 2013. U(VI) reduction in sulfate-reducing subsurface sediments amended with ethanol or acetate Appl Environ Microbiol **79:**4173–4177. http://dx.doi.org/10.1128/AEM.00420-13.
2. **Barlett M, Moon HS, Peacock AA, Hedrick DB, Williams KH, Long PE, Lovley D, Jaffe PR.** 2012. Uranium reduction and microbial community development in response to stimulation with different electron donors. Biodegradation **23:**535–546. http://dx.doi.org/10.1007/s10532-011-9531-8.
3. **Boonchayaanant B, Nayak D, Du X, Criddle CS.** 2009. Uranium reduction and resistance to reoxidation under iron-reducing and sulfate-reducing conditions. Water Res **43:**4652–4664. http://dx.doi.org/10.1016/j.watres.2009.07.013.
4. **Merroun ML, Nedelkova M, Ojeda JJ, Reitz T, Fernández ML, Arias JM, Romero-González M, Selenska-Pobell S.** 2011. Bio-precipitation of uranium by two bacterial isolates recovered from extreme environments as estimated by potentiometric titration, TEM and X-ray absorption spectroscopic analyses. J Hazard Mater **197:**1–10. http://dx.doi.org/10.1016/j.jhazmat.2011.09.049.
5. **Choudhary S, Sar P.** 2011. Uranium biomineralization by a metal resistant *Pseudomonas aeruginosa* strain isolated from contaminated mine waste. J Hazard Mater **186:**336–343. http://dx.doi.org/10.1016/j.jhazmat.2010.11.004.
6. **Acharya C, Chandwadkar P, Apte SK.** 2012. Interaction of uranium with a filamentous, heterocystous, nitrogen-fixing cyanobacterium, *Anabaena torulosa*. Bioresour Technol **116:**290–294. http://dx.doi.org/10.1016/j.biortech.2012.03.068.
7. **Akhtar K, Waheed Akhtar M, Khalid AM.** 2007. Removal and recovery of uranium from aqueous solutions by *Trichoderma harzianum*. Water Res **41:**1366–1378. http://dx.doi.org/10.1016/j.watres.2006.12.009.
8. **Akhtar K, Khalid AM, Akhtar MW, Ghauri MA.** 2009. Removal and recovery of uranium from aqueous solutions by Ca-alginate immobilized *Trichoderma harzianum*. Bioresour Technol **100:**4551–4558. http://dx.doi.org/10.1016/j.biortech.2009.03.073.
9. **VanEngelen MR, Field EK, Gerlach R, Lee BD, Apel WA, Peyton BM.** 2010. UO_2^{2+} speciation determines uranium toxicity and bioaccumulation in an environmental *Pseudomonas* sp. isolate. Environ Toxicol Chem **29:**763–769. http://dx.doi.org/10.1002/etc.126.
10. **Malekzadeh F, Farazmand A, Ghafourian H, Shahamat M, Levin M, Colwell RR.** 2002. Uranium accumulation by a bacterium isolated from electroplating effluent. World J Microbiol Biotechnol **18:**295–302. http://dx.doi.org/10.1023/A:1015215718810.
11. **Kulkarni S, Ballal A, Apte SK.** 2013. Bioprecipitation of uranium from alkaline waste solutions using recombinant *Deinococcus radiodurans*. J Hazard Mater **262:**853–861. http://dx.doi.org/10.1016/j.jhazmat.2013.09.057.
12. **Nedelkova M, Merroun ML, Rossberg A, Hennig C, Selenska-Pobell S.** 2007. *Microbacterium* isolates from the vicinity of a radioactive waste depository and their interactions with uranium. FEMS Microbiol Ecol **59:**694–705. http://dx.doi.org/10.1111/j.1574-6941.2006.00261.x.
13. **Liang X, Hillier S, Pendlowski H, Gray N, Ceci A, Gadd GM.** 2015. Uranium phosphate biomineralization by fungi. Environ Microbiol **17:**2064–2075. http://dx.doi.org/10.1111/1462-2920.12771.
14. **Newsome L, Morris K, Lloyd JR.** 2014. The biogeochemistry and bioremediation of uranium and other priority radionuclides. Chem Geol **363:**164–184. http://dx.doi.org/10.1016/j.chemgeo.2013.10.034.

15. **Markich SJ.** 2002. Uranium speciation and bioavailability in aquatic systems: an overview. ScientificWorldJournal **2:**707–729.
16. **Belli KM, DiChristina TJ, Van Cappellen P, Taillefert M.** 2015. Effects of aqueous uranyl speciation on the kinetics of microbial uranium reduction. Geochim Cosmochim Acta **157:**109–124. http://dx.doi.org/10.1016/j.gca.2015.02.006.
17. **Carvajal DA, Katsenovich YP, Lagos LE.** 2012. The effects of aqueous bicarbonate and calcium ions on uranium biosorption by *Arthrobacter* G975 strain. Chem Geol **330–331:**51–59.
18. **Gorman-Lewis D, Elias PE, Fein JB.** 2005. Adsorption of aqueous uranyl complexes onto *Bacillus subtilis* cells. Environ Sci Technol **39:**4906–4912. http://dx.doi.org/10.1021/es047957c.
19. **Krestou A, Panias D.** 2004. Uranium (VI) speciation diagrams in the $UO_2^{2+}/CO_3^{2-}/H_2O$ system at 25°C. Eur J Miner Process Environ Prot **4:**113–129.
20. **Sheng L, Fein JB.** 2014. Uranium reduction by *Shewanella oneidensis* MR-1 as a function of $NaHCO_3$ concentration: surface complexation control of reduction kinetics. Environ Sci Technol **48:**3768–3775. http://dx.doi.org/10.1021/es5003692.
21. **Macaskie LE, Empson RM, Cheetham AK, Grey CP, Skarnulis AJ.** 1992. Uranium bioaccumulation by a *Citrobacter* sp. as a result of enzymically mediated growth of polycrystalline HUO_2PO_4. Science **257:**782–784. http://dx.doi.org/10.1126/science.1496397.
22. **Macaskie LE, Jeong BC, Tolley MR.** 1994. Enzymatically accelerated biomineralization of heavy metals: application to the removal of americium and plutonium from aqueous flows. FEMS Microbiol Rev **14:**351–367. http://dx.doi.org/10.1111/j.1574-6976.1994.tb00109.x.
23. **Seetharam C, Soundarajan S, Udas AC, Rao AS, Apte SK.** 2009. Lyophilized, non-viable, recombinant *E. coli* cells for cadmium bioprecipitation and recovery. Process Biochem **44:**246–250.
24. **du Plessis EM, Theron J, Joubert L, Lotter T, Watson TG.** 2002. Characterization of a phosphatase secreted by *Staphylococcus aureus* strain 154, a new member of the bacterial class C family of nonspecific acid phosphatases. Syst Appl Microbiol **25:**21–30. http://dx.doi.org/10.1078/0723-2020-00098.
25. **Vincent JB, Crowder MW, Averill BA.** 1992. Hydrolysis of phosphate monoesters: a biological problem with multiple chemical solutions. Trends Biochem Sci **17:**105–110. http://dx.doi.org/10.1016/0968-0004(92)90246-6.
26. **Gandhi NU, Chandra SB.** 2012. A comparative analysis of three classes of bacterial non-specific acid phosphatases and archaeal phosphoesterases: evolutionary perspective. Acta Inform Med **20:**167–173. http://dx.doi.org/10.5455/aim.2012.20.167-173.
27. **Beazley MJ, Martinez RJ, Sobecky PA, Webb SM, Taillefert M.** 2007. Uranium biomineralization as a result of bacterial phosphatase activity: insights from bacterial isolates from a contaminated subsurface. Environ Sci Technol **41:**5701–5707. http://dx.doi.org/10.1021/es070567g.
28. **Benzerara K, Miot J, Morin G, Ona-Nguema G, Skouri-Panet F, Férard C.** 2011. Significance, mechanisms and environmental implications of microbial biomineralization. C R Geosci **343:**160–167. http://dx.doi.org/10.1016/j.crte.2010.09.002.
29. **Misra CS, Appukuttan D, Kantamreddi VSS, Rao AS, Apte SK.** 2012. Recombinant *D. radiodurans* cells for bioremediation of heavy metals from acidic/neutral aqueous wastes. Bioeng Bugs **3:**44–48.
30. **Appukuttan D, Rao AS, Apte SK.** 2006. Engineering of *Deinococcus radiodurans* R1 for bioprecipitation of uranium from dilute nuclear waste. Appl Environ Microbiol **72:**7873–7878. http://dx.doi.org/10.1128/AEM.01362-06.
31. **Appukuttan D, Seetharam C, Padma N, Rao AS, Apte SK.** 2011. PhoN-expressing, lyophilized, recombinant *Deinococcus radiodurans* cells for uranium bioprecipitation. J Biotechnol **154:**285–290. http://dx.doi.org/10.1016/j.jbiotec.2011.05.002.
32. **Nilgiriwala KS, Alahari A, Rao AS, Apte SK.** 2008. Cloning and overexpression of alkaline phosphatase PhoK from *Sphingomonas* sp. strain BSAR-1 for bioprecipitation of uranium from alkaline solutions. Appl Environ Microbiol **74:**5516–5523. http://dx.doi.org/10.1128/AEM.00107-08.
33. **Ames BN.** 1966. Assay of inorganic phosphate, total phosphate and phosphatases, Methods Enzymol **8:**115–118.
34. **Peterson GL.** 1977. A simplification of the protein assay method of Lowry et al. which is more generally applicable. Anal Biochem **83:**346–356. http://dx.doi.org/10.1016/0003-2697(77)90043-4.
35. **Francis A, Dodge C, Gillow J, Papenguth H.** 2000. Biotransformation of uranium compounds in high ionic strength brine by a halophilic bacterium under denitrifying conditions. Environ Sci Technol **34:**2311–2317. http://dx.doi.org/10.1021/es991251e.
36. **Acharya C, Joseph D, Apte S.** 2009. Uranium sequestration by a marine cyanobacterium, *Synechococcus elongatus* strain BDU/75042 Bioresour Technol **100:**2176–2181.
37. **Fritz JS, Bradford EC.** 1958. Detection of thorium and uranium. Anal Chem **30:**1021–1022.
38. **Riccio ML, Rossolini GM, Lombardi G, Chiesurin A, Satta G.** 1997. Expression cloning of different bacterial phosphatase-encoding genes by histochemical screening of genomic libraries onto an indicator medium containing phenolphthalein diphosphate and methyl green. J Appl Microbiol **82:**177–185. http://dx.doi.org/10.1111/j.1365-2672.1997.tb02848.x.
39. **Van Loosdrecht MC, Lyklema J, Norde W, Schraa G, Zehnder AJ.** 1987. Electrophoretic mobility and hydrophobicity as a measured to predict the initial steps of bacterial adhesion. Appl Environ Microbiol **53:**1898–1901.
40. **French S, Puddephatt D, Habash M, Glasauer S.** 2013. The dynamic nature of bacterial surfaces: implications for metal-membrane interaction. Crit Rev Microbiol **39:**196–217. http://dx.doi.org/10.3109/1040841X.2012.702098.
41. **Macaskie LE, Bonthrone KM, Yong P, Goddard DT.** 2000. Enzymically mediated bioprecipitation of uranium by a *Citrobacter* sp.: a concerted role for exocellular lipopolysaccharide and associated phosphatase in biomineral formation. Microbiology **146:**1855–1867. http://dx.doi.org/10.1099/00221287-146-8-1855.
42. **Jeong BC, Hawes C, Bonthrone KM, Macaskie LE.** 1997. Localization of enzymically enhanced heavy metal accumulation by *Citrobacter* sp. and metal accumulation *in vitro* by liposomes containing entrapped enzyme. Microbiology **143:**2497–2507. http://dx.doi.org/10.1099/00221287-143-7-2497.
43. **Nesmeyanova MA, Tsfasman IM, Karamyshev AL, Suzina NE.** 1991. Secretion of the overproduced periplasmic PhoA protein into the medium and accumulation of its precursor in *phoA*-transformed *Escherichia coli* strains: involvement of outer membrane vesicles. World J Microbiol Biotechnol **7:**394–406. http://dx.doi.org/10.1007/BF00329408.
44. **Rothfuss H, Lara JC, Schmid AK, Lidstrom ME.** 2006. Involvement of the S-layer proteins Hpi and SlpA in the maintenance of cell envelope integrity in *Deinococcus radiodurans* R1. Microbiology **152:**2779–2787. http://dx.doi.org/10.1099/mic.0.28971-0.
45. **Morcillo F, Gonźalez-Muñoz MT, Reitz T, Romero-Gonźalez ME, Arias JM, Merroun ML.** 2014. Biosorption and biomineralization of U(VI) by the marine bacterium *Idiomarina loihiensis* MAH1: effect of background electrolyte and pH. PLoS One **9:**e91305. http://dx.doi.org/10.1371/journal.pone.0091305.
46. **Sani RK, Peyton BM, Dohnalkova A.** 2006. Toxic effects of uranium on *Desulfovibrio desulfuricans* G20. Environ Toxicol Chem **25:**1231–1238. http://dx.doi.org/10.1897/05-401R.1.
47. **Sepulveda-Medina PM, Katsenovich YP, Wellman DM, Lagos LE.** 2015. The effect of bicarbonate on the microbial dissolution of autunite mineral in the presence of Gram-positive bacteria. J Environ Radioacst **144:**77–85. http://dx.doi.org/10.1016/j.jenvrad.2015.03.002.
48. **VanEngelen MR, Szilagyi RK, Gerlach R, Lee BD, Apel WA, Peyton BM.** 2011. Uranium exerts acute toxicity by binding to pyrroloquinoline quinone cofactor. Environ Sci Technol **45:**937–942. http://dx.doi.org/10.1021/es101754x.
49. **Fortin C, Dutels L, Garnier-Laplace J.** 2004. Uranium complexation and uptake by a green alga in relation to chemical speciation: the importance of the free uranyl ion. Environ Toxicol Chem **23:**974–981. http://dx.doi.org/10.1897/03-90.

AUTHOR QUERIES

AUTHOR PLEASE ANSWER ALL QUERIES 1

AQau—Please confirm the given-names and surnames are identified properly by the colors. ■= Given-Name, ■= Surname

AQaff—Please confirm the following full affiliations or correct here as necessary. This is what will appear in the online HTML version:

[a]Molecular Biology Division, Bhabha Atomic Research Centre, Mumbai, India
[b]Homi Bhabha National Institute, Anushaktinagar, Mumbai, India

AQaff—This affiliation line will appear in the PDF version of the article and matches that on page 1 of the proof; corrections to this affiliation line may be made here **or** on page 1 of the proof:

Molecular Biology Division, Bhabha Atomic Research Centre, Mumbai, India[a]; Homi Bhabha National Institute, Anushaktinagar, Mumbai, India[b]

AQA—To ensure sequential order, references have been renumbered in text and in References. Please check and correct the renumbering if necessary. If any reference should be deleted from the References list, please mark "Reference deleted" in the margin next to that entry; do not renumber subsequent references.

AQB—Please define "*Dr-pRAD1*."

AQC—In the "U precipitation assays were..." sentence, please check that the edits retain the intended meaning, or edit further as necessary.

AQD—The slash here was changed to "or," as slashes are not allowed between genes except in the case of diploid/haploid genes.

AQE—Please indicate the significance of the +/− data in Table 2.

AQF—Bold type is not allowed per ASM style and was deleted in Table 3. If there is a particular meaning for the bold type in the table, please reunderline the correct sections and add a footnote to explain the significance of it.

AQG—Is Choudhury also the surname for "Chitra R."? Please clarify.

AQH—Please indicate the significance of the arrows in Fig. 3.